

Evaluation of persulfate for the treatment of manufactured gas plant residuals

by

Angela McIsaac

A thesis
presented to the University of Waterloo
in fulfillment of the
thesis requirement for the degree of
Master of Applied Science
in
Civil Engineering

Waterloo, Ontario, Canada, 2013

© Angela McIsaac 2013

I hereby declare that I am the sole author of this thesis. This is a true copy of the thesis, including any required final revisions, as accepted by my examiners.

I understand that my thesis may be made electronically available to the public.

Abstract

The presence of coal tars in the subsurface associated with former manufactured gas plants (MGPs) offers a remediation challenge due to their complex chemical composition, dissolution behaviour and recalcitrant characteristics. A former MGP site in Clearwater Beach, Florida was characterized and bench-scale analyses were conducted to assess the potential for *in situ* chemical oxidation (ISCO) using persulfate to treat MGP residuals.

Completion of a conceptual site model identified a homogeneous, silty sand aquifer, with an average hydraulic conductivity of approximately 2.3×10^{-3} cm/s and a groundwater flow rate of 2 cm/day in the direction of S20°E. Six source zones, three near the water table and three in the deep aquifer were estimated to have a total volume of 108 m³. A multi-level well transect was installed to monitor concentrations of dissolved compounds and to estimate mass discharge downgradient of the source zones over time. On average, the morphology of the aqueous concentrations remained consistent with time. A total mass discharge across the transect of 94 mg/day was estimated for site-specific compounds.

Bench-scale tests were conducted on aquifer sediments and groundwater samples. The aquifer was determined to have a low buffering capacity, low chemical oxygen demand, and low natural oxidant interaction (NOI) with persulfate. Aqueous batch experiments identified the potential for iron (II) activated persulfate to reduce concentrations of BTEX and PAHs below method detection limits (MDLs). Unactivated persulfate was able to reduce BTEX concentrations to below MDLs after 14 days; however, the concentration of PAH compounds remained above MDLs after 14 days. Higher iron doses within the system were shown to be more effective in reducing BTEX and PAH compounds.

Column experiments designed to mimic site conditions were used to evaluate the feasibility of persulfate treatment on impacted sediments from the Clearwater site. Two sets of column experiments were conducted: one using unactivated persulfate followed by alkaline activated persulfate; and one using iron (II) activated persulfate. On average, unactivated persulfate was able to reduce BTEX and PAH aqueous effluent concentrations by > 75% and 40%, respectively, after a total dose of 60 g/g soil. Two additional doses of alkaline activated persulfate (total persulfate dose of ~80g/g soil) in these columns were able to further reduce effluent BTEX and PAH concentrations by > 90% and > 75%, respectively. Iron (II) activated persulfate reduced effluent BTEX concentrations by > 70% and PAHs by > 65% after a total dose of 35 g/g soil. Average reductions in mass for BTEX and PAH compounds were approximately of 48% and 26% respectively in the iron (II) activated persulfate columns, and 24% and 10%, respectively in the alkaline activated persulfate columns.

The potential for the ability to use *in situ* chemical oxidation using persulfate for the remediation of MGP residuals in the subsurface is evaluated using field measurements and bench-scale experimentation. The reductions observed in aqueous phase compounds in MGP groundwater as observed in the laboratory indicate the potential for reductions in groundwater concentrations at this and other contaminated former MGP sites. However, column experiments, indicating the inability for activated persulfate to reduce all identified compounds in the MGP NAPL suggest source treatment with activated persulfate would not reduce concentrations to below Florida Department of Environmental Protection natural attenuation concentrations.

Acknowledgements

Firstly, I would like to thank my thesis supervisor, Neil Thomson for his guidance and assistance with my research over the past two years. Also, I would like to thank Andrew Brey, ARCADIS®, Brian Langinlle, Clearwater Gas Systems, and William Pence and Lyndie James, Baker and Hostetter.

Finally, I would like to thank all those who helped me in the laboratory: Mark Sobon, Shirley Chatten, Marianne VanderGriendt, Laurel Thomas-Arrigo, and Wayne Noble, those who helped in the field: Michelle Cho, Nick Doucette, and Bob Ingleton and those who helped me de-stress and enjoy the process: Simon Haslam, Richard Simms, Joanna Hamely, Andrea Atkinson, Elleana Hoekstra, and Michael McIsaac.

Funding was provided by Arcadis Canada Inc. (N. Thomson, PI).

Dedication

I would like to dedicate this thesis to my parents who have provided me with unconditional love and support in all areas of my life making all of my achievements, including making this graduate degree possible.

Table of Contents

List of Tables	viii
List of Figures	ix
Chapter 1	1
Introduction	1
1.1 Remediation of MGP Residuals	3
1.1.1 <i>In Situ</i> Chemical Oxidation (ISCO).....	4
1.2 Thesis Objectives	5
1.3 Site History	5
1.4 Existing Site Conceptual Model.....	6
1.5 Thesis Organization.....	7
Chapter 2	18
2.1 Field Activities	18
2.2 General Stratigraphy.....	18
2.3 Grain Size Distribution.....	18
2.4 Hydrogeology	19
2.4.1 Permeability.....	19
2.4.3 Slug Tests	20
2.4.4 Groundwater Flow and Travel Time	21
2.5 MGP Source Material.....	22
2.6 Source Material Concentrations	24
2.7 Dissolved Phase Concentrations.....	25
2.7.1 Cation/Anion Scan.....	25
2.7.2 BTEX and PAH Concentrations.....	26
2.8 Mass Discharge	28
2.9 Current Conceptual Site Model	29
Chapter 3	57
3.1 Buffering Capacity	57
3.2 Chemical Oxygen Demand (COD) Tests	58
3.3 NOI Tests	59
3.4 Aqueous Treatability Studies	59
3.4.1 Unactivated Persulfate.....	59
3.4.2 Iron (II) Activated Persulfate.....	61
3.5 Column Experiments	62

3.5.1 Materials and Methods	63
3.5.2 Unactivated Column Results	65
3.6 Summary	70
Chapter 4	87
References	91
Appendices	95
Appendix A	96
Appendix B.....	102
Appendix C.....	112
Appendix D	122
Appendix E.....	133
Appendix F.....	149
Appendix G	169

List of Tables

Table 1.1. MGP residuals and sources.....	8
Table 1.2. Summary of ISCO studies.	9
Table 1.3. Summary of previous site investigations.	16
Table 1.4. Florida groundwater clean-up standards for site specific compounds.....	17
Table 2.1. Summary of field activities.....	30
Table 2.2. Concentrations of coal tar compounds in site soil.....	36
Table 2.3. Slug test results.....	37
Table 2.4. Observed MGP impacts from borings.	38
Table 2.5. Volume of NAPL source zones.	39
Table 2.6. NAPL composition	42
Table 2.7. Coal tar chemical compositions.....	43
Table 2.8. Groundwater geochemical parameters.....	44
Table 2.9. Mass discharge across transect.	56
Table 3.1. COD test results.	73
Table 3.2. Reaction rate coefficients from aqueous treatability studies.	75
Table 3.3. Minimum Detectable Levels for site-specific compounds.	76
Table 3.4. NAPL concentrations in unactivated/base activated persulfate columns.	82
Table 3.5. Initial and Final NAPL saturation in treatment and control columns.....	83
Table 3.6. NAPL concentrations in iron activated treatment columns.	86

List of Figures

Figure 1.1 Layout of former Clearwater MGP (circa 1957).....	14
Figure 1.2 Previous installations conducted at the former Clearwater MGP site.....	15
Figure 2.1. Particle size distribution for samples.....	32
Figure 2.2. Hydraulic conductivity profiles.....	33
Figure 2.3. Pressure transducer response during a slug tests.....	34
Figure 2.4. Transducer measurements.....	35
Figure 2.5: NAPL saturated pores in DPT 23.....	37
Figure 2.6. Estimated extent of observed source zones < 4.5 m bgs (shallow).....	40
Figure 2.7. Estimated extent of observed source zones > 4.5 m (15 ft) bgs (deep).....	41
Figure 2.8. Schematic of multilevel (ML) monitoring well construction.....	45
Figure 2.9. Benzene transect iso-concentration profiles.....	46
Figure 2.10. Naphthalene transect iso-concentration profiles.....	47
Figure 2.11. Ethylbenzene transect iso-concentration profiles.....	48
Figure 2.12. 1-Methylnaphthalene transect iso-concentration profiles.....	49
Figure 2.13. 2-Methylnaphthalene transect iso-concentration profiles.....	50
Figure 2.14. Acenaphthalene transect iso-concentration profiles.....	51
Figure 2.15. Concentration profiles from ML-11.....	52
Figure 2.16. Concentration profiles from ML-12.....	52
Figure 2.17. Concentration profiles from ML-13.....	53
Figure 2.18. Concentration profiles from ML-14.....	53
Figure 2.19. Concentration profiles from ML-3.....	54
Figure 2.20. Concentration profiles from ML-5.....	54
Figure 2.21. Concentration profiles from ML-8.....	55
Figure 3.1. Buffering capacity for randomly selected sediment.....	73
Figure 3.2. Persulfate decomposition due to natural oxidant demand.....	74
Figure 3.3. Unactivated persulfate treatability results for the COC.....	74
Figure 3.4. Iron(II) activated persulfate treatability results.....	77
Figure 3.5. Column schematic.....	78
Figure 3.6. Unactivated persulfate effluent concentration.....	78
Figure 3.7. Unactivated/base activated persulfate dose-response curves.....	79
Figure 3.8. Persulfate breakthrough curves.....	80
Figure 3.9. Relationships between SCAP and BTEX compounds.....	81
Figure 3.10. Iron activated persulfate effluent concentration.....	84
Figure 3.11. Iron activated persulfate dose-response curves.....	84
Figure 3.12. SCAP concentrations from iron activated columns.....	85

Chapter 1

Introduction

Manufactured gas was the dominant fuel source in the United States, Europe, and Canada from the early 1800s through to the mid-1900s (Hatheway, 2006). Manufactured gas plants (MGPs) generated fuel through the purification and processing of an organic feedstock. The most common feedstocks used were liquid oils and solid carbon based fuels, which included anthracite, bituminous coal, and coke (Harkins et al., 1988). The processes used to manufacture gas produced various by-products and wastes. Leaks, spills, and improper disposal methods were common and led to environmental contamination (Harkins et al., 1988).

During peak periods of gas production, there were an estimated 10,000 plants operating in North America and Europe (Fischer et al., 1999). Following World War II, advances in technology lead to the exploitation of natural gas, a more economical and environmentally friendly fuel option (EPA, 1999). As a result, MGPs ceased manufacturing and were abandoned or upgraded to distribute natural gas. It is estimated that in the United States and Europe there are approximately 30,000-65,000 abandoned MGP sites (4000 in Canada) where many persistent by-products and wastes are still present (Hatheway, 2006). The volume, characteristics, and toxicity of the wastes generated depend on a variety of factors including the type of feedstock and gas manufacturing processes that were used.

In general, MGPs consisted of a generator where the feedstock (commonly coal or oil) was heated in an anoxic environment to generate gas. The off-gas contained energy rich compounds such as hydrogen, methane and carbon dioxide, and was stored for lighting, heating, or as an industrial fuel source. The off-gas also contained impurities and tar extractors were commonly utilized for their removal. Additionally, naphthalene scrubbers were used to remove naphthalene in the off-gas that could cause problems in the distribution system. Finally, liquid purification systems were used to remove hydrogen sulfide from the gas. Following purification, the gas was metered and stored in holders for distribution (Hatheway, 2006).

There were three dominant processes used for manufacturing coal gas: coal carbonization, carbureted water gas (CWG), and oil gas (Hatheway, 2006). Coal carbonization was utilized between 1816 and 1875. In 1873, the CWG method was developed and used a type of oil known as blue gas, which increased the energy value of the produced gas making the process more efficient. This increased efficiency, coupled with a coal shortage from 1930 to 1960, facilitated

the rise of the oil gas manufacturing process and a growth in the MGP industry (Hatheway, 2006).

The types of waste residuals and their constituents vary between production processes (Table 1.1). Residuals were commonly discarded or stockpiled on site in the first couple of decades of gas manufacturing, and was the main source of contamination. However, as the industry progressed, residual recycling grew to be common practice and contamination from leaks and spills became more frequent (Hatheway, 2006). Additionally, when MGP sites were demolished, the residuals on site were typically buried with other debris (McGowan et al., 1996).

The most common by-product at MGP sites is coal tar. It is estimated that over 42 billion litres of coal tar was generated in the United States over the time period MGPs were operational (Eng and Menzies, 1985). Coal tar is of environmental concern since many of its constituents have been shown to be carcinogenic (Guerin, 1978; Warshawsky, 1999; USEPA 2006).

Coal tar is predominately composed of polycyclic aromatic hydrocarbons (PAHs) and benzene, toluene, ethylbenzene, and xylene (BTEX) compounds (Harkins et al., 1988). Up to 3000 separate PAHs (Hatheway, 2006) have been identified in coal tar; however, it is difficult to quantify all the constituents since identification of many of the compounds is not possible by chromatographic methods (Peters and Luthy, 1993). The exact chemical composition of coal tar is highly variable between sites as it is dependent on the feed material and the specific production process used (Hatheway, 2006). Analyses on the chemical composition of coal tar from former MGP sites have shown order of magnitude variations in compound concentrations (EPRI, 1993; Brown et al., 2005). Other properties such as phase stability (Peters et al. 2000), equilibrium aqueous phase concentrations (Lane and Loehr, 1992), mass transfer rates (Moo-Young and Brown, 2004), and bulk properties (EPRI, 1993; Peters and Luthy, 1993; Brown et al., 2006) of coal tar samples have been investigated and compared, also showing order of magnitude variations between sites.

Coal tar exists in the subsurface as a non-aqueous phase liquid (NAPL) acting as a continuous source of contamination. Coal tar can range in density from lighter than water (LNAPL) to denser than water (DNAPL) (Moo-Young et al., 2009) resulting in sources near the water table and in pools above impermeable boundaries (Murphy, 2005). Over time, lighter mass fractions in the coal tar will decrease due to weathering (i.e., volatilization, and degradation) (Moo-Young et al., 2009). Therefore, the concentrations of BTEX compounds and PAHs with low molecular weights diminish over time (Yeom et al., 1995). In contrast, heavier, less soluble compounds

(PAHs with 3 or more rings) will remain in the NAPL and amalgamate into a mass, reducing the potential for weathering, making them more persistent (Hatheway, 2006).

Coal tar migration in the subsurface is controlled by gravity, viscous and capillary forces. The dissolution mechanism is responsible for the presence of the associated aqueous phase compounds. Studies conducted to estimate groundwater concentrations of coal tar compounds at contaminated sites based on aqueous solubilities (Lane, et al., 1992; Lee, et al., 1992; Mackay, et al. 1991) and it has been determined that predicting aqueous solubilities of coal tar compounds using a modified version of Raoult's law agrees with experimental estimates (Lee et al., 1992; King and Barker, 1999). Therefore, the compounds in coal tar will dissolve into the groundwater phase depending on their mole fraction in the NAPL and their effective solubility (Moo-Young et al. 1999). BTEX compounds and low molecular weight PAHs have relatively high aqueous solubilities compared to high molecular weight PAHs, and are often seen in higher concentrations in groundwater plumes at former MGP sites (Pinto, 1993).

1.1 Remediation of MGP Residuals

The complex chemical composition of coal tar makes remediation a challenge. Remediation involves management of both groundwater and soil for LNAPL and DNAPL residuals. To date, there have been many investigations conducted on the remediation of MGP residuals including substantial laboratory and pilot-scale research, and some full-scale remediation activities.

Investigations of *ex situ* remediation techniques such as soil extraction (Luthy et al., 1994; Yeom et al. 1995), and thermal desorption (O'Shaughnessy and Nardini, 1997) have been conducted. However, due to increase costs related to hazardous waste disposal, *ex situ* treatment is commonly deemed infeasible (McGowan, et al., 1996).

In situ remediation addresses many of the shortcomings associated with *ex situ* methods and within the last decade have been developed and applied more frequently (Kavanaugh et al., 2003; ITRC, 2005; McGuire et al., 2006). *In-situ* full-scale treatment methods have been applied at BTEX and PAH contaminated sites using natural attenuation (Bockelmann et al., 2001), bioremediation (Schmitt et al., 1996), *in situ* solidification (Underhill et al., 2011), *in situ* air sparging with ozone (Nelson, 1997), and permeable reactive barriers (McGovern et al., 2002).

The efficiency of *in situ* technologies relies on contaminant characteristics and site hydrogeology. For MGP residuals, methods that rely on high dissolution rates, such as pump-and-treat, do not provide effective solutions for projects with time constraints due to the low solubility of many of the coal tar compounds (Luthy et al., 1992; Lane & Loehr, 1992). Similarly,

bioremediation and natural attenuation have time frames of decades to obtain remediation goals (EPA, 1999). *In situ* chemical oxidation has shown success in heterogeneous sediments and for a wide range of recalcitrant compounds in short time frames when used alone or coupled with other remediation technologies (Tsitonaki et al., 2006; Tsai and Kao, 2009; Krembs et al., 2010).

1.1.1 *In Situ* Chemical Oxidation (ISCO)

In situ chemical oxidation involves the delivery of an oxidant into an aquifer to oxidize organic contaminants. The benefit of this treatment technology compared to other *in situ* methods is that it enhances the dissolution and destruction of contaminants (Major, 2009). Typical oxidants include peroxide, catalyzed hydrogen peroxide (CHP), permanganate and persulfate. In the peer-reviewed literature the ability of these reagents to degrade BTEX and PAHs in both aqueous and slurry systems has been well-documented (Table 1.2). From these studies it is important to note that permanganate is unable to oxidize benzene, one of the main compounds in coal tar (Crimi and Taylor, 2007). Peroxide persistence in aquifer solids is dependent on aquifer type and is short-lived, with a typical half-life of several hours to several days, resulting in its decomposition before depletion of organic contaminants, increasing remediation costs and clean-up times (Ferrarese et al, 2008). Finally, treatment of coal tar compounds with CHP have shown its limited ability to degrade high molecular weight PAHs (4-20% removal) (Bogan and Trbovic, 2003; Lundstedt et al., 2006).

Persulfate is the most recent oxidant used for ISCO treatment and has advantages over other oxidants. Based on bench-scale tests conducted with persulfate (Table 1.2), it is known to degrade a wide variety of organic contaminants (Siegrist et al., 2011), have a low natural oxidant interaction (NOI) (Sra, 2010), and have a higher standard reduction potential (Latimer, 1952) compared to other oxidants (Yen et al., 2011). Additionally, once activated, persulfate generates free radicals, further increasing its oxidation potential. Aqueous studies using simulated groundwater have been conducted to show degradation of BTEX and PAH compounds using persulfate (>70%) (Block, 2004; Sra, 2010) and further reductions (>80%) were seen with activated persulfate. Positive results have also been observed with persulfate treatment of MGP contaminated soil (Killian et al., 2007; Ferrasse et al., 2008; Gryzenia et al., 2009), yielding >85% removal of compounds.

Although the results from aqueous and slurry batch tests have shown the ability of persulfate to treat MGP residuals (Nam et al. 2001; Sra et al. 2010), they are not representative of *in situ* conditions. The oxidant to solids mass ratio in a batch experiment is larger than what is encountered *in situ* and in column experiments, increasing effective interaction of persulfate and

the contaminants. As a result, reaction rates are often overestimated leading to unrealistic expectations of *in situ* treatment. To date there have been no peer-reviewed studies of column experiments, pilot-scale experiments, or full-scale trials on the ability of persulfate to treat MGP residuals. Such investigations are necessary to adequately evaluate the potential for ISCO using persulfate at former MGP sites.

1.2 Thesis Objectives

The content of this thesis fulfills the initial phases of a larger research project that aims to demonstrate the efficiency and effectiveness of *in situ* chemical oxidation using persulfate to treat MGP residuals beneath a former MGP. The project is a multi-year, pilot-scale evaluation at a former MGP site in Clearwater Beach, Florida. To achieve the project goal seven subtasks were defined: source area characterization, bench-scale experiments, push-pull tests, diffusion modeling, pilot-scale remediation, treatment and short-term monitoring, and long-term monitoring. The first two subtasks form the objectives of this thesis which are to:

- Develop a conceptual site model (CSM) by collecting sufficient background temporal information to establish a solid understanding of baseline conditions
- Design and conduct batch aqueous, batch slurry, and column treatability experiments to determine kinetic relationships between MGP residuals and persulfate, compare persulfate activation methods, determine dosing amounts, and quantify oxidant-solids interaction.

1.3 Site History

The Clearwater MGP operated between approximately 1924 and 1959 at 310 North Myrtle Avenue, Clearwater, Florida. As identified in Brown's Directory, the plant utilized the Tenny water gas process from 1924 to 1946, and then switched to the carbureted water gas (CWG) process. The plant was decommissioned in 1959. The former plant consisted primarily of buildings hosting retorts, a coke house, a compressor, scrubbers and purifiers, and above and below ground storage tanks (Figure 1.1).

The CWG process used steam to react with carbon to produce a fuel gas (known as blue gas) composed of carbon monoxide and hydrogen. Blue gas has a low fuel value and is lacking in illuminants. To overcome this drawback, the blue gas was thermally cracked with liquid

hydrocarbons to produce CWG, a gas with increased heating and illuminating power (Harkins et al., 1988).

The major by-product of the CWG process was tar from the uncracked portion of the liquid hydrocarbons. The amount of tar and its chemical composition depends on the original hydrocarbon feed material and the MGP production process. These tars predominately contain PAH and BTEX compounds (Harkins et al., 1988). However, unlike tars generated from the other MGP production processes, they contain trace amounts of nitrogen-based organics, cyanides, ammonia, and phenols. Additionally, tars and oils produced from the CWG process were usually less viscous, causing them to be more mobile (Harkins et al., 1988).

After the plant ceased operations in 1959, the structures were dismantled. Clearwater Gas System (CGS) now owns the property. The present surface conditions at the Site comprise a large paved parking area and operation buildings (meter shop, offices, and storage facilities) (Figure 1.2). The site is surrounded by residential properties to the north and west, and commercial properties south and east. A railway track is located on the southeast of the site and a public trail exists to the west just outside the limits of the site.

1.4 Existing Site Conceptual Model

Prior to the commencement of this thesis there were numerous subsurface investigations performed on site or downgradient on the Pinellas County Health Department property as detailed in Table 1.3. Additionally, some site characterization was conducted and instrumentation installed (Figure 1.2). Eleven boreholes, installed using direct-push technology (DPT), had been installed (denoted DPT-# in the order of their installation) and twenty monitoring wells (denoted MW-#), were installed. Wells IDs with a suffix of “D”, indicate a lower surficial monitoring well, while a “DV” suffix indicates a vertical extent monitoring well, and no suffix indicates an upper surficial monitoring well. Six off-site wells also exist which are named HDMW-1 through to -6, the “HD” prefix used to differentiate between wells located on the Pinellas County Health Department property and those installed for the former MGP site investigation.

The existing conceptual site model provided a general stratigraphic profile of the site which consists of 17 to 30 feet of surficial sands and silts (surficial aquifer), underlain by a competent, confining clay unit; underlying the clay unit is a buff-colored limestone. A depression in the clay layer was found at DPT-10. MGP residuals in the surficial sands and silts were observed and a source area was identified in the surficial aquifer south-east of the meter shop.

The groundwater flow direction was determined to be to the south-east in the surficial aquifer (shallow) and to the south-west in the aquifer underlying the clay unit (deep). Wells were sampled and analyzed for BTEX and PAH concentrations, and high concentrations of compounds were observed at MW-20 and MW-9D. Borehole installations confirmed a source zone in the area upgradient of MW-20. It was estimated that this source zone was contributing to the high groundwater concentrations observed at these well locations and most likely at downgradient wells HDMW-9, MW-9D, and HDMW-4D. Compounds of concern (COC) for the site were determined as: benzene, ethylbenzene, naphthalene, 1-methylnaphthalene, 2-methylnaphthalene, and acenaphthene based on groundwater concentrations that exceed groundwater clean-up target levels (GCTLs). State clean-up targets for the COC and other site-specific compounds are given in Table 1.4.

The existing conceptual site model provided some indication of the hydrogeology and extent of contamination at the site; however, many uncertainties still exist. For instance, the depth to the clay unit at DPT-10 was not measured, leaving uncertainty in the lithology and impacts in this area. The magnitude, direction and seasonal fluctuations in groundwater flow were not estimated. These hydrogeological conditions are important for predicting the movement and location of dissolved compounds. Finally, locations, extents and volumes of source zones were minimally characterized. Further site characterization is essential for designing an effective remediation strategy.

1.5 Thesis Organization

Chapter 2 focuses on development of the conceptual site model. In this chapter site geology, hydrogeology, source zones and the groundwater plume are discussed. Chapter 3 addresses the bench-scale studies completed including sediment buffering capacity, chemical oxygen demand and natural oxidant interaction tests, and treatability studies. Chapter 4 summarizes the conclusions and recommendations of this research.

Table 1.1. MGP residuals and sources.

Residual	Compounds	Production Method	Pathways
Coal Tar Tar Sludge Coke	PAHs, BTEX, and phenols	Coal Carbonization	Spills, leaks, dumps
Coal Tar Oil Tar Tar/Oil/Water Emulsion	PAHs, BTEX, and phenols	Carbureted Water Gas	Spills, leaks, dumps
Wastewater treatment sludge	PAHs, BTEX, phenols, nitrogen, sulfur, and metals	Coal Carbonization, Carbureted Water Gas	Spills, leaks, dumps
Spent purifier and scrubber wastes	Nitrogen, sulfur, inorganic compounds (mostly cyanide)	Coal Carbonization, Carbureted Water Gas	Leaks
Lampblack	PAHs and BTEX	Oil-gas	Dumps
Ammonia	Cyanides	Coal Carbonization, Carbureted Water Gas, Oil-gas	Discharge to sewer or ground

Table 1.2. Summary of ISCO studies to treat BTEX and PAH compounds using peroxide, permanganate and/or persulfate.

Author	System Type	Target Compounds	Source	Oxidant(s)	Oxidant System	Summary of Major Findings
Lou and Lee (1995)	aqueous	BTEX	spiked	peroxide	120 mg/L + 0, 100, 200, 400, 600 mg/L Fe(II)	Optimal pH value of 4 was found for degradation. Complete degradation of BTX in 10 minutes with 120 mg/L peroxide + 600 mg/L Fe(II)
Beltran et al. (1997)	aqueous	fluorene, phenanthrene, acenaphthene	spiked	CHP	10^{-5} , 10^{-4} , 10^{-3} , 10^{-2} , 10^{-1} M hydrogen peroxide + 7×10^{-5} M Fe(II)	Optimal hydrogen peroxide dose was 10^{-3} M. Optimal system yielded complete oxidation of PAHs within minutes
Kong (1998)	slurry	TPH	spiked	peroxide	0,1,7,15 and 35% by weight	Up to 70% degradation of petroleum compounds with 15% peroxide and 5% iron in 72 hours, no further degradation observed after 8 days
Gates-Anderson et al. (2001)	slurry	naphthalene, phenanthrene, and pyrene	spiked	peroxide permanganate	4.5; 25 g/kg soil; 4.5;25g/kg soil + 5mM iron 1.5; 15 g permanganate/kg soil	efficiency was dependent on soil type, iron addition yielded >95% degradation 99% degradation, quicker degradation at higher oxidant dose
Nam et al. (2001)	slurry	BTEX + PAHs	MGP soil	peroxide		80% of 2- and 3-ring hydrocarbons and 20-40% of 4- and 5-ring compounds were destroyed. 84.5% and 96.7% destruction of pyrene and benzo(a)pyrene reported.
Bogan et al. (2003)	slurry	PAHs	MGP soil	peroxide	10 mM peroxide	Low removal (5%) of high molecular weight PAHs (5 and 6 rings).
Brown et al (2003)		6 PAHs (anthracene, benzo(a)pyrene, chrysene, fluoranthene, phenanthrene, and pyrene)	spiked	permanganate	160 mM permanganate	Reactivity order of benzo(a)pyrene (72.1%)>pyrene (64.2%) > phenanthrene (56.2%) > anthracene (53.8%) > fluoranthene (13.4%) and chrysene (7.8%) was observed in 30 minutes with 160 mM of permanganate
Block et al. (2004)	aqueous	BTEX + PAHs	spiked	persulfate	10% persulfate, 10 % persulfate + 550mg/L Fe(II); 10% persulfate + 550 mg/L Fe(III); 10% persulfate + Fe(III)-EDTA	Fe(II) was the most effective activator, complete BTEX oxidation occurred in all systems.

Table 1.2 (continued). Summary of ISCO studies to treat BTEX and PAH compounds using peroxide, permanganate and/or persulfate.

Author	System Type	Target Compounds	Source	Oxidant(s)	Oxidant System	Summary of Major Findings
Forsey (2004)	slurry	PAHs + BTEX	spiked	CHP	0.014 M peroxide + 0.0037 M Fe	>92% oxidation of PAHs except for fluoroantene (71%) and 1-methylnaphthalene (80%). Pyrene did not decompose under CHP oxidation
				permanganate	0.0046 M permanganate	>90% oxidation of PAHs except for luoroantene (75%) and dibenzofuran (74%).
	column	PAHs + BTEX	spiked	permanganate	8 g/L permanganate	>88% oxidation of PAHs except for 1-methylnaphthalene (72%). Pyrene did not decompose under persulfate oxidation After 172 days and 3.61 L of permanganate injection, 36.2% PAH removal was measured in treatment columns, compared to 2.44% in the control column.
Goi (2004)	slurry	PAHs	spiked	peroxide	0.001:1:0.0002; 0.004/1/0; 0.004:1:0.0008 peroxide/sand/Fe (w/w/w)	increasing ratio did not enhance PAH removal. 60% degradation occurred after 24 hours. Stepwise addition of peroxide was more effective (80% vs 60% removal)
Kanel (2004)	slurry	phenanthrene, anthracene, and pyrene	spiked	peroxide	5 M	After 3 hours, 73% phenanthrene removal, 60% anthracene removal, and 55% pyrene removal
Huang et al. (2005)	aqueous	BTEX	spiked	persulfate	1g/L; 5g/L, 20;30;40°C	Higher temperature yielded quicker degradation rates. At 40°C and 1g/L persulfate, >95% degradation of naphthalene, xylene and toluene, 1,2,3TMB, 1,2,4 TMB, and 94.3% degradation of benzene
Kang (2005)	slurry	BTEX	spiked	peroxide	30, 150, 300 mM + Fe(II) or Fe(III); 2,5 and 10 mM	97% destruction after 3 hours with 300 mM peroxide + 10 mM Fe(III).
Nadim et al. (2005)	aqueous	16 USEPA priority PAHs	spiked	persulfate	5 g/L + Fe(II)-EDTA	all PAHs < MDL (1 µg/L)
	slurry	7 PAHs			5 g/L; 5 g/L + 0.124 g/L Fe(II)-EDTA	75-100% degradation of all PAHs in Fe(II) system

Table 1.2. (continued). Summary of ISCO studies to treat BTEX and PAH compounds using peroxide, permanganate and/or persulfate.

Author	System Type	Target Compounds	Source	Oxidant(s)	Oxidant System	Summary of Major Findings
Kulik (2006)	slurry	PAHs	spiked	peroxide	peroxide; 10:1 (peroxide to iron)	increasing peroxide/soil/iron ratio enhanced PAH removal (twofold increase = 24% more removal)
Crimi and Taylor (2007)	slurry	BTEX	spiked	hydrogen peroxide	10% peroxide + 500 g/L persulfate; 10% peroxide + 500g/L ferrous sulfate + 100 g/L citric acid	>88% removal of BTEX compounds. Depletion of hydrogen peroxide occurred in less than 24 hours.
				persulfate	10% peroxide + 500 g/L persulfate; 500 g/L persulfate + 500g/L FeSO4 + 100 g/L CA	Iron activated persulfate demonstrated greater contaminant destruction (>99%) and greater oxidation persistence than peroxide systems.
			spiked	persulfate	20:1 mole ratio of persulfate to BTEX, at pH =11	54-92% reduction over a 3 week period
Killian et al. (2007)	slurry	BTEX + PAHs	soil from MGP site	persulfate	2.0 M persulfate + 1.0 M citric acid / 0.04 M ferrous sulfate	Persulfate and citric acid chelated iron was most effective in destroying BTEX and PAH compounds. After two doses 99% of the total BTEX concentration and 92% of the total PAH concentrations were destroyed.
Ferrarese et al. (2008)	slurry	16 USEPA priority PAHs	soil sample from MGP site	peroxide	50;100;200 mmol/sample	above 90% removal efficiencies at higher doses (100-200)
				CHP	50;100;200 mmol/sample + 0.5;1;2 mmol/sample Fe(II)+ chelate	above 95% removal
				persulfate	50;100;200 mmol/sample + 2;4;4 mmol/sample Fe(II) +chelate	76-88% removal
				permanganate	50; 100; 200 mmol/sample permanganate, 25 mmol/sample permanganate + 50 mmol/sample peroxide	removal above 90% without peroxide, worse results with peroxide addition
			persulfate + peroxide	50 mmol/sample persulfate + 2 mmol/sample Fe(II) + chelate + 50 mmol/sample peroxide	92% removal for total PAHs (93% light, 90% heavy)	

Table 1.2 (continued). Summary of ISCO studies to treat BTEX and PAH compounds using peroxide, permanganate and/or persulfate.

Author	System Type	Target Compounds	Source	Oxidant(s)	Oxidant System	Summary of Major Findings
Liang et al. (2008)	aqueous	BTEX	spiked	persulfate	20 mM, 100 mM persulfate + thermal activation (20°C);	20 mM persulfate yielded BTEX half lives between 3-23.1 days, while 100 mM persulfate yielded half lived between 3.3-5.2 days. Removal percentages for high persulfate dose were: benzene (75.4%), ethylbenzene (65.5%), toluene (51.2%), xylene (47.3%)
	slurry				5,20,100 mM persulfate + 1,5, 20 mM Fe	Almost instantaneous degradation observed for all BTEX compounds
					20 mM, 100 mM persulfate + thermal activation (20°C);	Removal percentages for high persulfate dose were: benzene (9.7%), ethylbenzene (15.1%), toluene (30.7%), and xylene (34.6%).
Stavelova et al (2008)	slurry	PAHs	soil from former gas plant	CHP	15%, 20%, 30% peroxide + 1,3g Fe(II) + EDTA	Dosing in parts yielded better removal. 15% peroxide yielded 77% PAH removal
				CHP + persulfate	15%,20% peroxide + 1,3 g Fe(II) + 1,3 g persulfate+ EDTA	84% PAH removal with 15% peroxide and 3g persulfate
Thomson et al. (2008)	stop-flow column	PAHs + BTEX	spiked	permanganate	~ 29 g permanganate injected into the column	Overall 37% decrease in creosote mass. Compounds resistant to permanganate (i.e. biphenyl, and dibenzofuran) were still removed at greater percentages than the control column (77% vs. 14%).
	cont.-flow column	PAHs + BTEX	spiked	permanganate	~8.5g permanganate injected into the column	15-40% more removal than stop-flow columns. 25% decrease in mass discharge of contaminants and 33% decrease in compound mass.
	field (pilot-scale)	PAHs + BTEX	emplaced creosote plume	permanganate	125 kg permanganate injected	> 35% reduction for all monitored compounds except biphenyl, dibenzofuran and fluoroanthene after 150 days. Data after 1 & 2 years following treatment showed 10-60% decrease in mass discharge, however after 4 years, rebound to pretreatment concentration levels or higher occurred.

Table 1.2 (continued). Summary of ISCO studies to treat BTEX and PAH compounds using peroxide, permanganate and/or persulfate.

Author	System Type	Target Compounds	Source	Oxidant(s)	Oxidant System	Summary of Major Findings
Gryzenia et al. (2009)	slurry	PAHs	soil sample from former MGP site	peroxide	1L of 50% peroxide + 1g Fe(III) 200mg EDTA; 1L of 50% peroxide + 1g Fe(III) 200mg EDTA + 500g Cool-OX™	71.3% oxidation of PAHs, 92.3% oxidation with Cool-OX™ addition
				persulfate	20:1:5 (persulfate:EDTA:Fe(II))	88.5% oxidation of PAHs
Sra et al. (2010)	aqueous	BTEX + TMBs + naphthalene	spiked	persulfate	1 and 20g/L	<10% decrease in contaminants at 1g/L inactivated persulfate, >99% BTEX, >71% naphthalene, and >94% TMB degradation for inactivated persulfate at 20g/L
					20 g/L + 150 mg/L Fe(II); 20g/L + 600 mg/L Fe(II)	>99% TMB destruction, >85% naphthalene destruction, >99% BTEX destruction (0.1M peroxide), decrease in concentration was higher for 1M peroxide (<27%) than 0.1M peroxide (<11%)
	field				20 g/L / 0.1 M peroxide; 20 g/L / 1 M peroxide	TMB completely oxidized after 4 days (12 days for 150 mg/L Fe(II)). Fe(II) activation yielded higher reduction rates than other persulfate treatments (except for naphthalene)
					20g/L	Mass flux of gasoline compounds decreased 45-85% (benzene >50%, ethylbenzene >80%), Rebound (>805 ethylbenzene, >50% benzene) occurred
Yen et al. (2011)	slurry	BTEX + PAHs	spiked	persulfate		55% diesel degradation after 40 days, 60% degradation and 10% persulfate remaining after 150 days.
				permanganate		40% removal of diesel contaminants after 3 days, strongest oxidant, however no further removal due to lack of persistence
				peroxide		60% removal after 40 days and no further degradation for remainder of experiment

Notes: CA = citric acid
 FeSO₄ = ferrous sulfate
 EDTA = ethylenediaminetetraacetic acid



Figure 1.1 Layout of former Clearwater MGP (circa 1957).

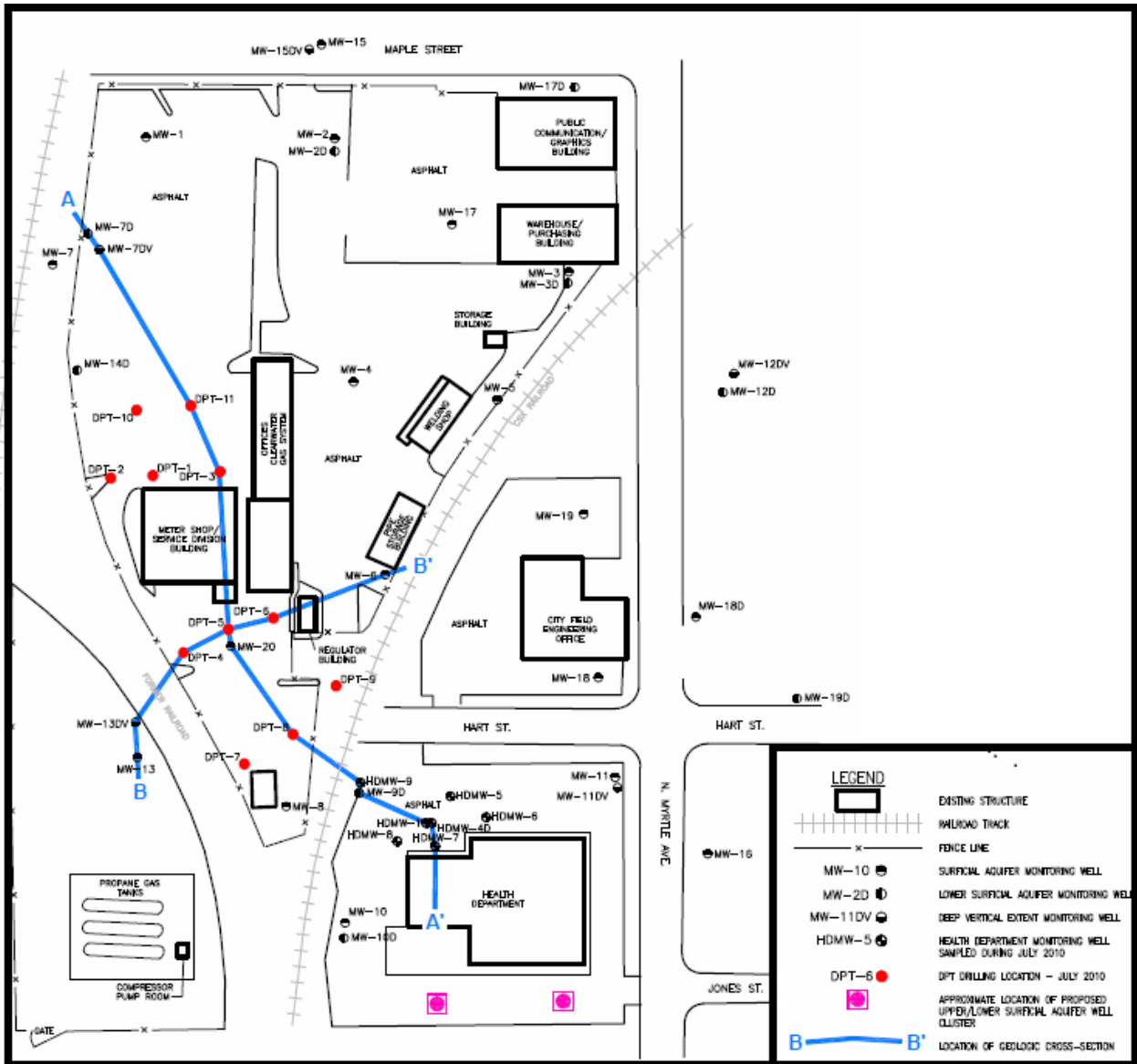


Figure 1.2 Previous installations at the former Clearwater MGP site.

Table 1.3. Summary of previous site investigations.

Year	Work Completed	Purpose	Report
1996	Installation of Test Trenches (#1-31)	Determine site lithology	ECT 1996
	Installation of Boreholes (GP-1 through to 35)	Determine site lithology	ECT 1999
1999	Installation of monitoring wells (MW-7DV, MW-12DV, and MW-13DV)	Determine groundwater properties (pH, DO, etc.), and analyze for BTEX and PAH compounds	ECT 1999
2003	Installation of 3 deep monitoring wells (MW-7DV and MW-13DV)	Determine site lithology, estimate groundwater flow direction, determine groundwater properties (pH, DO, etc.), and analyze for BTEX and PAH compounds	ECT 2003
	Collection of smear zone and vadose zone soil samples	Analyze for VOAs and cyanide	ECT 2003
	Groundwater elevation	Groundwater direction	ARCADIS 2010a
	Groundwater sampling	Develop current data set	
	Groundwater sampling from HDMW-1, HDMW-5, HDMW-6, HDMW-7, and HDMW-8	Analyze for BTEX and PAH compounds to determine dissolved phase concentrations	ARCADIS 2010b
2010	Drilling at temporary well locations (DPT-1 to DPT-11)	Characterize lithology and source of dissolved impacts downgradient	ARCADIS 2010b
	Sampling at select DPT locations	Analyze for BTEX and PAH compounds to determine dissolved phase concentrations	ARCADIS 2010b

Table 1.4. Florida groundwater clean-up standards for site specific compounds.

Compound	GCTL	NADC	Units
BTEX			
Benzene	1	100	ug/L
Ethylbenzene	30	300	ug/L
m-Xylene & p-Xylene	20	200	ug/L
o-Xylene	20	200	ug/L
Toluene	40	400	ug/L
Trime thylbe nze nes			
1,2,3-Trimethylbenzene	10	100	ug/L
1,2,4-Trimethylbenzene	10	100	ug/L
1,3,5-Trimethylbenzene	10	100	ug/L
PAHs			
1-Methylnaphthalene	28	280	ug/L
2-Methylnaphthalene	28	280	ug/L
Naphthalene	14	140	ug/L
Acenaphthene	20	200	ug/L
Acenaphthylene	210	2100	ug/L
Anthracene	2100	21000	ug/L
Benz [a] anthracene	0.05	5	ug/L
Benzo [a] pyrene	0.2	20	ug/L
Benz [b, k] fluoranthene	-	-	ug/L
Benzo [g,h,i] perylene	210	2100	ug/L
Biphenyl	0.5	50	ug/L
Carbazole	1.8	180	ug/L
Chrysene	4.8	480	ug/L
Dibenzofuran	28	280	ug/L
Fluoranthene	280	2800	ug/L
Fluorene	280	2800	ug/L
Indole	-	-	ug/L
Indeno[1,2,3-c,d] pyrene +	-	-	ug/L
Dibenz [a,h] anthracene	-	-	ug/L
Phenanthrene	210	2100	ug/L
Pyrene	210	2100	ug/L

Notes:

GCTL - FDEP Groundwater Cleanup Target Level

NADC - FDEP Natural Attenuation Default Concentration

Chapter 2

Enhancement of the Conceptual Site Model

2.1 Field Activities

Additional characterization of the site was required to enhance the existing conceptual site model (CSM) described in Chapter 1. Four site visits were conducted starting in March 2011 to complete focused site characterization tasks. This work included delineating the spatial extents and architecture of the MGP residuals, confirming groundwater flow direction and magnitude, and collecting soil cores to support the bench-scale efforts. A summary of the fieldwork completed and objectives are provided in Table 2.1. The site-wide monitoring well and borehole locations are shown on Figure 2.6. Full descriptions of site work completed are located in Appendix A.

2.2 General Stratigraphy

The site lithology was characterized by the installation of 24 additional boreholes. The installations were completed using direct-push technology (DPT) and boreholes were named DPT-# in the order of their installation, starting at DPT-12. In general the site lithology is comprised of a surficial sand and silt unit which sits on an olive green colored confining clay unit underlain by weathered limestone. The clay unit is encountered at a depth of between 6 and 12 m (20 and 40 ft) bgs, slopes west to south-west, and is ~3 m (10 ft) thick. The buff-coloured limestone unit extends to at least 15 m (50 ft) bgs. At borehole 27A, (DPT-27A) (Figure 3.1), a depression in the clay unit extends to 24 m (81 ft) bgs. The surficial aquifer is characterized as a fairly uniform fine to very fine grained sand. Horizontal laminations on the millimetre scale, organic silt nodules, organic muck, and tree rootlets are occasionally present (ARCADIS, 2010a).

2.3 Grain Size Distribution

Particle size distributions were determined by conducting grain size analyses on selected sediment samples. The purpose of these analyses was to provide an estimate of hydraulic conductivity. Sediment samples were chosen based on differences in color, composition, and texture as reported in the borehole logs.

A total of 32 samples were analyzed (Appendix B, Table B.2) using standard methods (ASTM D 422: Standard Test Method for Particle-Size Analysis of Soils; and ASTM D 6913: Particle Size Distribution of Soils Using Sieve Analysis). Samples were sieved using standard ASTM sieve sizes 10, 20, 40, 60, 100, 140, and 200. Grain size distribution curves were developed on a semi-log plot of the cumulative

percent passing each sieve versus the sieve mesh size. Figure 2.1 shows the grain size distributions for three samples, DTP-6 at 2.7 m (9 ft) bgs, DPT-18 at 7.6 m (25 ft) bgs and DPT-2 at 7 m (23 ft) bgs. The grain size distribution for DPT-18 and DPT-2 represent the envelope for all the other distributions determined while the distribution for DTP-6 represents the average distribution observed. In general, these distributions indicate that the sediments are very well-sorted or poorly graded, and are composed mostly of fine to medium sand, with some silt. There is little variability in the sediment grain size distribution across the site.

Using the grains size distributions, the hydraulic conductivity was estimated used the Hazen equation (Hazen, 1893)

$$K = Cd_{10} \quad (2.1)$$

where K is hydraulic conductivity in cm/s, d_{10} , the value where 10% of the sediment sample is finer, and C is a dimensionless coefficient that factors in the sorting characteristics of the sediment and was obtained from the grain size distributions. Hazen's equation was chosen since it is ideal for sand-sized sediment and is widely accepted (Eggleston and Rojstaczer, 2001). Since the grain size distributions have little variability, a C value of 50 indicating a well-sorted, mostly fine sand, was deemed to be appropriate for all samples.

Hazen's equation yielded hydraulic conductivity estimates ranging from 5.0×10^{-3} to 1.1×10^{-2} cm/s, with a harmonic mean ($n = 32$) of 8.0×10^{-3} cm/s. Vertical hydraulic conductivity profiles are shown in Figure 2.2 for DPT-13, DPT-17, and DPT-27. These data indicate the relative homogeneity in hydraulic conductivity with respect to depth.

2.4 Hydrogeology

2.4.1 Permeability

Falling-head permeameter tests were conducted at the University of Waterloo on the 32 sediment samples (Appendix B, Table B.2) using standard methods (ASTM D5084-10 Standard Test Methods for Measurement of Hydraulic Conductivity of Saturated Porous Materials Using a Flexible Wall Permeameter). The hydraulic conductivity estimated range from 4.0×10^{-3} to 1.1×10^{-2} cm/s with a harmonic mean of 8.0×10^{-3} cm/s. The results are consistent with the hydraulic conductivity values estimated from the grain size distributions (Figure 3.2). Full results for all sediment samples are given in Appendix B (Table B.2).

2.4.2 Porosity

Sediment porosity was estimated by standard methods (ASTM D5084-10 Standard Test Methods for Measurement of Hydraulic Conductivity of Saturated Porous Materials Using a Flexible Wall Permeameter). The estimated porosity varied from 0.30 to 0.39 with an average of 0.34 ± 0.03 (SD). Complete results are given in Appendix B (Table B.2).

2.4.3 Slug Tests

On November 2, 2011 rising and falling-head slug tests were performed on monitoring wells (MW) 7D, 23D, 24D and 25, where the D denotes lower surficial monitoring well (MW-7D, MW-23D, MW-24D, and MW-25). Tests were conducted using a slug constructed from 1 inch inner diameter PVC pipe (2.0 ft long, 1.315 inch outer diameter, volume of 0.22 ft^3) filled with sand and capped at both ends. A static water level reading was taken prior to commencement of each test. Following this initial measurement, a pressure transducer (HOBO™; U20; 69 to 207 kPa ($\pm 0.3\%$ FS, 0.62 kPa); 0° to 40°C (± 0.03)) U2) programmed to record pressure readings every second was deployed. The slug was then inserted into each well and left until a static water level was re-achieved and then removed until water levels returned to static conditions again. Slug tests were performed in triplicate in each well.

Figure 2.3 shows pressure profiles, for one slug test, in each well as captured by the pressure transducer during the slug tests. The profiles illustrate a quick hydraulic response for tests performed at MW-23D, MW-24, and MW-25. However, the test performed at MW-7D was significantly slower in response indicating that the screened interval for this well is in material with a lower hydraulic conductivity, possibly the underlying clay unit.

To interpret the collected slug test data, Hvorslev's method (1951) was chosen since it can be used in both confined and unconfined aquifers under a variety of well geometric and aquifer conditions. Additionally, site characterizations conducted in predominately sand environments have shown reliable and consistent estimates (Mes-Pla et al., 1997). The method makes use of some simplifying assumptions including homogeneous isotropic soil characteristics, "infinite" aquifer thickness, a horizontal potentiometric surface, negligible specific storage, and a finite effective radius (Bair and Lahm, 2006). However, since the slug test effective radius and hydraulic head differential is small the assumptions made with this method is not likely to produce erroneous results (Chirlin, 1989). The estimate of

hydraulic conductivity using Hvorslev's method is determined from

$$K = r^2 \ln\left(\frac{L}{R}\right) 2LT \quad (2.2)$$

where K is hydraulic conductivity in cm/s, r is the radius of the well casing in cm, R is the radius of the well screen in cm, L is the length of the well screen in cm, and T is the time it takes for the water level to rise or fall 37% of initial perturbation in seconds. Well construction details (Appendix B, Table B.3) and other information were taken from previous site assessment reports.

The Hvorslev method uses only rising-head data in the computation. Therefore, for the rising head results, pressure differences were plotted versus time on a semi-logarithmic scale. The straight-line portions of these plots were used to determine the time at which a 37% change from the initial hydraulic head occurred and used in Eq (1.2). Results from the Hvorslev analysis are given in Table 2.3. The results of the Hvorslev's analysis yielded a pooled harmonic mean of hydraulic conductivity of 2.3×10^{-3} cm/s with a standard deviation of 6.0×10^{-4} cm/s.

The average K estimate for MW-7D was 1.0×10^{-4} cm/s. This value is an order of magnitude lower than the other estimates. Upon review of the well construction log it was determined that a portion of the MW-7D well screen is in the clay unit and that during well development the "flow was very slow". Since MW-7D is not fully located in the sand and the response times are significantly different than the response times from the other three wells, it was decided that the results from the slug test performed on this well do not reflect the hydraulic conductivity of the surficial sand unit.

Note that this slug test hydraulic conductivity estimate (2.3×10^{-3} cm/s) is lower than the hydraulic conductivity estimated from the grain size distribution (8.0×10^{-3} cm/s) and permeameter tests (8.0×10^{-3} cm/s) (Figure 2.2). The use of grain size results often overestimate hydraulic conductivity since homogeneity is assumed, whereas in the field preferential flow paths may exist and *in situ* compaction can occur reducing hydraulic conductivity (Eggleston and Rojstaczer, 2001).

2.4.4 Groundwater Flow and Travel Time

Pressure transducers (HOBO™; U20; 69 to 207 kPa ($\pm 0.3\%$ FS, 0.62 kPa); 0° to 40°C (± 0.03)) were deployed in MW 7D, MW 23D, MW 24D, and MW 25 to collect data to estimate groundwater flow direction and magnitude. The pressure transducers recorded water pressure (kPa) and groundwater temperature (°C) hourly from March 2011 to February 2012.

Hourly atmospheric pressure data were obtained from National Oceanic and Atmospheric Administration sources (NOAA, 2012) for Clearwater, Florida (latitude of 27.98 N and longitude of 82.83 W). The transducer pressure observations were subtracted from the atmospheric pressure measurements and converted into height of water in meters. The top of well casing elevations from a Site survey performed in 2011 and the adjusted transducer data were used to determine the water elevation (ft amsl) at each well location. Fluctuations in water elevation and temperature were similar for all the wells. Figure 2.4(a) illustrates the fluctuations in water elevation and temperature observed in MW-7D. Results for all wells are located in Appendix B (Figure B.1).

A triangular discretization approach was used to calculate two hydraulic gradients (Pinder et al., 1981). Straight lines were used to connect transducer locations to form two triangles, and two plane surfaces were fit through the observed hydraulic head values. The slope of the resulting planes is taken to be the hydraulic gradient.

Monitoring wells MW-23D, 24D and 7D formed the upper triangle and MW-24D, 23D and 25 formed the lower triangle. Over the year, the calculated hydraulic gradients varied 0.0028 to 0.0036 m/m with a bearing that varied between 153° and 168°. The average hydraulic gradient was estimated to be $3.3 \pm 0.27 \times 10^{-3}$ (SD) for the lower triangle, and $2.9 \pm 0.14 \times 10^{-3}$ (SD) for the upper triangle, both in a direction of S23°E $\pm 0.2^\circ$. Figure 2.4(b) illustrates the temporal variation in gradient and bearing.

Groundwater velocity was estimated from

$$v = Ki/n \quad (2.3)$$

where v is the groundwater velocity (m/day). Using the average of the two interpolated hydraulic gradients ($i = 0.03$), and a hydraulic conductivity (K) of 2.3×10^{-3} cm/s, and a porosity of 0.34, the average groundwater velocity was determined to be 1.93 ± 0.51 (SD) cm/day (~2 cm/day). Considering this velocity and the area of the site, travel time estimates from MW-20, where groundwater impacts have been seen (Section 1.4), to the Health Department property (HDMW-9), a distance of approximately 60 m (~200 ft), would be 3000 days. Given that the former MGP was operating in 1924, calculations estimate migration distances of roughly 640 m at the time of publication.

2.5 MGP Source Material

The previously installed boreholes (DPT-1 through to 11) indicated a limited aerial extent of source material within the surficial aquifer that is suspected to be contributing to the groundwater plume. To further characterize this source and determine the existence of other sources, borings DPT-11 through to

35 were installed. MGP residuals in the form of sheens, blebs (isolated pore spaces containing NAPL), stringers (a small channel of NAPL, independent or occurring as a branch), and pockets of tar (Figure 2.5) were observed throughout much of the surficial aquifer. In total, visual impacts were observed in 15 of the 35 DPT borings completed (Table 2.4).

The following observations are noted:

- a sandy zone above the clay contact (7.3 m (24 ft) bgs) at boring DPT-1 contained an approximate 7.6 cm (3 inch) thick lense of non-aqueous phase liquid (NAPL)-saturated material, which was observed at the top of the clay contact.
- Boring DPT-12, north of the Meter Shop contained a NAPL lens at 6.5 m (21.2 ft) bgs and NAPL pooling was noted on a lense at 6.7 m (22 ft) bgs at the sand/clay contact.
- Boring DPT-13, located north of the Meter Shop contained discrete lenses of NAPL-saturated material in sands within a few feet above the clay unit; but no NAPL was present at the sand/clay interface.
- At boring DPT-14 NAPL stringer and residual tar in pores was observed between 4.5-6 m (15-20 ft) bgs and NAPL was observed to fully saturate pores between 7.5 to 9.0 m (25 to 30 ft) bgs.
- Inclined boring DPT-18 encountered a tar saturated lens at 9.5 linear meters (31 ft); ~0.6 m (2 ft) above the sand/clay contact.
- At DPT-30 NAPL blebs were observed from 9.4 to 9.8 m (30.8 to 32 ft) bgs, and NAPL lenses were present at 10.7 m (35.1 ft) bgs.
- Residual NAPL blebs were observed in sandy zones at 5.2-6 m (17-20 ft) bgs at DPT-5, ~0.5 m (1.5 ft) above the clay contact (6.5 m (21.5 ft) bls)
- At DPT-29 NAPL lenses were observed between 5.7 to 5.8 m (18.6 to 19.1 ft) bgs.

Other observed impacts, such as staining and sheens, were noted near the water table in DPT borings: DPT-7, DPT-11, DPT-20, DPT-24, and DPT-31.

The spatial extents of the residual MGP source material were estimated from the borehole logs, however, the complete geometry of these zones are not fully defined. Since the cross-sectional areas perpendicular to flow were approximately ellipses (Appendix B, Figures B.2 and B.3) and the depth of each source zone varied longitudinally, the equation for the volume of an ellipsoid was used for estimation of source zone volumes (Table 2.5). Major and minor axes of the ellipse were estimated from borehole logs and the vertical axis was taken to be the maximum depth of observed impact. Above 4.5 m bgs (< 15 ft) (shallow) there appear to be three source areas, with a major zone south of the Meter Shop (Figure 2.6). The volume of this source zone was estimated to be 85 m³ and a cross-sectional area of 42 m² parallel to groundwater flow. Below 4.5 m bgs (>15 ft) (deep) (Figure 2.7) there appear to be three impacted areas with the major source zone immediately northwest of the Meter Shop. The largest source

area encompasses DPT-1, -12, -13, -14, -29, and -30 is estimated to have a volume of 36 m³ and a cross-sectional area parallel to groundwater flow of 22 m². In total there is estimated to be 193 m³ of source zone on site.

2.6 Source Material Concentrations

During the borehole installation at DPT-23, two sediment samples were taken, one at a depth of 3-3.5 m (10-11.5 ft) and one at a depth 6 m (20 ft). Samples were placed in jars, put on ice, and shipped to the University of Waterloo for BTEX and PAHs analyses (EPA methods 8260 and 8270, respectively). This borehole was chosen since it had visual impacts in both shallow (<4.5 m) and high zones (>4.5 m) in the aquifer. Triplicate samples were taken at each sample depth and results (Appendix B, Table B.5) from the analyses were averaged (Table 2.2). There were no significant differences between the average compositions of the two samples at the 5% significance level (Appendix B, Tables B.5 and B.6).

Results from the composition analyses showed that of the detectable compounds, naphthalene was the most prevalent (27%), followed by 2-methylnaphthalene (18%), and 1-methylnaphthalene (10%). It is difficult to compare the concentrations of the contaminants in the soil phase with other studies since these measurements can differ up to an order of magnitude due to geological and hydrogeological conditions, the amount of weathering, MGP operations, and feedstock.

In order to determine the individual constituents in the NAPL, samples of free phase source material from DPT-23 at 3.04 m (10 ft) were sent to an external lab (ALPHA Analytical, Westborough, MA). Analyses for alkylated PAHs (EPA 8270C-SIM) and saturated hydrocarbons (EPA8015D) were completed (Table 2.6). Approximately 30% of the constituents in the coal tar were identified. Of these constituents naphthalene was the most prevalent (7%), followed by 2-methylnaphthalene (5%) and 1-methylnaphthalene (3%).

The composition of coal tars has been shown to be highly variable (on orders of magnitude) between sites (Brown et al., 2006). Data obtained from coal tars from 11 different MGP sites (Brown et al., 2006) and from four water-gas sites (Birak and Miller, 2008) were compiled (Table 2.7). The Clearwater site NAPL concentrations fall in the ranges observed by Brown et al. for all compounds except for naphthalene and benzo[g,h,i]perylene where results were above the observed range. Birak and Miller's results do not fit as well with the Clearwater NAPL data; Indeno[1,2,3-c,d] Pyrene + Dibenz [a,h] Anthracene, chrysene and benz[a]anthracene all fall below their observed ranges. Additionally, naphthalene again falls above the observed range. Across all data sets naphthalene was the most prevalent

constituent followed by 2-methylnaphthalene and 1-methylnaphthalene. The wide range of concentrations in coal tar, and the difficulty and variation associated with determining its individual compounds illustrate the importance of site specific characterization, remediation efforts, and clean-up targets.

2.7 Dissolved Phase Concentrations

Ten multilevel wells were installed evenly spaced in 2.7 m (9 ft) intervals to form a 27.7 m (91 ft) transect that spans the width of the dissolved phase plume (Figure 2.7 for location). The transect was oriented at approximately N65°E which, based on previous water level measurements taken at the site, represents a line that is approximately perpendicular to the mean groundwater flow (Section 2.4.4). Multilevel wells were selected since they are capable of providing discrete groundwater samples from various depths within a single borehole installation. Ports were evenly spaced every 0.67 m (2.2 ft) beginning at the groundwater table and extending to the clay unit (Figure 2.8). The multilevel wells were denoted ML 1-# to ML10-#, where the # indicates the sampling port as numbered from 1 to 10, starting at the groundwater table. Additional information on the design and location of the multilevel wells installed are given in Appendix A. This installation allows for the determination of baseline conditions in concentration and morphology of the dissolved phase plume, estimation of the mass loading of COC from the source area to the groundwater plume, and measurements of geochemical parameters.

Four additional multilevel wells were installed inside the meter shop building (Figure 2.7). Sampling ports were spaced every 1.5 m (5 ft) and the wells were denoted ML 11-# through to ML 14-#, where the # was 5,10,15, or 20 to indicate the depth of the port. These multilevel wells were required to determine the dissolved phase concentrations underneath the meter shop due to the source zone discovered upgradient.

2.7.1 Cation/Anion Scan

Samples were taken from ML1-1, ML5-5, and ML 5-7 and sent to an external laboratory (ALS, Waterloo, ON) to be analyzed for dissolved ions. Total alkalinity (EPA method 310.2) measurements, an anion scan (EPA method 300.0), and a total metal scan (EPA method 200.8) were completed. Relevant results from the general ion scan are given in Table 2.8. The observed sodium concentrations were high due to the addition of the biocide sodium azide that was added to all samples in the field. Dissolved total iron concentrations varied from 1.5 to 4.2 mg/L which may be naturally occurring or associated with iron-cyanide complexes (cyanide has been observed in samples from MW-5, MW-8, MW-20, and HDMW-9). Also, sulfate was the most abundant anion. This abundance is most likely associated with the gas and

liquor purification process at MGP sites where sulfur was released (Hatheway, 2010). Low dissolved oxygen levels (Appendix B, Table B.7), coupled with high iron and sulfate concentrations and low nitrogen are indicative of anaerobic conditions (Christensen et al., 2000). PAHs have shown to be persistent under these conditions (Mihelcic and Luthy, 1988), however benzene degradation is common (Edwards and Grbic-Galic, 1992).

2.7.2 BTEX and PAH Concentrations

In order to characterize the morphology and concentrations of the dissolved phase plume across this transect, three sampling episodes were conducted. Duplicate samples were taken from each multilevel port using a sampling glass vial (40 mL) placed between the multilevel port and a peristaltic pump. For sample collection, the glass vial was fitted to an in-line, stainless steel screw cap sample head. Several (2-3) groundwater volumes of the vial were passed through before the vial was detached from the sample head in order to prevent losses due to volatilization. Samples were preserved with sodium azide (0.4 mL of 10% solution), sealed with PTFE lined screw caps, and preserved in coolers with ice. All collected samples were shipped on ice to the University of Waterloo where they were stored at 4 °C and held for less than 14 days prior to analysis. Analyses of BTEX and PAHs were performed using gas chromatography techniques and methods in the Organics Laboratory at the University of Waterloo (see Freitas and Barker (2008) for details).

Results from the BTEX and PAH analyses for three sampling episodes are provided in Appendix C. Duplicate samples analyzed were checked to ensure variation of < 50%, which is indicative of sufficient error control during sampling (Barcelona et al., 1985). The first sampling episode was the only episode to yield values not meeting this criterion (Appendix F, Tables F.1 to F.3). Two sets of duplicate samples were calculated to be outside this range. These sample measurements were compared with measurements from sampling episodes 2 and 3. From this comparison, the measurements that fell outside the 50% range observed in episodes 2 and 3 was assumed to be erroneous and discarded. Using the resulting data, iso-concentration profiles (Figures 2.9 to 2.14) were created (above the natural attenuation default criteria (NADC) levels) along the ML transect. Iso-concentration contours for all monitored compounds are given in Appendix C (Figures C.1 to C.6).

In general, plume morphologies remain relatively constant over across the sampling periods. The highest concentrations were generally centered laterally around ML-5 for most quantified compounds. BTEX compounds were observed close to the water table, while trimethylbenzenes were predominately in the center of the aquifer, and PAHs were concentrated near the clay unit.

The following observations are evident from the iso-concentration figures:

- The core of the benzene plume is consistently near the water table, with a maximum observed concentration of 17000 ug/L, during the first sampling episode. The location of the maximum concentration does not change with time (remains at ML5-2) however, decreases in concentration are observed (15000 ug/L and 13000 ug/L) in sampling episodes 2 and 3 respectively.
- Ethylbenzene exhibits peak concentrations during sampling round 1 at ML-10 near the water table. It should be noted that during sampling round three no data was reported at this location since the port was dry from lowering of the water table.
- The morphologies of the BTEX plumes are all relatively similar. The center of mass of these plumes at the water table, between ML-4 to ML-6, except for ethylbenzene, which has a center of mass at ML-10.
- The naphthalene plume is more widespread across the monitoring transect relative to the benzene plume with multiple locations of elevated concentrations. The lateral extent and average concentration remained relatively constant.
- The trimethylbenzene plumes all have similar morphologies with a center of mass at ML-10 and few changes occur over the sampling periods for these compounds.
- Both the 1-methylnaphthalene and 2-methylnaphthalene plumes at the monitoring transect have increased in concentration over time. However, the lateral extents have not changed significantly.
- Concentrations of the BTEX plumes at the monitoring transect have not changed significantly over time. The lateral extents have not changed significantly except for toluene, P,M-xylene and O-xylene where these plume have appeared at ML-3 and no longer observed at ML-10.
- Observed acenaphthalene concentrations above the NADC at the monitoring transect have been minimal and only slight temporal variations have been observed.
- The concentrations of the remaining monitored compounds were all reported below NADC levels, except for benz(a)anthracene. Measurements in sampling episodes 1 and 2 each had one measurement (ML5-1) where benz(a)anthracene concentration exceeded NADC levels.

Figures 2.15 to 2.21 show COC concentration profiles for selected the MLs in the Meter Shop. COC profiles remain consistent along ML-3, ML-5, and ML-8 with the exception of benzene. Surprisingly,

the COC profiles along ML-14 are relatively lower compared to ML-11, ML-12 and ML-14. ML-14 is upgradient of ML-11 and ML-12 and downgradient of the NAPL impacted area to the north of the Meter Shop.

2.8 Mass Discharge

Mass discharge is a crucial parameter to measure remediation performance (ITRC, 2010). Initial mass discharge provides a baseline estimate of the strength of the source zone which can later be compared to post-remediation mass discharge to assess performance. The total mass discharge (mg/day) crossing the monitoring transect for each of the COC was estimated using:

$$\dot{M} = \sum_{i=1}^n C_i q_i A_i \quad (2.4)$$

where A_i is a subarea of the transect (m^2), defined as the midpoint point between measurement locations; C is the concentration in the defined area (mg/m^3); and q is the specific discharge (m/day) through area A .

Specific discharge (m/day) was calculated from $q = Ki$ where K is the hydraulic conductivity (m/s) and i is the hydraulic gradient (unitless). An average hydraulic conductivity from the slug tests (Section 2.4.3) was used for this calculation. The assumption of an average hydraulic conductivity for the entire site is based on the homogeneity seen in the soil samples during the permeameter and grain size analyses (statistical analyses of the results of these tests determined the samples to not be significantly different at the 95% confidence level). The hydraulic gradient was estimated as described in Section 2.4.4. A_i was assumed to be a rectangle with dimensions equal to half of the distance between sampling points for both lateral and longitudinal directions. For ports on the perimeter of the transect, lateral distances were determined as those for inner ports, however vertical distances were calculated as half the distance to the next port plus the distance from the port to the boundary.

Results from mass discharge calculations (Table 2.9) indicate that naphthalene has the highest average mass discharge (44 mg/day), followed by the BTEX compounds (9.1, 3.1, 12.5 and 7.1 mg/day for benzene, toluene, ethylbenzene and p,m-xylene, respectively). These values represent the initial conditions at the site and, as the project continues, they will be used as the baseline for comparison during and after *in situ* treatment.

Overall, differences in mass discharge between all three sampling episodes were relatively insignificant at the 5% significance level (Appendix B, Table B.8). However, sources of error and uncertainty can exist with this method of calculating mass flux. Calculation uncertainty is possible since the transect only captures discrete points and interpolation between points could be erroneous depending on the temporal

variability within the aquifer. However, it has been estimated that by sampling 6-7% of the groundwater, an appropriate estimate of mass discharge is obtained (Li et al. 2007), which was achieved in each sampling episode (~7%). Additionally, for relatively homogeneous aquifers, concentration variations can create uncertainty. It was found that sample ports spaced 30 cm apart in an aquifer with an aged (decades) DNAPL source zone had samples vary by more than three orders of magnitude in concentration (Guilbeault et al., 2005).

2.9 Current Conceptual Site Model

The site conceptual model resulting from the field investigations and laboratory experiments is described in the following paragraphs. This model provides information for the design and implementation of bench-scale testing (Chapter 3) and full-scale remediation (future work).

The site lithology is spatially consistent and is composed of a fine to very fine sand ($K = 2.3 \times 10^{-3} \pm 6.0 \times 10^{-4}$ cm/s (SD) and a porosity of 0.34 ± 0.03 (SD)). The water table exists at approximately 1.5 m bgs and a clay layer underlying the aquifer exists at 7.5 m bgs, with the exception of a depression at DPT-27A, where the clay unit is encountered at 25 m bgs.

Dissolved iron concentrations above NADC levels (3 mg/L) were observed in groundwater samples and assumed to be natrogenic or associated with iron-cyanide complexes since low levels (below NADC) of cyanide have been observed. Additionally, low measurements of dissolved oxygen indicate anaerobic conditions within the aquifer.

Three shallow (< 4.5 m bgs) source zones exist in the aquifer: upgradient of MW-20, southeast of the meter shop; upgradient of the metershop encompassing DPT-1, -14, and -29; and surrounding DPT-11. These three sources are estimated to have a cumulative volume of 153 m^3 . Three deep source zones were identified: surrounding DPT-1, -12, -13, -29, and -30; northwest of the meter shop, at MW-26; and underneath the southwest corner of the meter shop. It is estimated that a total source volume of 39 m^3 exists in the deep portion of the aquifer. Uncertainty exists in all estimates of source zone spatial extents since areas of contamination were interpolated between boreholes. Additionally, the spatial extents of the north-west corner of the shallow and deep source zones upgradient of the meter shop were approximated since the depth of the depression in the clay layer made comprehensive drilling infeasible due to time and cost constraints. Further, the extents of the south east corner of the shallow source zone were approximated because borehole installation was infeasible through the foundation of the metershop.

These uncertainties could provide erroneous estimates of source zone volumes, subsequent oxidant dosages, and anticipated clean-up target levels.

Based on calculations using transducer data, the aquifer has a Darcy flux of 0.0193 m/day (SD \pm 0.0051) in the direction of S20°E. This flux suggests that off-site migration of contaminants is likely. Sources of error associated with the velocity estimate are inherent in the assumption that hydraulic conductivity is homogeneous across the site. Even though lab tests validate this assumption, the overall site geology was generalized since stratigraphy was interpolated between boreholes. It is possible that areas of heterogeneity could exist with zones of higher or lower than estimated permeability. Lack of information on these zones could result in errors in the estimation of groundwater velocity and contaminant mobility. Additionally, uncharacterized heterogeneous zones could impact remediation goals since oxidant-contaminant interaction could be lower than anticipated in areas of lower than estimated permeability.

Highest concentrations of COC are observed downgradient of the source zones, specifically around ML-5. It is expected that these high concentrations are associated with the shallow source zone located south-east of the meter shop as it has a center of mass upgradient of ML-5. In general, BTEX plumes are predominately located at the water table, trimethylbenzene plumes are located between the water table and clay unit and PAH plumes are predominately located near the clay unit. The location and morphologies of these plumes indicate contamination exists at all depths within the aquifer. Therefore, the full-scale remediation design must deliver the oxidant to a variety of depths to maximize exposure to all COC.

Measured groundwater concentrations and calculations of mass discharge across the site provide baseline conditions for comparison following oxidant doses. However, it is important to note that while a representative sample size was used, concentrations between sample points were interpolated and may not be fully representative. Additionally, mass discharge was estimated assuming a constant Darcy flux across the entire site. While this assumption agrees with laboratory testing, it is possible that uncharacterized heterogeneous zones exist impacting the calculated mass discharge of contaminants.

To accommodate gaps in the conceptual site model, appropriate safety factors should be used when determining oxidant dosage amounts and calculations of contaminant mobility. Additionally, estimates of oxidant delivery, timeframes for remediation, and clean-up objectives should be calculated conservatively and monitored, re-evaluated, and altered as necessary throughout remediation efforts.

Table 2.1. Summary of field activities

Date	Work Completed	Purpose
Mar 7-11, 2011	Installation of additional boreholes (DPT-12 through to DPT-27)	Determine lithology and location and extent of MGP source material
	Collection of soil samples	Provide material for bench scale testing
	Collection of undisturbed core samples	Provide material for bench scale testing
	Collection of free NAPL	Determine NAPL composition
Jul 17- 22, 2011	Installation of additional monitoring wells (MW-23D, MW-24D, MW-25, MW-25D and MW-26)	Groundwater sampling and transducer deployment
	Deployment of Pressure Transducers	Estimate groundwater flow direction and magnitude
	Construction and installation of multi-level transect (ML-1 to ML-10)	Estimate aqueous mass discharge
	Construction and installation of multi-level wells in Meter Shop (ML-11, ML 12, ML-13, ML-14)	Determine dissolved phase concentration below Meter Shop
	Groundwater sampling of transect and Meter Shop multi-level wells	Determine dissolved plume concentrations for mass discharge estimate
	Download transducer data	Estimate groundwater flow direction and magnitude
Oct 31 - Nov 3, 20	Groundwater sampling of transect and Meter Shop multi-level wells	Determine dissolved plume concentrations for mass discharge estimate
	Download transducer data	Estimate groundwater flow direction and magnitude
	Completion of slug tests	Estimate <i>in situ</i> hydraulic conductivity
Feb 13 - 17, 2012	Groundwater sampling of transect and Meter Shop multi-level wells	Determine dissolved plume concentrations for mass discharge estimate
	Download transducer data	Estimate groundwater flow direction and magnitude

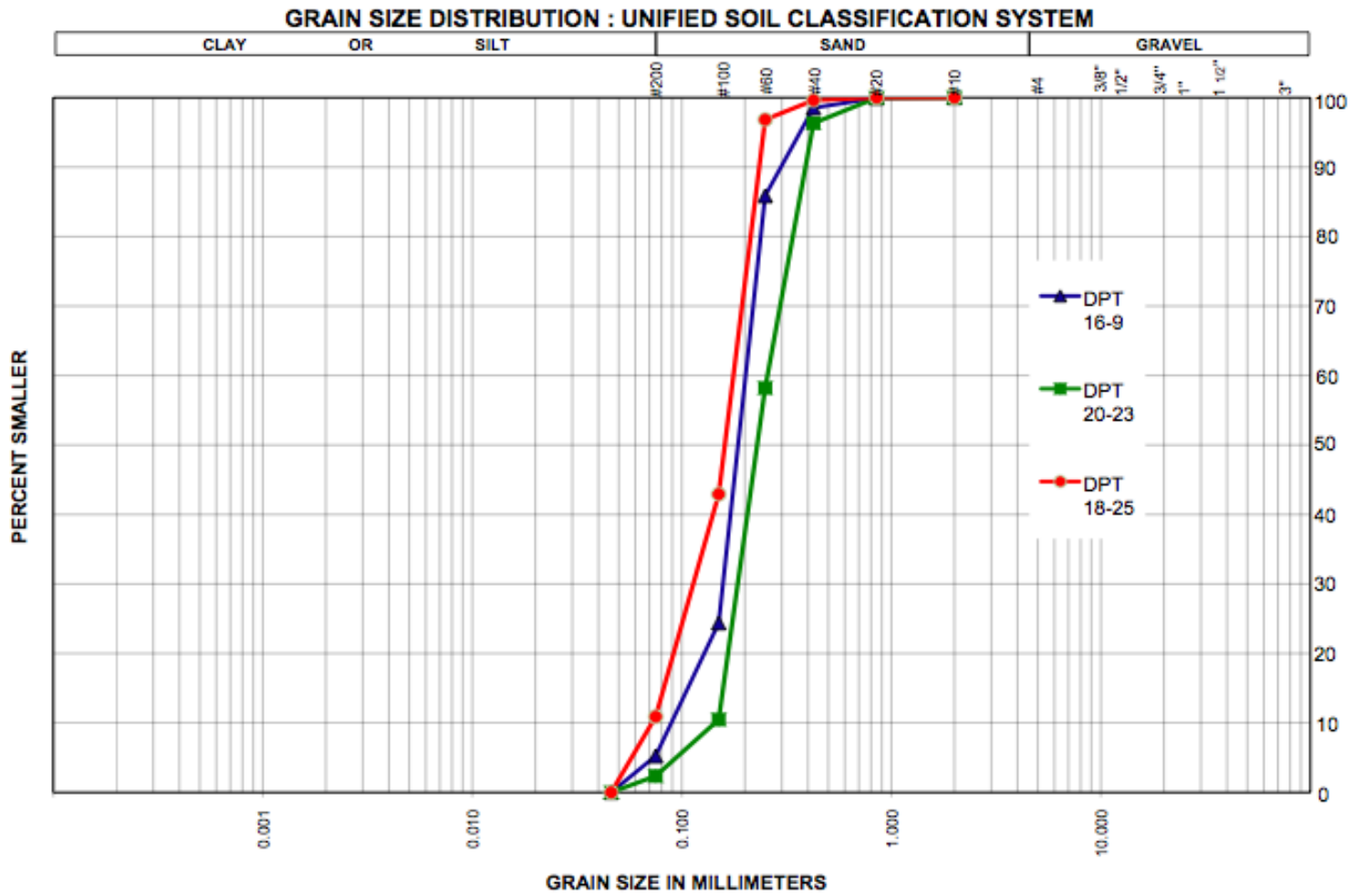


Figure 2.1. Particle size distribution for samples DTP 6 at 2.7 m (9ft) bgs, DPT 18 at 7.6 m (25 ft) bgs and DPT-20 at 7 m (23 ft) bgs.

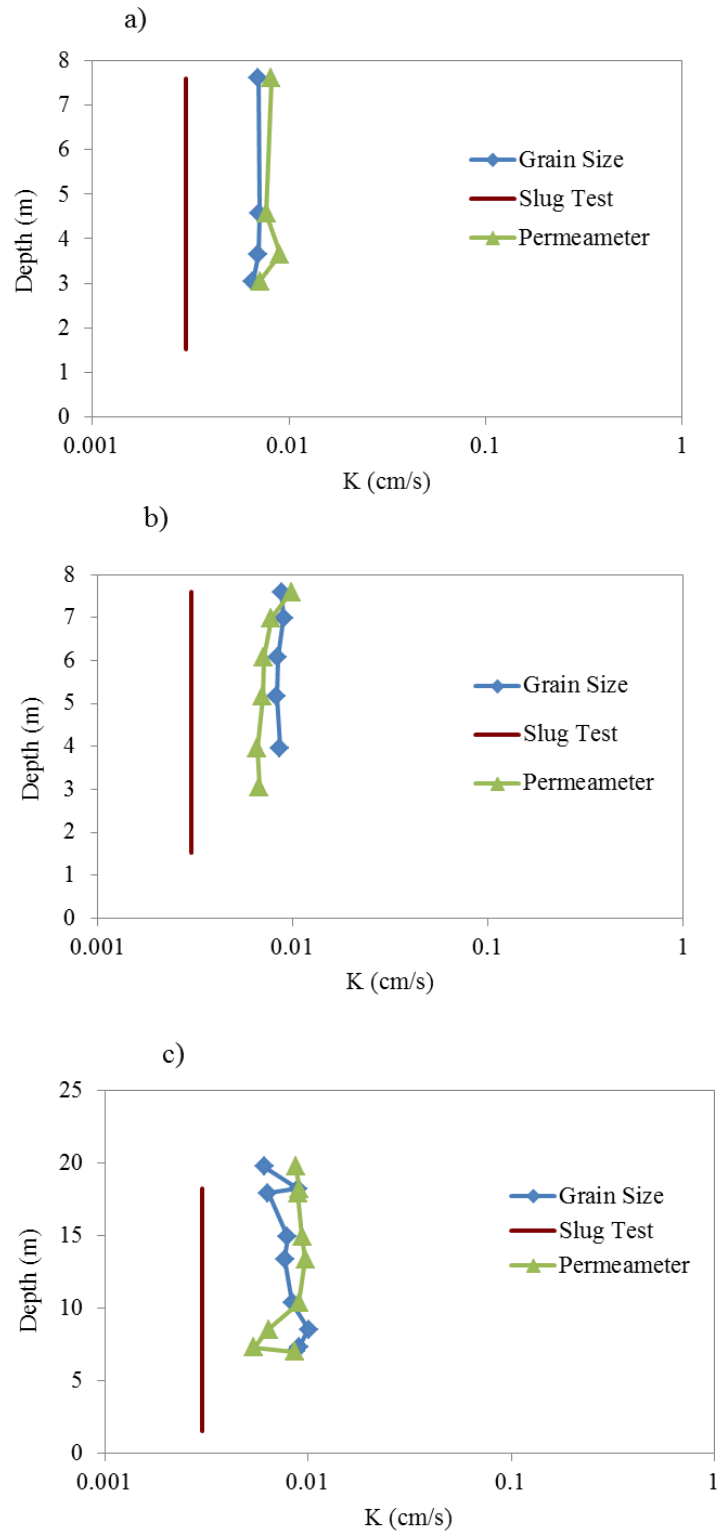


Figure 2.2. Hydraulic conductivity profiles at (a) DPT-13, (b) DPT-17 and (c) DPT-27.

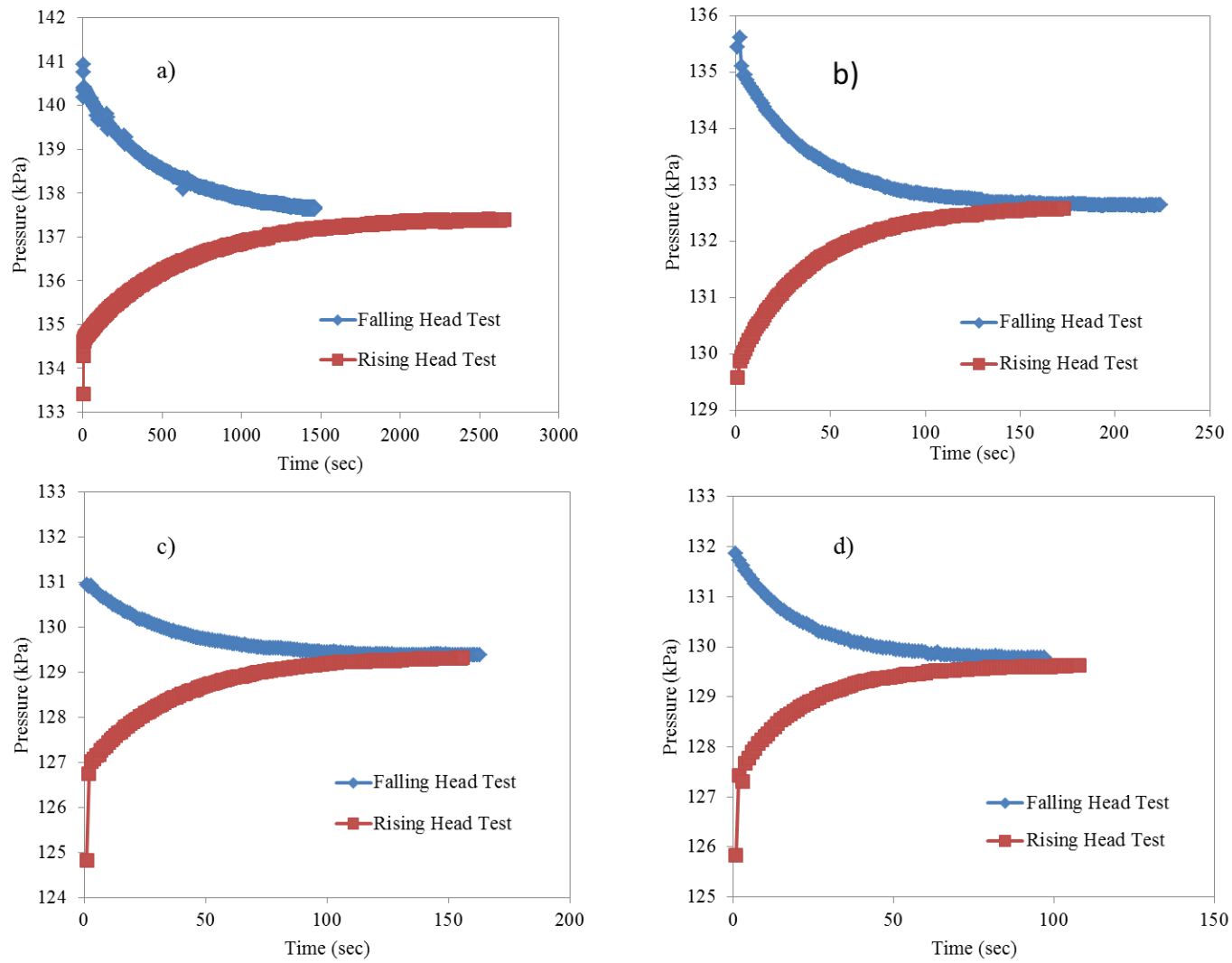


Figure 2.3. Pressure transducer response during a slug test performed at (a) MW-7, (b) MW-23D, (c) MW-24, (d) MW-25.

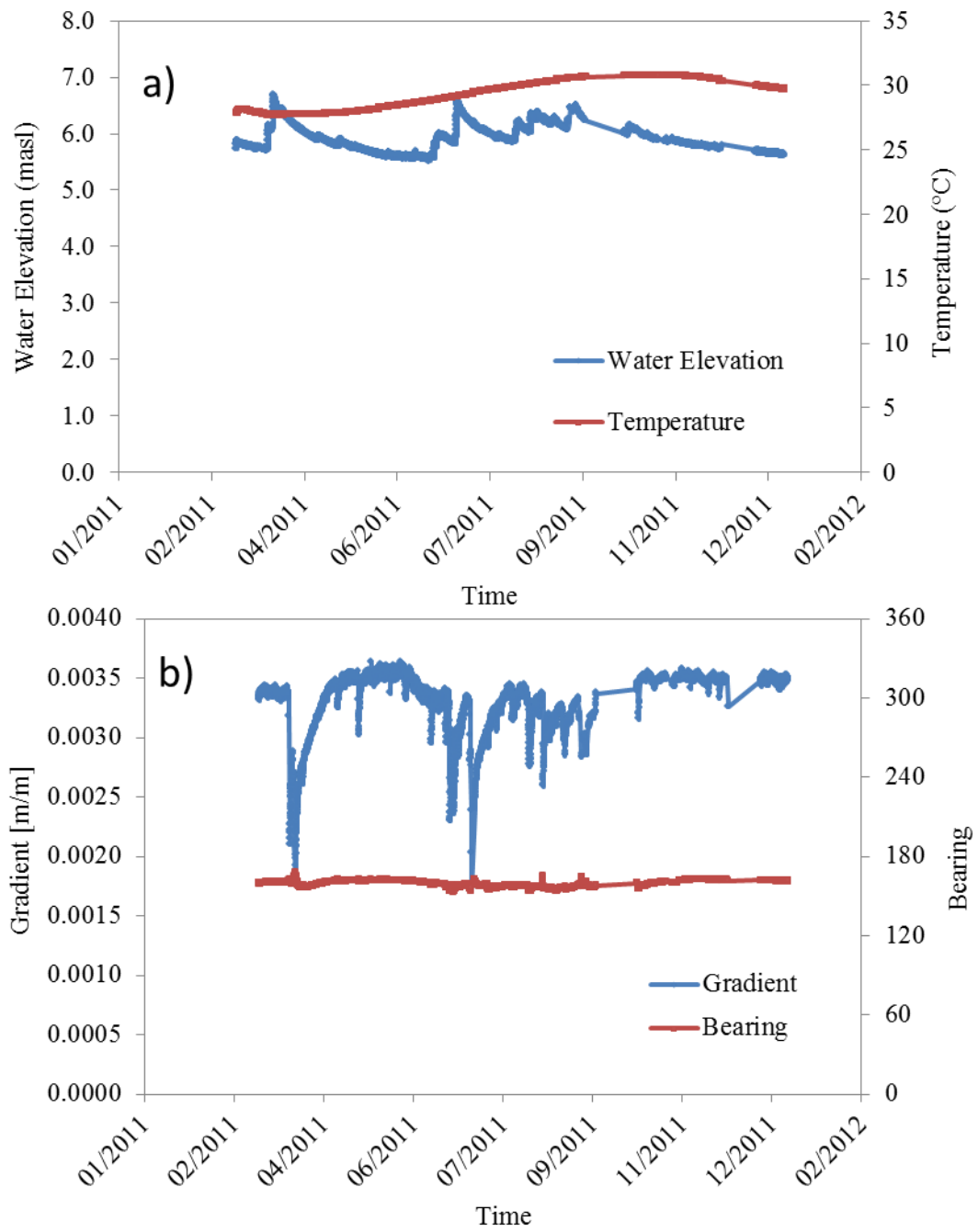


Figure 2.4. (a) Water elevation and temperature profile at MW-7D and (b) average hydraulic gradient and bearing for the site.

Table 2.2. Average measured concentrations of MGP compounds in aquifer material taken from DPT-23 at 0.9 m (3 ft).

Compound	Concentration (mg/kg)
BTEX	
Benzene	12
Toluene	75
Ethylbenzene	72
p,m-Xylene	110
o-Xylene	70
Trimethylbenzenes	
1,3,5-Trimethylbenzene	31
1,2,4-Trimethylbenzene	140
1,2,3-Trimethylbenzene	50
PAHs	
Naphthalene	960
Indole	9.7
2-Methylnaphthalene	670
1-Methylnaphthalene	390
Biphenyl	81
Acenaphthylene	130
Acenaphthene	57
Dibenzofuran	55
Fluorene	120
Phenanthrene	340
Anthracene	40
Carbazole	< MDL
Fluoranthene	82
Pyrene	140
Benz [a] anthracene	27
Chrysene	27
Benz [b] Fluoranthene +	
Benz [k]Fluoranthene	27
Benzo [a] Pyrene	21
Indeno[1,2,3-c,d] Pyrene	
+ Dibenz [a,h]	
Anthracene	3.6
Benzo [g,h,i] Perylene	6

Table 2.3. Slug test results.

Well	Test	T (sec)	K (cm/s)	Average (cm/s)	Standard Deviation (cm/s)
25	1	20	2.44E-03		
25	2	20	2.44E-03	2.48E-03	7.42E-05
25	3	19	2.57E-03		
24	1	20	2.44E-03		
24	2	17	2.87E-03	2.86E-03	4.07E-04
24	3	15	3.25E-03		
23	1	27	1.81E-03		
23	2	32	1.53E-03	1.56E-03	2.28E-04
23	3	36	1.36E-03		



Figure 2.5: NAPL saturated pores in DPT 23.

Table 2.4. Observed MGP impacts from borings.

Location	1.5-3 m (5-10 ft) bgs	3-4.5 m (10-15 ft) bgs	4.5-6 m (15-20 ft) bgs	> 6 m (>20 ft) bgs
DPT-1	NAPL blebs and stringers, sheens	trace black tar bleb	trace black tar blebs, stained patches	staining with tar blebs, strong odors, 3 inch zone of NAPL saturated sands on top of clay (24 ft)
DPT-5		staining, sheen streaks (throughout)	NAPL present in pores, heavy sheen, NAPL blebs (17-20)	
DPT-7		sheen streaks		
DPT-11	trace sheens			
DPT-12				NAPL lens (21.2 ft); NAPL pooling in lens (22 ft) at clay contact (22.1 ft)
DPT-13				Visible NAPL at discrete intervals from 25 to 26 ft; sheens from 26 to 28 ft; no NAPL at clay contact (29 ft)
DPT-14	staining and trace sheens; diesel odor	sheen throughout	NAPL stringers and residual tar in pores; NAPL pooling in indentations	NAPL fully saturate pores; present throughout (25 to 30 ft); NAPL at clay contact (32.5 ft)
DPT-18				Tar saturated lens, pore filled with NAPL (31 linear ft); no NAPL at clay contact (33.4 linear ft)
DPT-20	Light staining (2 ft)			
DPT-21	Tar and wood mix (3 ft)	Trace NAPL blebs		
DPT-23	Fully saturated with NAPL	NAPL saturated, heavy sheens (10 - 15 ft)	Saturated NAPL in pores at 19.4-20 ft	Moderate sheens (20 -21 ft); NAPL at clay contact (21 ft)
DPT-24	Some staining			
DPT-29	NAPL present in pores (5-7 ft)		NAPL lenses (18.6 - 19.1 ft)	
DPT-30				NAPL blebs (31 - 32 ft) NAPL lenses in sand horizon
DPT-31	Heavy sheen (3-5')	Sporadic sheen (6.8 - 8.1 ft)		

Table 2.5. Volume of NAPL source zones.

Source Zone	Zone	Location	Maximum Depth of Impact (m)	Major Axis (m)	Minor Axis (m)	Area (m ²)	Volume (m ³)
1	Deep	DPT-1, -12, -13, -14, -29, -30	2.5	7.6	3.6	22	36
2	Deep	DPT-23, MW-26	0.5	4.0	3.0	9.4	3.1
3	Deep	SW corner of Meter Shop	0.4	2.0	1.0	1.6	0.4
4	Shallow	DPT-14, -29, -31	3.0	7.0	6.0	33	66
5	Shallow	DPT-5, -20, -21, -23, -24, MW-26	3.0	9.0	6.0	42	85
6	Shallow	DPT-11	1.5	2.0	1.5	2.4	2.4

Notes:

Maximum depths of impact were calculated based on observed impacts from borings (Table 3.4).

Plume locations and major and minor axes are shown in Figures C.1 (deep) and C.2 (shallow).

Source values were calculated using the equation for the volume of an ellipsoid.

Area is the cross sectional area parallel to groundwater flow.

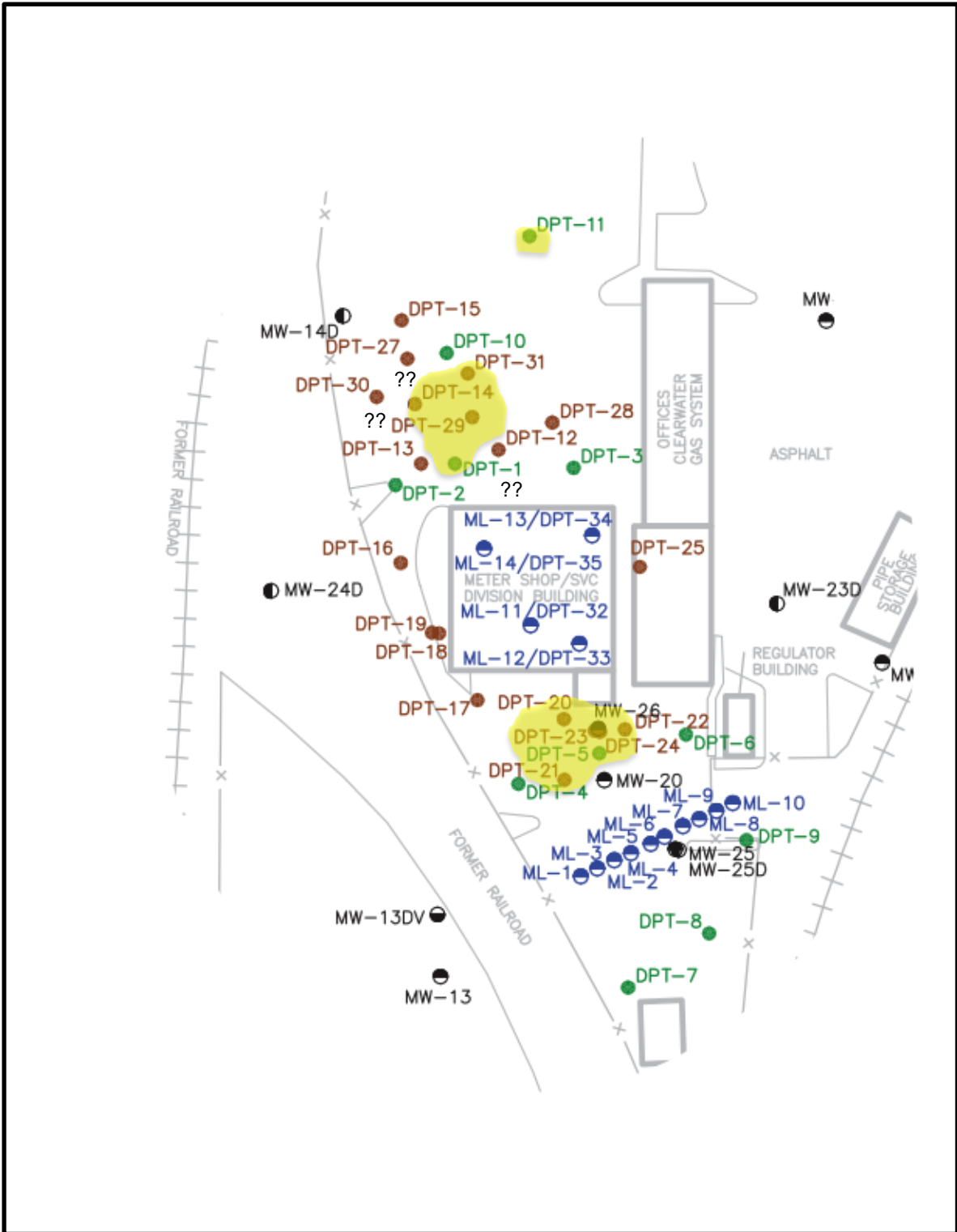


Figure 2.6. Estimated extent of observed source zones < 4.5 m (15 ft) bgs (shallow).

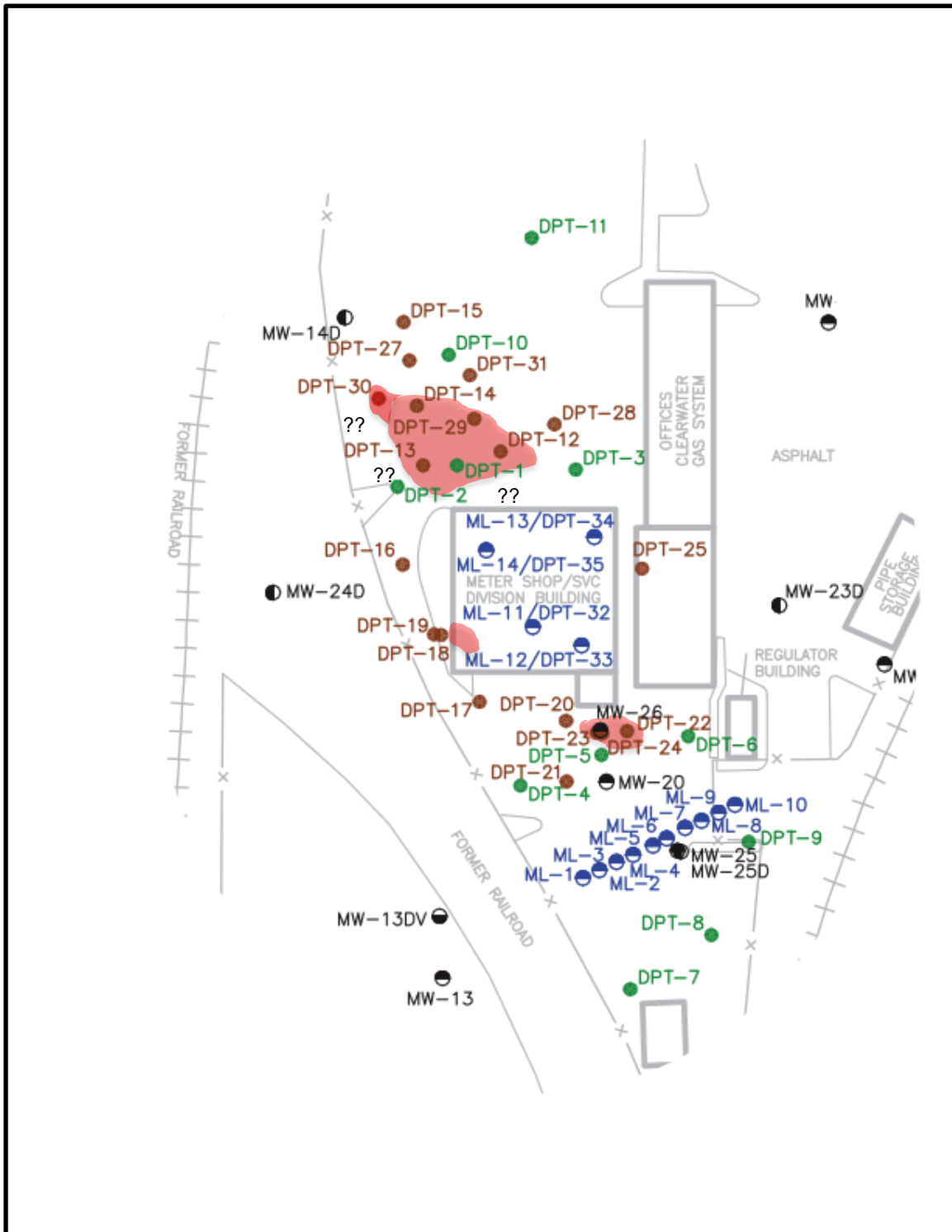


Figure 2.7. Estimated extent of observed source zones > 4.5 m (15 ft) bgs (deep).

Table 2.6. Concentrations of compounds in residual MGP NAPL taken from DPT-23 at 0.9 m (3 ft).

Contaminant	Concentration (mg/kg NAPL)	% Composition
BTEX		
Benzene	72.7	7.26E-03
Toluene	635	6.34E-02
Ethylbenzene	486	4.85E-02
P,M-xylene	990	9.89E-02
O-xylene	467	4.66E-02
Trimethylbenzenes		
1,3,5-Trimethyl-Benzene	225	2.25E-02
1,2,4-Trimethyl-Benzene	767	7.66E-02
1,2,3-Trimethyl-Benzene	248	2.48E-02
PAHs		
1-Methylnaphthalene	27700	2.77E+00
2-Methylnaphthalene	47200	4.71E+00
Acenaphthene	2250	2.25E-01
Acenaphthylene	6580	6.57E-01
Anthracene	2980	2.98E-01
Benz [a] anthracene	2230	2.23E-01
Benz [b] Fluoranthene + Benz [k]Fluoranthene	2001	2.00E-01
Benzo [a] Pyrene	2060	2.06E-01
Benzo [g,h,i] Perylene	2992	2.99E-01
Biphenyl	3360	3.36E-01
Carbazole	106	1.06E-02
Chrysene	2150	2.15E-01
Dibenzofuran	1130	1.13E-01
Fluoranthene	4860	4.85E-01
Fluorene	5530	5.52E-01
Indeno[1,2,3-c,d] Pyrene + Dibenz [a,h] Anthracene	865	8.64E-02
Indole	< MDL	-
Naphthalene	72800	7.27E+00
Phenanthrene	17400	1.74E+00
Pyrene	7680	7.67E-01
Other		
1,4-Dimethyl-N-Ethylbenzene	278.4	2.78E-02
1-Methyl-2-Ethylbenzene	88.4	8.83E-03
1-Methyl-3-Ethylbenzene	246	2.46E-02
1-Methyl-4-Ethylbenzene	172	1.72E-02
1-Methyl-N-Propylbenzene	84.9	8.48E-03
1-Methylphenanthrene	2700	2.70E-01
2,3,3-Trimethylpentane	41.1	4.11E-03
2,3,4-Trimethylpentane	38.6	3.86E-03
2,3,5-Trimethylnaphthalene	1100	1.10E-01
2,6-Dimethylnaphthalene	11300	1.13E+00
Benzothiopene	1190	1.19E-01
C21-C31	6060	6.05E-01
C9 - C20	43078	4.30E+00
Decalin	1415	1.41E-01
Dibenzothiophene	1600	1.60E-01
Indane	259	2.59E-02
Indene	1770	1.77E-01
Isooctane	58.8	5.87E-03
Isopentane	73.1	7.30E-03
Isopropylbenzene	26.1	2.61E-03
Naphthobenzothiophene	534	5.33E-02
Norpristane	1180	1.18E-01
n-Propylbenzene	47.4	4.73E-03
PentaDecane	132	1.32E-02
Perylene	285	2.85E-02
Phytane	3310	3.31E-01
Pristane	1030	1.03E-01
Styrene	242	2.42E-02
Unknown		
Unknown	707015.5	7.06E+01

Note: C9-C31 : Hydrocarbon chains

Table 2.7. Coal tar chemical compositions.

Compound	Clearwater	Brown et al. (2006)			Birak and Miller (2009)		
	Concentration (mg/kg NAPL)	Concentration (mg/kg NAPL)			Concentration (mg/kg NAPL)		
		Max	Min	Average	Max	Min	Average
BTEX							
Benzene	72.7	3390	47.5	1020	1000	11.0	514
Toluene	635	11900	210	3560	2120	53.0	1040
Ethylbenzene	486	3790	48.4	1490	3400	300	1850
P,M-xylene	990	8100	284	2830	-	-	-
O-xylene	467	4170	148	1400	-	-	-
Trimethylbenzenes							
1,3,5-Trimethylbenzene	225	-	-	-	-	-	-
1,2,4-Trimethylbenzene	767	3680	323	1680	-	-	-
1,2,3-Trimethylbenzene	248	-	-	-	-	-	-
PAHs							
Naphthalene	72800	68200	7700	29400	70000	21600	60900
Indole	< MDL	-	-	-	-	-	-
2-Methylnaphthalene	47200	38300	4230	14400	53000	37400	40300
1-Methylnaphthalene	27700	24300	1390	9120	38000	21500	27700
Biphenyl	3360	-	-	-	-	-	-
Acenaphthylene	6580	20000	567	6200	12100	610	5800
Acenaphthene	2250	2300	430	1090	15200	900	10300
Dibenzofuran	1130	5250	180	1520	-	-	-
Fluorene	5530	9510	716	3570	14000	1800	8570
Phenanthrene	17400	27200	2160	10800	32600	1600	18100
Anthracene	2980	634	8310	3310	20000	5420	9970
Carbazole	106	-	-	-	-	-	-
Fluoranthene	4860	8690	572	3760	13400	3000	6670
Pyrene	7680	11400	762	4550	13200	3200	7070
Benzo [a] anthracene	2230	4390	347	2020	10000	3100	5090
Chrysene	2150	3930	339	1870	5100	2340	3440
Benzo [b] Fluoranthene + Benz [k]Fluoranthene	2001	4350	292	1940	5200	2000	4220
Benzo [a] Pyrene	2060	4100	268	1660	3900	1560	3020
Indeno[1,2,3-c,d] Pyrene + Dibenz [a,h] Anthracene	865	1530	85.4	661	2610	1810	1850
Benzo [g,h,i] Perylene	2990	1930	100	766	3110	1270	2190

(-) no data reported

Table 2.8. Groundwater geochemical parameters.

Parameter	Units	ML 1-1	ML 5-5	ML 8-7	Average
Alkalinity	mg/L	137	168	287	197
Anions					
Chloride	mg/L	24.1	31.3	16.9	24.1
Bromide	mg/L	<0.500	<0.500	<0.500	<0.500
Fluoride	mg/L	<0.500	<0.500	<0.500	<0.500
Nitrite-N	mg/L	<0.500	<0.500	<0.500	<0.500
Nitrate-N	mg/L	<0.500	<0.500	<0.500	<0.500
Sulphate	mg/L	17.4	31.3	<10	24.4
Cations					
Aluminum	mg/L	25.9	2.3	21.6	16.6
Calcium	mg/L	12.8	83.1	40.2	45.4
Chromium	mg/L	0.044	0.006	0.054	0.03
Iron	mg/L	4.17	1.51	1.62	2.40
Lead	mg/L	0.026	<0.010	0.019	0.020
Phosphorous	mg/L	3.49	<0.500	1.10	2.30
Silicon	mg/L	31.0	<10	26.0	28.5
Sodium	mg/L	102	88.1	97.4	95.8
Strontium	mg/L	0.163	0.181	0.244	0.200
Titanium	mg/L	0.050	<0.020	0.057	0.05

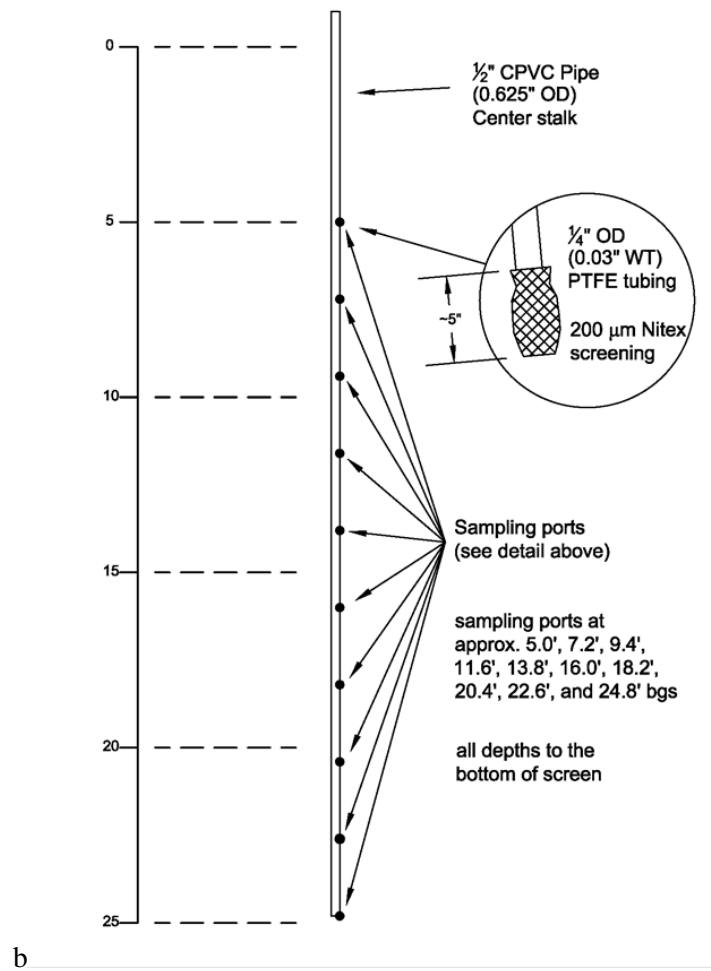


Figure 2.8. Schematic of multilevel (ML) monitoring well construction.

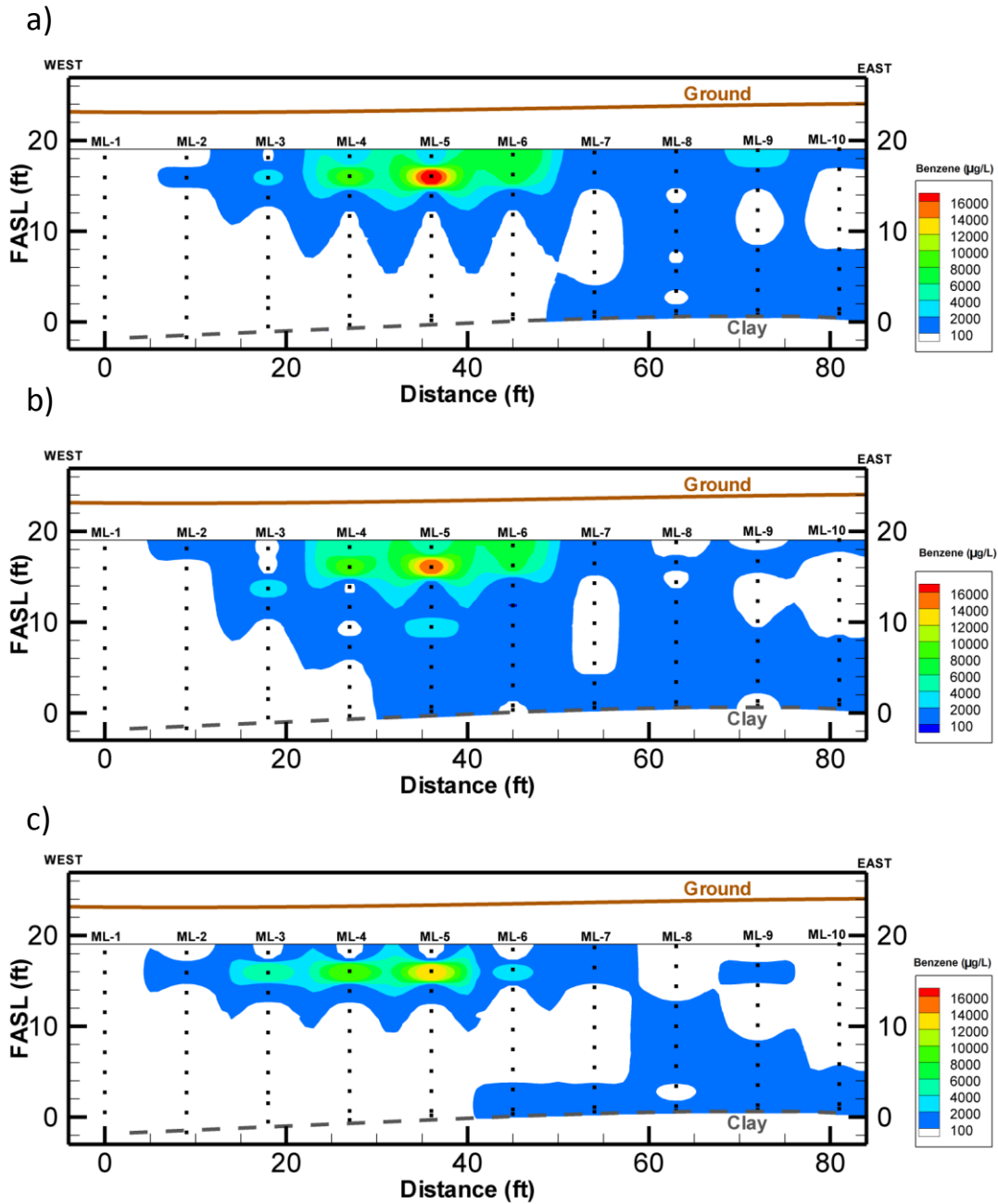


Figure 2.9. Benzene transect iso-concentration profile from a) July 2011, b) November 2011, and c) February 2012.

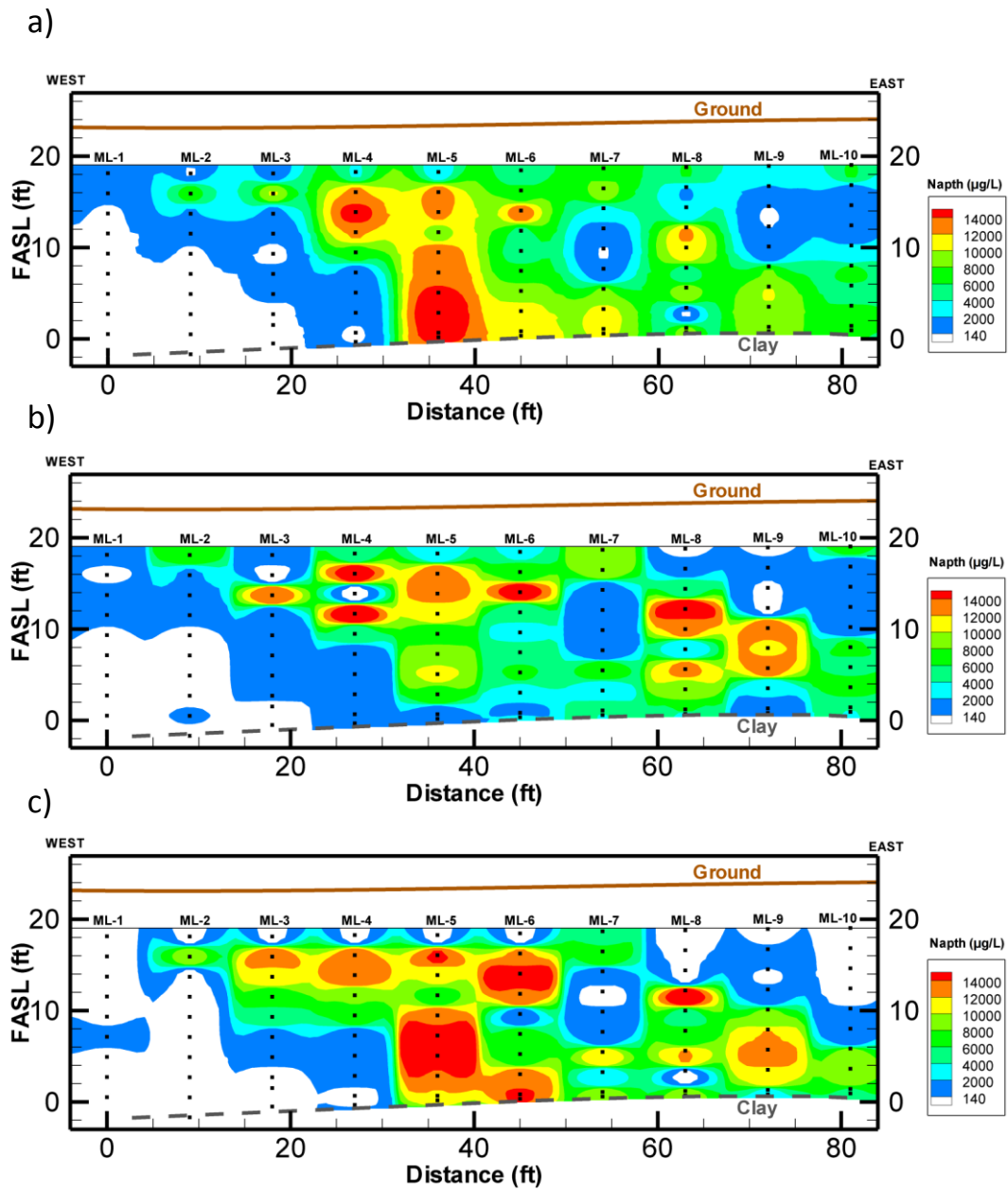


Figure 2.10. Naphthalene transect iso-concentration profile from a) July 2011, b) November 2011, and c) February 2012.

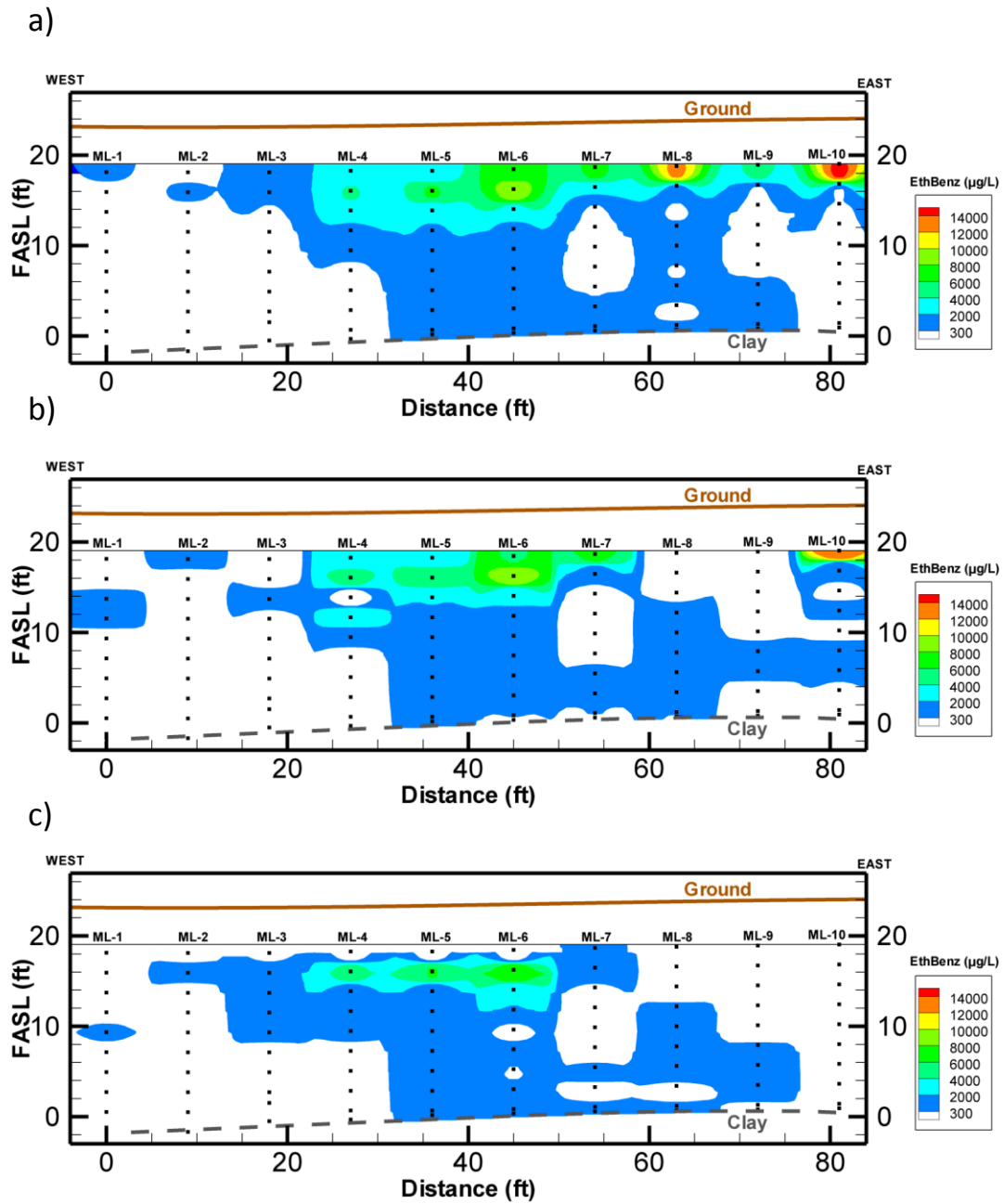


Figure 2.11. Ethylbenzene transect iso-concentration profile from a) July 2011, b) November 2011, and c) February 2012.

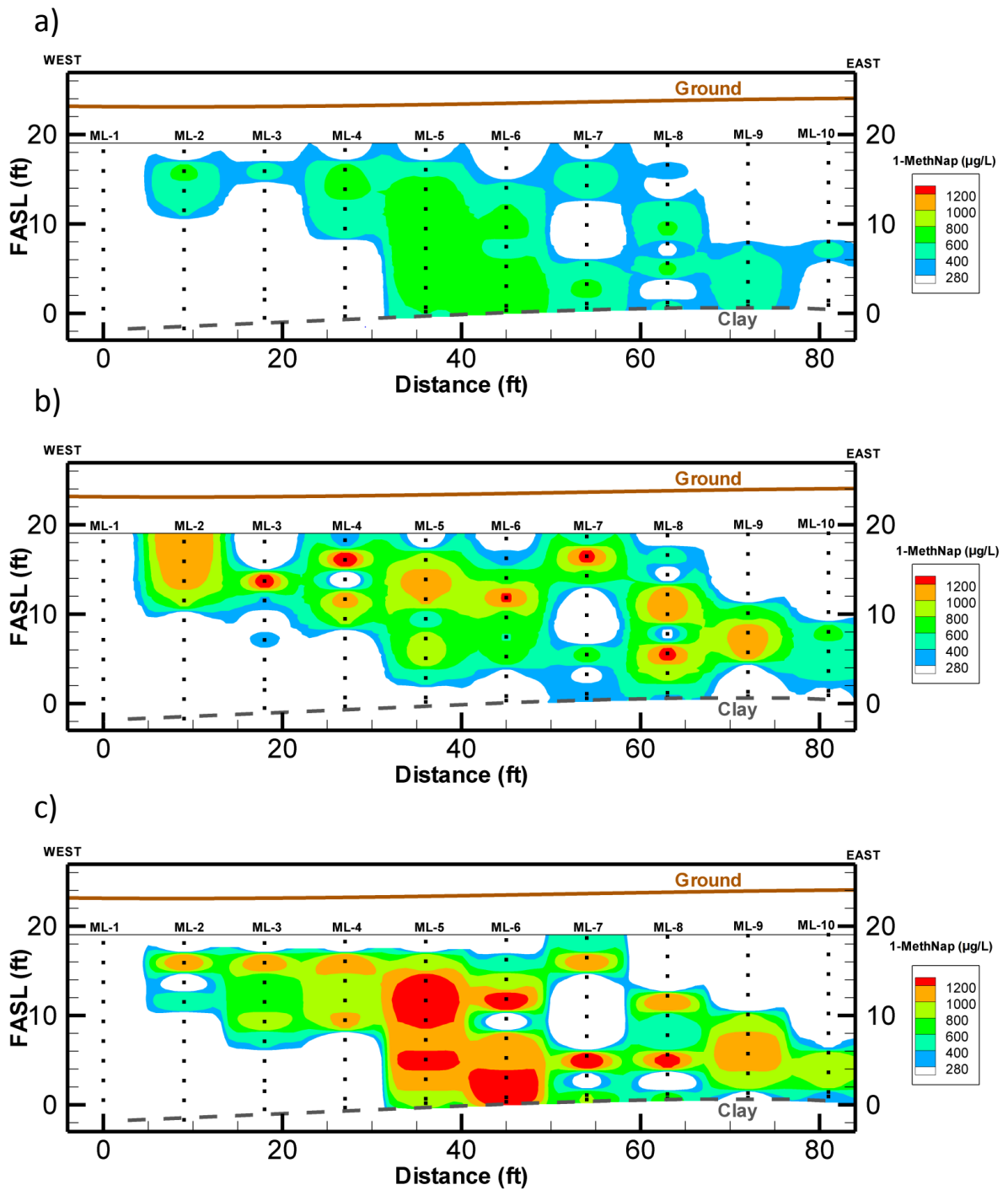


Figure 2.12. 1-Methylnaphthalene transect iso-concentration profile from a) July 2011, b) November 2011, and c) February 2012.

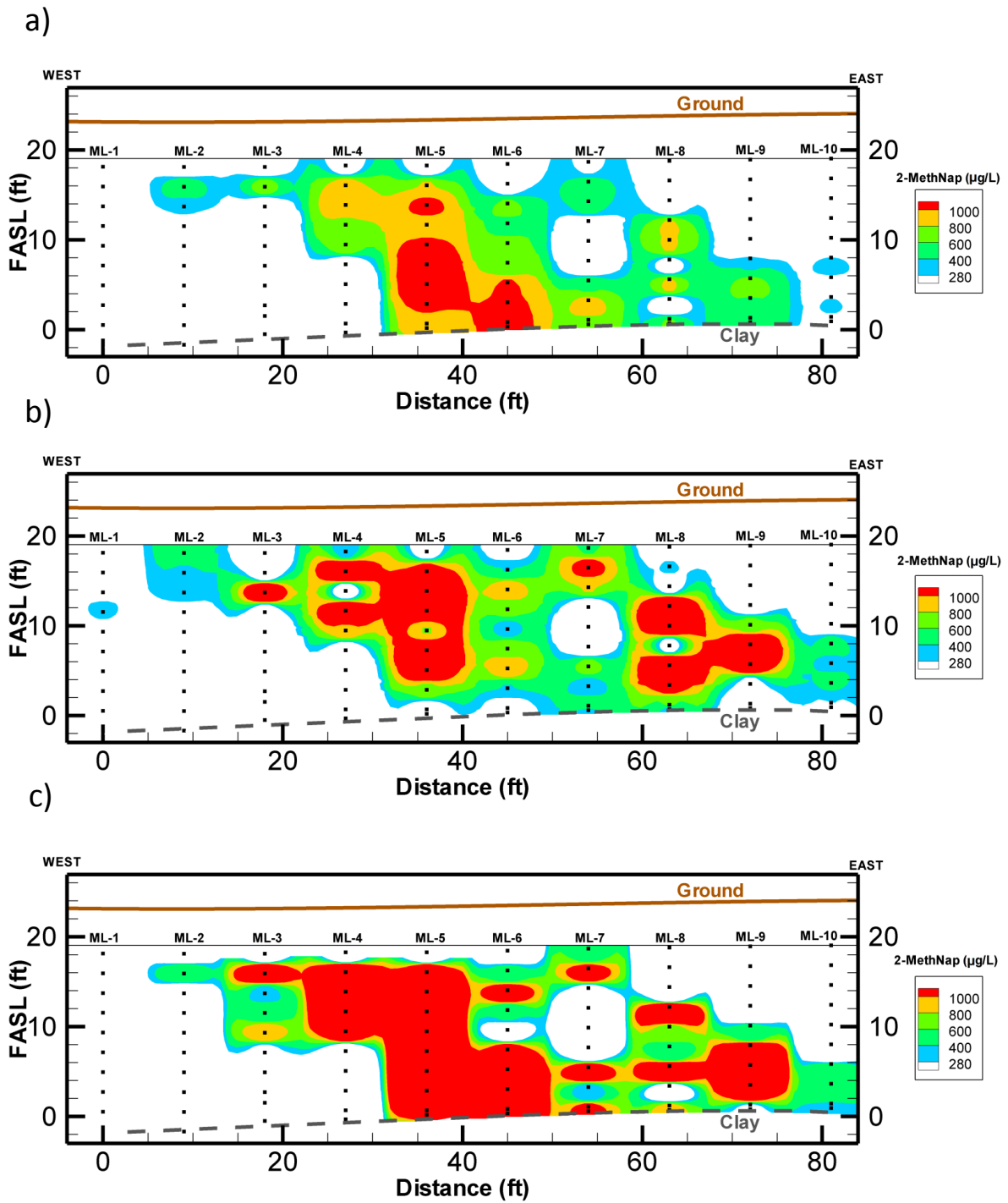


Figure 2.13. 2-Methylnaphthalene transect iso-concentration profile from a) July 2011, b) November 2011, and c) February 2012.

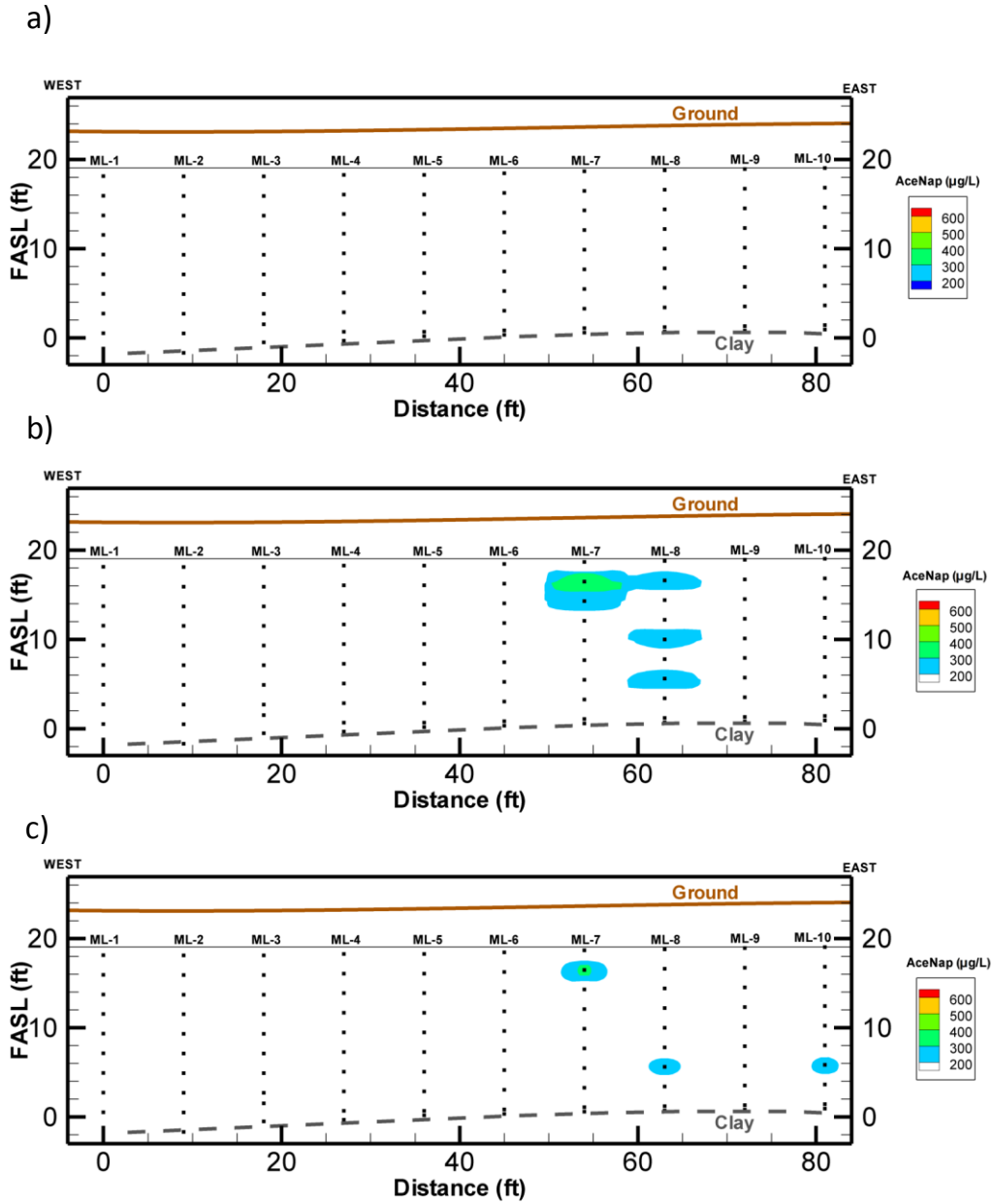


Figure 2.14. Acenaphthalene transect iso-concentration profile from a) July 2011, b) November 2011, and c) February 2012.

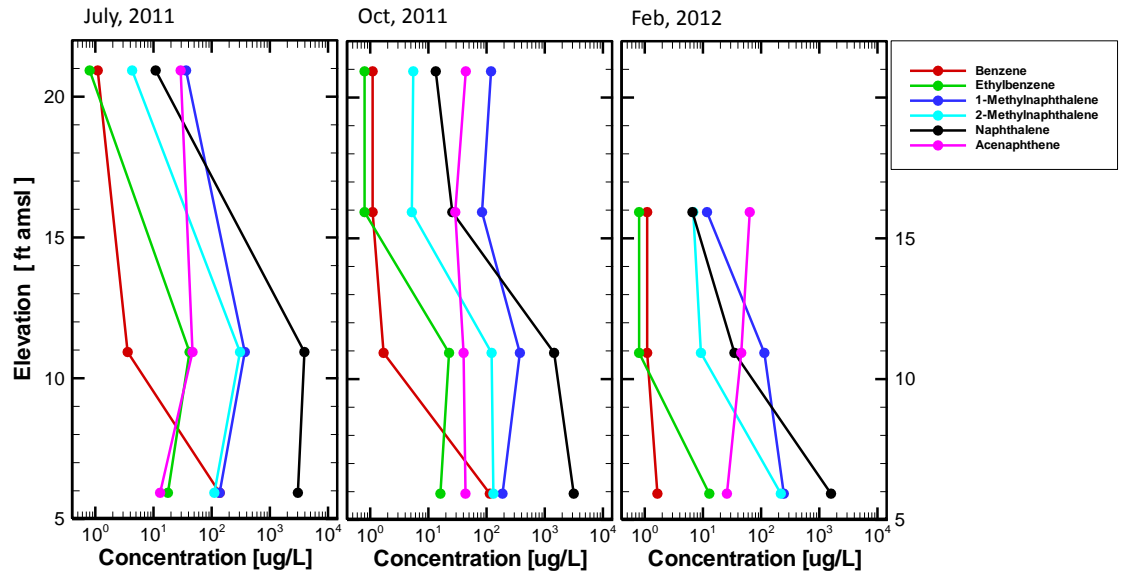


Figure 2.15. Concentration profiles from ML-11.

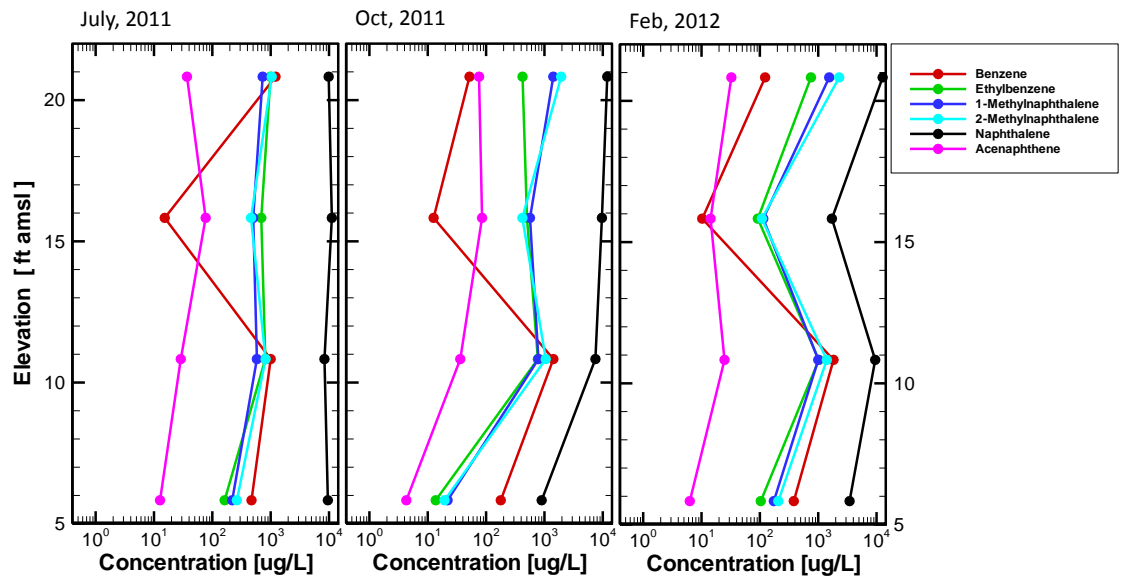


Figure 2.16. Concentration profiles from ML-12.

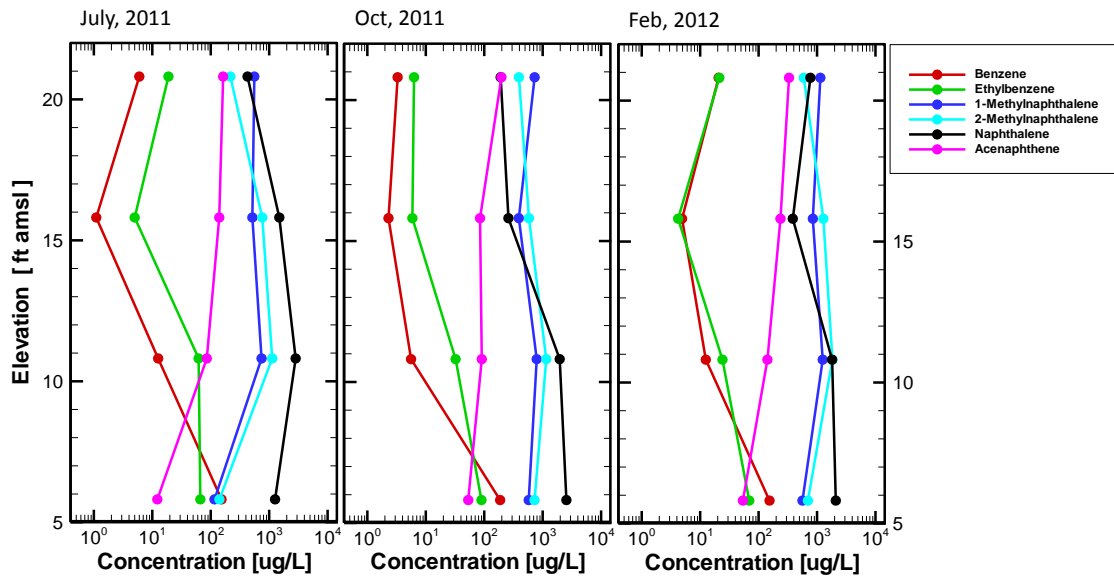


Figure 2.17. Concentration profiles from ML-13.

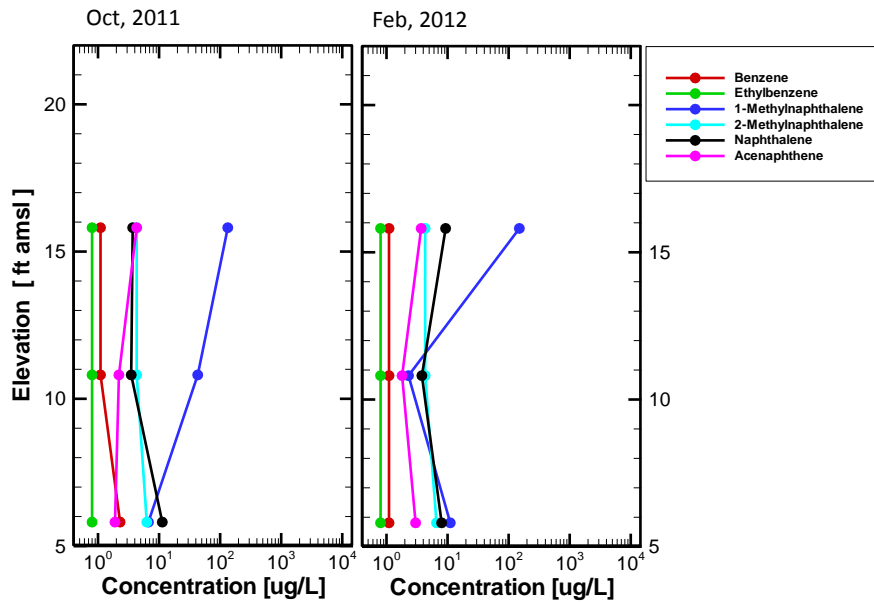


Figure 2.18. Concentration profiles from ML-14.

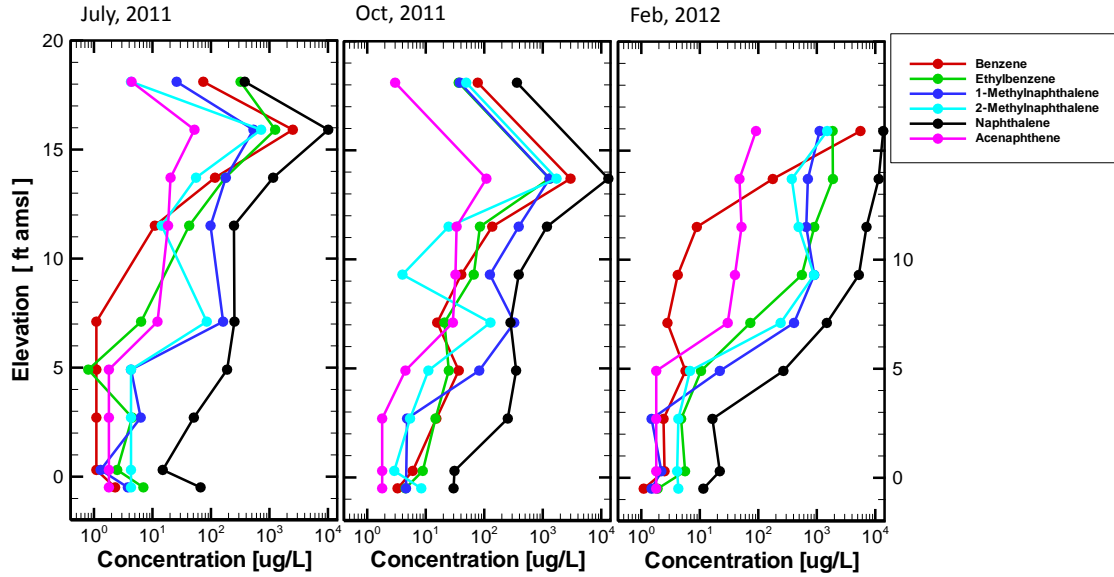


Figure 2.19. Concentration profiles from ML-3.

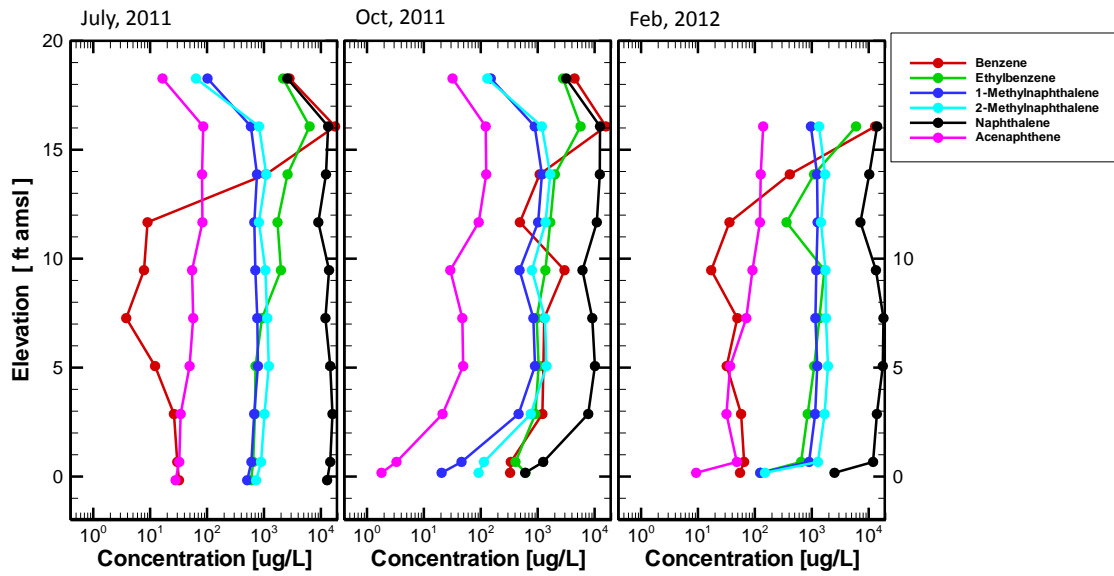


Figure 2.20. Concentration profiles from ML-5.

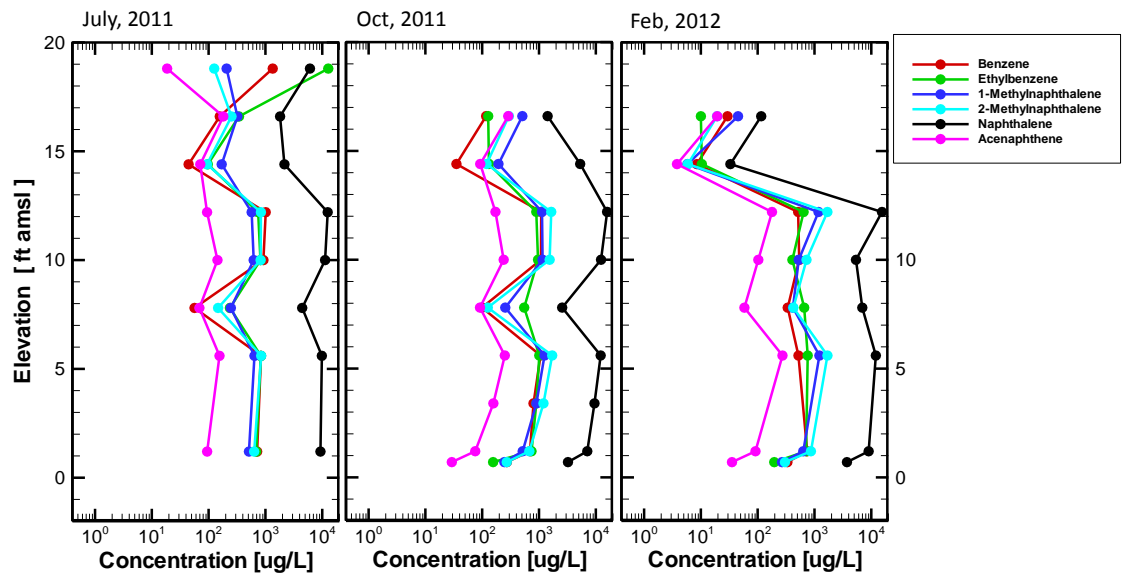


Figure 2.21. Concentration profiles from ML-8.

Table 2.9. Mass discharge across transect.

Contaminant	Round 1	Round 2	Round 3	Average Mass
	Mass Flux (mg/day)	Mass Flux (mg/day)	Mass Flux (mg/day)	Flux (mg/Day)
BTEX				
Benzene	12.7	9.75	7.80	10.1
Toluene	4.50	2.50	2.50	3.17
Ethylbenzene	21.2	11.5	8.68	13.8
P,M-xylene	10.3	6.13	4.81	7.08
O-xylene	5.45	2.51	2.61	3.52
Trimethylbenzenes				
1,3,5-Trimethylbenzene	0.560	0.475	0.524	0.52
1,2,4-Trimethylbenzene	1.57	1.31	1.60	1.49
1,2,3-Trimethylbenzene	0.86	0.80	0.96	0.87
PAHs				
Naphthalene	56.8	38.0	37.8	44.2
Indole	-	-	-	-
2-Methylnaphthalene	3.67	4.28	4.69	4.21
1-Methylnaphthalene	3.26	3.76	3.63	3.55
Biphenyl	0.249	0.225	0.230	0.235
Acenaphthylene	0.261	0.256	0.253	0.257
Acenaphthene	0.459	0.617	0.520	0.532
Dibenzofuran	0.155	0.187	0.232	0.191
Fluorene	0.298	0.411	0.363	0.357
Phenanthrene	0.248	0.282	0.264	0.265
Anthracene	0.034	0.013	0.013	0.020
Carbazole	0.033	0.045	0.040	0.039
Fluoranthene	0.015	0.011	0.011	0.012
Pyrene	0.016	0.010	0.007	0.011
Benz [a] anthracene	-	-	-	-
Chrysene	-	-	-	-
Benz [b] Fluoranthene +				
Benz [k] Fluoranthene	-	-	-	-
Benzo [a] Pyrene	-	-	-	-
Indeno[1,2,3-c,d] Pyrene				
+ Dibenz [a,h]				
Anthracene	-	-	-	-
Benzo [g,h,i] Perylene	-	-	-	-
Indeno[1,2,3-c,d] Pyrene				
+ Dibenz [a,h]				
Anthracene	-	-	-	-
Benzo [g,h,i] Perylene	-	-	-	-

Note: (-) < MDL

Chapter 3

Bench Scale Experiments

This chapter discusses the design and results of bench-scale experiments that were performed to gain insight into the behaviour of persulfate with uncontaminated site sediments, impacted groundwater and MGP impacted sediments. The buffering capacity of the soil was analyzed to determine the extent of the pH shift that occurs with the addition of persulfate. The reductive capacity of the aquifer was estimated through chemical oxygen demand tests. Persulfate degradation due to oxidant-solid interaction was quantified for aquifer sediments using NOI tests. Aqueous treatability experiments were conducted to determine reaction kinetics for unactivated and iron activated persulfate schemes. Finally, column experiments were used to determine potential treatability end-points and dosing requirements for push-pull tests and pilot-scale designs.

3.1 Buffering Capacity

The decomposition of persulfate generates protons that will potentially raise or lower the pH of the groundwater. The amount the pH decreases or increases are dependent on the buffering capacity, or the ability of the aquifer to resist changes in pH, and the oxidant dose (Siegrist et al., 2011). Mathematically, buffering capacity is defined as

$$\beta = \frac{dC}{dpH} \quad (3.1)$$

where dC is concentration of acid or base added to the sediment (eq/L), and dpH is the change in pH after the addition. The higher the buffering capacity, the less sensitive the material is to additions of acid or base. The impacts of potential pH shifts are important to consider because they determine persulfate activation pathways and hence oxidation effectiveness (Siegrist et al., 2011). Acid and base titrations were conducted to determine the natural alkaline and acidic buffering capacities of the site sediments and anticipate the *in situ* pH response to persulfate addition.

Based on the sediment types determined through grain size analyses (Appendix B, Table B.2), random samples were chosen in order to yield an unbiased characterization of the buffering capacity of the aquifer. A titration approach, modified from Zoltan (2010) was used to assess the ability for each sediment type to resist a shift in pH. For each strata, batch reactors containing 10 g of soil were submersed in 100 mL of distilled water. Following a 24-hour reaction period, the initial pH of the system was measured and NaOH or H₂SO₄ was added to the reactor to yield a concentration of 0.01 eq/L.

Additional additions of NaOH or H₂SO₄ were added to achieve concentrations of 0.05, 0.1, 0.5, 1, 5 and 10 meq/L. Controls were prepared without aquifer sediments. Measurements were taken with a pH probe (Orion, 209A) 24 hours following each addition of acid or base to allow sufficient time for a stable pH to be reached.

Theoretical pH values were calculated for the control reactors based on the amount of acid or base added and this estimate is consistent with the pH observations (Appendix D, Figure D.1). In general, the sediment samples showed buffering capacity for an acid or base concentration below 1 meq/L equivalent in both alkaline and acidic solutions (Figure 3.1). This is illustrated by the slope of the titration profile being less steep than the control. However, the sediment was ineffective at buffering conditions higher than 1 meq/L, indicated by a greater than or equal to the control. An addition of 20 g/L of persulfate will generate a theoretical hydrogen ion concentration of 0.175 meq/L (Sra et al., 2010). At this concentration, an *in situ* pH of around 4 is expected for sediments types of very fine silty sand, and sand with silt; and an *in situ* pH of around 6 is expected for fine sand and fine silty sand.

Alkaline activated persulfate has been shown to be the most aggressive persulfate activation scheme. This scheme generates three free radicals; the hydroxyl, super oxide, and sulfate free radicals (Siegrist et al., 2011). For this scheme to be effective a system pH >11 is ideal (Siegrist et al., 2011). Since the buffering capacity of this soil is depleted quickly (Figure 3.1), altering the system with an injection of a base *in situ* could be a feasible option.

3.2 Chemical Oxygen Demand (COD) Tests

To quantify the natural reductive capacity of the aquifer solids, chemical oxygen demand (COD) tests were performed. The tests were performed in triplicate for each of the lithotypes identified in the grain size analyses (Appendix B, Table B.5) following the method described Xu and Thomson (2008). This method measured the absorbance of a potassium dichromate solution added to a reactor filled with dried aquifer material. A standard curve was then utilized to quantify the COD.

The COD results (Table 3.1) are expressed in terms of mg O₂/g. This value was converted to an equivalent mass of permanganate (KMnO₄) for comparison with the results in Xu and Thomson (2008). The results indicate that the site sediments are at low end of the aquifer materials studied by Xu and Thomson (2008), and hence have a low total reductive capacity (between 0.09 and 0.17 meq/g).

The results for the COD tests performed within a given sample set (sediment type) were compared to the other sample sets to determine if it was possible that the sample sets were from the same statistical

population (i.e., if there was a significant difference in the COD results between soil types). Based on a one-way ANOVA (Appendix D, Table D.1), it was concluded at a 95% confidence interval that the 16 samples were not statistically distinguishable. Therefore, a single COD value could be considered representative of all the samples analyzed. An average value of 0.138 meq/g of aquifer material was estimated with a standard deviation of 0.025 meq/g.

3.3 NOI Tests

Natural oxidant interaction (NOI) tests were conducted to quantify the reduction in persulfate concentration due to the natural interaction with aquifer materials. NOI decreases oxidant mobility, reaction rates with the COC, and the mass of oxidant available. Therefore, NOI is an important site-specific measurement that should be quantified in order to design a cost-efficient treatment system.

Samples were randomly selected for analysis to provide an unbiased estimate of the NOI of aquifer sediments. Tests were performed in triplicate following the method outlined by Xu and Thomson (2009) and modified as outlined by Sra (2010). The experiment was completed after 50 days. Persulfate measurements were taken daily for the first 4 days and less frequently for the remainder of the experiment (Figure 3.2). Sand with silt and clay samples had the highest NOI, yielding persulfate reductions of 22.7 and 23.4%. Reactors with very fine sand, and very fine sand with silt had persulfate degradations of 14.4% and 15.1%, respectively. The control sample, which contained persulfate and Milli-Q water, saw a 0.04% overall decrease in persulfate concentration over the experimental period. The decomposition of persulfate appeared to follow a first-order mass action law for all aquifer materials ($r^2 > 0.89$) (Appendix D, Figure D.2). The average reaction rate coefficient for the sediments was $1.4 \times 10^{-5} \text{ hr}^{-1}$ with a range of 2×10^{-5} to $7 \times 10^{-6} \text{ hr}^{-1}$.

3.4 Aqueous Treatability Studies

3.4.1 Unactivated Persulfate

Batch experiments were conducted to determine the potential for unactivated persulfate to oxidize the contaminants of concern (COC) as defined in Section 1.4. Groundwater from MW-20, preserved with sodium azide, was used. MW-20 was chosen since it is directly downgradient from a known MGP residual source and has exhibited high COC concentrations.

Glass reactors (40 mL) were labeled and weighed prior to the commencement of the experiment. A groundwater sample volume of 36 mL was added to each reactor, followed by 2 mL of a 20 g/L stock persulfate ($\text{Na}_2\text{S}_2\text{O}_8$, ACS; Aldrich, Milwaukee) solution. The reactors were then capped with a Teflon

lined cap and re-weighed. A dose of 20 g/L was chosen based on successful BTEX and PAH decomposition shown by Sra et al. (2012).

Experimental and persulfate control samples were prepared for each temporal sample interval and initial concentration measurements were taken at time zero. The samples were placed in the dark at room temperature (~20 °C) to prevent persulfate photo-degradation. Upon analysis, samples were removed and reweighed to ensure no loss in the reactor. Persulfate concentrations were measured following Huang et al. (2002). Measurements of BTEX and PAH compounds were performed by solvent extraction with methylene chloride followed by gas chromatography. A detailed description of the method can be found in Freitas and Barker (2008). Measurements were taken daily for the first three days, and at longer intervals for the remainder of the experiment (total of 14 days). Reactors were prepared and analyzed in triplicate.

Results from the control reactors indicate that the concentration of BTEX and PAH compounds remained constant over the 14-day experimental period (Appendix D, Figure D.5). Results from the treatment reactors show concentration reductions of all the COC (Figure 3.3) (See Appendix D, Figure D.4 for all compounds). Benzene, ethylbenzene, and acenaphthalene were quickly oxidized to below method detection limit (MDL) (MDL values located in Table 3.3) by Day 7. Naphthalene (and other PAHs), 1-methylnaphthalene and 2-methylnaphthalene however had concentrations above MDL at Day 14. After 14 days all the COC had reached a concentration below 10% of their initial concentration. Persulfate concentration varied little over the 14-day experimental period (Appendix D, Figure D.3).

Oxidation kinetics remained fairly constant for all COC except for acenaphthalene which appeared faster at earlier times ($t < 3$ days) and more slowly. Reaction rate coefficients (k_{obs}) were calculated using the pseudo first-order rate law. A pseudo first-order rate law was used since persulfate concentration remained relatively constant over the experimental period. A full description of the method is given in Sra (2010).

The first-order rate law represented the data well for all compounds ($r^2 > 0.9$) (Table 3.2), except for 1,2,3 trimethylbenzene (0.863) and 2-methylnaphthalene (0.875). For the COC, k_{obs} was largest for ethylbenzene, followed by benzene, 1-methylnaphthalene, 2-methylnaphthalene, acenaphthalene, and naphthalene.

3.4.2 Iron (II) Activated Persulfate

Site water from MW-20 was also used to determine the potential for iron-activated persulfate to oxidize the COC. It was expected that the addition of iron in the reactor would significantly increase degradation rates of the COC as observed in Crimi and Taylor, 2007 and Sra et al., 2010. Two series of batch experiments were performed, one with a high (600 mg-Fe(II)/L) iron concentration, and one with a low iron concentration (150 mg-Fe(II)/L). These concentrations were chosen since they correspond with the lower and upper bounds of iron dosages typically used (Block, 2008).

Glass reactors (40 mL) were prepared as described for the unactivated persulfate experiment (Section 3.4.1); however, a 1:1 mole ratio of iron ($\text{FeSO}_4 \cdot 7\text{H}_2\text{O}$) (ACS; J.T.Baker, Phillipsbourg, NJ) and citric acid ($\text{C}_6\text{H}_8\text{O}_7$) (Fischer; Fair Lawns, NJ) were added to the reactors. Citric acid (CA) was added as a chelating agent. Samples were collected and analyzed in duplicate every 3 hours for the first 9 hours and then daily for a total of 14 days.

The presence of iron accelerated the rate of reaction for both low and high iron concentrations explored (Table 3.4). This increase is a result of the generation of the sulfate free radical ($\text{SO}_4^{\cdot -}$) through a one electron transfer process. This process increases the activation potential of persulfate from 2.1 V to 2.6 V (Siegrist et al. 2011). Except for naphthalene, all COC reached MDL by 96 hours. Degradation rates of COCs in the high iron system (Figure 3.4(b)) were faster than in the low iron system (Figure 3.4(a)) (see Appendix D, Figures D.6 (low) and D.8 (high) for other compounds). Persulfate decomposition occurred in the reactors for the low iron series (Appendix D, Figure D.10). An average concentration reduction of 17% was observed.

For the low iron case, k_{obs} was calculated using a pseudo first-order rate law outlined in Sra (2010). The persulfate degradation observed was minimal enough to assume that persulfate was still in excess within the system, making the pseudo first-order assumption valid. The first-order rate law represented the data well for all compounds ($r^2 > 0.9$) (Table 4.5). For the COC, the k_{obs} was largest for 2-methylnaphthalene followed by 1-methylnaphthalene, ethylbenzene, acenaphthene, benzene, and naphthalene.

For the high iron series, persulfate was not in excess for the duration of the experiment (Appendix D, Figure D.10). By the end of the 14-day experiment, persulfate consumption reached 78%. As a result, the assumptions undertaken to utilize a pseudo first-order rate equation are not valid. In order to calculate a reaction rate coefficient, the differential method of analysis was used (Levenspiel, 1998). This method

evaluates all terms in the differential rate equation (Equation 3.2) and tests the goodness of fit of the equation with the experimental data (Appendix D, Table D.2 and Figure D.11).

$$\frac{dC_A}{dt} = -kC_A^n \quad (3.2)$$

Where dC_A/dt is the change in concentration (mol/L-s), k is the reaction rate coefficient ($L^n/mol^n\text{-sec}$), and C_A is the concentration of compound A at time t (mol/L). The generated rate equations represented the data sufficiently for all compounds ($r^2 > 0.901$) (Table 3.5).

Compound reductions were faster in the Fe(II)-600 experiment compared to the Fe(II)-150 experiment. However, the Fe(II)-600 experiment showed limited persulfate persistence and resulted in ~60% less persulfate in the system at the end of the experiment compared to the low iron experiment (Appendix D, Figure D.10). Complete oxidation of 600 mg/L of Fe (II) requires 1.28 g/L of persulfate (Sra, 2010). At the end of both series of experiments, the final concentration was greater than 1.28 g/L meaning a 600 mg-Fe(II)/L activation scheme would be more effective in reducing aqueous COC concentrations than a low iron scheme.

Results from this experiment agree with other aqueous treatability studies that have been conducted with iron activated persulfate schemes. Almost instantaneous degradation of BTEX compounds has been observed (Liang, 2008; Sra, 2010) PAH removal below MDL levels has been shown (Nadim, 2005; Ferrasse, 2008).

3.5 Column Experiments

Two series of column experiments were performed to investigate the ability of persulfate to treat MGP impacted sediments. The goal of these experiments was to help to design full-scale treatment approaches and develop realistic treatment goals. To achieve this, the experiments were designed (Appendix E, Table E.4) to mimic *in situ* conditions such as velocity and porosity as well as aspects of potential pilot-scale treatment variables such as persulfate injection rates, frequency, doses, and reaction times. The columns were packed with MGP impacted sediment taken and the pumping rate into the columns was equivalent to the estimated groundwater flow rate determined from transducer measurements.

For the first series of column experiments, multiple doses of unactivated persulfate were administered, followed by two doses of alkaline activated persulfate. Unactivated persulfate was initially used to determine its potential for remediation of impacted sediments as an unactivated scheme would be easier to

design and is more cost effective. Further doses using alkaline-activated persulfate were conducted for contrast since it is known to be the most effective persulfate activation method (Siegrist et al., 2011).

For the second series of column experiments, doses of 600 mg-Fe(II)/L activated persulfate with a citric acid chelate (600 mg/L) were used. The results from the aqueous treatability experiments indicated that 600 mg-Fe(II)/L was more effective in reducing COC than unactivated persulfate and persulfate activated with 150 mg-Fe(II)/L. Effluent concentrations of BTEX and PAHs were measured following a 4-day reaction period to determine reduction in dissolved effluent concentrations. Initial and final concentrations of the column sediments were also compared to assess mass removal.

3.5.1 Materials and Methods

MGP impacted sediments collected from DPT-23 (10-12 and 20 ft bgs) were homogenized and packed into two series of four short PVC columns (diameter 3.81 cm, length 10 cm). This sample was selected since it contained MGP residual in shallow and deep zones and the impacts of contamination were previously quantified (Chapter 2). Three columns in each series were treatment columns and one column was a control. The bottom of each column was filled with glass beads (Potter Industries Ltd.) of 0.59 to 0.84 mm in diameter, followed by a thin layer of glass wool (Pyrex, VWR) and a wire mesh of 0.178 mm aperture size. The next 10 cm of the column was packed with impacted sediments, followed by another layer of wire, glass beads, and wool (photos in Appendix G, Figures G.6 to G.11). Packing was conducted in 1 cm lifts and 5 mg samples from the bottom, middle and top lifts were taken for baseline BTEX and PAH analyses (Appendix G, Figure G.7).

The experimental set-up (Figure 3.5) consisted of an open system where a reservoir was connected with 1.42 mm I.D. tubing (Masterflex) to a peristaltic pump (Cole-Parmer Instrument Co.) that forced the flushing solution upwards through the column. Solution leaving the column entered a closed sample vial and then discharged to an effluent tank.

To commence the experiment, the reservoir was filled with Milli-Q water. At a rate of 0.025 mL/min, the Milli-Q water was flushed through all four columns. Once two pore had passed through the columns samples were taken from the vials attached to each column to determine the baseline concentrations of BTEX and PAHs. It was assumed that two pore volumes would provide sufficient time for equilibrium conditions to be attained (Forsey, 2010). Following the Milli-Q flush, the reservoir was filled with a prescribed sodium persulfate solution. This persulfate solution was flushed through the three treatment

columns, at a flow rate of 0.18 ml/min, and Milli-Q was flushed through the control column at the same rate. The flow rate was increased during persulfate injections to mimic an injection episode.

An electrical conductivity (EC) (Orion, 5* Plus) meter was installed in-line with one treatment column and recorded measurements at 30-minute intervals to monitor persulfate solution breakthrough. Once breakthrough occurred, the pump was turned off. Following a four-day reaction period, which was to allow for sufficient time for kinetic processes to occur, the reservoir was refilled with Milli-Q water and the columns were flushed until EC readings indicated that the persulfate solution had exited the system (approximately two pore volumes).

From the sampling vial attached to each column, duplicate 40-mL samples were taken and analyzed for selected organic compounds following the method from Thomson et al. (2008). Persulfate concentrations were also measured following the method by Huang et al. (2002). Additionally, duplicate 10 mL samples were taken for short-chained alkylphenol (SCAP) analysis. Standard water quality measurements of temperature, pH, Eh, dissolved oxygen (DO), and EC were also taken at sampling times that occurred following Milli-Q and persulfate flushes (Appendix E, Tables E.1 and E.2). This sequence was repeated for the entire experiment.

As stated, when packing the columns, three 5 mg soil samples were taken from the bottom, top and middle of each column to determine the baseline concentrations for the COC (Table 3.4). The samples were analyzed for BTEX and PAH concentrations (EPA Methods 8260 and 8270). Following the experiment, the columns were split open and three 5 mg soil samples were taken from the same locations for comparison. Sediment samples collected and analyzed prior to packing the columns indicated a homogenous mixture across and between columns.

Short chained alkylphenols (SCAP) analysis was completed (method from Huling et al. 2011) following Milli-Q flushes after doses of unactivated persulfate and iron activated persulfate. No samples were collected or analyses performed on the alkaline activated persulfate flushes, therefore results from these columns only represent unactivated persulfate treatment. The analyses completed included measurements of phenol, cresols, dimethyl, ethylphenols, trimethyl, ethyl-methyl and propylphenols concentrations. The purpose of this work was to determine if BTEX oxidation yielded SCAP by-products.

Series one of the column experiments were treated with unactivated persulfate ($\text{Na}_2\text{S}_2\text{O}_8$) (ACS; Aldrich, Milwaukee). On Day 58, these treatments were no longer causing a significant reduction in the effluent organic compound concentrations. In order to determine if further degradation was possible, two

doses of base activated persulfate were administered. A $S_2O_8^{2-} + NaOH$ solution was prepared to achieve a desired pH of 11. The pH of the injection solution was monitored hourly to ensure pH remained constant. Series two of the treatment columns were flushed with 600 mg-Fe(II)/L ($FeSO_4 \cdot 7H_2O$) (ACS, J.T.Baker, Phillipsbourg, NJ) activated persulfate. A persulfate stock solution was prepared using 600 mg/L iron concentration and 600 mg/L citric acid chelate ($C_6H_8O_7$, Fischer, Fair Lawns, NJ).

3.5.2 Unactivated Column Results

For the unactivated column experiment, a total of nine treatment episodes (7 unactivated persulfate, 2 base activated persulfate) were conducted over 75 days. During this time period approximately 20 g of persulfate was injected into each treatment column. The timeline for the experiment, injection concentrations, and water quality measurements taken are given in Appendix E (Table E.1). Photos showing set-up, materials, and packing of the columns are given in Appendix G (Figures G.6 to G.11).

Effluent PAH and BTEX concentrations from the control column showed a decrease between 10 and 40% (Appendix E, Figure E.8). Effluent concentrations of the control column were always higher than the treatment columns. Additionally, the initial anticipated effluent concentrations based on aqueous solubility values were always higher than the measured values (Appendix E, Table E.5). This over-estimation is likely a result of not being able to identify all the compounds in the impacted sediments (~70% bulk). Of the COCs, benzene was reduced 17% followed by ethylbenzene (21%), naphthalene (23%), 1-methylnaphthalene (33%), and 2-methylnaphthalene (45%). Overall, the control column had a 22% loss of MGP soil concentration after flushing with ~1.5 L of water.

Persulfate doses into the column increased over time to promote degradation and to ensure there was always an excess of persulfate in the system (Figure 3.6). Persulfate concentrations in the effluent never decreased below 50% of the injection concentrations suggesting that dosage amounts were sufficient to maintain persulfate presence. Between injection episodes persulfate measurements were less than the MDL indicating that all the persulfate had been flushed from the system.

Duplicate samples taken from each column were averaged and normalized to the baseline measurements for all measured compounds. These values were then adjusted for the losses seen in the control column to estimate losses solely due to persulfate degradation. Persulfate dose, *Dose* (g persulfate/g of soil), was calculated using:

$$Dose = \frac{PV \sum C_i}{m} \quad (3.3)$$

where PV is the pore volume (L) in the column, C_i (g/L) is the oxidant injection concentrations, and m is the mass of sediment in the column (g). Dose-response curves were generated for each column, and for the average of the three treatment columns by plotting the normalized concentration versus dose (Appendix E, Figures E.6 to E.9). Additionally, a plot of the average over the three columns was plotted for the COC before the base activated injection and after the base activated injection (Figure 3.7).

After the first injection, the concentrations of all the COC decreased. Each subsequent injection yielded further reductions in all the compounds until a dose of ~ 50 g/g of soil, at which point no additional changes in the effluent concentrations of the COC were observed. At this point, no COC were reduced to below MDL levels; acenaphthalene was the most persistent (68% of initial concentration remaining), followed by naphthalene, 1-Methylnaphthalene and 2-Methylnaphthalene, ethylbenzene, and benzene (88% reduction). These results indicate the potential for unactivated persulfate to treat dissolved COC *in situ*, and allow for the prediction of full-scale treatability endpoints. However, based on the average groundwater concentrations measured on site, reductions of this magnitude would not satisfy NADC guidelines (Table 1.4).

To determine if further reduction in effluent COC concentrations were possible, two base activated persulfate treatments were administered. Following these injections, effluent concentrations of acenaphthalene and benzene were reduced to below detection limits. Ethylbenzene was reduced another 15% (98% reduction), followed by 2-methylnaphthalene, 1-Methylnaphthalene and naphthalene (75%). These results indicate that base-activated persulfate is a more aggressive and effective remediation option compared with unactivated persulfate in the treatment reducing effluent concentrations of the COC. Additionally, NADC guidelines were achieved for all compounds except for naphthalene.

Measurements of EC were taken from treatment column 1 during persulfate flushing. Resulting EC measurements were plotted versus time to generate breakthrough curves (Figure 3.8). The gradual slope of the curve shows that mixing processes are present and plug-flow through the column is not occurring. Comparing the initial and final breakthrough curves (Appendix E, Figure E.10) show that dispersion within the column increases over time since breakthrough occurs at later times. The longitudinal diffusion coefficient was calculated from the average results. It was estimated to be $1.03 \times 10^{-7} \text{ m}^2/\text{sec}$ ($\pm 1.2 \times 10^{-7} \text{ m}^2/\text{sec}$) using the method outlined in Levenspiel (1998). This value is comparable to typical values of a fine sand aquifer (Batu, 2006). Persulfate breakthrough was estimated based on the time for 50% change in EC reading to occur. Therefore, the time at which the normalized EC measurement of 0.50 occurred

was used to back calculate a value for the column porosity (Appendix E, Table E.3). A porosity of 0.33 was calculated, which is similar to the porosity estimated from permeameter analyses (0.34).

Phenol measurements taken after Milli-Q flushes indicated indirect relationships between SCAP and BTEX compounds. Decreasing benzene concentration in the effluent was correlated with an increase in effluent phenol concentrations. Once benzene concentrations reached < MDL, phenol concentrations decreased (Figure 3.9(a)). Concentrations measured from the effluent in the control columns remained at or below baseline concentrations. Similar relationships were shown for ethylbenzene and ethylphenol (Figure 3.9(b)), toluene and creosol (Figure 3.9(c)), and xylene and dimethylphenol (Figure 3.9(d)) (Thomas-Arrigo, 2012). SCAP concentrations were shown to increase at the 20g/kg dose and after additional doses concentrations subsided. All these by-products have been shown to be harmful and some of these by-products are more toxic than the parent phenol compound (e.g. o-creosol and p-creosol) (HSBD, 1985). Therefore, sufficient dosing of unactivated persulfate is required to eliminate the threat of phenol compounds.

Soil samples from the bottom, middle and top of the treatment and control columns were compared to the initial soil samples that were taken when the columns were packed (Table 3.4). Raw data are given in Appendix F (Table F.11). Results from the control column were also compared to the results from the treatment columns. Initial soil concentrations showed little variation with depth (less than 3% difference between top and bottom of column). Therefore, the column experiment was constructed such that, initially, the column had a homogenous soil concentration. Final soil concentration measurements indicate that more of the NAPL had degraded near the at the top of the column (10% difference between top and bottom).

Results show that approximately 400 mg of mass was removed from the control column. On average, reductions in the control column were higher for BTEX compounds than PAH compounds. This outcome was expected since BTEX compounds are more soluble. Even in the control, benzene, Indeno[1,2,3-c,d] Pyrene + Dibenz [a,h] Anthracene, and Benzo [g,h,i] Perylene, were reduced 100%, indicating that flushing alone is sufficient to remove these contaminants. Similar reductions (less than 2% difference) were seen in the control and treatment columns for naphthalene, dibenzofuran, biphenyl, phenanthrene, fluoranthene, and pyrene, indicating that persulfate was not assisting in the removal of these compounds.

Results from the treatment columns showed a reduction in soil concentration of 526 mg (23% more removal than observed in the control column). Therefore, it can be concluded that persulfate assisted with

the removal of NAPL from the soil. Also, indole, acenaphthalene and anthracene were shown to be oxidized by persulfate in all treatment columns (18%, 18%, and 19% more reduction in treatment columns compared to control columns, respectively). However, results indicate that persulfate did not significantly assist in the removal of BTEX compounds (42% removal in treatment columns compared with 40% removal in the control column). All other compounds showed reductions of less than 5% compared to the control column.

NAPL soil saturation was estimated before and after treatment using

$$S_n = \frac{\sum_{k=1}^n C_s^k \rho_b}{\sum_{k=1}^n C_n^k \phi \rho_n} \quad (3.4)$$

where C_s the average measured concentration for compound k (Table 2.2), ρ_b is the soil density, C_n is the measured concentration of contaminant k in the NAPL (Table 2.7), ϕ is the porosity in the column calculated from persulfate breakthrough curves (Appendix E, Table E.3), and ρ_n is the density of the NAPL (assumed to be 1083 kg/m^3). This value was taken from the low-end of the range of coal tar densities examined by Lee et al. (1992). The low-end value was taken since LNAPL and DNAPL exist at the Clearwater site. Soil saturation was calculated to be approximately 4.0% before treatment, and 3.7% after treatment (Table 3.5). The saturation level in the control column was 3.8% at the end of the experiment. The $\sim 0.2\%$ change in saturation levels is attributed to reductions in the PAH compounds. Reductions in higher soluble compounds (BTEX and trimethylbenzenes) were similar in treatment and control columns.

3.5.3 Iron Activated Persulfate Results

For the iron activated persulfate column series, a total of seven treatment episodes were conducted over 60 days. During this time period approximately 15 g of iron activated persulfate solution was flushed through each treatment column. The timeline for the experiment, injection concentrations, and water quality measurements taken can be found in Appendix E (Table E.2).

Persulfate doses were increased over time to promote degradation of the contaminants and to ensure there was always an excess of persulfate in the system (Figure 3.6). Effluent persulfate concentrations never decreased below 10% of the injection concentrations. It is believed that the effluent concentrations were lower than the unactivated persulfate experiment due to scavenging of sulfate radicals by the iron.

Between injection episodes persulfate measurements were below detection limits indicating that all the persulfate had been removed from the system.

Duplicate samples taken from each column were averaged and to the baseline measurements for all measured compounds. These values were then adjusted for the losses seen in the control column to determine losses solely due to persulfate degradation. An average dose-response curve was created for the effluent COC across the three columns (Figure 3.9). Plots for each column including the control are located in Appendix E (Figures E.1 to E.5).

After the first injection, the concentrations of all the COCs decreased. Each subsequent injection yielded further reductions in all the compounds. Upon completion of the experiment, no concentration was reduced 100%. Acenaphthalene was most persistent with approximately 50% of initial concentration remaining, followed by naphthalene, 1-Methylnaphthalene and 2-Methylnaphthalene, ethylbenzene, benzene, which was least persistent with approximately 98% reduction inside the column. Similar to the unactivated columns, benzene and acenaphthalene were the only two COC reduced to below MDL levels.

Samples were taken following Milli-Q flushes and analyzed for SCAP concentrations. Unlike the unactivated persulfate treatment columns, SCAP effluent concentrations decreased after each persulfate dose (Figure 3.12). It was argued that iron-activated persulfate is more efficient in the destruction of coal tar and no phenol by-products are produced (Thomas-Arrigo, 2012). This conclusion agrees with the results from the effluent organic concentrations. On average, following a total dose of 20 g/g, BTEX concentrations were less than 20% of their original concentrations in the effluent of the iron activated treatment columns. However, after this dose, average BTEX effluent concentrations in the unactivated persulfate treatment columns were less than 40% of original concentrations. For these reasons, iron activated persulfate would be more beneficial for a full-scale treatment than unactivated persulfate.

Following all dosing episodes, soil samples were taken from the bottom, middle and top of the control and treatment columns and analyzed for BTEX and PAH concentrations (Table 3.6). Raw data are located in Appendix F (Table F.11). Approximately 400g of NAPL was removed in the control column. Similarly to the unactivated column experiment, reductions in the control column were highest for BTEX compounds (>25%) and 100% reduction was seen in benzene, indeno[1,2,3-c,d] pyrene + dibenz [a,h] anthracene, and benzo [g,h,i] perylene. Reductions with less than 2% difference were seen between control and treatment columns for 1-methylnaphthalene, biphenyl, acenaphthylene and chrysene indicating that iron-activated persulfate did not assisting in the removal of these compounds in the NAPL.

Treatment columns showed more reduction in soil concentrations (550 mg) than the control column (27% more reduction observed). Results in reduction in BTEX compounds agree with those seen in the treatment columns; persulfate did not significantly contribute to BTEX reductions (48% in treatment compared to 44% in control). Oxidation of indole, acenaphthalene and anthracene were shown in the treatment columns (22%, 12% and 5% more reduction in treatment columns, respectively). All other compounds showed reduction of less than 5% compared to the control column.

The average initial sediment saturation level in the iron treatment columns was 3.99%. Final control and treatment column saturation levels were 1.51 and 1.44%, respectively.

3.6 Summary

Aquifer solids taken from the Clearwater site were analyzed to determine buffering capacity, COD and NOI. Poorly buffering solids were observed and could be advantageous for an alkaline activated persulfate system, however, it could also lead to enhanced persulfate degradation. The aquifer solids were also determined to have a COD between 0.09 and 0.17 meq/g. Comparing results from Clearwater samples to other COD investigations, it was determined that the aquifer has a relatively low COD. A low COD in the aquifer allows for a more efficient persulfate system since persulfate will persist for longer periods of time targeting contaminants as opposed to aquifer materials. Finally, the NOI of the soil with persulfate was determined. Persulfate degradation between 23.4 and 14.4% were observed over a 50-day period.

Batch aqueous experiments determined the potential for persulfate to oxidize the COC. Fe(II) (600 mg/L) activated persulfate was the most effective oxidation scheme, generating reaction rates up to 6 times faster than the Fe(II) (150 mg/L) case and up to 50 times faster than the unactivated case. With the higher iron concentration, all COCs were reduced < MDL within 6 hours, while in the lower iron experiment all COCs were reduced < MDL within 12 hours. Unactivated persulfate was able to reduce BTEX concentrations <MDL, however naphthalene and other PAHs were still > MDL after 14 days. Persulfate reduction for the unactivated, 150mg/L iron activated, and 600 mg/L iron activated experiments were 10%, 17%, and 60% respectively.

Column experiments, designed to mimic site conditions, determined the potential for persulfate to oxidize MGP contaminated sediments. Analyses of the effluent from the unactivated persulfate columns had benzene as the only COC < MDL, while acenaphthalene showed the most persistence with ~50% reduction, followed by naphthalene with ~60% reduction by the end of the experiment. Additional flushes

with alkaline activated persulfate reduced ethylbenzene and acenaphthalene concentrations to < MDL, and naphthalene concentrations by an additional 20%. Soil samples taken after the experiment showed 23% more removal in compounds than in the control column. Analyses of the effluent from the iron activated persulfate columns measured benzene and ethylbenzene < MDL, while naphthalene was the most persistent with 65% degradation. Soil samples from these columns taken at the conclusion of the experiment showed 27% more reduction in compounds than the control column. Results from the sediment analyses indicate the inability for persulfate to enhance the removal of source zone concentrations of: biphenyl in both explored persulfate systems; naphthalene, dibenzofuran, phenanthrene, fluoranthene, and pyrene in alkaline activated persulfate systems; and 1-methylnaphthalene, acenaphthylene and chrysene in iron activated persulfate systems. Finally, the results from the column experiments indicate that persulfate was not essential for removal of benzene compounds from the sediment.

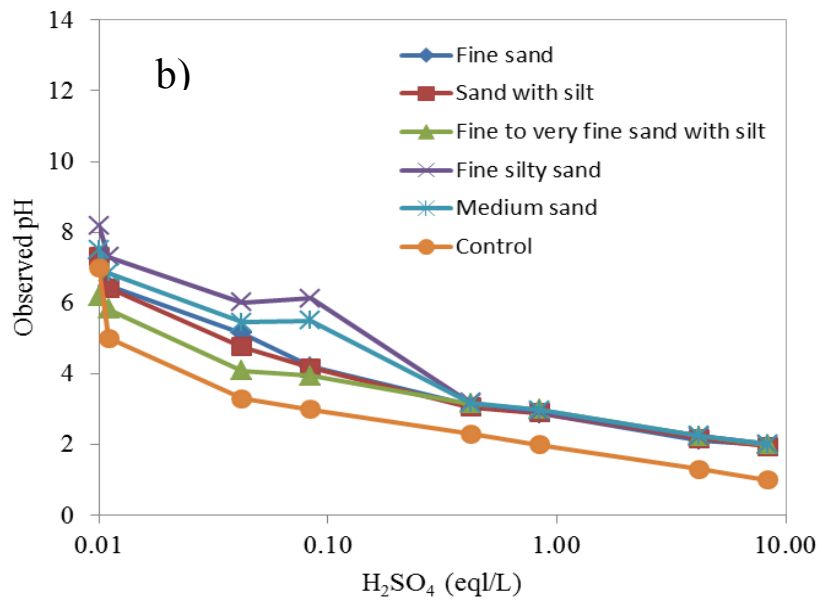
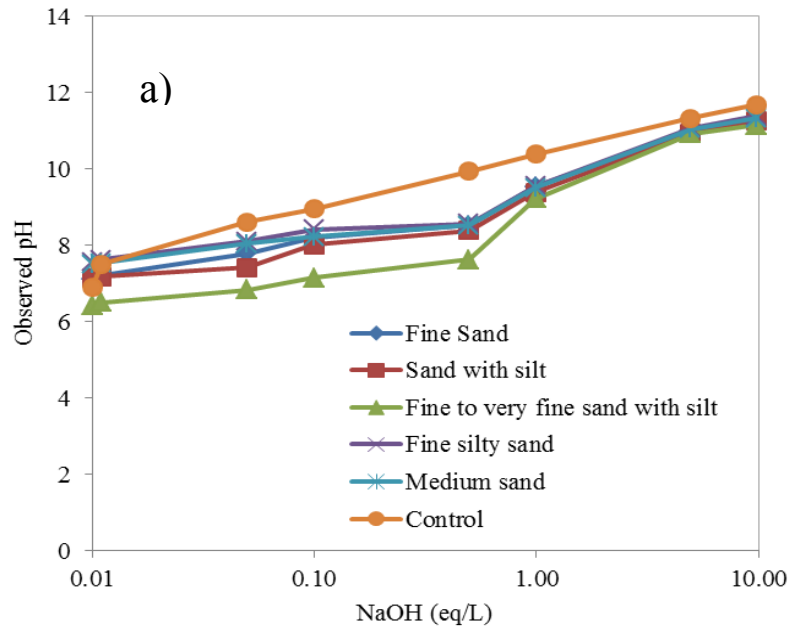


Figure 3.1. Buffering capacity in (a) basic and (b) acidic conditions for randomly selected sediment.

Table 3.1. COD of soil samples collected from randomly selected boreholes.

Description	Sample	Depth (m)	COD	Avg	Std Dev
			meq/g		
Fine sand	DPT - 19	4.3	0.086	0.102	0.022
Fine sand	DPT - 16	5.8	0.118		
Fine sand with silt	DPT - 26	4.3	0.109	0.121	0.011
Fine sand with silt	DPT - 18	6.1	0.123		
Fine sand with silt	DPT - 13	7.6	0.131		
Fine silty sand	DPT - 22	4.0	0.122	0.116	0.009
Fine silty sand	DPT - 18	7.6	0.110		
Fine to very fine silty sand	DPT - 13	4.6	0.123	0.118	0.008
Fine to very fine silty sand	DPT - 17	7.6	0.113		
Sand with silt and clay	DPT - 25	7.6	0.168	0.139	0.041
Sand with silt and clay	DPT - 25	8.5	0.110		
Very fine sand	DPT - 12	6.1	0.096	0.113	0.017
Very fine sand	DPT - 24	6.1	0.129		
Very fine sand	DPT - 17	7.0	0.113		
Very fine silty sand	DPT - 20	6.7	0.099	0.131	0.044
Very fine silty sand	DPT - 20	7.0	0.162		

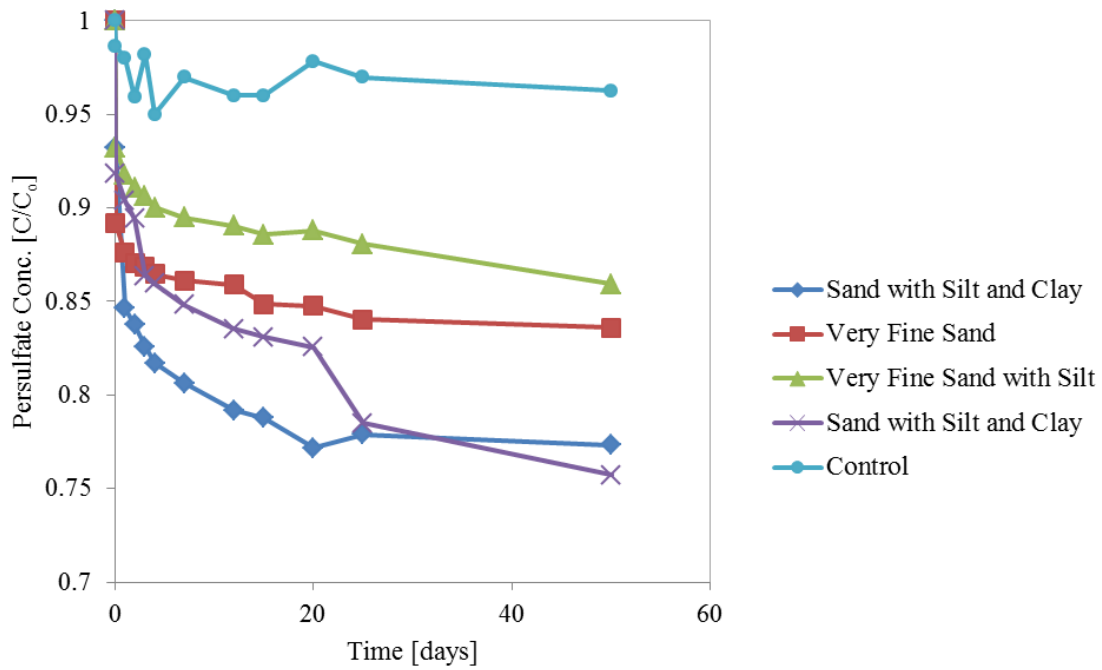


Figure 3.2. Persulfate decomposition due to natural oxidant demand for randomly selected sediment.

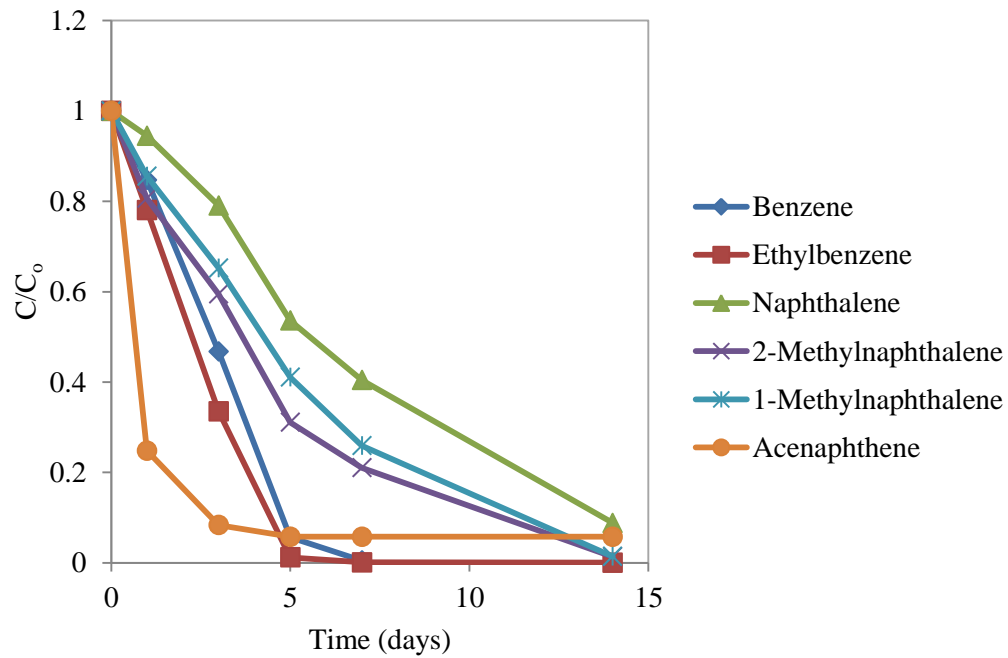


Figure 3.3. Degradation of the COC in unactivated persulfate aqueous treatability study.

Table 3.2. Reaction rate coefficients from aqueous treatability studies.

Compound	Unactivated - 20		Low		High - 600	
	k_{obs} (/day)	R^2	k_{obs} (/day)	R^2	k (mol ⁿ /L ⁿ /day) [n]	R^2
BTEX						
Benzene	0.068 ± 0.050	0.981	0.159 ± 0.016	0.955	0.007 ± 0.003 [1.03]	0.951
Toluene	0.080 ± 0.012	0.992	0.167 ± 0.014	0.947	0.021 ± 0.003 [1.03]	0.962
Ethylbenzene	0.072 ± 0.015	0.991	0.536 ± 0.021	0.989	0.059 ± 0.006 [0.743]	0.901
P,M-xylene	0.092 ± 0.015	0.919	0.543 ± 0.011	0.988	0.021 ± 0.005 [1.25]	0.931
O-xylene	0.108 ± 0.002	0.957	0.855 ± 0.005	0.958	0.042 ± 0.006 [0.866]	0.933
Trimethylbenzenes						
1,3,5-TMB	0.078 ± 0.017	0.910	0.144 ± 0.005	0.985	- ^a	- ^a
1,2,4-TMB	0.053 ± 0.005	0.958	0.690 ± 0.001	0.910	0.025 ± 0.009 [1.02]	0.956
1,2,3-TMB	0.077 ± 0.000	0.863	0.557 ± 0.015	0.995	0.026 ± 0.001 [1.02]	0.966
PAHs						
Naphthalene	0.009 ± 0.020	0.900	0.008 ± 0.006	0.988	0.051 ± 0.001 [0.289]	0.974
Indole	-	-	-	-	-	-
2-Methylnaphthalene	0.039 ± 0.030	0.875	0.998 ± 0.006	0.953	0.063 ± 0.003 [1.47]	0.944
1-Methylnaphthalene	0.062 ± 0.040	0.958	1.318 ± 0.006	0.986	0.013 ± 0.004 [1.44]	0.926
Biphenyl	0.007 ± 0.026	0.965	0.699 ± 0.102	0.962	1.99x10 ⁻⁶ ± 1x10 ⁻¹² [3.93]	0.940
Acenaphthylene	-	-	-	-	-	-
Acenaphthalene	0.029 ± 0.085	0.891	0.253 ± 0.01	0.962	- ^a	- ^a
Dibenzofuran	0.018 ± 0.098	0.926	0.151 ± 0.022	0.900	0.022 ± 0.002 [1.14]	0.941
Fluorene	0.023 ± 0.079	0.980	0.183 ± 0.005	0.990	- ^a	- ^a
Phenanthrene	0.015 ± 0.001	0.944	0.219 ± 0.002	0.937	1.5x10 ⁻⁶ ± 1x10 ⁻⁸ [2.15]	0.978
Anthracene	-	-	-	-	-	-
Carbazole	-	-	-	-	-	-
Fluoranthene	-	-	-	-	-	-
Pyrene	-	-	-	-	-	-
Benz [a] anthracene	-	-	-	-	-	-
Chrysene	-	-	-	-	-	-
Benz [b] Fluoranthene +	-	-	-	-	-	-
Benz [k]Fluoranthene	-	-	-	-	-	-
Benzo [a] Pyrene	-	-	-	-	-	-
Indeno[1,2,3-c,d] Pyrene +	-	-	-	-	-	-
Dibenz [a,h] Anthracene	-	-	-	-	-	-
Benzo [g,h,i] Perylene	-	-	-	-	-	-

^a insufficient data

- concentration > MDL

Table 3.3. Minimum Detectable Levels for site-specific compounds.

Compound	MDL (ug/L)
BTEX	
Benzene	1.11
Ethylbenzene	0.77
m-Xylene & p-Xylene	1.46
o-Xylene	0.37
Toluene	0.83
Trimethylbenzenes	
1,2,3-Trimethylbenzene	0.76
1,2,4-Trimethylbenzene	0.82
1,3,5-Trimethylbenzene	0.74
Naphthalene	6.61
PAHs	
1-Methylnaphthalene	1.31
2-Methylnaphthalene	4.27
Naphthalene	2.2
Acenaphthene	1.83
Acenaphthylene	1.53
Anthracene	5.53
Benz [a] anthracene	4.77
Benzo [a] pyrene	13.33
Benz [b, k] fluoranthene	5.62
Benzo [g,h,i] perylene	11.49
Biphenyl	3.26
Carbazole	7.18
Chrysene	5.75
Dibenzofuran	3.31
Fluoranthene	1.8
Fluorene	1.88
Indole	6.36
Indeno[1,2,3-c,d] pyrene + Dibenz [a,h] anthracene	18.65
Phenanthrene	3.78
Pyrene	1.6

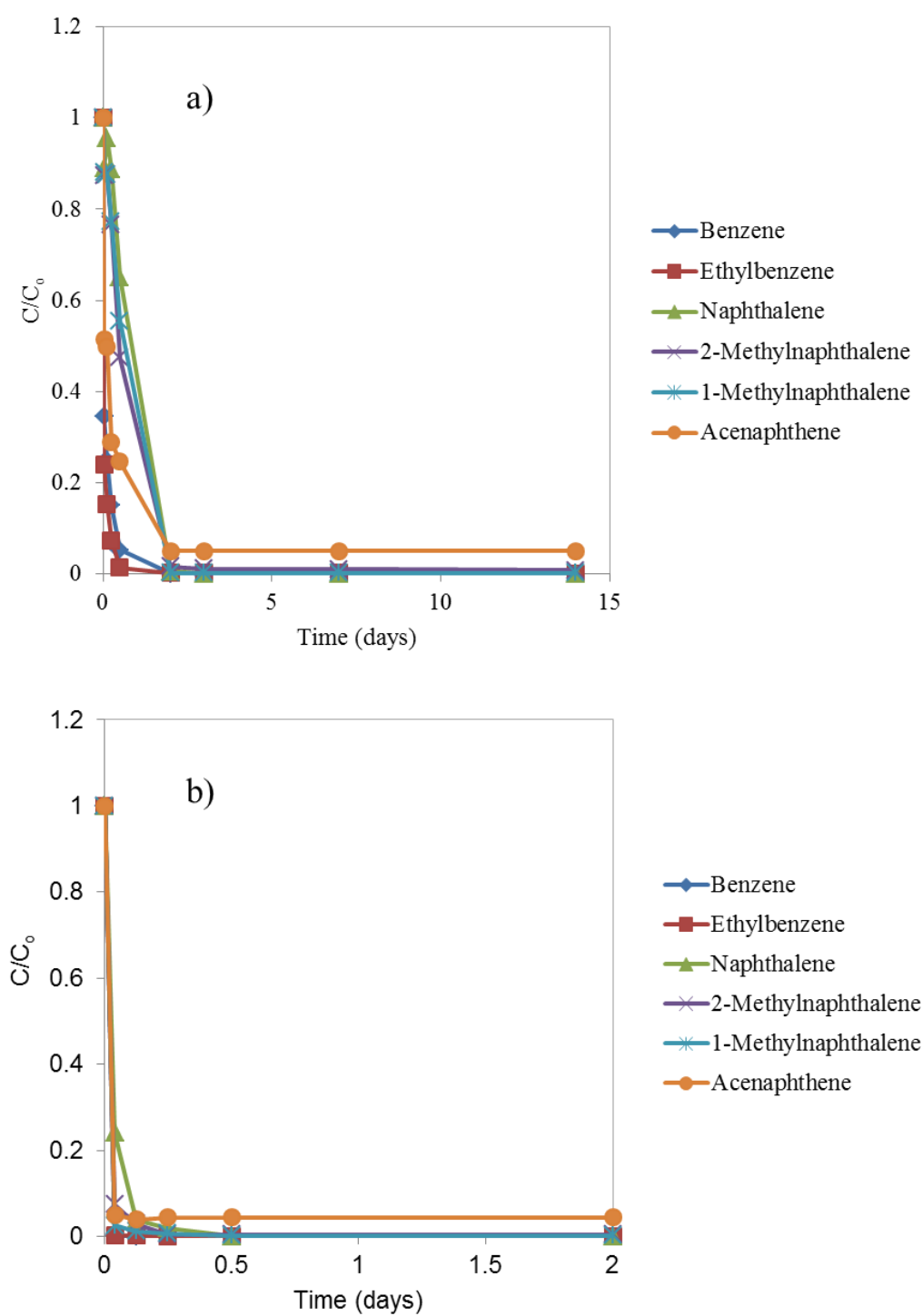


Figure 3.4. Iron(II) activated persulfate treatability for COC at a) low Fe, b) high Fe.

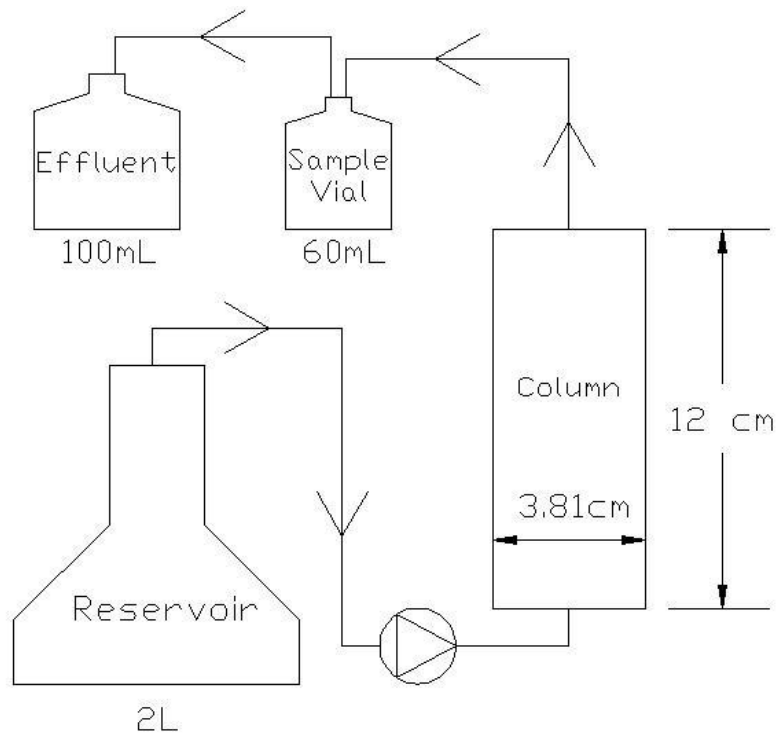


Figure 3.5. Column schematic.

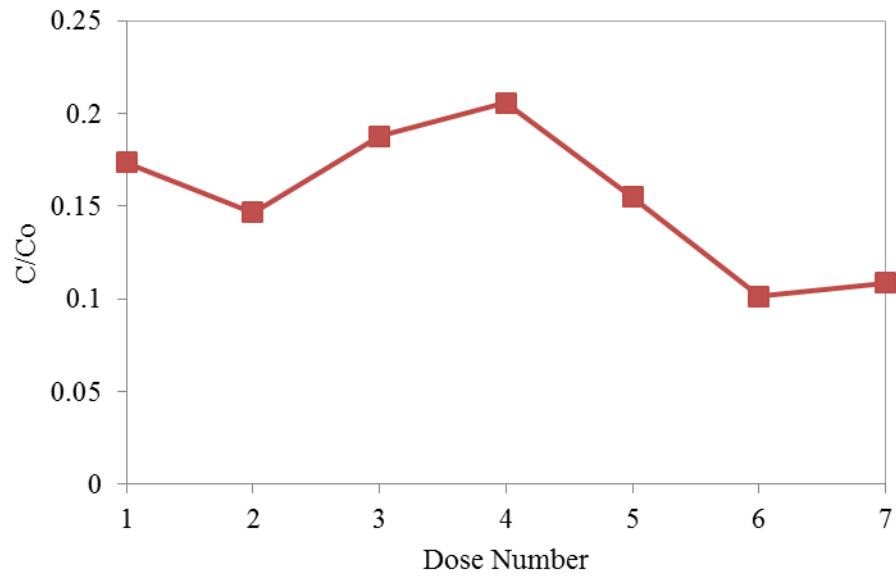


Figure 3.6. Unactivated persulfate effluent concentration following each dosing episode.

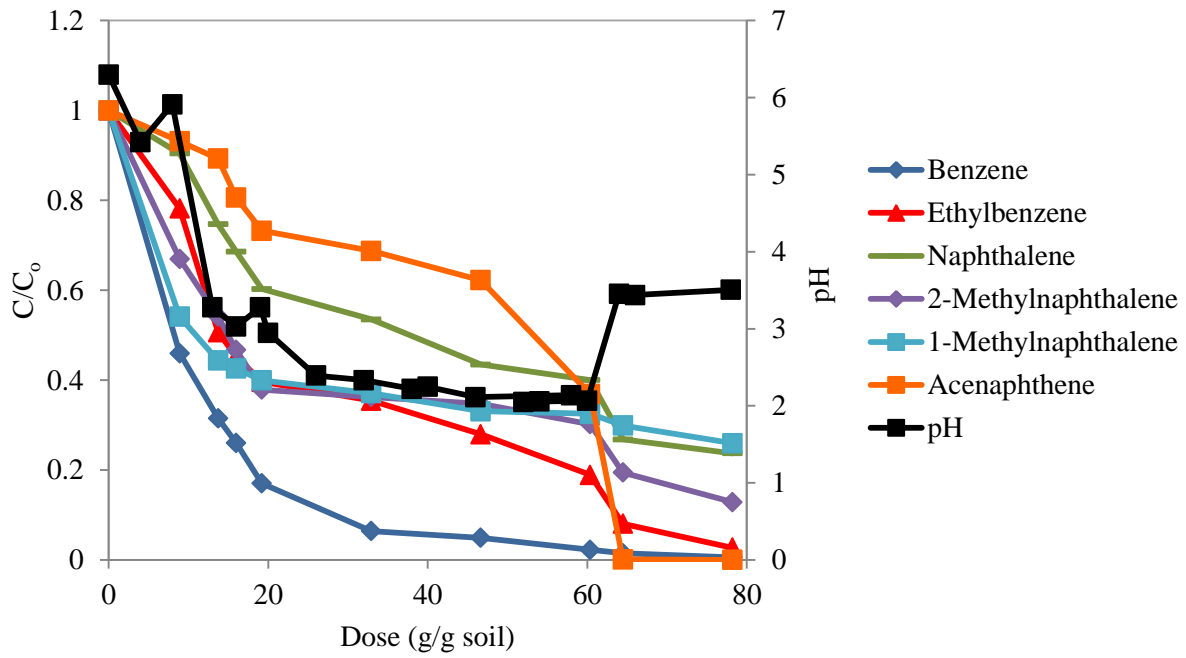


Figure 3.7. Dose-response curve for the average COC depletion for unactivated/alkaline activated persulfate columns. (Last two points represent samples taken after alkaline activated flushes).

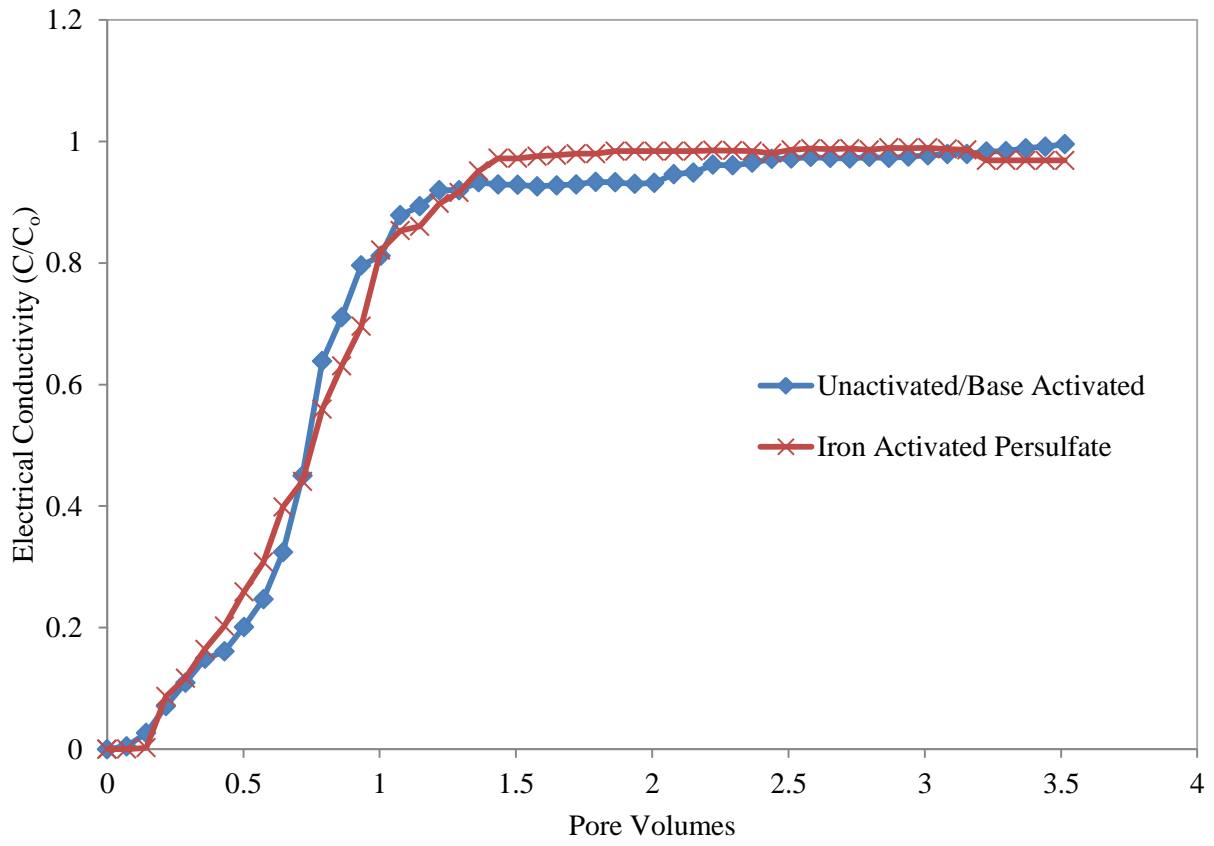


Figure 3.8. Persulfate breakthrough curves in column #1 for both series of column experiments.

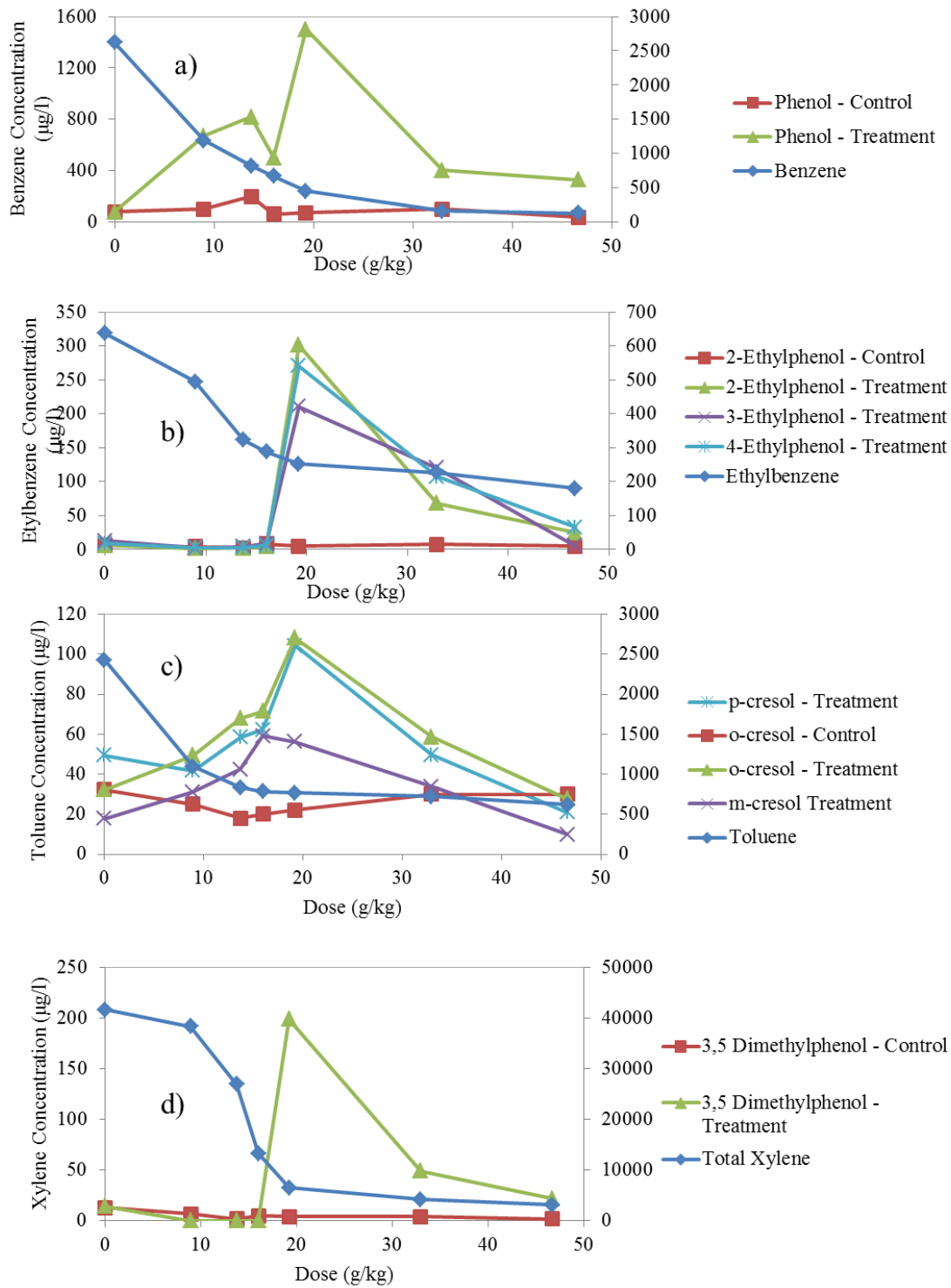


Figure 3.9. Relationships between SCAP and BTEX compounds (a) benzene and phenol, (b) ethylbenzene and ethylphenol, (c) toluene and cresol, (d) xylene and dimethylphenol.

Table 3.4. Average NAPL concentrations in unactivated/base activated persulfate columns.

Contaminant	Initial (mg/kg)			Final - Treatment (mg/kg)			% Reduction	Final- Control (mg/kg)			% Reduction
	Low (0-2 cm)	Middle (2-5 cm)	High (5-8 cm)	Low (0-2 cm)	Middle (2-5 cm)	High (5-8 cm)		Low (0-2 cm)	Middle (2-5 cm)	High (5-8 cm)	
BTEX											
Benzene	11.5	11.0	12.3	<MDL	<MDL	<MDL	100	<MDL	<MDL	<MDL	100
Toluene	79.7	70.0	70.5	10.6	12.5	3.49	87.90	15.6	17.3	14.25	78.6
Ethylbenzene	77.8	73.5	65.0	49.7	59.4	35.0	33.4	56.7	69.0	18.5	33.3
P,M-xylene	123	116	102	90.2	104	64.0	24.3	98.2	125	47.8	20.7
O-xylene	76.5	72.5	63.2	58.8	65.1	45.5	20.2	67.5	77.7	33.5	15.8
Trimethylbenzenes											
1,3,5-Trimethyl-Benzene	34.4	33.5	38.1	31.6	34.2	29.3	10.3	31.7	36.5	22.4	10.3
1,2,4-Trimethyl-Benzene	151	147	122	128	140	120	7.38	143	161.59	98.62	7.38
1,2,3-Trimethyl-Benzene	51.4	49.7	41.4	41.1	44.3	36.8	14.3	48.1	54.1	30.6	14.3
PAHs											
Naphthalene	1040	1010	1040	951	974	869	9.6	946	1029	623	16.0
Indole	10.0	10.4	8.78	5.91	6.31	5.00	40.96	7.98	8.51	6.34	21.7
2-Methylnaphthalene	728	729	723	701	732	644	4.78	686	742	515	10.9
1-Methylnaphthalene	420	424	443	413	430	378	5.13	405	437	305	10.9
Biphenyl	89	87	70	46	48	41	45.0	45	47	33.8	48.8
Acenaphthylene	141	140	116	93	100	87	29.2	124	133	91.6	12.1
Acenaphthene	61.0	60.5	49.7	53	55	48	8.36	56.6	60.4	41.3	7.6
Dibenzofuran	58.8	58.1	57.7	54	56	48	9.79	52.9	56.4	39.0	15.1
Fluorene	151	159	170	159	165	127	5.89	170	182	124	0.729
Phenanthrene	363	361	366	345	354	310	7	334	356	242	14.5
Anthracene	41.7	42.6	35.2	30.9	32.1	26.7	24.9	41.4	43.6	27.1	6.11
Carbazole	<MDL	<MDL	<MDL	<MDL	<MDL	<MDL	<MDL	<MDL	<MDL	<MDL	<MDL
Fluoranthene	92.3	91.0	93.9	83.7	84.0	75.5	12.3	79.7	83.9	55.4	21.0
Pyrene	154	153	154	129	127	116	19.4	128	133	87.9	24.3
Benz [a] anthracene	29.2	28.9	29.9	24.5	24.5	24.0	17.1	24.4	25.9	15.2	25.6
Chrysene	29.2	28.7	27.9	28.0	27.8	27.0	3.64	26.5	27.7	17.3	16.7
Benz [b] Fluoranthene + Benz [k] Fluoranthene	31.4	32.7	30.9	25.8	24.1	22.2	24.0	22.9	23.4	15.0	35.4
Benzo [a] Pyrene	23.1	22.7	17.8	13.3	11.9	13.2	39.7	14.1	14.8	9.31	39.8
Indeno[1,2,3-c,d] Pyrene + Dibenz [a,h] Anthracene	4.1	5.6	2.2	<MDL	<MDL	<MDL	100.00	<MDL	<MDL	<MDL	100.00
Benzo [g,h,i] Perylene	7.1	7.4	2.2	<MDL	<MDL	<MDL	100.00	<MDL	<MDL	<MDL	100.00

Note: MDL = minimum detectable level

Table 3.5. Average initial and final NAPL saturation in treatment and control columns.

Compound	C _n	Initial		Final			
		Unactivated C _s	Iron Activated C _s	Unactivated Treatment C _s	Unactivated Control C _s	Iron Activated Treatment C _s	Iron Activated Control C _s
		g/kg	g/kg	g/kg	g/kg	g/kg	g/kg
BTEX							
Benzene	78.7	32.6	38.8	-	-	-	-
Toluene	0.635	20.1	236	23.8	42.1	24.0	22.4
Ethylbenzene	0.486	194	224	129	129	121	131
P,M-xylene	6.14E+03	306	350	231	242	222	237
O-xylene	0.467	191	217	151	160	141	157
Trimethylbenzenes							
1,3,5-Trimethylbenzene	0.225	85.5	96.4	85.0	81.0	86.9	90.4
1,2,4-Trimethylbenzene	2.49E+04	375	423	348	360	345	370
1,2,3-Trimethylbenzene	0.248	127	145	109	119	110	116
PAHs							
Naphthalene	72.8	2.58E+03	2.92E+03	2.32E+03	2.50E+03	2.56E+03	2.69E+03
Indole	2.15E+05	26.1	29.6	20.4	15.4	15.4	16.1
2-Methylnaphthalene	47.2	1.78E+03	2.02E+03	1.74E+03	1.86E+03	1.88E+03	1.98E+03
1-Methylnaphthalene	-	1.05E+03	1.18E+03	1.03E+03	1.09E+03	1.12E+03	1.17E+03
Biphenyl	3.36	218	243	113	121	124	128
Acenaphthylene	-	353	395	312	2.51E+02	252	267
Acenaphthene	2.25	152	172	141	1.40E+02	144	149
Dibenzofuran	1.13	146	165	133	141	146	150
Fluorene	5.53	322	452	426	404	371	427
Phenanthrene	17.4	908	1016	833	903	937	964
Anthracene	2.98	106	117	100.3	80.2	83.0	84.9
Carbazole	0.106	-	-	-	-	-	-
Fluoranthene	4.86	229	256	196	218	227	233
Pyrene	7.68	384	430	312	332	347	356
Benz [a] anthracene	2.23	71.4	80.4	58.6	65.2	70.2	70.9
Chrysene	2.15	72.0	81.2	64.0	74.0	74.7	80.1
Benz [b] Fluoranthene + Benz [k]Fluoranthene	2.00	72.0	80.9	54.9	64.5	71.1	71.9
Benzo [a] Pyrene	2.06	56.3	62.5	34.2	34.3	38.5	37.7
Indeno[1,2,3-c,d] Pyrene + Dibenz [a,h] Anthracene	0.865	9.55	6.78	-	-	-	-
Benzo [g,h,i] Perylene	2.99	16.0	16.4	-	-	-	-
SUM	2.46E+05	9.88E+03	1.14E+04	8.96E+03	9.43E+03	9.51E+03	9.99E+03
% Saturation		4.02	4.66	3.65	3.83	3.87	4.07

Note: (-) < MDL

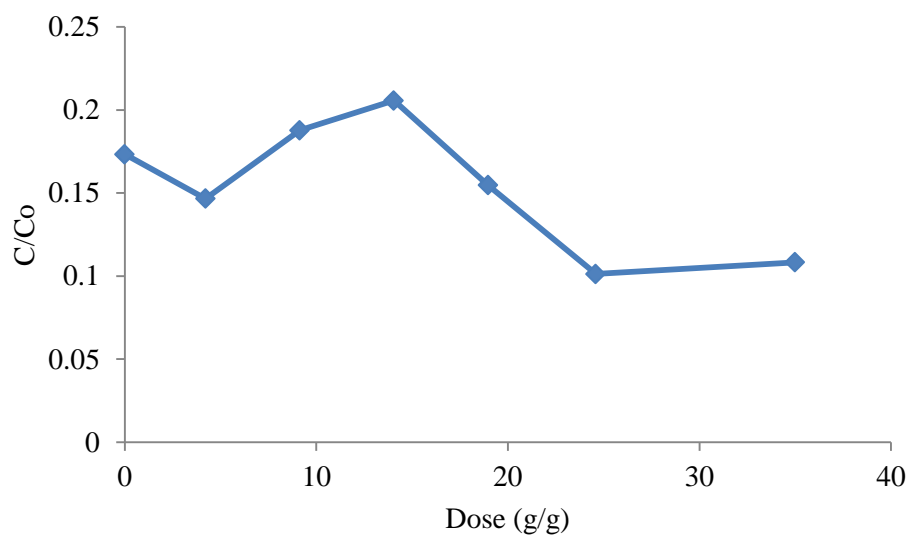


Figure 3.10. Iron activated persulfate effluent concentration.

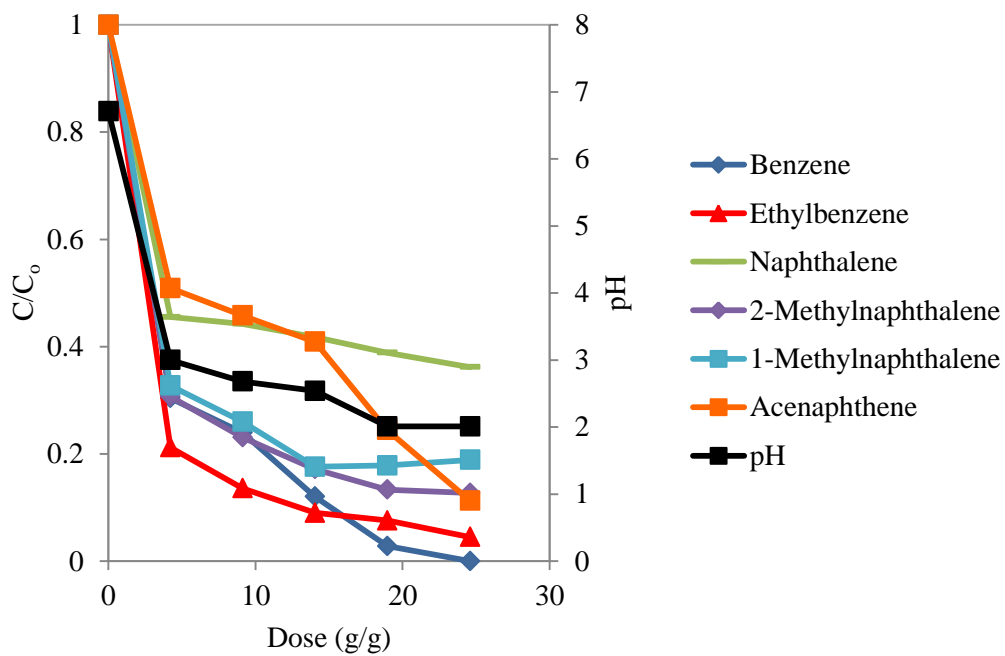


Figure 3.11. Average dose-response curves for the average COC depletion in the iron activated persulfate columns.

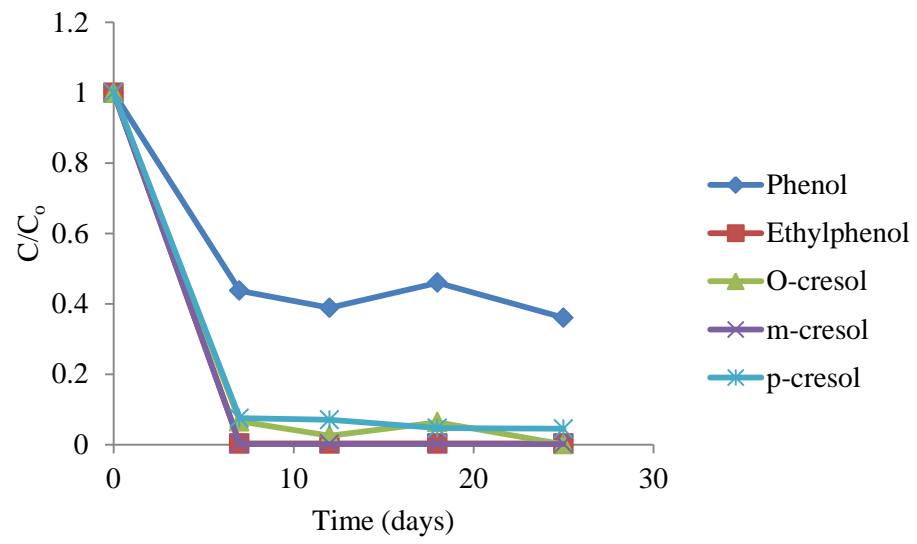


Figure 3.12. SCAP concentrations from iron activated columns.

Table 3.6. NAPL concentrations in iron activated treatment columns.

Contaminant	Initial Average Soil Concentrations - Treatment (mg/kg)			Final Soil Average Concentrations - Treatment (mg/kg)			% Reduction	Average Final Soil Concentration - Control (mg/kg)	% Reduction
	Low (0-2 cm)	Middle (2-5 cm)	High (5-8 cm)	Low (0-2 cm)	Middle (2-5 cm)	High (5-8 cm)			
BTEX									
Benzene	15.9	12.8	14.6	<MDL	<MDL	<MDL	100	<MDL	100
Toluene	89.4	90.7	83.6	5.20	9.38	10.4	90.5	8.95	87.1
Ethylbenzene	84.3	88.5	77.2	49.9	47.2	49.4	41.4	45.2	37.8
P,M-xylene	129	141	121	90.7	84.1	89.7	32.5	82.8	28.0
O-xylene	79.3	87.5	75.5	62.9	53.6	58.6	27.7	52.7	26.7
Trime thylbenzenes									
1,3,5-Trimethyl-Benzene	35.2	39.1	33.4	40.4	29.3	31.5	6.18	32.4	2.21
1,2,4-Trimethyl-Benzene	156	171	147	165	120	128	12.7	129	11.3
1,2,3-Trimethyl-Benzene	53.1	59.3	49.7	51.2	37.7	41.0	19.9	40.9	16.9
PAHs									
Naphthalene	1080	1170	1010	1200	857	949	7.8	953	4.49
Indole	11.2	11.4	10.5	6.80	5.31	5.89	45.7	5.75	43.2
2-Methylnaphthalene	741	823	694	878	639	699	1.85	702	0.245
1-Methylnaphthalene	436	474	407	515	375	412	1.09	418	0.377
Biphenyl	89.6	100	81.5	55.9	42.0	45.8	47.1	46.1	46.4
Acenaphthylene	146	160	136	120	86	93	32.4	94.1	31.9
Acenaphthene	63.0	70.1	59.0	65.8	48.2	53.1	13.0	53.7	10.3
Dibenzofuran	60.5	67.2	56.9	65.8	48.7	53.4	9.10	54.5	5.20
Fluorene	163	177	166	175	144	158	5.5	138	8.58
Phenanthrene	377	410	349	422	312	344	5.10	349	1.96
Anthracene	45.1	45.5	39.7	36.6	27.6	30.7	27.2	30.9	25.6
Carbazole	<MDL	<MDL	<MDL	<MDL	<MDL	<MDL	<MDL	<MDL	<MDL
Fluoranthene	94	104	88	103	74	83	8.96	84.7	5.82
Pyrene	159	177	145	158	112	128	17.3	129	14.1
Benz [a] anthracene	28.6	33.4	27.8	33	22	24	11.8	26.2	8.92
Chrysene	29	34	28	37.03	24.64	27.89	1.41	27.8	2.21
Benz [b] Fluoranthene + Benz [k]Fluoranthene	29.9	33.7	26.9	33.2	21.5	25.7	11.1	26.5	6.41
Benzo [a] Pyrene	22.9	25.8	21.1	18.4	10.7	13.1	39.6	14.3	35.9
Indeno[1,2,3-c,d] Pyrene + Dibenz [a,h]	1.8	3.5	2.2	<MDL	<MDL	<MDL	100.00	<MDL	100
Anthracene									
Benzo [g,h,i] Perylene	7.9	8.3	2.3	<MDL	<MDL	<MDL	100.00	<MDL	100

Chapter 4

Conclusions and Recommendations

The research conducted for this thesis enhanced the site conceptual model and evaluated the potential for persulfate to treat residuals at a former MGP site. This evaluation was achieved through bench-scale, batch aqueous and column treatability studies.

An extensive site characterization was conducted at the former Clearwater Beach MGP site in Florida. The lithology of the site is spatially consistent with a homogeneous sand aquifer (water table at 1.5 m (5 ft) bgs) overlying a clay unit (~7.5 m, (25 ft) bgs). The aquifer was estimated to have a porosity of 0.34 and an average hydraulic conductivity, determined from slug tests, of 2.3×10^{-3} cm/s. Using pressure transducer measurements the groundwater flow was characterized to have a Darcy flux of 0.0193 m/day in the direction of S20°E.

Extents of source areas in both deep (>4.5 m) and shallow (<4.5 m) zones of the aquifer were estimated based on borehole logs and soil and water sample analyses. A total source volume of approximately 84.8 m³ exists in the shallow zone of the aquifer and a total source volume of approximately 42.4 m³ exists in the deep zone of the aquifer. Downgradient of these source zones, a transect of ten multilevel wells was installed perpendicular to groundwater flow to determine dissolved BTEX and PAH concentrations and mass discharge across the site. BTEX plumes were determined to be predominately located at the water table, trimethylbenzene plumes in the middle of the aquifer, and PAH plumes near the clay unit. On average, the groundwater plumes were relatively constant in concentration and morphology over the 12 month sampling period. Total mass discharge of contaminants across the site was estimated to be 94 mg/day. Of the compounds measured, the mass discharge of naphthalene was greatest (44 mg/day).

Samples of MGP residual were analyzed to characterize the source material. Approximately 30% of the constituents were identified. Of this 30%, naphthalene was the predominant compound (27%), followed by 2-methylnapthalene (18%), and 1-methylnapthalene (10%).

Bench-scale tests were conducted to determine buffering capacity, COD and NOI of the Clearwater aquifer sediments. Poor buffering capacity was observed, indicating the probability of

pH shifts during persulfate injections. These shifts could be advantageous for an alkaline activated persulfate system. COD tests indicate that the aquifer has a low reductive capacity, between 0.09 and 0.17 meq/g. Finally, NOI results indicated minimal degradation of persulfate due to aquifer interactions (~14-23%). Knowledge of this range will be applied when determining the optimal full-scale injection dose to ensure persulfate persistence within the aquifer.

Batch aqueous experiments were conducted and showed the ability for persulfate and iron activated persulfate to oxidize PAHs and BTEX in site groundwater. Persulfate (20g/L) activated with 600 mg/L-Fe(II) was the most effective oxidation system tested. Degradation of all COCs was observed within 6 hours after the commencement of this experiment. Reaction rates were calculated to be up to 6 times faster than using 20g/L persulfate activated with 150mg/L-Fe(II) and 50 times faster than using 20g/L of unactivated persulfate. However, persulfate decomposition was greater with the increased iron dosage (60% consumed, compared to 17%). Unactivated persulfate was unable to reduce some PAHs below MDL by the end of the 14-day experiment.

Two series of column experiments were conducted to determine the potential for persulfate to oxidize MGP impacted sediments. The first experiment, conducted with unactivated persulfate, yielded final reductions in effluent concentrations of BTEX and PAHs between 78-98% and 45-87%, respectively. Additional flushes were conducted with alkaline activated persulfate and yielded further reductions in effluent concentrations (94-99% and 75-99%). Soil samples taken from the columns indicated that persulfate removed 23% more mass than the control column but did not assist in the removal of BTEX compounds and had no impact on naphthalene, dibenzofuran, phenanthrene, fluoranthene, biphenyl and pyrene concentrations. The second experiment, conducted with iron activated persulfate, yielded final reductions in effluent concentrations of BTEX and PAHs between 70-99% and 65-97%, respectively. Soil samples taken at the conclusion of the experiment showed iron activated persulfate increased reduction in compounds by 27% relative to water flushing but, similar to the first experiment, removal of BTEX compounds were independent of iron activated persulfate addition and it was unable to oxidize 1-methylnaphthalene, acenaphthylene and chrysene.

4.1 Recommendations

The conceptual site model could be enhanced through additional borehole installations surrounding source zones to further characterize their spatial extents. Specifically, the large shallow and deep sources located upgradient of the metershop. Additionally, further groundwater sampling of the transect would provide a better understanding of long-term changes in the movement of the plumes and mass discharge across the site. Currently, the degree of contamination in the clay unit is unknown. Samples from this unit should be collected and analyzed in order to provide an estimate of the degree of contamination.

Additional bench-scale tests would be beneficial in the determination of treatability endpoints. In the high (600 mg-Fe(II)/L) iron-activated persulfate treatability study, reactions occurred very quickly. Measurements taken in shorter sampling intervals would provide a better estimation of reaction kinetics for the COC. The column experiments provided insight on the treatability of impacted sediments with unactivated, Fe(II)-activated, and alkaline activated persulfate. Completion of another series of column experiments, increasing the reaction period (from 4 days to 8 days), may be beneficial. Originally, a four day reaction period was selected to allow for kinetic processes to occur within the columns after a persulfate dose. However, there is a possibility that this timeframe may be too short. Measurements of effluent persulfate concentration taken after doses indicate an excess of persulfate within the system, meaning the potential for further oxidation. Therefore increasing the reaction period could be beneficial in promoting degradation of COC.

The next step in the project is to conduct push-pull tests (PPTs) to further and more accurately assess the ability for persulfate to treat MGP residuals *in situ*. Based on the site characterization, proposed locations for the PPTs are: between DPT-5 and DPT-23 (18' – 19.5' bgs) and between DPT-22 and DPT-23 (11'-12.5' bgs). These locations were chosen to assess treatability potential in the shallow and deep zones of the aquifer. Additionally, borehole installations indicated these areas are heavily saturated with NAPL.

Based on the completed bench-scale tests, iron activated persulfate (600 mg/L iron) or alkaline activated persulfate are recommended for the PPTs. Treatability studies showed that these schemes are more aggressive and effective than unactivated persulfate for the oxidation of MGP residuals, especially with higher molecular weight PAHs. Injections of activated persulfate are anticipated to reduce aqueous concentrations of both BTEX and PAHs to below NADC levels.

Based on the mass removal observed in the column analyses conducted, it is expected that complete oxidation is not realistic using either unactivated, iron (II) activated, or alkaline activated persulfate. Activated persulfate showed the most potential for mass reduction, however, final concentrations measured in column sediments indicate that, for the majority of compounds, alkaline-activated persulfate doses were not more effective than water flushing in the reduction of BTEX and PAH compounds. Therefore, further investigation into other treatment options for source depletion is recommended.

References

- Batu, V. 2006. Applied flow and solute transport modeling in aquifers: fundamental principles and analytical and numerical methods. CRC Press. Boca Raton, FL, USA.
- Beltran, F.J., Gonzalez, M., Rivas, F., Alvarez, P., 1997. Fenton reagent advanced oxidation of polynuclear aromatic hydrocarbons in water. Departamento de Ingenieria Quimica y Energetica, Universidad de Extremadura, Badajoz, Spain.
- Block, P.A., Brown, R.A., Robinson, D. 2004. Novel Activation Technologies for Sodium Persulfate *In Situ* Chemical Oxidation, Proceedings of the Fourth International Conference on the Remediation of Chlorinated and Recalcitrant Compounds. Monterey, CA.
- Bockelmann, A., Ptak, T., Teutsch, G. 2001. An analytical quantification of mass fluxes and natural attenuation rate constants at a former gasworks site. *J. Contam. Hydrol.* 53, 429-453.
- Bogan B.W., Trbovic V. 2003. Effect of sequestration on PAH degradability with Fenton's reagent: Roles of total organic carbon, humin, and soil porosity. *J. Hazard Materials.* 100, 285-300.
- Bogan, B., Trbovic V., Paterek, R.J. 2003. Inclusion of vegetable oils in Fenton's chemistry for remediation of PAH-contaminated soils. *Chem.* 50 (1), 15-21.
- Brown, D.G., Knightes C.D., Peters, C.A. 1999. Risk assessment for polycyclic aromatic hydrocarbon NAPLs using component fractions. *Environ. Sci. Technol.* 33, 4357-4363.
- Brown, G.S., Barton, L.L., Thomson, B.M. 2003. Permanganate oxidation of sorbed polycyclic aromatic hydrocarbons. *Waste Management* 23, 737-740.
- Chapman M.J., Gallaher B.M., Early D.A. 1990 A preliminary investigation of the hydrogeology and contamination in the area of an abandoned manufactured gas plant in Albany, Georgia. US Geological Survey Water-Resources Investigations Report 90-4141.
- Crimi M., Taylor J. 2007. Experimental Evaluation of Catalyzed Hydrogen Peroxide and Sodium Persulfate for Destruction of BTEX Contaminants. *Soil and Sed. Contam.* 16(1), 29-45.
- Eberhardt, C., Grathwohl, P. 2002. Time scales of organic contaminant dissolution from complex source zones: coal tar pools vs. blobs. *J. Contam., Hydrol.* 59(1-2), 45-66.
- Eng R. 1985. Survey of Town Gas and By-product Production and Location in the United States (1880-1950). U.S. Environmental Protection Agency. Washington, D.C.
- EPA (Environmental Protection Agency). 1999. A rational approach to the remediation of soil and ground water and MGP sites: A resource for MGP site characterization and remediation. U.S. Environmental Protection Agency, Washington D.C.
- EPA (Environmental Protection Agency). 1999. A resource for MGP site characterization and remediation expedited site characterization and source remediation at former manufactured gas plant sites, U.S. Environmental Protection Agency, Washington, D.C.
- Fischer, C., Schmitter, R., Lane, E. 1999. Manufactured gas plants: the environmental legacy. Georgia Institute of Technology, Atlanta, Georgia, USA.
- Ferrarese, E., Andreottola, G., Oprea, I.A. 2008. Remediation of PAH-contaminated sediments by chemical oxidation, *J. Hazard. Mater.* 152;1,128-139.
- Forsey, S.P. 2004. In situ chemical oxidation of creosote/coal tar residuals: experimental and numerical investigation. Ph.D. Thesis, University of Waterloo, Waterloo, ON.
- Freitas, J.G., Barker, J.F. 2008. Sampling VOCs with porous suction samplers in the presence of ethanol: How much are we losing? *Ground Water Monit. Rem.* 28(3),83-92.
- Gates-Anderson, D.D., Siegrist, R.L., Cline, S.R. 2001. Comparison of potassium permanganate and hydrogen peroxide as chemical oxidants for organically contaminated soils. *J. Environ. Eng.* 127:337-347.

- Goi, A., Trapido, M. 2004. Degradation of polycyclic aromatic hydrocarbons in soil: the Fenton reagent versus ozonation. *Environ. Tech.* 25:2, 155-164.
- Goltz, M.N., Kim, S., Hyouk, Y., Park, J., 2007. Review of groundwater contaminant mass flux measurement. *Korean Society of Environ. Eng.* 12(4):176-193.
- Gryzenia, J., Cassidy, D., Hampton, D. 2009. Production and accumulation of surfactants during the chemical oxidation of PAH in soil. *Chem.* 77, 540-545.
- Guilbeault, M.A., Parker B.L. and Cherry, J.A.. 2005. Mass and flux distributions from DNAPL zones in sandy aquifers. *Ground Water.* 43(1), 70-86.
- Haley, J.L., Hanson, B., Enfield, C. and Glass, J., 1991. Evaluating the effectiveness of groundwater extraction systems. *Ground Water Monit.* 11(1): 119-124.
- Hsu I-Y, Masten S.J. 2001. Modeling transport of gaseous ozone in unsaturated soils. *J. Env. Eng.* 127:546-554.
- Huang, K., Zhao, Z., Hoag, G.E., Dahmani, A., Block, P. 2005. Degradation of volatile organic compounds with thermally activated persulfate oxidation. *Chem.* 61, 551-560.
- ITRC (Interstate Technology and Research Council). 2005. Technical and regulatory guidance for in situ chemical oxidation of contaminated soil and groundwater, ISCO-2. Washington, D.C., Interstate technology & Regulatory Council, *In Situ Chemical Oxidation Team*, 2nd ed.
- ITRC (Interstate Technology and Research Council). 2010. Use and Measurement of Mass Flux and Mass Discharge. Washington, D.C., Interstate technology & Regulatory Council, Integrated DNAPL Site Strategy Team.
- Kanel, S.R., Neppolian, B., Jung, H., Choi, H. 2004. Comparative removal of polycyclic aromatic hydrocarbons using iron oxide and hydrogen peroxide in soil slurries. *Environ. Eng. Sci.* 21 (6), 741-751.
- Kang, N., Hua, I. 2005. Enhanced chemical oxidation of aromatic hydrocarbons in soil systems. *Chem.* 61,909-922.
- Kavanaugh, M.C., S.C. Rao, L. Abriola, J. Cherry, G. Destouni, R. Falta, D. Major, J. Mercer, C. Newell, T. Sale, S. Shoemaker, R. Siegrist, G. Teutsch, K. Udell. 2003. The DNAPL remediation challenge: Is there a case for source depletion? U.S. EPA: National Risk Management Research Laboratory, Ada, Ok.
- Kong, S., Watts, R.J., Choi, J. 1998. Treatment of petroleum contaminated soils using iron mineral catalyzed hydrogen peroxide. *Chem.* 37 (8), 1473-1482.
- Killian, P.F., Bruell, C.J. Liang, C., Marley, M.C. 2007. Iron (II) activated persulfate oxidation of MGP contaminated soil. *Soil and Sed. Contam.* 16, 523-537.
- King, M.W.G., Barker, J.F. 1999. Migration and natural fate of a coal tar creosote plume 1. Overview and plume development. *J. of Cont. Hydrol.* 39, 249-279.
- Krembs, F., Siegrist, R., Crimi, M., Furrer, R., and Petri, B. 2010. ISCO for Groundwater Remediation: Analysis of Field Applications and Performance. *Ground Water Monit. Remediat.*, 30(4),42-53.
- Lane W.F., Loehr, R.C. 1992. Predicting aqueous concentrations of polynuclear aromatic hydrocarbons in complex mixtures. *Environ. Sci. Technol.* 26, 983-990.
- Lee, L.S., Rao, P.S., Okuda, I. 1992. Equilibrium partitioning of polycyclic aromatic hydrocarbons from coal tar into water. *Environ. Sci. Technol.* 26 (11), 2110-2115.
- Levenspiel, O. 1998. Chemical reaction engineering – 3rd Edition. Wiley. Hoboken, NJ, USA.
- Lou, J.C., Lee, S.S. 1993. Chemical oxidation of BTX using Fenton's reagent. *Hazard. Waste and Hazard. Mater.*, 12 (2),186-193.
- Lehr, J., Hyman, M., Gass, T., and Seevers, W. 2001. Handbook of Complex Environmental Remediation Problems. McGraw-Hill, New York, NY.

- Liang, C., Hyang, C., Chen, Y. 2008. Potential for activated persulfate degradation of BTEX contamination. *Water Res.*, 42(15),4091-4100.
- Lundstedt S, Persson Y, Oberg L. 2006. Transformation of PAHs during ethanol-Fenton treatment of an aged gasworks' soil. *Chem.* 65:1288–1294.
- Luthy, R.G., Dzombak, D.A., Peters C.A., Roy, S.B., Ramaswami, A., Nakles, D.V., Nott, B.R. 1994. Remediating tar-contaminated soils at manufactured gas plant sites. *Environ. Sci. Tech.* 28,266A-276A.
- Major, D. 2009. Remediation of DNAPL through sequential in situ chemical oxidation and bioaugmentation. Prepared for ESTCP (Project ER-200116), Arlington, Virginia. Final Report.
- MacKay, A.A., Gschwend P.M. 2001. Enhanced concentrations of PAHs in groundwater at a coal tar site. *Environ. Sci. Tech.* 35 (7), 1320–1328.
- Marvin, B. K., Nelson, C. H., Clayton, W., Sullivan, K. M., Skladany, G. 1998. In-situ chemical oxidation of Pentachlorophenol and polycyclic aromatic hydrocarbons: From laboratory tests to field demonstration. *The First International Conference on Remediation of Chlorinated and Recalcitrant Compounds, Vol. C1-5: Physical, Chemical, Thermal Technologies, Monterey, CA*, pp. 383-388.
- McGowan, T., Greer, B., Lawless, M. 1996. Thermal treatment and non-thermal treatment technologies for remediation of manufactured gas plant sites. *Waste Management* 16(8)691-698.
- McGovern, T.; Guerin, T. F.; Horner, S.; Davey, B. 2002. Design, construction and operation of a funnel and gate in-situ permeable reactive barrier for remediation of petroleum hydrocarbons in groundwater. *Water, Air, Soil Pollution*. 136, 11-31.
- McGuire, T. M., J. M. McDade, C.J. Newell. 2006. Performance of DNAPL source depletion technologies at 59 chlorinated -solvent-impacted sites. *Ground Water Monit. Remediat.* 26,1; 73–84.
- Moo-Young, H., Brown, D. 2004. Laboratory assessment of leaching potential of coal tar at MGP sites. EPRI, Palo Alto, CA.
- Moo-Young, H., Mo, X., Waterman, R., Coleman, A., Saroff, S. 2009. Investigation of coal tar mobility at a former MGP site. *J. Hydrol. Eng.* 14,11;1221-1234.
- Nam, K., Rodriguez, W., Kukor, J.J. 2001. Enhanced degradation of polycyclic aromatic hydrocarbons by biodegradation combined with a modified Fenton reaction. *Chem.* 45, 11-20.
- Nadim, F., Huang, K. C., Dahmani, A.M. 2005. Remediation of soil and ground water contaminated with PAH using heat and Fe(II)-EDTA catalyzed persulfate oxidation. *Water Air Soil Pollution Focus.* 6,227–232.
- Nelson, C.H. 1997. Ozone sparging for the remediation of MGP contaminants. *Proceedings of the Fourth Symposium on In Situ and On Site Bioremediation, New Orleans, LA, U.S.A.*
- O'Shaughnessy, J.C. and C. Nardini. 1997. Heating the tar out. *Soil and Groundwater Cleanup*, June: 7-13.
- Peters, C., Luthy, R. 1993. Coal Tar dissolution in water-miscible solvents: experimental evaluation. *Environ. Sci. Tech.* 27, 2831-2843.
- Schmitt, R.; Langguth, H. R., Puttmann, W., Rohns, H. P., Eckert, P., Schubert, J. 1996. Biodegradation of aromatic hydrocarbons under anoxic conditions in a shallow sand and gravel aquifer of the Lower Rhine Valley, Germany. *Org. Geochem.* 25, 41-50.
- Shin W-T, Garanzuay X, Yiacoumi S, Tsouris C, Gu B, Mahinthakumar G. 2004. Kinetics of soil ozonation: An experimental and numerical investigation. *J. Cont. Hydrol.* 72:227–243.

- Sra, K., Thomson, N.R., Barker, J.F. 2008. In situ chemical oxidation of gasoline compounds using persulfate. Proceedings of the Petroleum Hydrocarbons and Organic Chemicals in Ground Water Conference, Houston, TX, November 3–5.,76.
- Sra, K., Thomson, N.R., Barker, J.F. 2010. Persistence of persulfate in uncontaminated aquifer materials. *J. Env. Sci. Tech.*, 44(8), 3098–3104
- Siegrist, R.L. 2011. *In Situ Chemical Oxidation for Groundwater Remediation*. Springer Science, New York, NY Ch. 2, 6.
- Stravelova, M., Pokorny, A. 2008. Chemical oxidation of PAHs using modified Fenton's reagent and Persulfate. Earth Tech CZ, Ltd., Trojska 92, 171 00 Prague, Czech Republic.
- Thomson, N., Fraser, M.J., Lamarche, C., Barker, J.F., Forsey, S.P. 2008. Rebound of a coal tar creosote plume following partial source zone treatment with permanganate. *J. Contam. Hydrol.* 102, 154-171.
- Pinto, P. 1993. Treatability of groundwater from a plume contaminated with PAHs and gasoline hydrocarbons. Master of Science Thesis, University of Cincinnati, Ci, OH.
- Warshawsky, D. 1999. Polycyclic aromatic hydrocarbons in carcinogenesis. *Environ. Health Persp.* 107(4),317-319.
- Wick, A., Haus, N., Sukkariyah, B., Haering, K., Daniels, W. 2011. Remediation of PAH-Contaminated Soils and Sediments: A Literature Review. Virginia Polytechnic Institute, Blacksburg, VA.
- Yen, C., Chen, K., Kao, C., Liang, S., Chen, T. 2011. Application of persulfate to remediate petroleum hydrocarbon-contaminated soil: Feasibility and comparison with common oxidants. *J. Hazard. Mater.* 186(2-3), 2097-2102.
- Yeom, I., Ghosh, M., Cox, C., Robinson, K. 1993. Micellular solubilization of polynuclear aromatic hydrocarbons in coal tar-contaminated soils. *Environ. Sci. Tech.*, 29, 3015-3021.

Appendices

Appendix A:

Site Work Completed

March 2011

During the week of March 7, 2011 ARCADIS and personnel from UW mobilized to the site to conduct additional soil borings (DPT-12 to DPT-27) and monitoring well installations (MW-23D, MW-24D, MW-25, MW-25D and MW-26) in the area surrounding the Meter Shop building and to deploy pressure transducers at select monitoring well locations. The field-work performed in March 2011 was primarily focused on the collection of additional information on the architecture of surficial aquifer source material, including soil cores for laboratory and bench-scale testing.

Pressure transducers were deployed at monitoring well locations MW-7D, MW-23D, MW-24D and MW-25D for the purpose of refining surficial aquifer groundwater flow direction and magnitude in the area surrounding the “meter shop”.

Temporary groundwater screening/sampling was not performed at any of the locations drilled in March 2011. Total boring depths, depending on the depth of the clay contact, ranged from 20 to 88 feet below ground surface (ft bgs). GeoProbe™ macro-core sampling with piston assembly was used to advance the borings and to collect soil core samples. The borings were abandoned via tremie-grout methods.

During the installations of boreholes DPT-12 to DPT-27, core was logged on Site. At changes in lithology, grab samples were collected transferred to plastic bags and preserved in coolers with ice. At DPT locations where MGP residuals were observed near the sand/clay interface in a core sample, a secondary borehole installation was conducted approximately 1 foot away. At this secondary location, an intact core sample was collected by driving the macro-core sampling system to the required depth. The intact core samples were stored on Site in coolers with ice. All collected samples were shipped to the University of Waterloo for laboratory analyses. Upon arrival at the university, the samples were logged and then stored at 4 °C. Tables 3 and 4 list the sediment and intact core samples collected, respectively. The borehole logs were re-examined and the sediments were assigned a lithotype and weighed. Sediment samples were denoted by the DPT location and depth bgs; for example sample DTP-6 9 is obtained from location DPT-6 at 9 feet bgs.

July 2011

During the week of July 18, 2011 ARCADIS and personnel from UW mobilized to the site to conduct additional soil borings (DPT-28 to DPT-35) and multilevel (ML) monitoring well installations in the area surrounding the Meter Shop building and within the Meter Shop building. The purpose of these borings and well installation work was to provide additional information on the architecture of surficial aquifer source material contributing to the groundwater plume in the vicinity and downgradient of MW-20, and to complete installation of additional long-term groundwater monitoring points within the surficial aquifer.

Fourteen (14) multilevel wells were installed between July 18 and 22, 2011 using direct push Geoprobe™ equipment (ML well locations are shown as blue symbols on Figure 2). The multilevel design was selected because of its capability to obtain discrete groundwater samples from various depths within a single borehole installation. Ten (10) multilevel wells denoted as ML-1 to ML-10 were evenly spaced at 9 foot intervals along an 81 foot wide transect located north of the MW-25/MW-25D well cluster, south of

the Meter Shop building. This transect was oriented at approximately 65° east of north which, based on previous water level measurements taken at the site, represents a line that is approximately perpendicular to the mean groundwater flow direction, south of the Meter Shop building. These ML monitoring wells were installed using a track-mounted Geoprobe™ 6610DT drilling rig. Four (4) multilevel wells denoted as ML-11 to ML-14 were installed inside the Meter Shop at strategic locations. These four locations were installed utilizing a dolly-mounted, low clearance Geoprobe™ GP420M mobile rig due to the access constraints (i.e., low ceiling and walls) inside the Meter Shop.

Based on designs utilized by UW on other remediation monitoring projects in the State of Florida, the following methodology was used to construct ML monitoring wells at the site during July 2011. The core (center stock) of each multilevel well was a length of nominal 0.50 inch CPVC pipe (0.625 inch outside diameter) with lengths of polytetrafluoroethylene (PTFE) tubing (0.25 inch outside diameter and 0.03 inch wall thickness) fastened to the center stock with electrical tape. The bottom approximately 5 inches of each PTFE tube was slotted (sampling port) and covered with a 200 micrometer (µm) mesh Nitex screen (45% open area) to prevent fine particles from entering the sample tubing. The Nitex screen was attached to the PTFE tube using stainless steel wire.

For ML-1 to ML-10, 10 sampling ports were spaced at nominal 2.2 foot intervals, and for ML-11 to ML-14, 4 sampling ports were spaced at nominal 5 foot intervals. Each ML well was constructed on Site and inserted into the center of the probe rods driven to the target depth using an expendable knock-out tip. As the probe rods were withdrawn the formation was allowed to collapse around the multilevel well. Filter sand with a grout collar was used to fill the ML well annular space above the water table (~ 5 feet below ground surface [ft bgs]) to 12 inches below ground surface. A cement well pad with 8-inch diameter flush-mounted well cover was installed as surface protection at each ML well location. Each sampling port was developed using a peristaltic pump until the extracted groundwater was visually free of fine sediment.

Soil boring locations included borings DPT-28 to DPT-35 (Figure 2). Borings DPT-32 to DPT-35, located within the Meter Shop were converted to ML monitoring well points (ML-11 through ML-14, respectively) as described above after reaching total drilling depth. Temporary groundwater screening/sampling was not performed at any of the locations drilled in July 2011. Total boring depths, depending on the depth of the clay contact, ranged from 20 to 40 ft bgs. GeoProbe™ macro-core sampling with piston assembly was used to advance the borings and to collect soil core samples. The soil borings were abandoned via tremie-grout methods, unless converted to a ML monitoring well.

During the installations of boreholes DPT-28 to DPT-35, core was logged on Site. At changes in lithology, grab samples were collected transferred to plastic bags and preserved in coolers with ice. All collected samples were shipped to the University of Waterloo for laboratory analyses. Upon arrival at the university, the samples were logged (Table 3) and then stored at 4 °C.

Following development of each ML sampling port, duplicate samples were collected from each multilevel port using a sampling glass vial (40 mL) placed between the multilevel port and a peristaltic pump. For sample collection, the glass vial was fitted to an in-line, stainless steel screw cap sample head. Several (2-3) groundwater volumes of the vial were passed through before the vial was detached from the sample head. Samples were preserved with sodium azide (0.4 milliliters [mL] of 10% solution), sealed with PTFE lined screw caps, and preserved in coolers with ice. All collected samples were shipped to the

University of Waterloo for laboratory analyses. All samples were stored at 4 °C and held for less than 14 days prior to analysis at the Organics Laboratory at the University of Waterloo.

October 2011

During the week of October 31, 2011 personnel from UW mobilized to the site to sample the transect and Meter Shop ML wells, perform slug tests on MW-7D, MW-23D, MW-24, and MW-25, and download the pressure transducer data. Groundwater samples were collected and handled as described in Section 2.1.2.

February 2012

During the week of February 14, 2012 personnel from UW mobilized to the site to sample the transect and Meter Shop ML wells, and download the pressure transducer data. Groundwater samples were collected

Table A.1 Transect multi-level well installation details.

Well ID	Top of Center Stock Elevation [ft amsl]	Port Number	Port Elevation [ft amsl]
ML-1	23.13	1	18.13
		2	15.93
		3	13.73
		4	11.53
		5	9.33
		6	7.13
		7	4.93
		8	2.73
		9	0.53
		10	-1.67
ML-2	23.11	1	18.11
		2	15.91
		3	13.71
		4	11.51
		5	9.31
		6	7.11
		7	4.91
		8	2.71
		9	0.51
		10	-1.69
ML-3	23.11	1	18.11
		2	15.91
		3	13.71
		4	11.51
		5	9.31
		6	7.11
		7	4.91
		8	2.71
		9	0.31
		10	-0.49

Well ID	Top of Center Stock Elevation [ft amsl]	Port Number	Port Elevation [ft amsl]
ML-4	23.27	1	18.27
		2	16.07
		3	13.87
		4	11.67
		5	9.47
		6	7.27
		7	5.07
		8	2.87
		9	0.47
		10	-0.33
ML-5	23.27	1	18.27
		2	16.07
		3	13.87
		4	11.67
		5	9.47
		6	7.27
		7	5.07
		8	2.87
		9	0.67
		10	0.17
ML-6	23.44	1	18.44
		2	16.24
		3	14.04
		4	11.84
		5	9.64
		6	7.44
		7	5.24
		8	3.04
		9	0.84
		10	0.34

Table A.1 cont'd. Transect multi-level well installation details.

Well ID	Top of Center Stock Elevation [ft amsl]	Port Number	Port Elevation [ft amsl]
ML-7	23.68 *	1	18.68
		2	16.48
		3	14.28
		4	12.08
		5	9.88
		6	7.68
		7	5.48
		8	3.28
		9	1.08
		10	0.58
ML-8	23.8 *	1	18.80
		2	16.60
		3	14.40
		4	12.20
		5	10.00
		6	7.80
		7	5.60
		8	3.40
		9	1.20
		10	0.70
ML-9	23.92	1	18.92
		2	16.72
		3	14.52
		4	12.32
		5	10.12
		6	7.92
		7	5.72
		8	3.52
		9	1.32
		10	0.82

Well ID	Top of Center Stock Elevation [ft amsl]	Port Number	Port Elevation [ft amsl]
ML-10	24.03	1	19.03
		2	16.83
		3	14.63
		4	12.43
		5	10.23
		6	8.03
		7	5.83
		8	3.63
		9	1.43
		10	0.93

Table A.1 cont'd. Meter Shop multi-level well installation details.

Well ID	Top of Center Stock Elevation [ft amsl]	Port Number	Port Elevation [ft amsl]
ML-11	25.93	1	20.93
		2	15.93
		3	10.93
		4	5.93
ML-12	25.83 *	1	20.83
		2	15.83
		3	10.83
		4	5.83
ML-13	25.81	1	20.81
		2	15.81
		3	10.81
		4	5.81
ML-14	25.81	1	20.81
		2	15.81
		3	10.81
		4	5.81

Appendix B: Site Characterization Data

Table B.1 Sediment grad samples collected.

Location	Depth	Mass (g)	Lithotype
DPT-12	9'	586.79	Fine SAND
	14'	482.1	Fine SAND
	15'	457.05	Fine SAND
	18'	485.27	Very Fine SAND
DPT-13	9'	552.67	Fine SAND
	25'	488.28	Fine SAND with Silt
DPT-14	3'	230.9	Peaty SAND
	5'	427.26	Peaty SAND
	10'	529.36	Fine SAND
DPT-16	32'	425.48	Clay
DPT-17	10-13'	506.93	Fine SAND with Silt
	15'	497.44	Fine to Very Fine Silty SAND
	17-19'	450.11	Very Fine SAND
	23-25'	513.38	Fine to Very Fine Silty SAND
DPT-24	30'	396.65	Fine to Very Fine Silty SAND
	20 LF	420.42	Very Fine SAND
	25 LF	501.14	Fine to Very Fine SAND
DPT-25	15'	451.51	Fine SAND
	19'	447.95	Fine SAND
	25'	595.17	SAND with Silt
	28'	587.42	SAND with Silt
DPT-26	7'	442.37	Fine SAND
	9'	423.22	Fine SAND
	14'	410.91	Fine SAND with Silt
DPT-27	16'	447.25	Fine SAND with Silt
	23'-24'	564.72	Fine to Very Fine Silty SAND
	24' #2	478.86	Fine to Very Fine Silty SAND
	28'	581.33	Medium SAND
	34'	571.67	Fine to Very Fine Silty SAND
	39'	518.93	Fine to Very Fine Silty SAND
	44'	540.02	SAND and SILT
	49'	516.95	SAND and SILT
	54'	413.89	SILT
	59'	433.05	SAND and SILT
	60'-65'	615.42	Fine Silty SAND
	65'-70'	488.91	Fine to Very Fine SAND
DPT-28	70'-75'	616.92	Fine to Very Fine SAND
	80'	534.68	Fine to Very Fine SAND
	83'	369.49	Medium SAND
	86'	370.3	Fine Silty SAND
	88'	169.16	Fine Silty SAND
	7'	150.43	Fine Silty SAND
	12'	232.15	Fine SAND
	19'	211.11	Fine Silty SAND
DPT-29	8'	321.14	Fine to Very Fine SAND
	20'	122.4	Fine SAND
DPT-30	14'	245.23	Fine SAND
	20'	217.65	Very Fine SAND
DPT-31	8'	287.3	Fine SAND
	15'	243.3	Fine SAND
	28'	231.12	Fine Silty SAND
DPT-32	12'	200.14	Fine to Very Fine SAND
	16'	288.43	Very Fine SAND
DPT-33	9'	216.54	Very Fine SAND
	15'	233.51	Very Fine SAND
	26'	244.32	Very Fine SAND
DPT-34	14'	209.22	Very Fine SAND
	24'	254.44	SAND and SILT
DPT-35	15'	232.4	Fine SAND
	20'	344.29	SAND and SILT

Table B.2 Intact core samples collected.

Location	Depth	Mass (g)
DPT-12A	21.7'-24'	2160.85
	24'-25'	841.96
DPT-13A	26.8'-28.4'	1553.38
	28.4'-30'	1466.77
DPT-14	31.5'-33.3'	1343.52
	33.3'-35'	1484.06
DPT-16A		1182.08
	28.3'-30'	1167.67
DPT-23A	5'-10'	2141.85
	10'-15'	1901.75
	18'-20'	1908.82
	20'-22'	1407.41

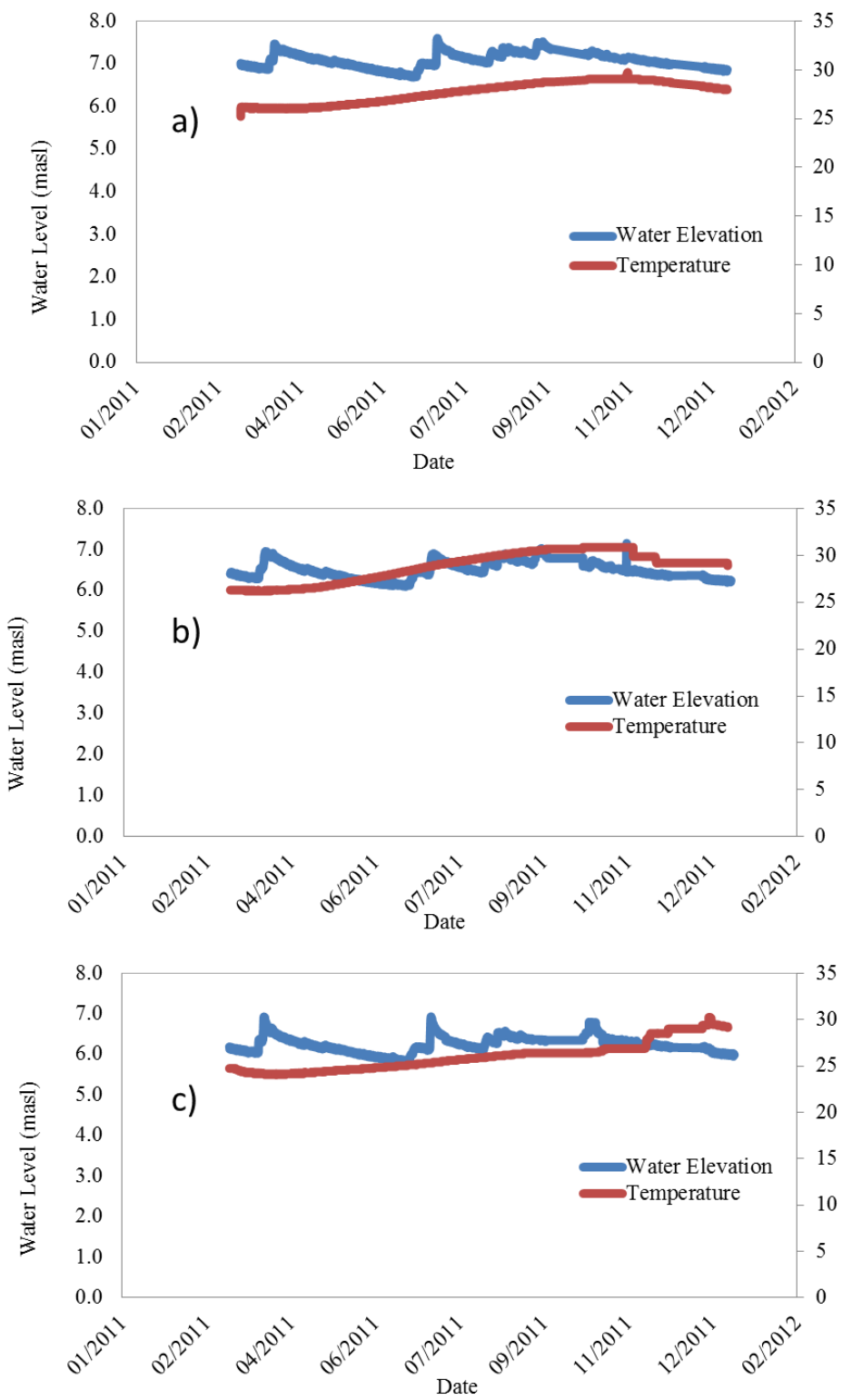


Figure B.1. Water elevation and temperature profiles at (a) MW-25, (b) 23D, and (c) 24D.

Table B.2: Soil sample grain size, permeameter and porosity results.

Location	Borehole Description	Sample Mass (g)	Grain Size	Permeameter	n
			K (cm/s)	K (cm/s)	
DPT - 12 9'	Fine SAND	465.5	9.28E-03	8.82E-03	3.56E-01
DPT - 16 19'	Fine SAND	389.1	6.15E-03	7.01E-03	3.47E-01
DPT - 19 14'	Fine SAND	253.7	6.52E-03	7.11E-03	-
DPT - 16 9'	Fine to Very Fine SAND	393.1	7.32E-03	9.01E-03	3.53E-01
DPT - 17 13'	Fine to Very Fine SAND	390	8.55E-03	7.70E-03	3.52E-01
DPT - 27 65'	Fine to Very Fine SAND	345.6	6.05E-03	8.15E-03	3.96E-01
DPT - 12 20'	Very fine SAND	436.3	6.53E-03	5.68E-03	3.75E-01
DPT - 17 23'	Very fine SAND	219.7	8.95E-03	6.57E-03	2.98E-01
DPT - 24 20'	Very fine SAND	310.5	6.90E-03	6.70E-03	3.03E-01
DPT - 13 10'	Fine to Very Fine Silty SAND	363.1	6.55E-03	6.55E-03	3.02E-01
DPT - 13 12'	Fine to Very Fine Silty SAND	522.4	6.99E-03	7.00E-03	3.10E-01
DPT - 13 15'	Fine to Very Fine Silty SAND	429.2	7.09E-03	7.07E-03	3.21E-01
DPT - 17 25'	Fine to Very Fine Silty SAND	232.5	8.73E-03	7.75E-03	2.85E-01
DPT - 27 34'	Fine to Very Fine Silty SAND	403.1	8.35E-03	9.77E-03	3.68E-01
DPT - 20 22'	Very fine SILTY SAND	313.6	7.79E-03	6.96E-03	2.96E-01
DPT - 20 23'	Very fine SILTY SAND	369.2	1.12E-02	9.45E-03	3.33E-01
DPT - 18 25'	Fine Silty SAND	236.7	5.33E-03	8.01E-03	-
DPT - 22 13'	Fine Silty SAND	302.7	6.12E-03	6.50E-03	2.38E-01
DPT - 27 60'	Fine Silty SAND	477.2	8.86E-03	6.96E-03	3.22E-01
DPT - 25 25'	SAND with SILT and CLAY	443.6	9.41E-03	6.71E-03	3.18E-01
DPT - 25 28'	SAND with SILT and CLAY	405.4	9.68E-03	7.02E-03	3.46E-01
DPT - 17 10'	Fine SAND with SILT	344.7	6.01E-03	8.13E-03	3.61E-01
DPT - 17 17'	Fine SAND with SILT	453.2	8.22E-03	8.00E-03	3.64E-01
DPT - 17 20'	Fine SAND with SILT	309.2	8.35E-03	8.54E-03	3.66E-01
DPT - 13 25'	Fine SAND with SILT	374.1	6.99E-03	5.39E-03	3.66E-01
DPT - 26 14'	Fine SAND with SILT	323.5	6.88E-03	6.37E-03	3.11E-01
DPT - 27 23'	Fine to Very Fine SAND with SILT	446.8	8.66E-03	8.99E-03	3.28E-01
DPT - 27 24'	Fine to Very Fine SAND with SILT	380.4	8.97E-03	9.68E-03	3.68E-01
DPT - 27 28'	Fine to Very Fine SAND with SILT	462.4	1.00E-02	9.35E-03	3.38E-01
DPT - 27 44'	SAND and SILT	366.5	7.67E-03	8.85E-03	3.85E-01
DPT - 27 49'	SAND and SILT	373.6	7.90E-03	9.03E-03	3.97E-01
DPT - 27 59'	SAND and SILT	304.5	6.31E-03	8.67E-03	3.60E-01

Table B.3: Well construction details.

Well	MW25	MW24D	MW23D	MW7
Elevation (m)	7.12	7.70	7.15	8.24
Depth to TOC (m)	4.52	4.71	4.27	5.21
Easting	405704.3	405486.9	405751.7	405521.7
Northing	1322892	1323040	1323003	1323250
Average static pressure (m)	2.82	2.7921	3.111	3.635
Static water level elevation (m)	5.91	6.26	6.51	7.15
Transducer rise adjust (m)	0.492	0.48	0.517	0.4853
Adjusted transducer depth (m)	4.028	4.23	3.75	4.72
Screen start depth (m)	0.9144	4.88	4.11	0.61
Screen end depth (m)	3.9624	6.40	5.64	4.57
Static column height or well length (m)	2.7544	4.96	5.00	3.48
Clay elevation (m)	0.82	0.42	1.88	-1.63
Saturated thickness (m)	5.09	5.84	4.62	8.78
Casing I.D.	0.0508	0.0508	0.0508	0.0508
Screen I.D. (m)	0.0508	0.0508	0.0508	0.0508
Hydraulic conductivity, K (m/s)	8.30E-05	8.30E-05	8.30E-05	8.30E-05
Well I.D. (m)	0.1524	0.1524	0.1524	0.1524

Table B.4. Calculation of source zone volumes.

Source Zone	Zone	Location	Maximum Depth of Impact (m)	Major Axis (m)	Minor Axis (m)	Volume (m ³)
1	Deep	DPT-1, -12, -13, -14, -29, -30	2.5	7.6	3.6	20.1
2	Deep	DPT-23, MW-26	0.5	4	3	1.8
3	Deep	SW corner of Meter Shop	0.4	2	1	0.2
4	Shallow	DPT-14, -29, -31	3	7	6	37.1
5	Shallow	DPT-5, -20, -21, -23, -24, MW-26	3	9	6	47.7
6	Shallow	DPT-11	1.5	2	1.5	1.3

Notes:

Maximum depths of impact were calculated based on observed impacts from borings (Table 3.4).

Plume locations and major and minor axes are shown in Figures C.1 (deep) and C.2 (shallow).

Source values were calculated using the equation for the volume of an ellipsoid.

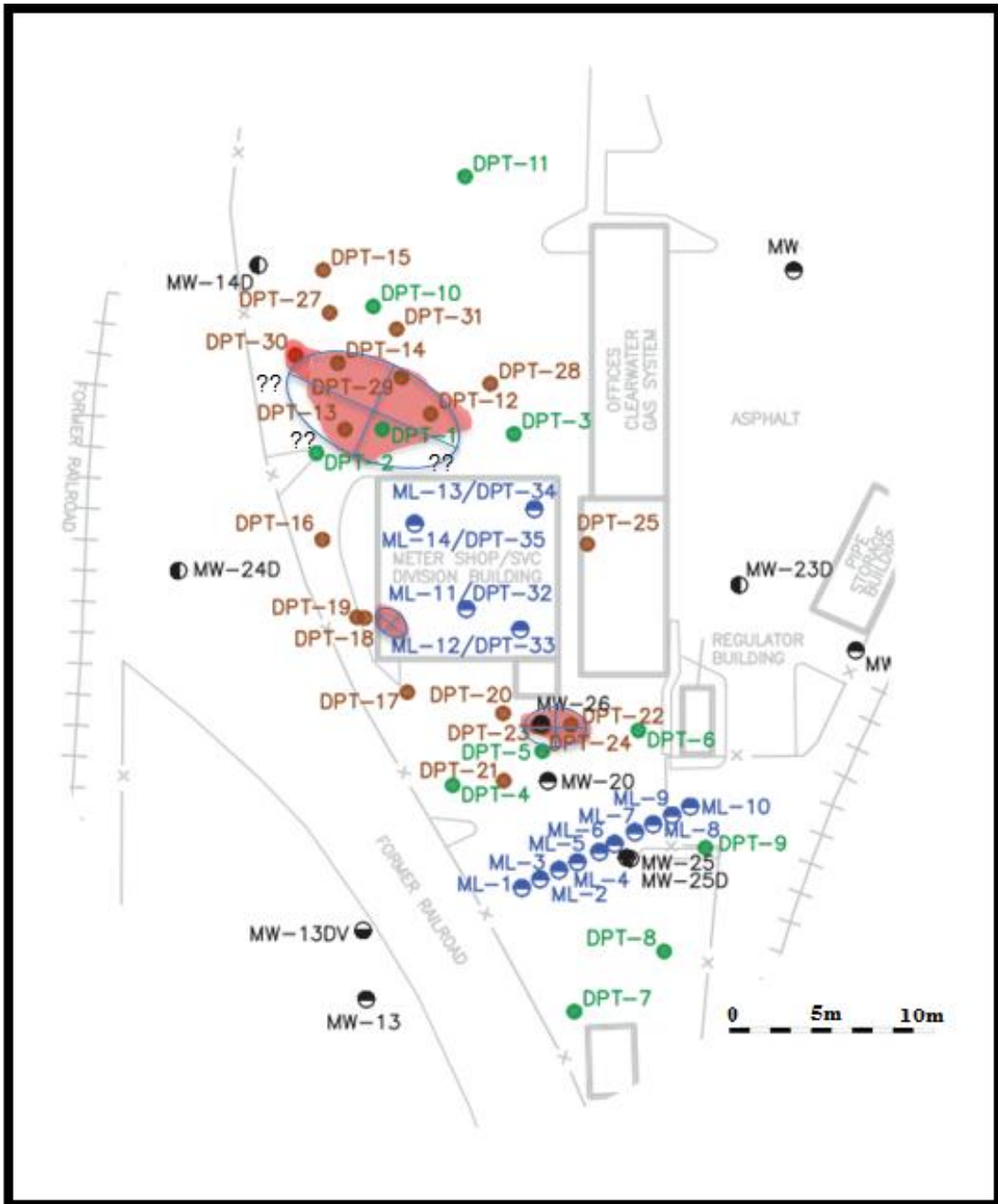


Figure B.2. Areas for source zone estimation for observed source zone > 4.5 m bgs (15 ft) (deep).

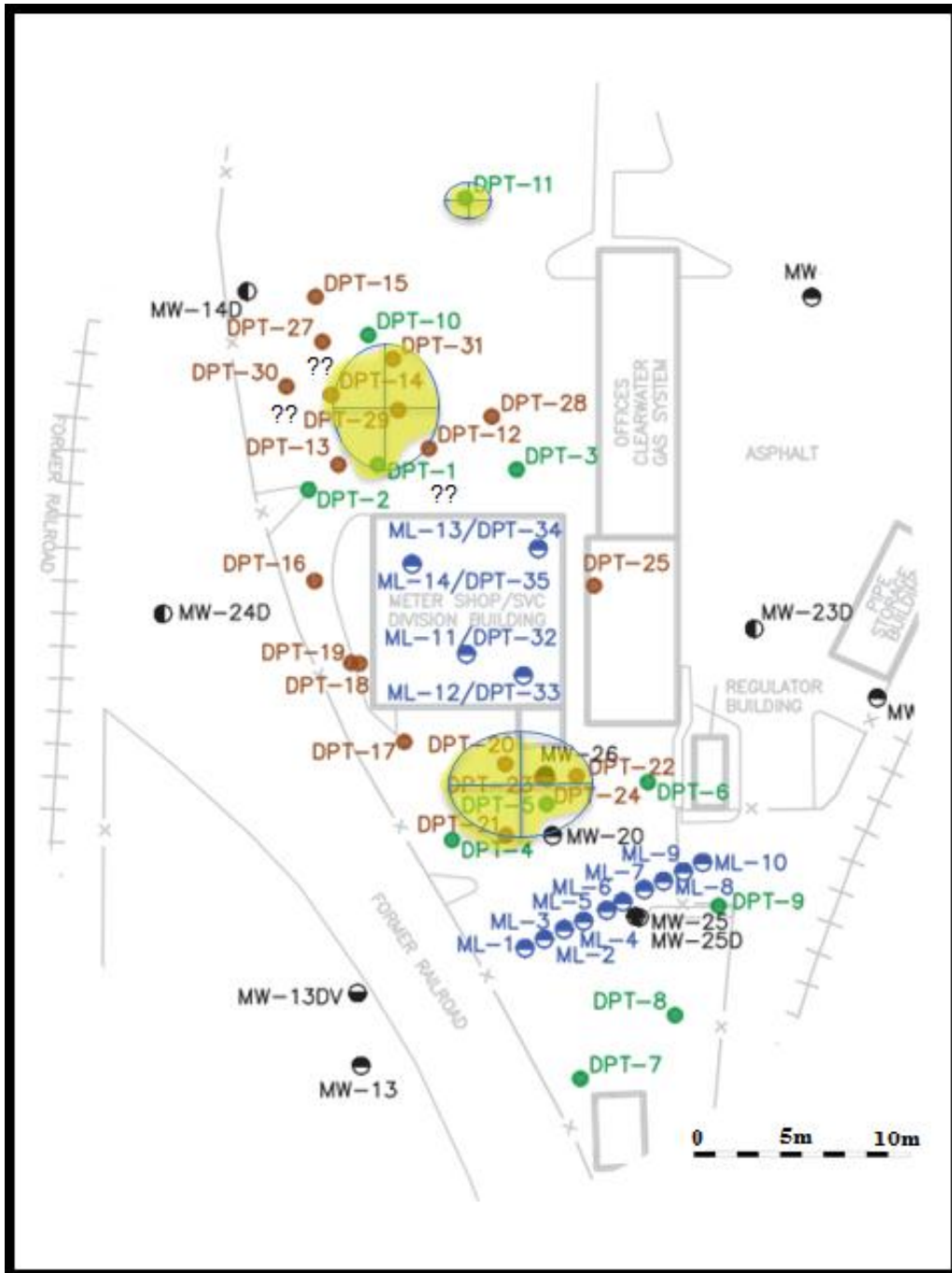


Figure B.3. Areas for source zone estimation for observed source zone >4.5 m bgs (15 ft) (shallow).

Table B.5. Triplicate results for soil samples taken from DPT-23 at 3-3.5 m and 6m.

Compound	Concentration (mg/kg)					
	Depth = 3-3.5 m			Depth = 6 m		
BTEX						
Benzene	11.5	11.2	11.1	11.9	12.8	11.6
Toluene	79.7	80.0	85.2	89.4	90.7	83.6
Ethylbenzene	77.2	75.0	73.0	84.3	88.5	77.2
P,M-xylene	123	121	122	129	121	121
O-xylene	66.3	62.0	65.4	69.3	67.5	65.5
Trimethylbenzenes						
1,3,5-Trimethylbenzene	33.9	33.7	32.4	34.2	32.1	33.6
1,2,4-Trimethylbenzene	155	150	149	156	151	157
1,2,3-Trimethylbenzene	41.9	41.0	42.3	43.1	50.0	49.1
PAHs						
Naphthalene	1080	1090	1080	1080	1170	1010
Indole	9.0	10.0	8.91	11.2	11.1	10.5
2-Methylnaphthalene	724	725	720	811	823	834
1-Methylnaphthalene	420	424	443	456	474	477
Biphenyl	88.5	86.2	88.5	89.6	89.6	88.8
Acenaphthylene	125	115	116	146	160	136
Acenaphthene	45.1	49.5	49.7	68.0	77.1	78.1
Dibenzofuran	68.4	68.1	67.5	56.3	59.2	57.0
Fluorene	177	179	175	143	147	136
Phenanthrene	315	321	316	397	406	399
Anthracene	41.7	42.6	39.7	45.1	45.5	45.7
Carbazole	-	-	-	-	-	-
Fluoranthene	92.2	93.0	93.8	94.4	94.6	89.9
Pyrene	154	153	154	159	167	165
Benz [a] anthracene	29.2	28.9	22.9	28.6	33.4	27.9
Chrysene	29.4	27.4	29.4	27.8	32.0	29.6
Benz [b] Fluoranthene + Benz [k]Fluoranthene	27.7	28.7	28.9	29.0	32.3	28.1
Benzo [a] Pyrene	17.9	17.5	17.8	22.3	26.1	21.1
Indeno[1,2,3-c,d] Pyrene + Dibenz [a,h] Anthracene	4.42	4.56	4.26	3.75	3.09	2.09
Benzo [g,h,i] Perylene	7.22	7.42	7.12	7.81	8.94	8.27

Notes: (-) < MDL

Table B.6. ANOVA analysis for soil samples taken from DPT-23 at depths of 3.5 and 6 m.

Source of Variation	SS	df	MS	F	P-value	F crit
Between Groups	1583.766	1	1583.766	0.025476	0.873804	4.026631
Within Groups	3232645	52	62166.25			
Total	3234229	53				

Table B.7. Field parameters for monitoring wells on-site.

Parameter	Units	MW-7D	MW- 23D	MW-24	MW-25D
Purge Volume	L	3.5	3.60	2.65	4.92
Water Level	m (bgs)	0.84	1.31	1.66	1.34
pH	-	10.11	5.96	6.23	6.19
Temperature	°C	27.13	29.7	25.9	29.0
Conductivity	µS/cm	291	401	458	367
Dissolved Oxygen	mg/L	0.46	0.189	0.268	0.380
Turbidity	NTUs	9.72	30.8	14.3	120
Colour	-	clear	brown	yellow	gray
Odor	-	none	MGP	none	MGP

Table B.8. ANOVA for mass discharge calculations across sampling events.

Sampling Episode	Source of Variation	SS	df	MS	F	P-value	F crit
1 & 2	Between Groups	26.09606	1	26.09606	0.299902	0.586045	4.006873
	Within Groups	5046.891	58	87.01536			
	Total	5072.987	59				
1 & 3	Between Groups	33.86982	1	33.86982	0.395925	0.531672	4.006873
	Within Groups	4961.67	58	85.54604			
	Total	4995.54	59				
2 & 3	Between Groups	0.506017	1	0.506017	0.009885	0.921146	4.006873
	Within Groups	2969.141	58	51.19208			
	Total	2969.647	59				

Appendix C:

Transect Data

Table C.1. Meter Shop Concentrations July 2011.

ML ID:	GCTL	NADC	MDL	Units	ML-11 -20	ML-11 -15	ML-11 -10	ML-11 -5	ML-12 -20	ML-12 -15	ML-12 -10	ML-12 -5	ML-13 -20	ML-13 -15	ML-13 -10	ML-13 -5
Port Depth (ft bls):																
BTEX																
Benzene	1	100	1.11	ug/L	137	3.7	<MDL	<MDL	470	11.8	15.3	1210	153	12.7	<MDL	6.3
Ethylbenzene	30	300	0.77	ug/L	17.7	41.7	<MDL	<MDL	163	81.4	69.3	995	66.5	62	5	18.9
m-Xylene & p-Xylene	20	200	1.46	ug/L	42.7	53.6	<MDL	<MDL	161	649	223	788	25.2	37.2	3.9	9.9
o-Xylene	20	200	0.37	ug/L	71.9	59.5	<MDL	<MDL	245	397	49.3	491	42.7	32.7	2.3	4.6
Toluene	40	400	0.83	ug/L	3.4	12.1	<MDL	3.4	82.9	1250	4.6	1540	16.1	7.7	<MDL	<MDL
Trimethylbenzenes																
1,2,3-Trimethylbenzene	10	100	0.76	ug/L	35.4	38.4	<MDL	<MDL	65.5	145	95.7	162	17.6	6.9	39.4	7.6
1,2,4-Trimethylbenzene	10	100	0.82	ug/L	44.7	97	<MDL	<MDL	119.2	420	120	456	45.5	19.9	13.4	18.9
1,3,5-Trimethylbenzene	10	100	0.74	ug/L	19.4	27.8	<MDL	<MDL	33.9	72.4	3.7	88.2	9.7	48.3	3.3	8.5
PAHs																
1-Methylnaphthalene	28	280	1.31	ug/L	137	372	<MDL	36.3	219	58.7	52.8	73.4	117	741	516	557
2-Methylnaphthalene	28	280	4.27	ug/L	111	37.4	<MDL	<MDL	263	819	462	143.7	14.9	1130	764	217
Naphthalene	14	140	2.2	ug/L	334	3930	<MDL	<MDL	9560	8360	11200	9880	1260	2840	1490	430
Acenaphthene	20	200	1.83	ug/L	13.5	46.9	<MDL	29.3	12.7	28.8	76.9	36.8	12.2	85.7	140	163.1
Acenaphthylene	210	2100	1.53	ug/L	13.9	26.5	<MDL	7.6	16.7	73.4	2.5	57.8	8.6	64.7	41.5	24
Anthracene	2100	21000	5.53	ug/L	<MDL	5.8	<MDL	<MDL	<MDL	<MDL	8.5	5.7	<MDL	6.3	<MDL	<MDL
Benz [a] anthracene	0.05	5	4.77	ug/L	<MDL	<MDL	<MDL	<MDL	<MDL	<MDL	<MDL	<MDL	<MDL	<MDL	<MDL	<MDL
Benzo [a] pyrene	0.2	20	13.3	ug/L	<MDL	<MDL	<MDL	<MDL	<MDL	<MDL	<MDL	<MDL	<MDL	<MDL	<MDL	<MDL
Benz [b, k] fluoranthene	-	-	5.62	ug/L	<MDL	<MDL	<MDL	<MDL	<MDL	<MDL	<MDL	<MDL	<MDL	<MDL	<MDL	<MDL
Benzo [g,h,i] perylene	210	2100	11.5	ug/L	<MDL	<MDL	<MDL	<MDL	<MDL	<MDL	<MDL	<MDL	<MDL	<MDL	<MDL	<MDL
Chrysene	4.8	480	5.75	ug/L	<MDL	<MDL	<MDL	<MDL	<MDL	<MDL	<MDL	<MDL	<MDL	<MDL	<MDL	<MDL
Fluoranthene	280	2800	1.8	ug/L	<MDL	2.9	<MDL	<MDL	<MDL	1.8	2.6	<MDL	<MDL	<MDL	<MDL	1.2
Fluorene	280	2800	1.88	ug/L	31.7	51.1	<MDL	19.7	11.9	36	37.7	43.8	7.9	6.6	64.3	39.4
Indeno[1,2,3-c,d] pyrene + Dibenz [a,h] anthracene	-	-	18.7	ug/L	<MDL	<MDL	<MDL	<MDL	<MDL	<MDL	<MDL	<MDL	<MDL	<MDL	<MDL	<MDL
Phenanthrene	210	2100	3.78	ug/L	35.3	54.9	<MDL	28.5	<MDL	<MDL	21.9	23.7	5.2	48.7	46.4	31.1
Pyrene	210	2100	1.6	ug/L	<MDL	4.3	<MDL	<MDL	<MDL	2.6	3.6	2.2	<MDL	<MDL	<MDL	2.4

Notes:

- GCTL - FDEP Groundwater Cleanup Target Level
- NADC - FDEP Natural Attenuation Default Concentration
- MDL - minimum detection limit
- PAHs - polycyclic aromatic hydrocarbons
- ft bls - feet below land surface
- ug/L - micrograms per liter
- ML - multi-level monitoring well

Table C.2. Meter shop concentrations November 2011.

ML ID: Port Depth (ft bls):	GCTL	NADC	MDL	Units	ML-11	ML-11	ML-11	ML-11	ML-12	ML-12	ML-12	ML-12	ML-13	ML-13	ML-13	ML-13	ML-14	ML-14	ML-14	ML-14
					-20	-15	-10	-5	-20	-15	-10	-5	-20	-15	-10	-5	-20	-15	-10	-5
BTEX																				
Benzene	1	100	1.11	ug/L	114	1.7	<MDL	<MDL	180	1420	-	52	188	5.7	2.3	3.3	<MDL	2.3	<MDL	<MDL
Ethylbenzene	30	300	0.77	ug/L	16.6	22.7	<MDL	<MDL	13.7	772	52	422	89.8	32.4	5.9	6.3	1.3	<MDL	<MDL	<MDL
m-Xylene & p-Xylene	20	200	1.46	ug/L	38.6	27.9	<MDL	<MDL	16.2	618	175	331	36.1	2.3	3.5	2.7	<MDL	<MDL	<MDL	<MDL
o-Xylene	20	200	0.37	ug/L	67.4	35.9	1.5	<MDL	18.5	383	38.2	221	52.2	17.3	2.3	<MDL	<MDL	<MDL	<MDL	<MDL
Toluene	40	400	0.83	ug/L	3.4	8.7	<MDL	<MDL	17.5	1570	9.6	164	13.3	4.2	0.9	<MDL	<MDL	<MDL	<MDL	<MDL
Trimethylbenzenes																				
1,2,3-Trimethylbenzene	10	100	0.76	ug/L	29.6	34.3	1.8	1.7	2.6	916	78.5	152	29.2	33.4	4.1	9.6	<MDL	<MDL	<MDL	<MDL
1,2,4-Trimethylbenzene	10	100	0.82	ug/L	39.8	49.6	2.2	2.4	3.4	261	89.7	445	85.1	110	13.3	19.9	<MDL	<MDL	<MDL	<MDL
1,3,5-Trimethylbenzene	10	100	0.74	ug/L	14.2	14.1	<MDL	<MDL	<MDL	51.7	2.6	74.9	18.2	26.6	4.3	5.8	<MDL	<MDL	<MDL	<MDL
PAHs																				
1-Methylnaphthalene	28	280	1.31	ug/L	188	374	83.7	120	21.9	789	566	142	577	79.4	392	728	3.9	6.7	43.4	134
2-Methylnaphthalene	28	280	4.27	ug/L	131	122	5.2	5.5	19.4	155	419	1940	726	1150	583	393	<MDL	6.3	<MDL	<MDL
Naphthalene	14	140	2.2	ug/L	3160	145.1	25.8	13.4	897	7490	9680	12000	2550	1960	260	191	6.9	11.3	3.5	3.7
Acenaphthene	20	200	1.83	ug/L	43.4	4.3	29.2	44	4.3	36.6	85.3	75.8	53.3	9.9	84.8	197	17.2	1.9	2.2	4.3
Acenaphthylene	210	2100	1.53	ug/L	14.5	27.9	13.9	21.8	2.8	83	29.4	141	39.6	54.2	38.3	23.7	<MDL	<MDL	<MDL	<MDL
Anthracene	2100	21000	5.53	ug/L	<MDL	<MDL	<MDL	<MDL	<MDL	<MDL	<MDL	<MDL	<MDL	<MDL	<MDL	<MDL	<MDL	<MDL	<MDL	<MDL
Benz [a] anthracene	0.05	5	4.77	ug/L	<MDL	<MDL	<MDL	<MDL	<MDL	<MDL	<MDL	<MDL	<MDL	<MDL	<MDL	<MDL	<MDL	<MDL	<MDL	<MDL
Benzo [a] pyrene	0.2	20	13.33	ug/L	<MDL	<MDL	<MDL	<MDL	<MDL	<MDL	<MDL	<MDL	<MDL	<MDL	<MDL	<MDL	<MDL	<MDL	<MDL	<MDL
Benz [b, k] fluoranthene	-	-	5.62	ug/L	<MDL	<MDL	<MDL	<MDL	<MDL	<MDL	<MDL	<MDL	<MDL	<MDL	<MDL	<MDL	<MDL	<MDL	<MDL	<MDL
Benzo [g,h,i] perylene	210	2100	11.49	ug/L	<MDL	<MDL	<MDL	<MDL	<MDL	<MDL	<MDL	<MDL	<MDL	<MDL	<MDL	<MDL	<MDL	<MDL	<MDL	<MDL
Chrysene	4.8	480	5.75	ug/L	<MDL	<MDL	<MDL	<MDL	<MDL	<MDL	<MDL	<MDL	<MDL	<MDL	<MDL	<MDL	<MDL	<MDL	<MDL	<MDL
Fluoranthene	280	2800	1.8	ug/L	<MDL	2.5	<MDL	<MDL	<MDL	2.4	1.8	2.5	<MDL	<MDL	<MDL	<MDL	<MDL	<MDL	<MDL	<MDL
Fluorene	280	2800	1.88	ug/L	3.4	51.3	37.7	59.5	<MDL	4.9	38.8	75.3	36.7	54.8	61	41.9	<MDL	<MDL	<MDL	<MDL
Indeno[1,2,3-c,d] pyrene + Dibenz[a,h] anthracene	-	-	18.65	ug/L	<MDL	<MDL	<MDL	<MDL	<MDL	<MDL	<MDL	<MDL	<MDL	<MDL	<MDL	<MDL	<MDL	<MDL	<MDL	<MDL
Phenanthrene	210	2100	3.78	ug/L	19.2	50.1	26.2	42.4	<MDL	19.9	15.3	29.6	14.7	35.4	32.2	27	<MDL	<MDL	<MDL	<MDL
Pyrene	210	2100	1.6	ug/L	<MDL	3.5	1.7	2.7	<MDL	2.7	1.8	1.8	<MDL	<MDL	<MDL	3	<MDL	<MDL	<MDL	<MDL

Notes:

- GCTL - FDEP Groundwater Cleanup Target Level
- NADC - FDEP Natural Attenuation Default Concentration
- MDL - minimum detection limit
- PAHs - polycyclic aromatic hydrocarbons
- ft bls - feet below land surface
- ug/L - micrograms per liter
- ML - multi-level monitoring well

Table C.3 Meter shop groundwater concentrations Feb 2012.

ML ID: Port Depth (ft bls):	GCTL	NADC	MDL	Units	ML-11	ML-11	ML-11	ML-11	ML-12	ML-12	ML-12	ML-12	ML-13	ML-13	ML-13	ML-13	ML-14	ML-14	ML-14	ML-14
					-20	-15	-10	-5	-20	-15	-10	-5	-20	-15	-10	-5	-20	-15	-10	-5
BTEX																				
Benzene	1	100	1.11	ug/L	1.6	< MDL	< MDL	< MDL	382	184	1.3	123	154	12.5	4.9	2.7	<MDL	<MDL	<MDL	<MDL
Ethylbenzene	30	300	0.77	ug/L	12.9	<MDL	<MDL	<MDL	13.7	130	92.3	752	69.2	24.1	4.2	21.3	<MDL	<MDL	<MDL	<MDL
m-Xylene & p-Xylene	20	200	1.46	ug/L	12.1	1.7	<MDL	<MDL	66.6	819	39.4	612	28.5	14.8	3.2	4.6	1.8	<MDL	<MDL	<MDL
o-Xylene	20	200	0.37	ug/L	31.2	<MDL	<MDL	<MDL	86	495	1.7	368	41.2	13.4	2.8	4.5	1.4	<MDL	7.8	<MDL
Toluene	40	400	0.83	ug/L	5.6	<MDL	<MDL	<MDL	2.8	265	4.1	549	11.5	4.9	2.8	2.2	<MDL	7.8	<MDL	<MDL
Trimethylbenzenes																				
1,2,3-Trimethylbenzene	10	100	0.76	ug/L	12.5	4.7	<MDL	<MDL	22.3	119	12.9	17.9	21.3	27.5	4.2	11.5	<MDL	<MDL	<MDL	<MDL
1,2,4-Trimethylbenzene	10	100	0.82	ug/L	39.5	7	<MDL	<MDL	44.9	363	2.7	500	62.8	95.9	15.7	33.1	1.4	<MDL	<MDL	<MDL
1,3,5-Trimethylbenzene	10	100	0.74	ug/L	2	2.6	<MDL	<MDL	13	68.7	5.2	95.3	15	28.9	6.3	15	<MDL	<MDL	<MDL	<MDL
PAHs																				
1-Methylnaphthalene	28	280	1.31	ug/L	246	114	12	<MDL	174	12.6	115	1550	564	1250	848	115	11.9	2.3	81.2	<MDL
2-Methylnaphthalene	28	280	4.27	ug/L	218	9.2	6.8	<MDL	27.3	147.1	18.4	229.3	698	1830	1280	595	6.6	<MDL	<MDL	<MDL
Naphthalene	14	140	2.2	ug/L	1590	34.9	6.7	<MDL	3450	9500	1720	12700	295	1810	385	77.6	8	3.8	5.8	<MDL
Acenaphthene	20	200	1.83	ug/L	25.9	45.6	63.8	<MDL	6.3	24.8	14.3	32.5	53.9	142	238	332	3.4	<MDL	1.9	<MDL
Acenaphthylene	210	2100	1.53	ug/L	18.4	23.1	13.3	<MDL	9.2	129.3	21.9	124.1	29.7	76.5	63.3	45.9	<MDL	<MDL	<MDL	<MDL
Anthracene	2100	21000	5.53	ug/L	<MDL	< MDL	<MDL	<MDL	<MDL	2.3	1.8	<MDL	4.9	3.2	<MDL	<MDL	<MDL	<MDL	<MDL	<MDL
Benz [a] anthracene	0.05	5	4.77	ug/L	<MDL	<MDL	<MDL	<MDL	<MDL	<MDL	<MDL	<MDL	<MDL	<MDL	<MDL	<MDL	<MDL	<MDL	<MDL	<MDL
Benzo [a] pyrene	0.2	20	13.3	ug/L	<MDL	<MDL	<MDL	<MDL	<MDL	<MDL	<MDL	<MDL	<MDL	<MDL	<MDL	<MDL	<MDL	<MDL	<MDL	<MDL
Benz [b, k] fluoranthene	-	-	5.62	ug/L	<MDL	<MDL	<MDL	<MDL	<MDL	<MDL	<MDL	<MDL	<MDL	<MDL	<MDL	<MDL	<MDL	<MDL	<MDL	<MDL
Benzo [g,h,i] perylene	210	2100	11.5	ug/L	<MDL	<MDL	<MDL	<MDL	<MDL	<MDL	<MDL	<MDL	<MDL	<MDL	<MDL	<MDL	<MDL	<MDL	<MDL	<MDL
Chrysene	4.8	480	5.75	ug/L	<MDL	<MDL	<MDL	<MDL	<MDL	<MDL	<MDL	<MDL	<MDL	<MDL	<MDL	<MDL	<MDL	<MDL	<MDL	<MDL
Fluoranthene	280	2800	1.8	ug/L	2.3	3.3	<MDL	<MDL	<MDL	1.8	<MDL	2.6	<MDL	<MDL	2.4	3.2	<MDL	<MDL	<MDL	<MDL
Fluorene	280	2800	1.88	ug/L	30	7.9	35.6	<MDL	<MDL	54.4	8.7	87.1	36.5	9.7	113	73.9	<MDL	<MDL	<MDL	<MDL
Indeno[1,2,3-c,d] pyrene + Dibenz[a,h] anthracene	-	-	18.7	ug/L	<MDL	<MDL	<MDL	<MDL	<MDL	<MDL	<MDL	<MDL	<MDL	<MDL	<MDL	<MDL	<MDL	<MDL	<MDL	<MDL
Phenanthrene	210	2100	3.78	ug/L	27.9	58.3	38.5	<MDL	<MDL	26.6	<MDL	38.5	<MDL	65.1	7.5	45	<MDL	<MDL	<MDL	<MDL
Pyrene	210	2100	1.6	ug/L	2.8	3.8	<MDL	<MDL	<MDL	1.6	<MDL	2.5	<MDL	1.6	<MDL	5.3	<MDL	<MDL	<MDL	<MDL

Notes:

- GCTL - FDEP Groundwater Cleanup Target Level
- NADC - FDEP Natural Attenuation Default Concentration
- MDL - minimum detection limit
- PAHs - polycyclic aromatic hydrocarbons
- ft bls - feet below land surface
- ug/L - micrograms per liter
- ML - multi-level monitoring well

Table C.4. Summary of groundwater concentrations from transect samples.

	GCTL	NADC	MDL	Units	July 2011			November 2011			February 2012		
					Max	Min	Average	Max	Min	Average	Max	Min	Average
BTEX													
Benzene	1	100	1.11	ug/L	17800	1.8	530	15800	1.1	714	13000	1.3	505
Ethylbenzene	30	300	0.77	ug/L	14800	1.6	810	8660	1.3	817	6990	0.8	432
m-Xylene & p-Xylene	20	200	1.46	ug/L	9290	1.8	537	7640	1.3	478	6220	1.4	475.3
o-Xylene	20	200	0.37	ug/L	4036	1.5	304	3240	1.5	239	2680	1.3	279.9
Toluene	40	400	0.83	ug/L	7820	1.7	248	7850	0.9	245	11300	1.5	289
Trimethylbenzenes													
1,2,3-Trimethylbenzene	10	100	0.76	ug/L	1160	1.9	107	917	1.4	78	554	1.5	104.9
1,2,4-Trimethylbenzene	10	100	0.82	ug/L	1970	1.7	214	1190	1.8	131	1240	1.9	174
1,3,5-Trimethylbenzene	10	100	0.74	ug/L	417	1.5	59	315	1.7	38	335	1.5	67.8
PAHs													
1-Methylnaphthalene	28	280	1.31	ug/L	784	1.0	260	1360	1.8	400	1550	1.1	456
2-Methylnaphthalene	28	280	4.27	ug/L	1210	0.8	297	1960	2.1	430	1950	1.4	392
Naphthalene	14	140	2.2	ug/L	16000	1.5	4090	15800	3.8	3873	17700	1.2	3740
Acenaphthene	20	200	1.83	ug/L	183	0.8	38.4	345	1.6	58.4	332	1.2	66
Acenaphthylene	210	2100	1.53	ug/L	73	1.1	20.1	141	0.6	24.5	148	1.6	37.3
Anthracene	2100	21000	5.53	ug/L	12	1.3	2.71	10	1.1	1	8.4	1.3	3
Benz [a] anthracene	0.05	5	4.77	ug/L	22	1.0	0.8	14.6	3.3	1.4	14.9	0.7	2.8
Benzo [a] pyrene	0.2	20	13.33	ug/L	<MDL	<MDL	<MDL	<MDL	<MDL	<MDL	2.2	1.4	1.7
Benzo [b, k] fluoranthene	-	-	5.62	ug/L	2.37	1.3	0.04	13.9	6.9	0.2	<MDL	<MDL	<MDL
Benzo [g,h,i] perylene	210	2100	11.49	ug/L	<MDL	<MDL	<MDL	<MDL	<MDL	<MDL	<MDL	<MDL	<MDL
Biphenyl	0.5	50	3.26	ug/L	94.8	0.7	19.9	94.8	0.7	19.9	<MDL	<MDL	<MDL
Carbazole	1.8	180	7.18	ug/L	12.3	1.1	2.5	12.3	1.1	2.5	<MDL	<MDL	<MDL
Chrysene	4.8	480	5.75	ug/L	<MDL	<MDL	<MDL	<MDL	<MDL	<MDL	<MDL	<MDL	<MDL
Dibenzofuran	28	280	3.31	ug/L	52.7	0.9	13.2	52.7	0.9	13.2	<MDL	<MDL	<MDL
Fluoranthene	280	2800	1.8	ug/L	5.99	0.7	0.8	6.4	0.4	0.8	14.2	1.4	3.3
Fluorene	280	2800	1.88	ug/L	84.8	0.9	25.1	132	1.4	37.2	137	1.3	45.8
Indole	-	-	6.36	ug/L	<MDL	<MDL	<MDL	<MDL	<MDL	<MDL	<MDL	<MDL	<MDL
Indeno[1,2,3-c,d] pyrene + Dibenz [a,h] anthracene	-	-	18.65	ug/L	<MDL	<MDL	<MDL	<MDL	<MDL	<MDL	<MDL	<MDL	<MDL
Phenanthrene	210	2100	3.78	ug/L	117	0.8	19.9	160	1.1	23.7	167	1.4	37
Pyrene	210	2100	1.6	ug/L	7.0	0.8	1.2	8.4	0.4	0.9	7.8	1.3	3.1

Notes:

- GCTL - FDEP Groundwater Cleanup Target Level
- NADC - FDEP Natural Attenuation Default Concentration
- MDL - minimum detection limit
- Max - maximum concentration in transect
- Min - minimum concentration in transect
- Average - average concentration in transect

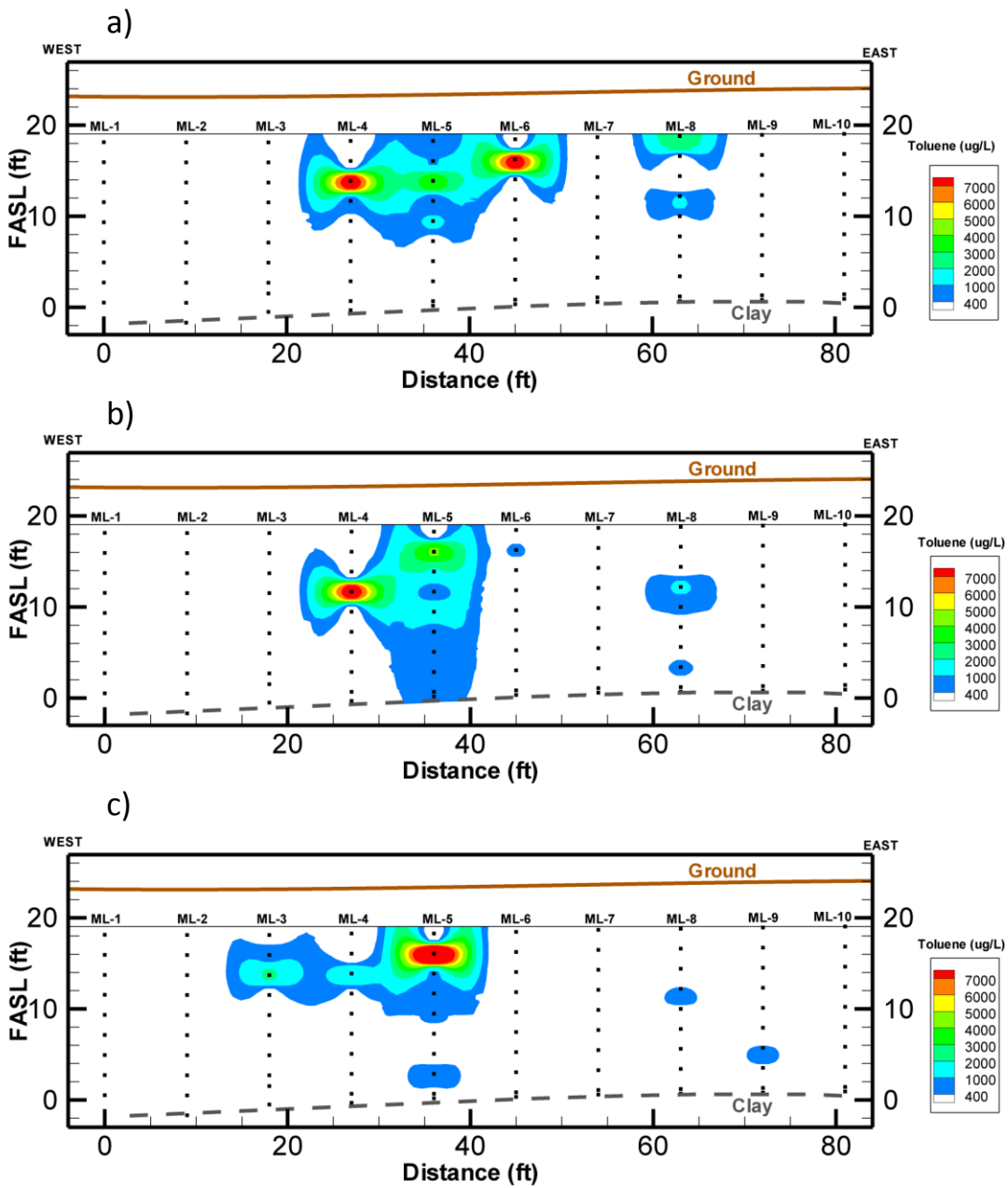


Figure C.1. Toluene transect iso-concentration profile from a) July 2011, b) November 2011, and c) February 2012.

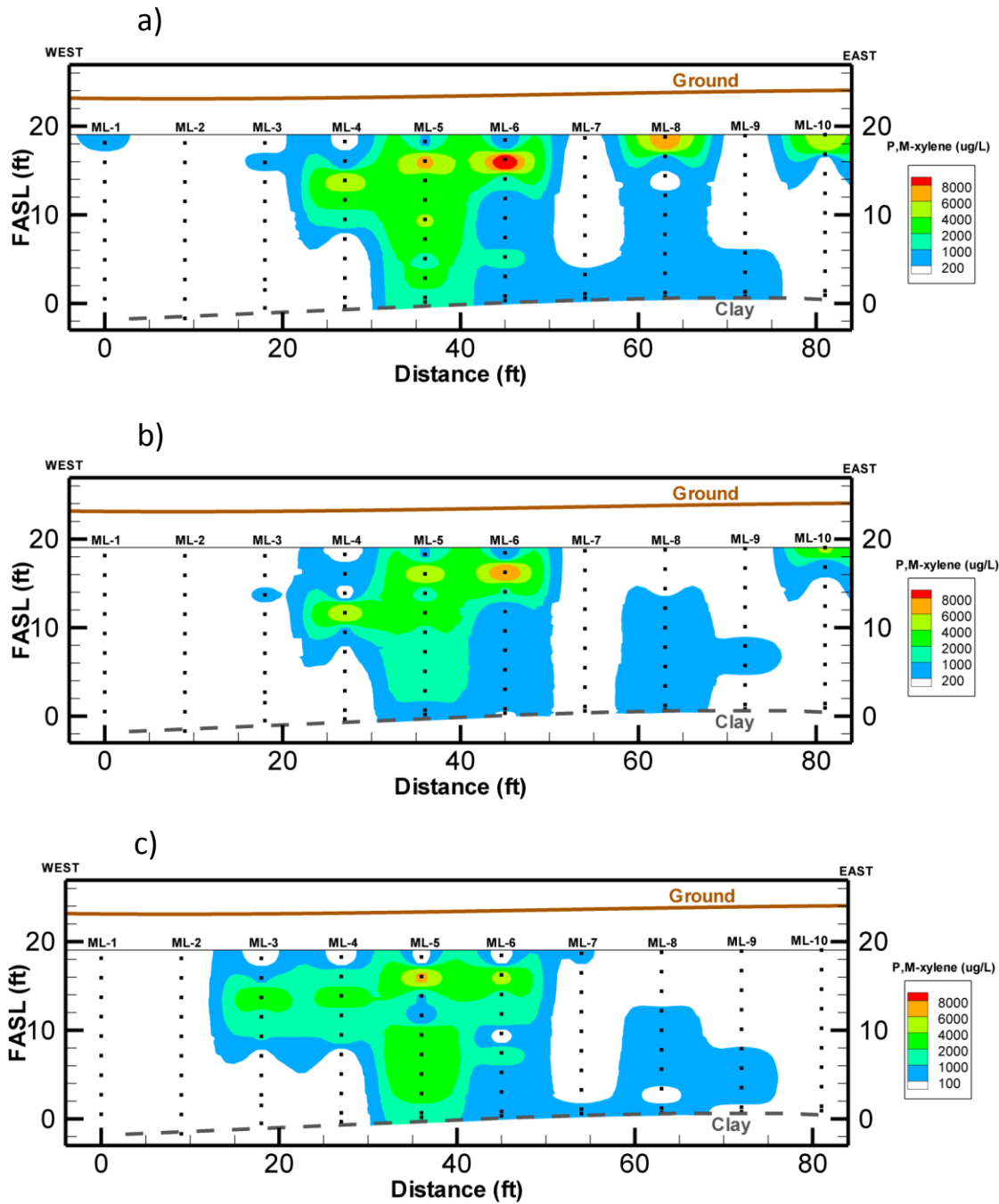


Figure C.2. P,M-xylene transect iso-concentration profile from a) July 2011, b) November 2011, and c) February 2012.

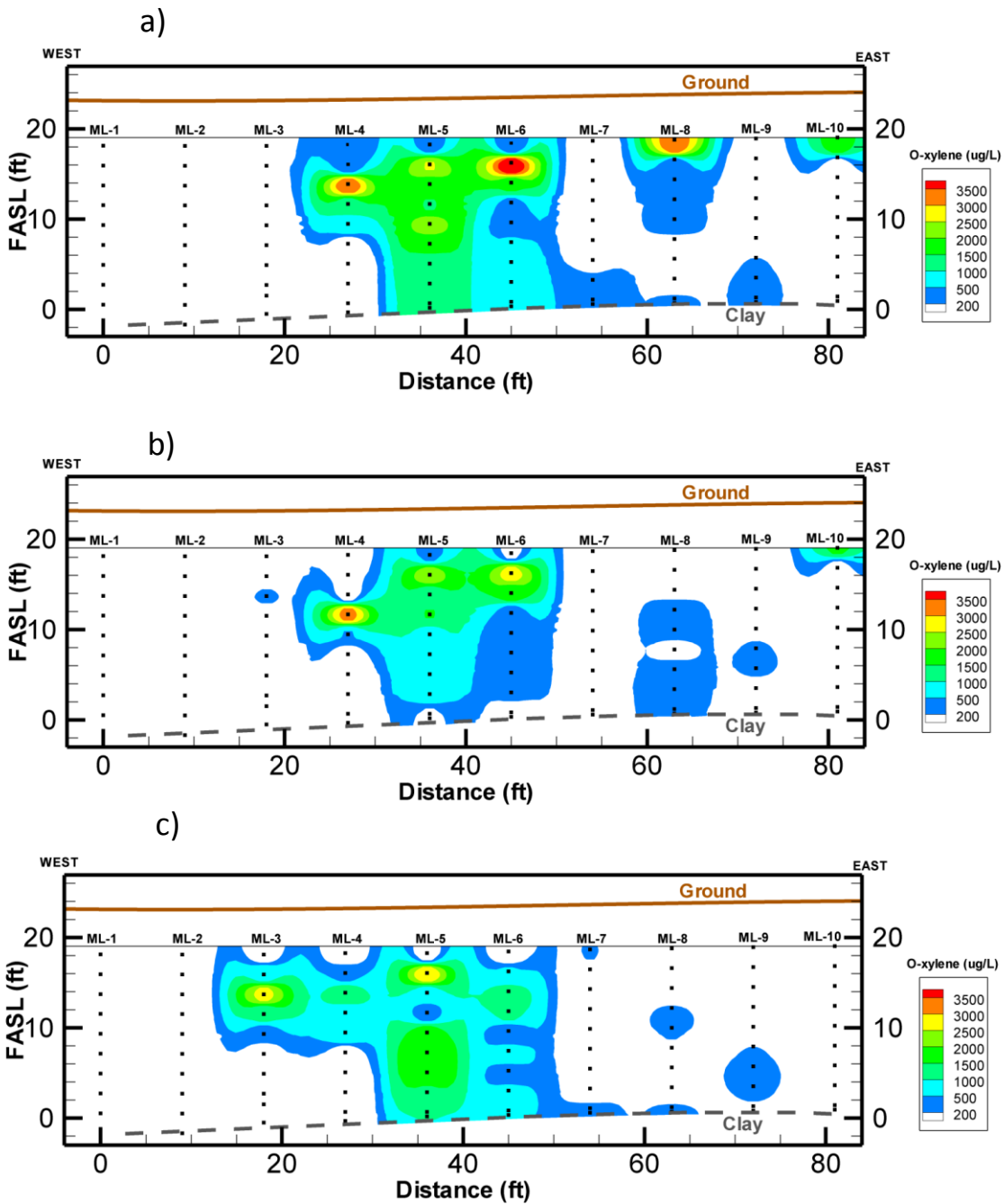


Figure C.3. o-xylene transect iso-concentration profile from a) July 2011, b) November 2011, and c) February 2012.

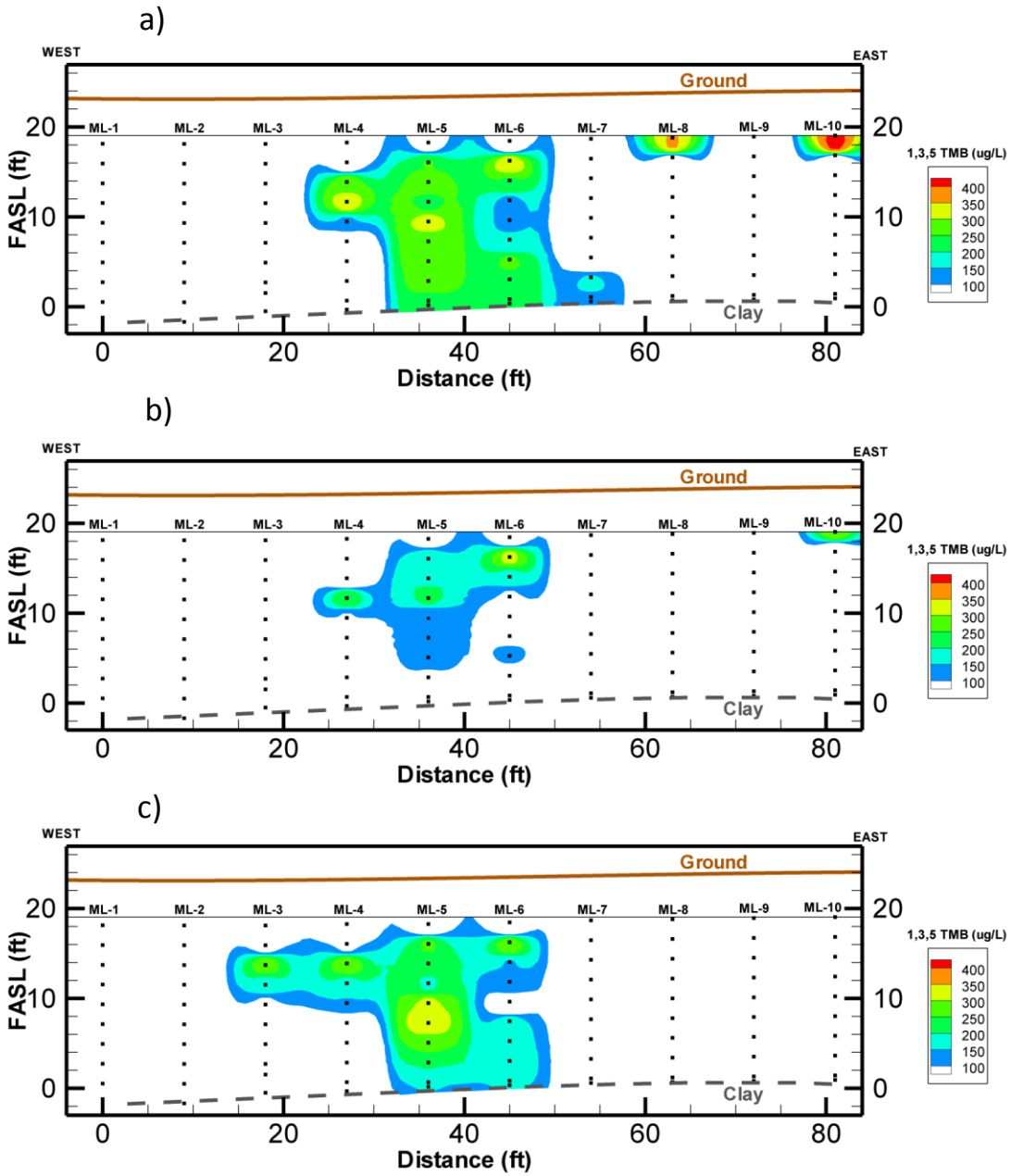


Figure C.4. 1,3,5-trimethylbenzene transect iso-concentration profile from a) July 2011, b) November 2011, and c) February 2012.

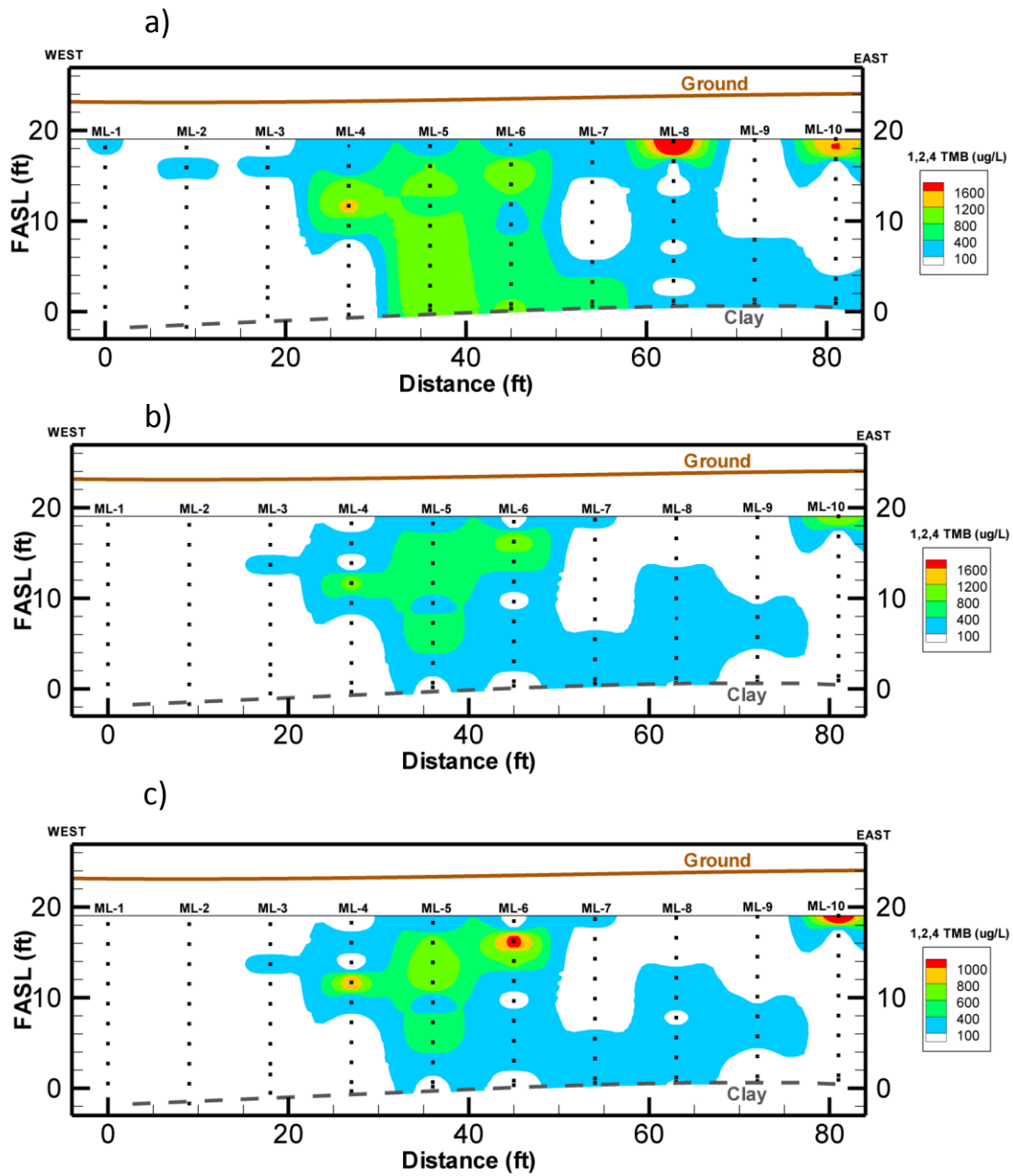


Figure C.5. 1,2,4-trimethylbenzene transect iso-concentration profile from a) July 2011, b) November 2011, and c) February 2012.

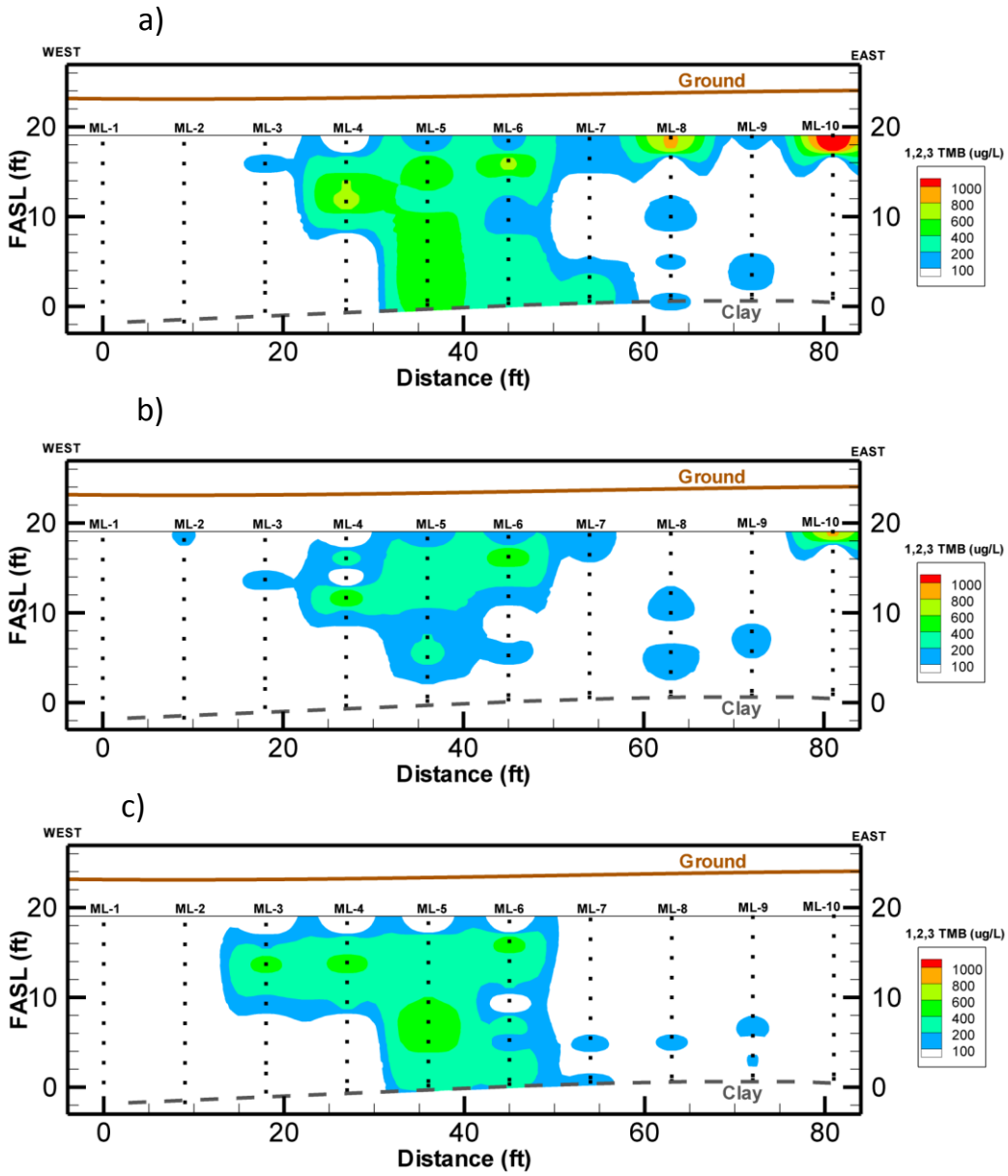


Figure C.6. 1,2,3-trimethylbenzene transect iso-concentration profile from a) July 2011, b) November 2011, and c) February 2012.

Appendix D: Bench Scale Data

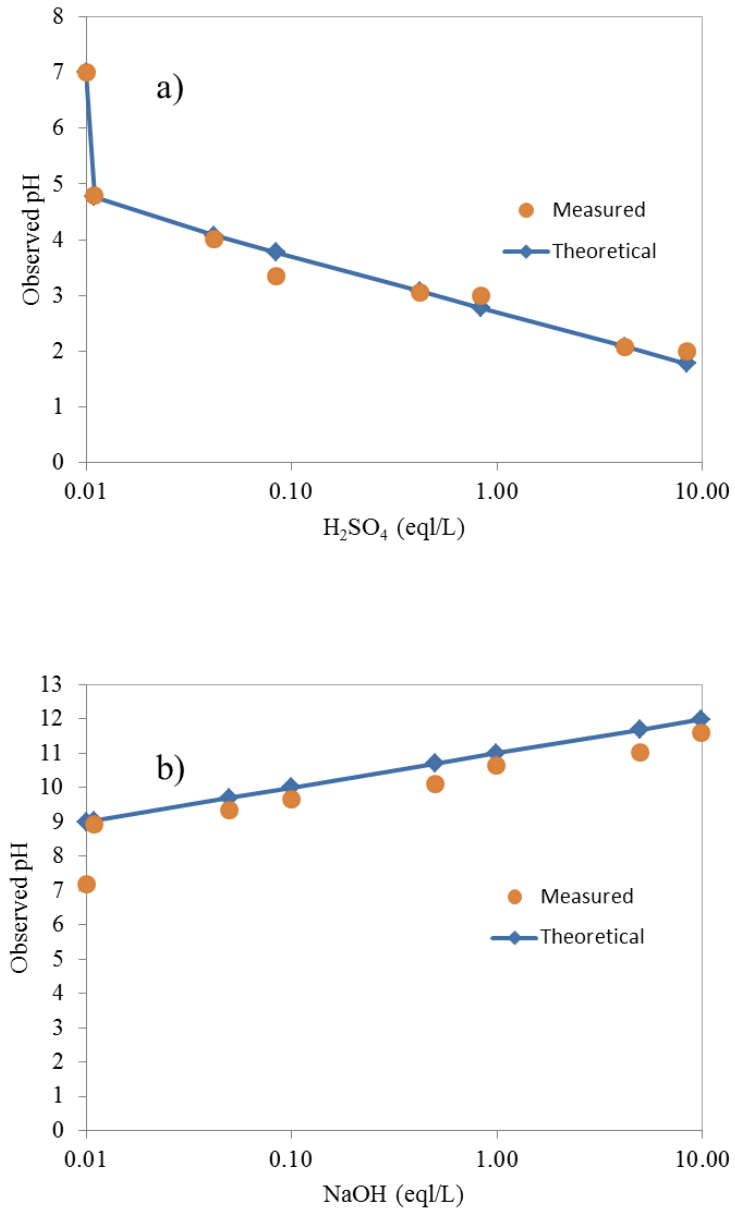


Figure D.1. Measured pH and theoretical pH curves of control reactors for (a) acid and (b) base titration.

Table D.1. COD ANOVA analysis.

Source of Variation	SS	df	MS	F	P-value	F crit
Rows	0.073221328	2	0.036610664	0.354787415	0.708437173	3.885293835
Columns	0.673711854	6	0.112285309	1.088136906	0.422190785	2.996120378
Error	1.238285091	12	0.103190424			
Total	1.985218274	20				

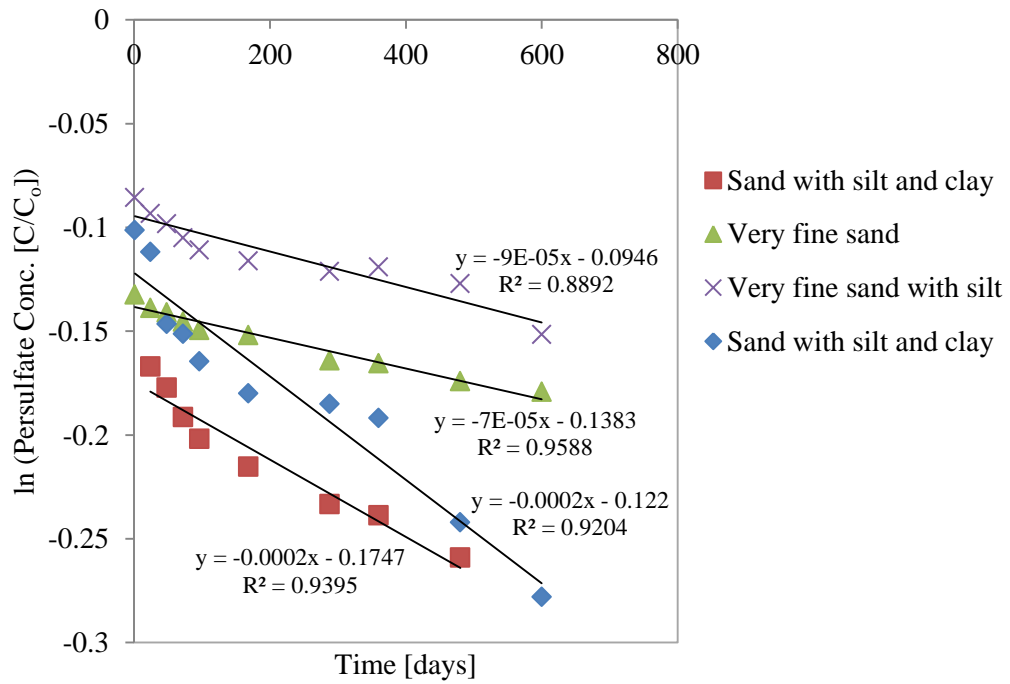


Figure D.2. Mass action law reaction rates for NOI test results.

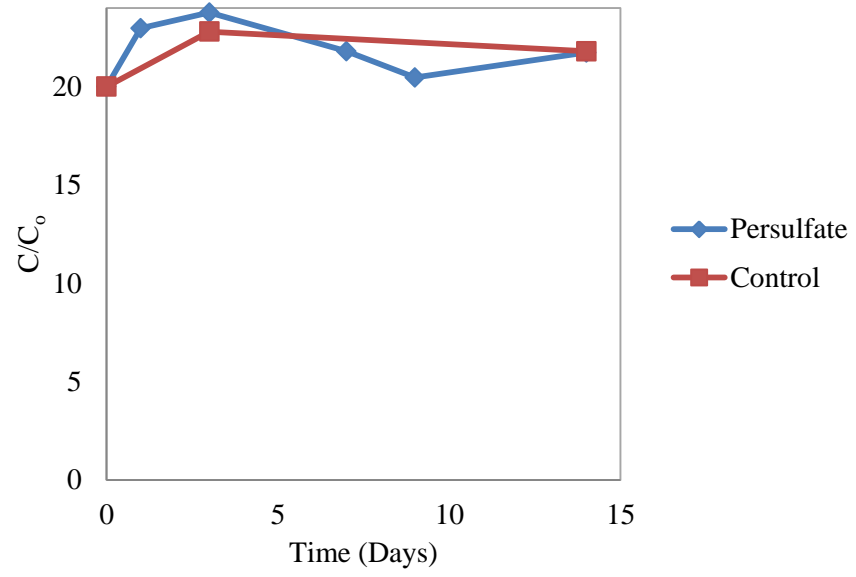


Figure D.3 Unactivated persulfate treatability results for persulfate concentration.

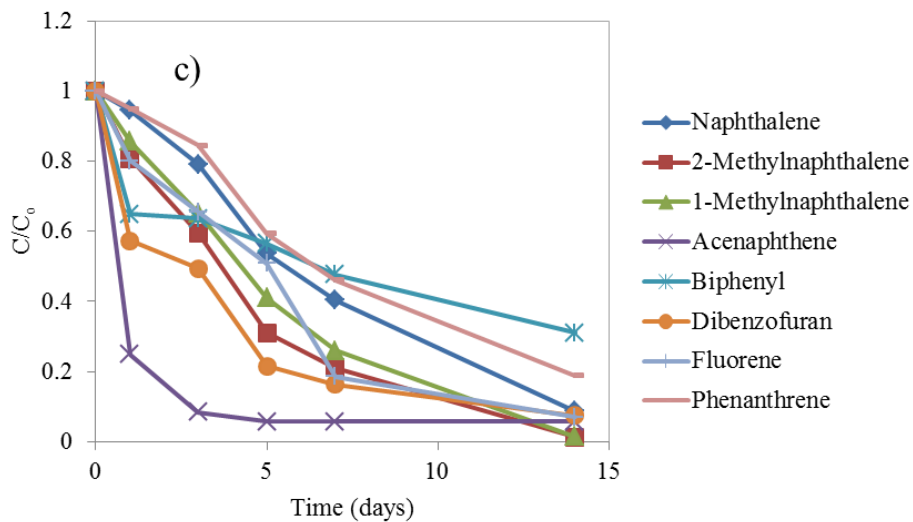
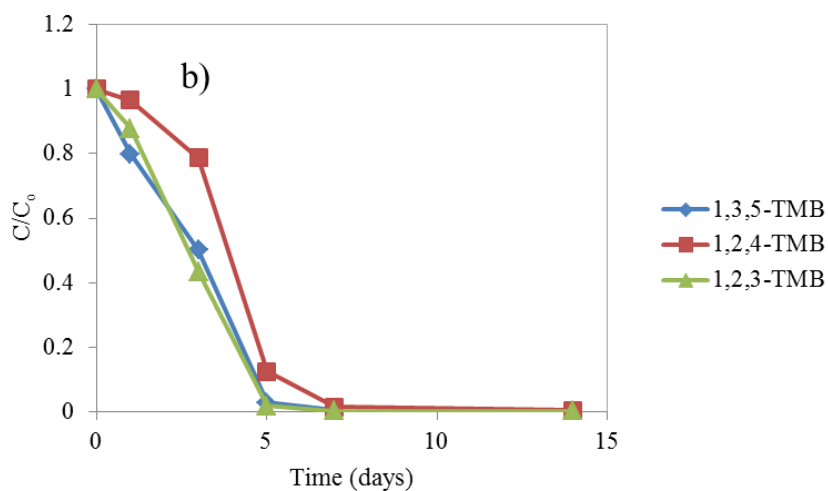
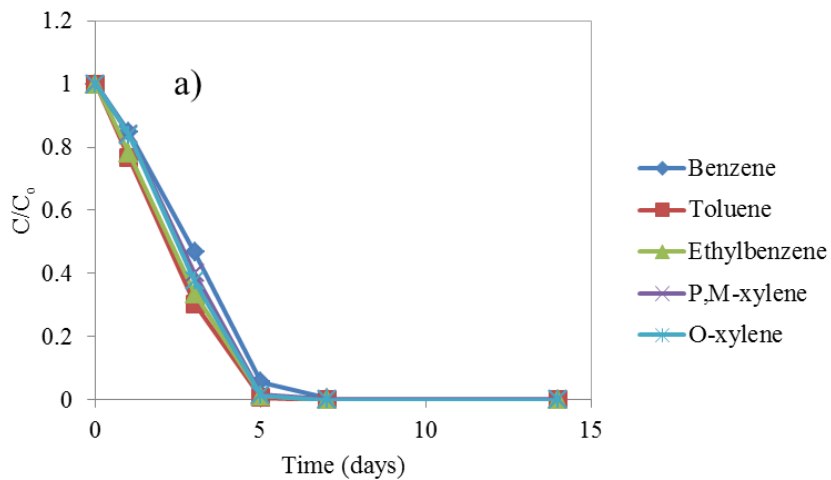


Figure D.4. Treatability results of unactivated persulfate for (a) BTEX (b) Trimethylbenzenes and (c) PAH compounds.

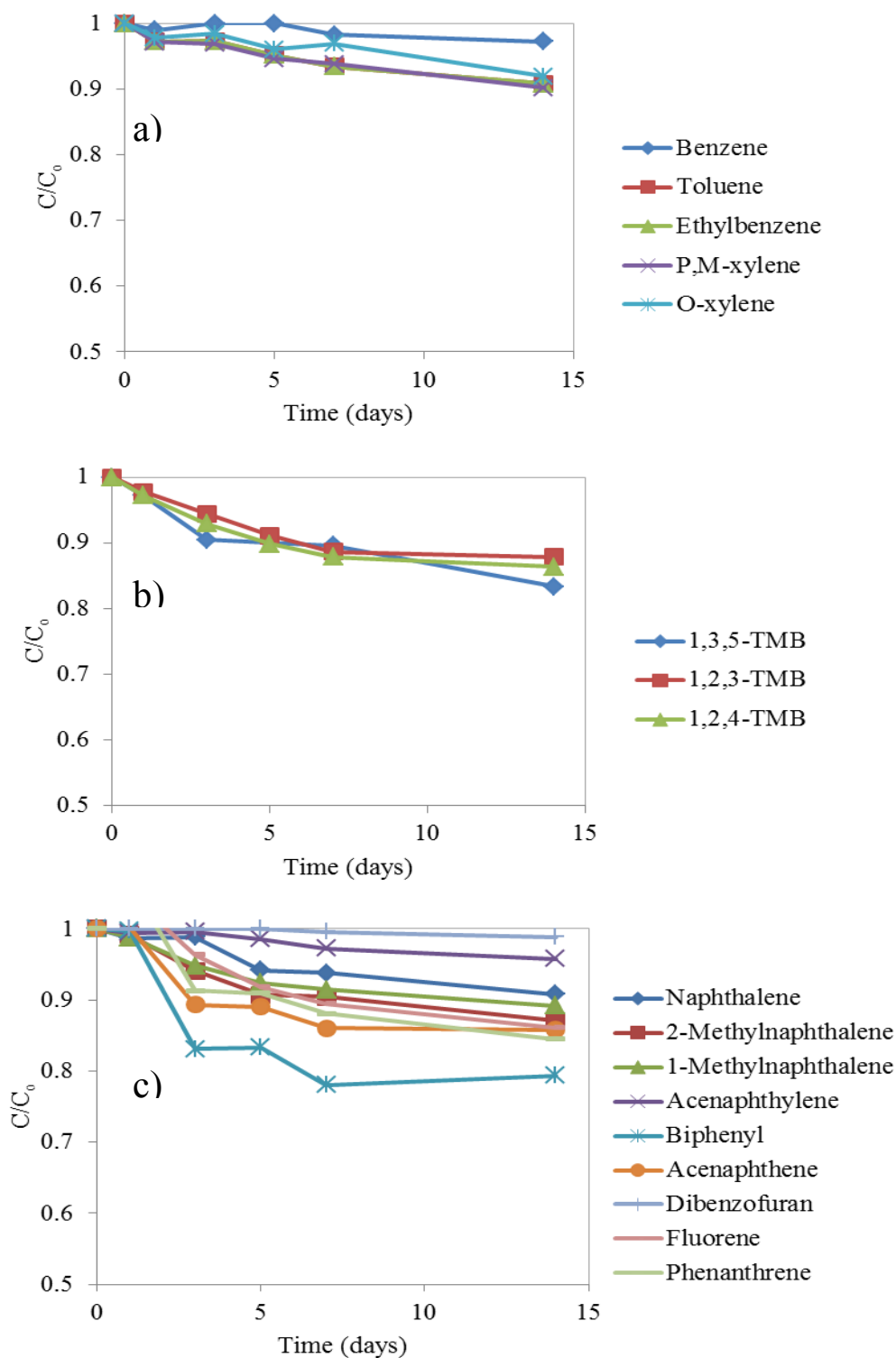


Figure D.5. Control results for unactivated persulfate treatability study for (a) BTEX (b) Trimethylbenzenes and (c) PAH compounds.

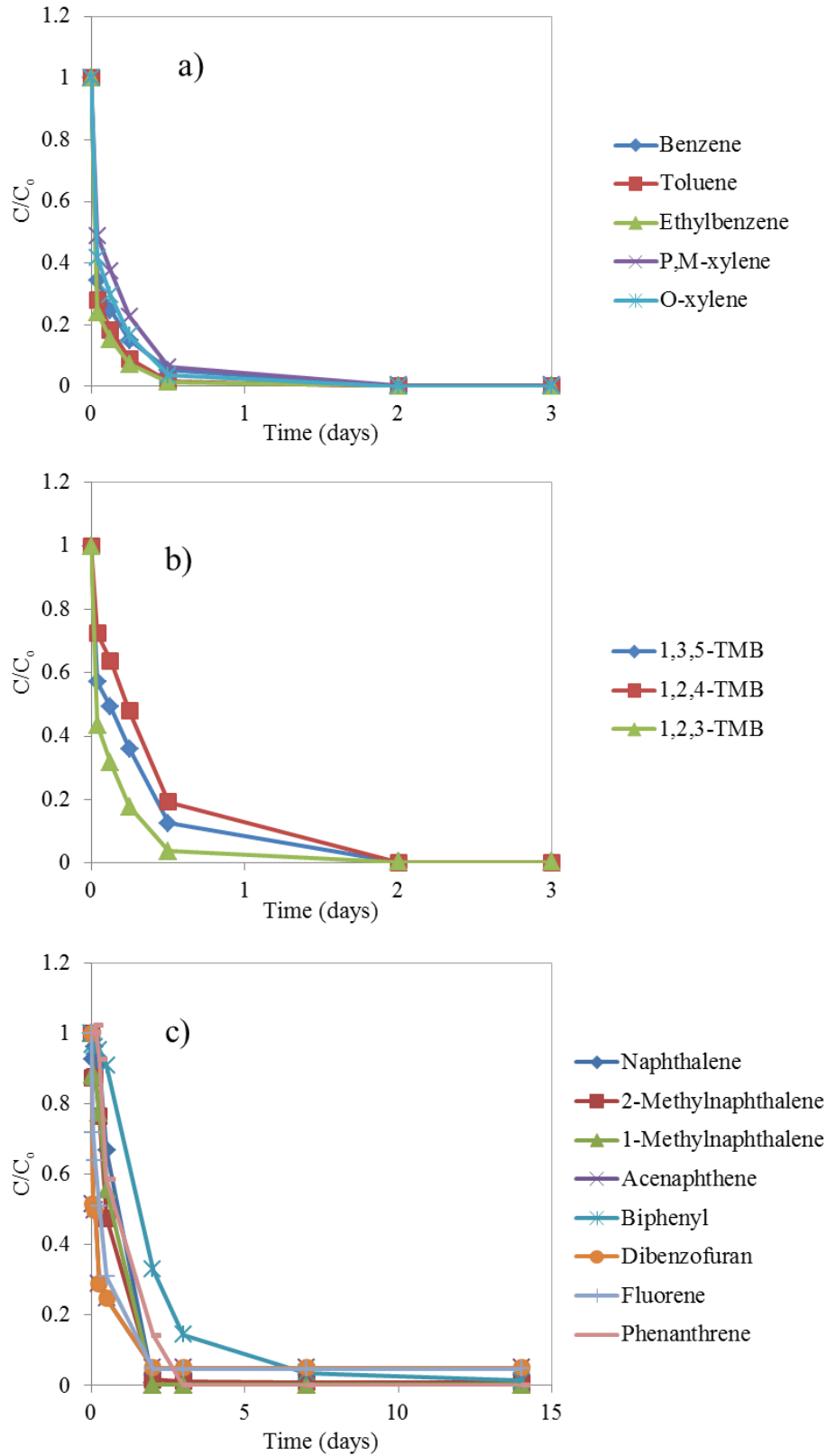


Figure D.6. Treatability results of 150 mg/L-Fe(II) activated persulfate for (a) BTEX (b) Trimethylbenzenes and (c) PAH compounds.

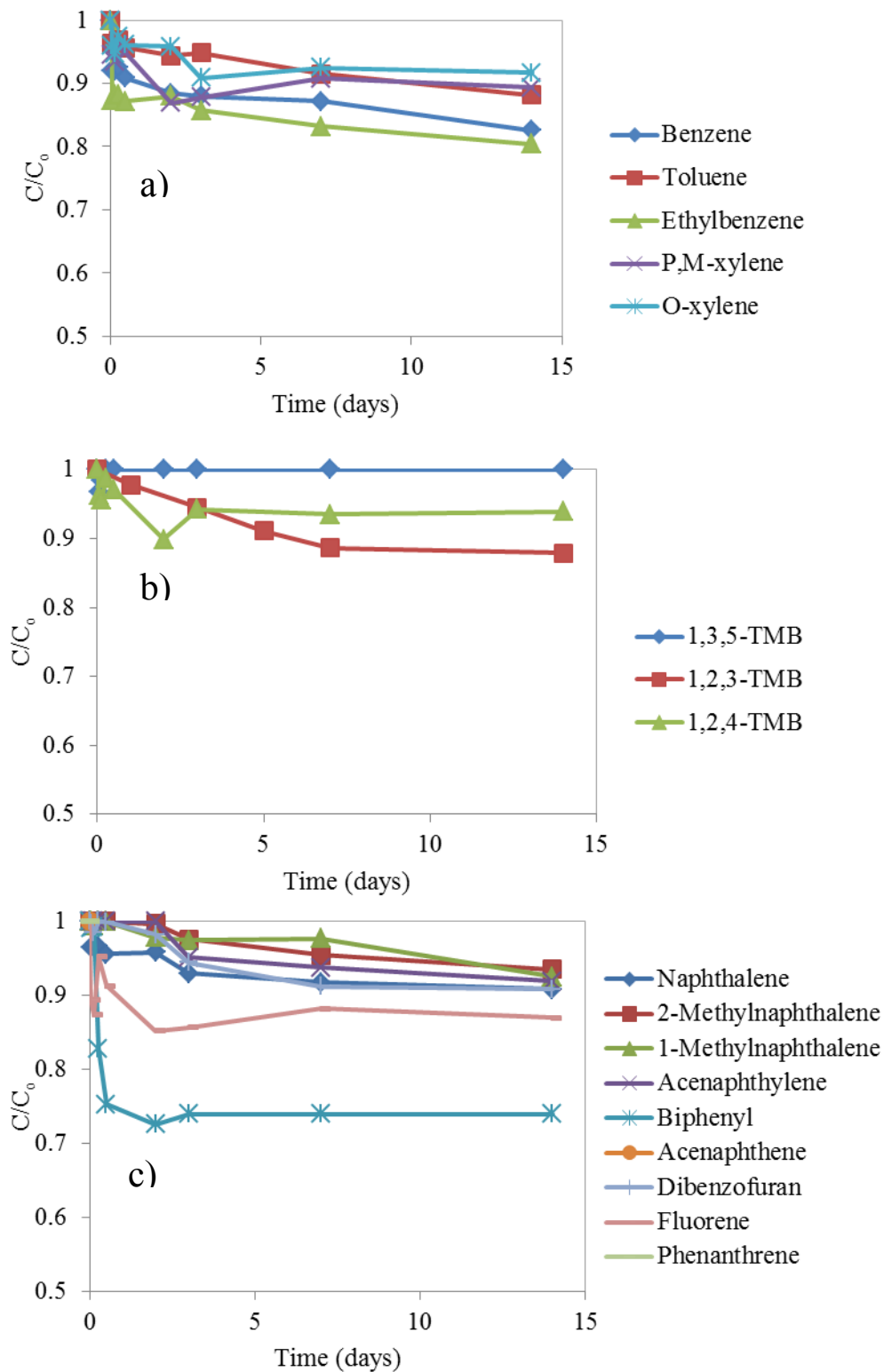


Figure D.7. Control results of 150 mg/L-Fe(II) activated persulfate treatability study for (a) BTEX (b) Trimethylbenzenes and (c) PAH compounds.

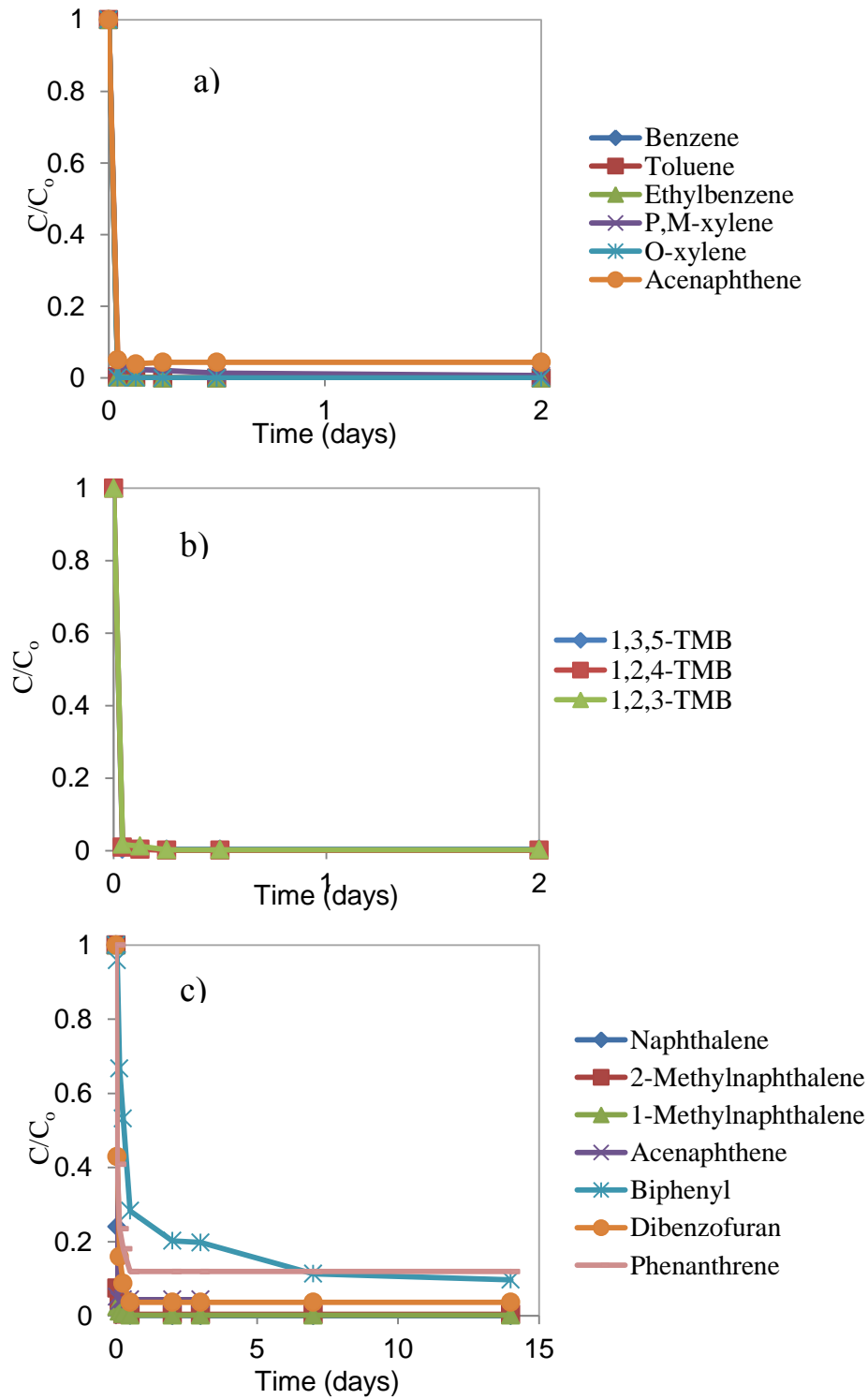


Figure D.8. Treatability results of 600 mg/L-Fe(II) activated persulfate for (a) BTEX (b) Trimethylbenzenes and (c) PAH compounds.

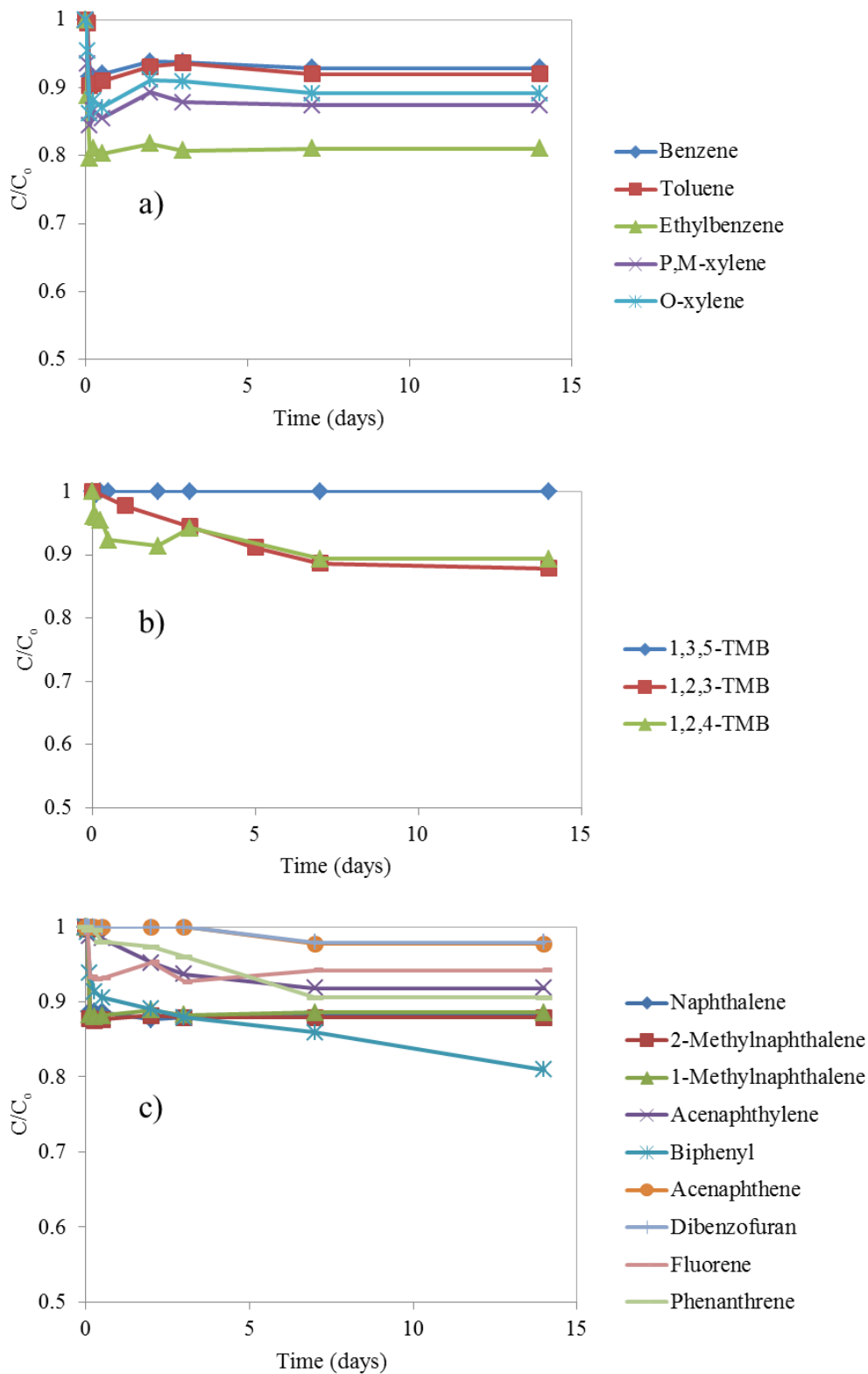


Figure D.9. Control results of 600 mg/L-Fe(II) activated persulfate treatability study for (a) BTEX (b) Trimethylbenzenes and (c) PAH compounds.

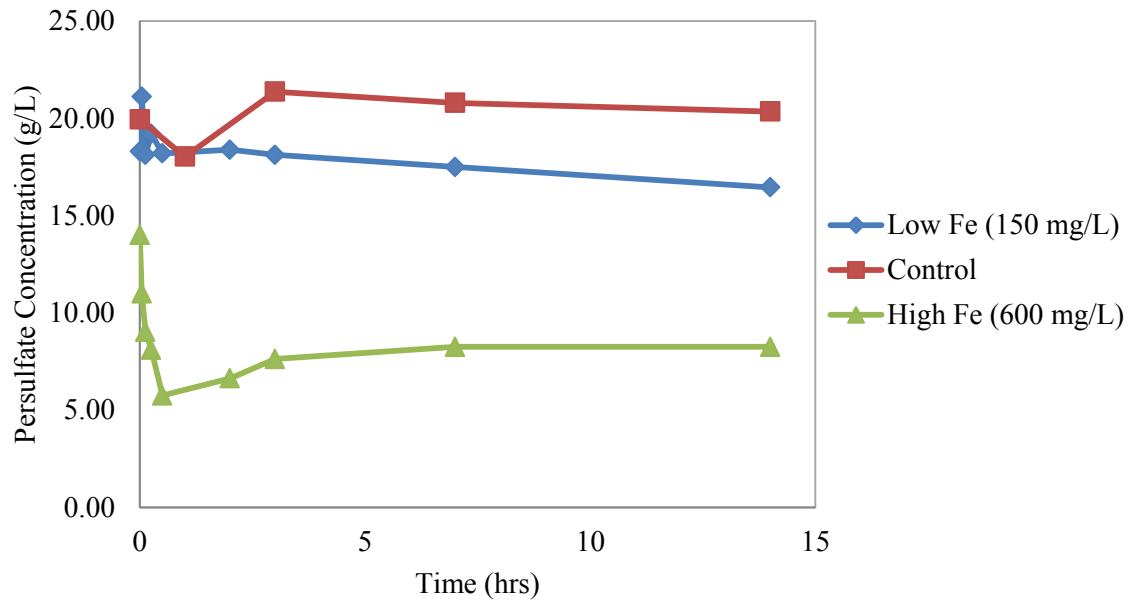


Figure D.10. Persulfate concentrations for iron activated treatability study.

Table D.2. Differential method to calculation reaction rate coefficient for benzene in high iron treatability study.

Time (s)	C (mg/L)	dC/dt	log(-dC/dt)	log(C)
0.000	9.17E-02	-10.2	1.01	-1.04
0.042	2.00E-04	-0.0100	-2.00	-3.70
0.125	1.35E-04	-0.0070	-2.15	-3.87
0.250	4.10E-05	-0.0060	-2.22	-4.39
0.500	1.41E-05	-0.0010	-3.00	-4.85

$$k = 103.2761406$$

$$n = 0.7408$$

$$r = 2.27Ca^{0.741}$$

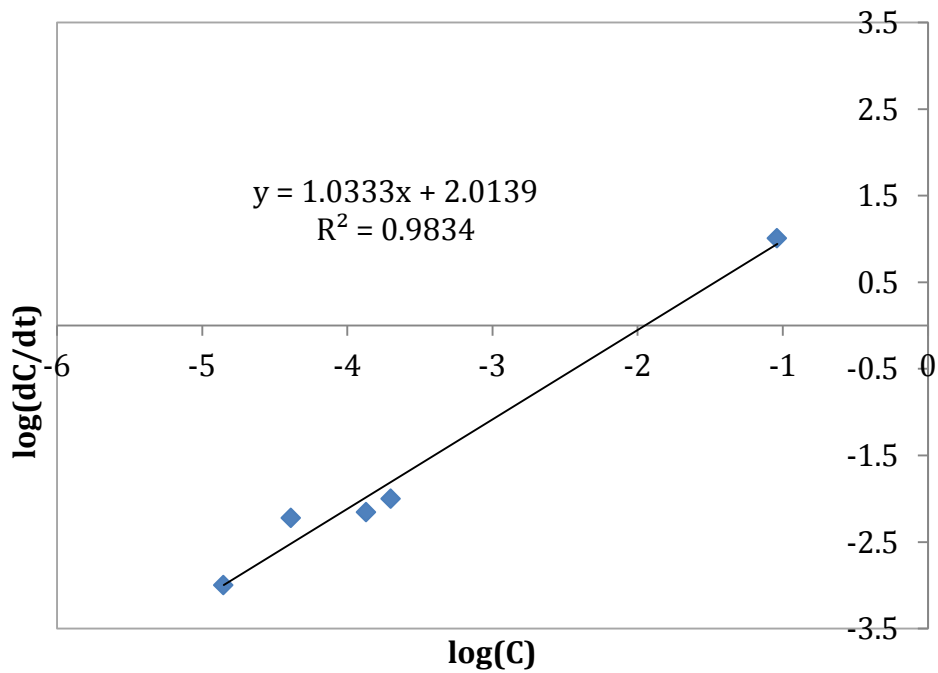


Figure D.11. Best fit line to determine the reaction rate coefficient using the differential method for benzene in high iron treatability study.

Appendix E: Column Data

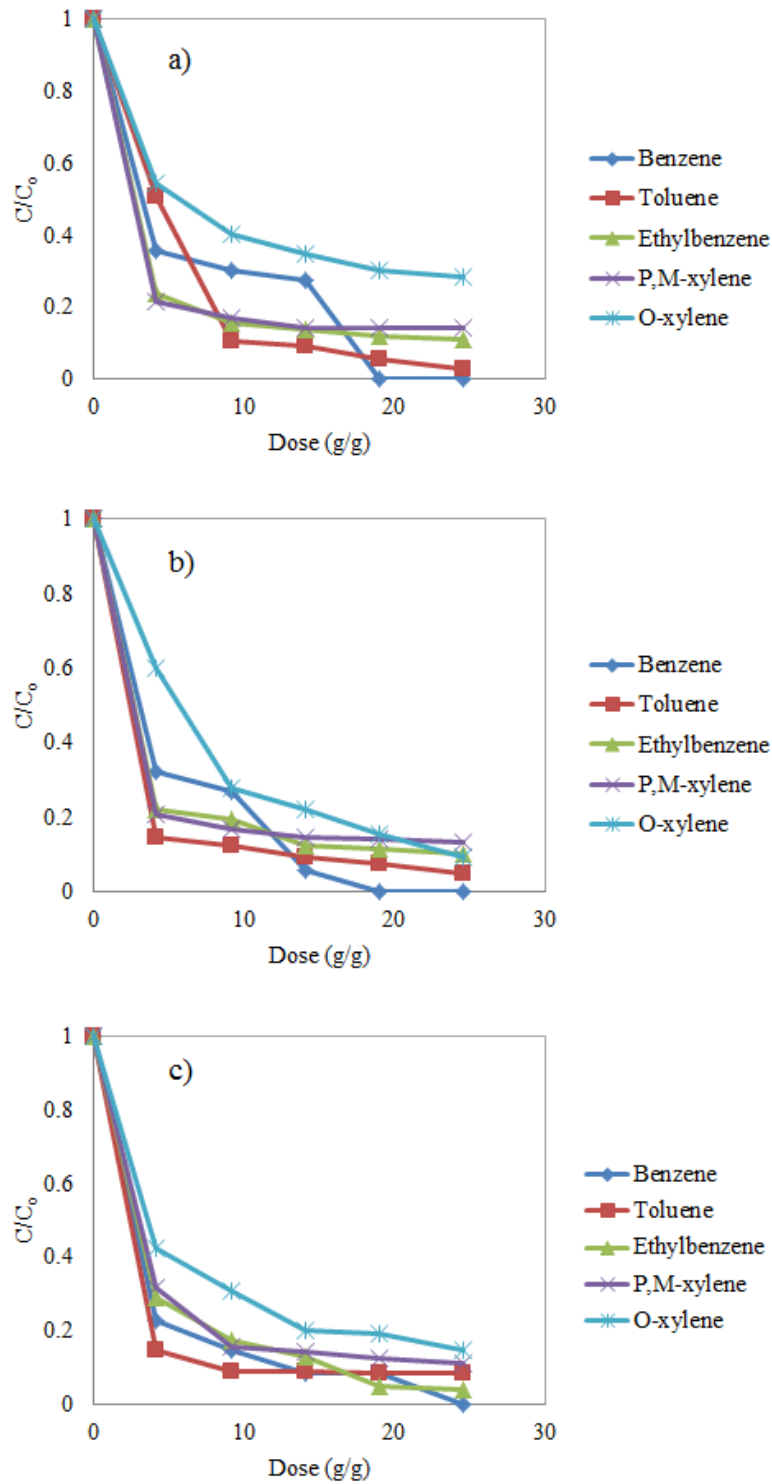


Figure E.1. Iron(II) activated persulfate dose-response curve for BTEX in (a) column 1, (b) column 2 and (c) column 3

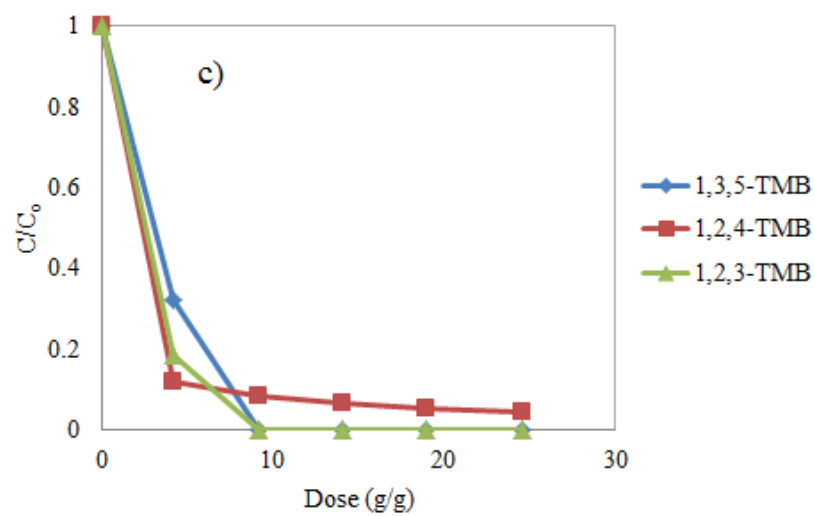
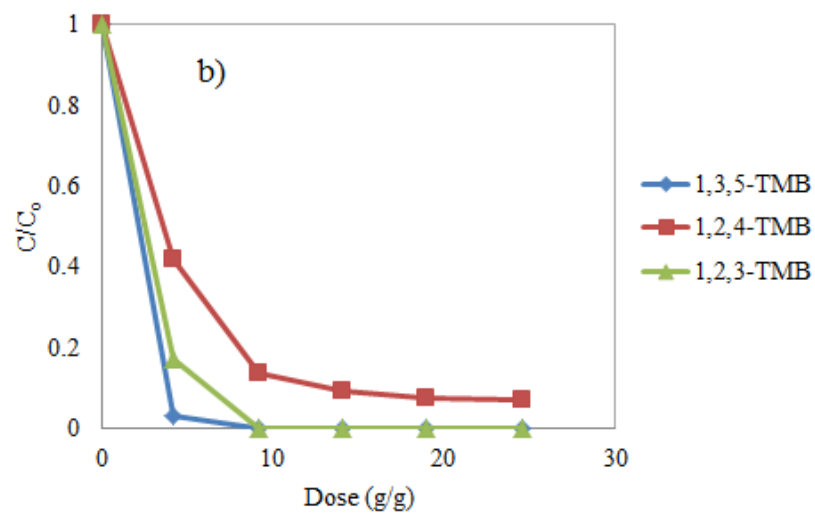
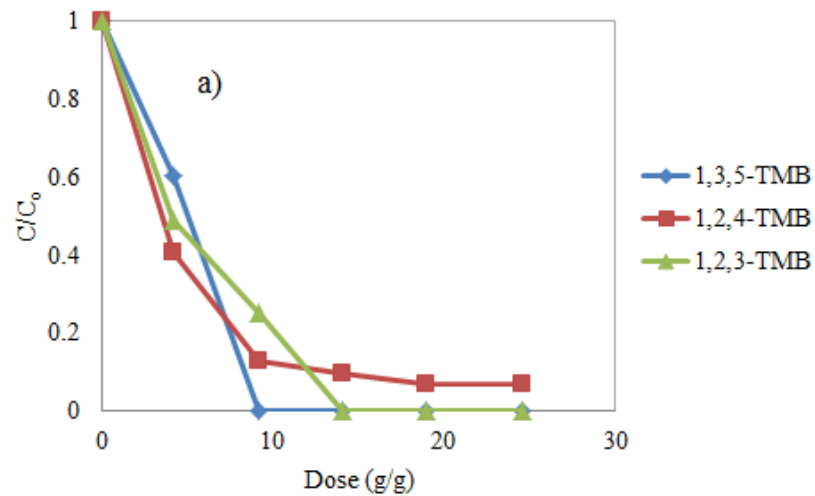


Figure E.2. Iron(II) activated persulfate dose-response curve for trimethylbenzenes in (a) column 1, (b) column 2 and (c) column 3

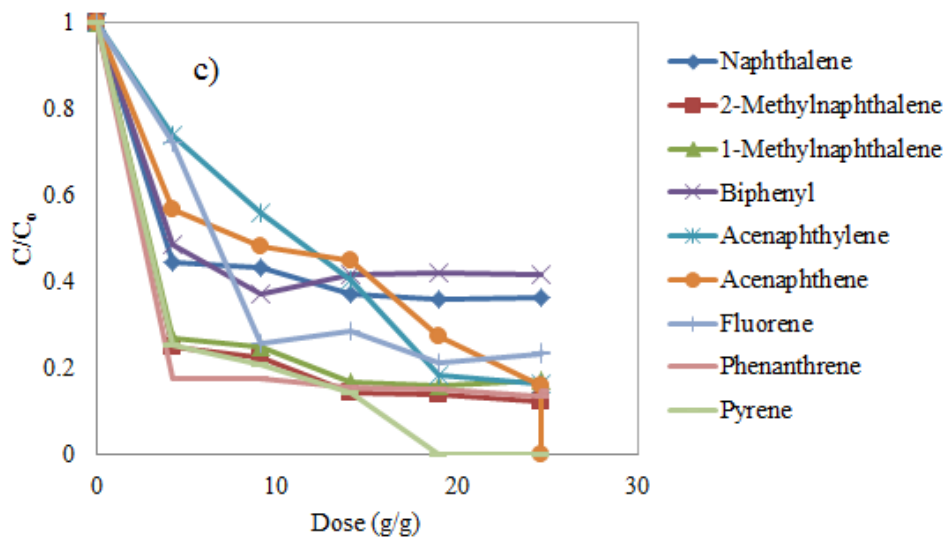
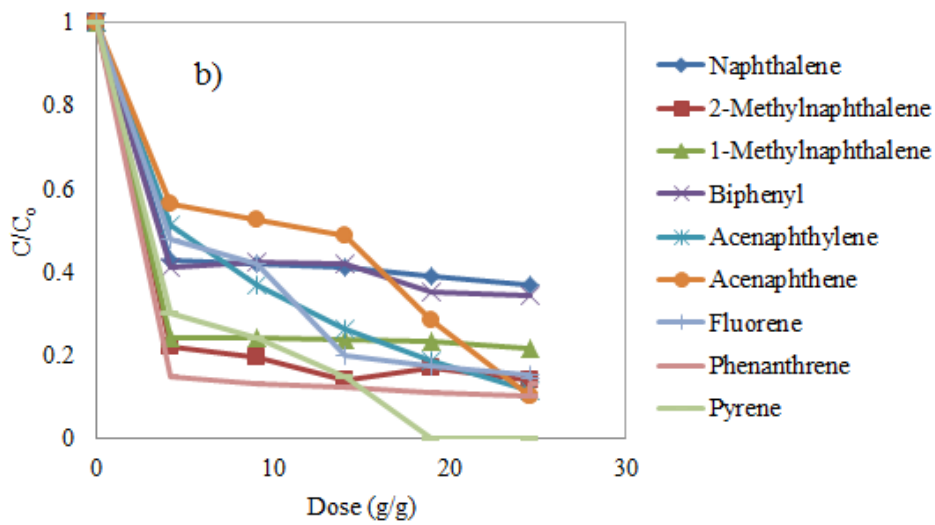
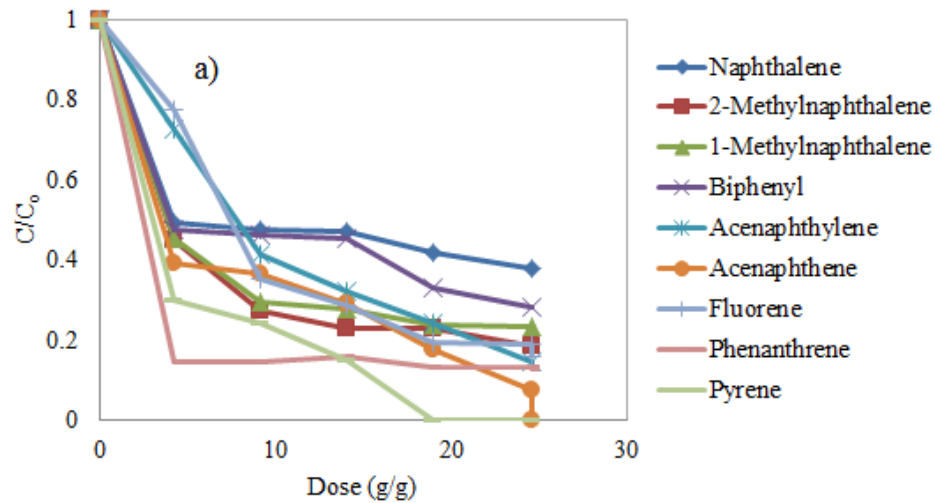


Figure E.3. Iron(II) activated persulfate dose-response curve for PAHs in (a) column 1, (b) column 2 and (c) column 3

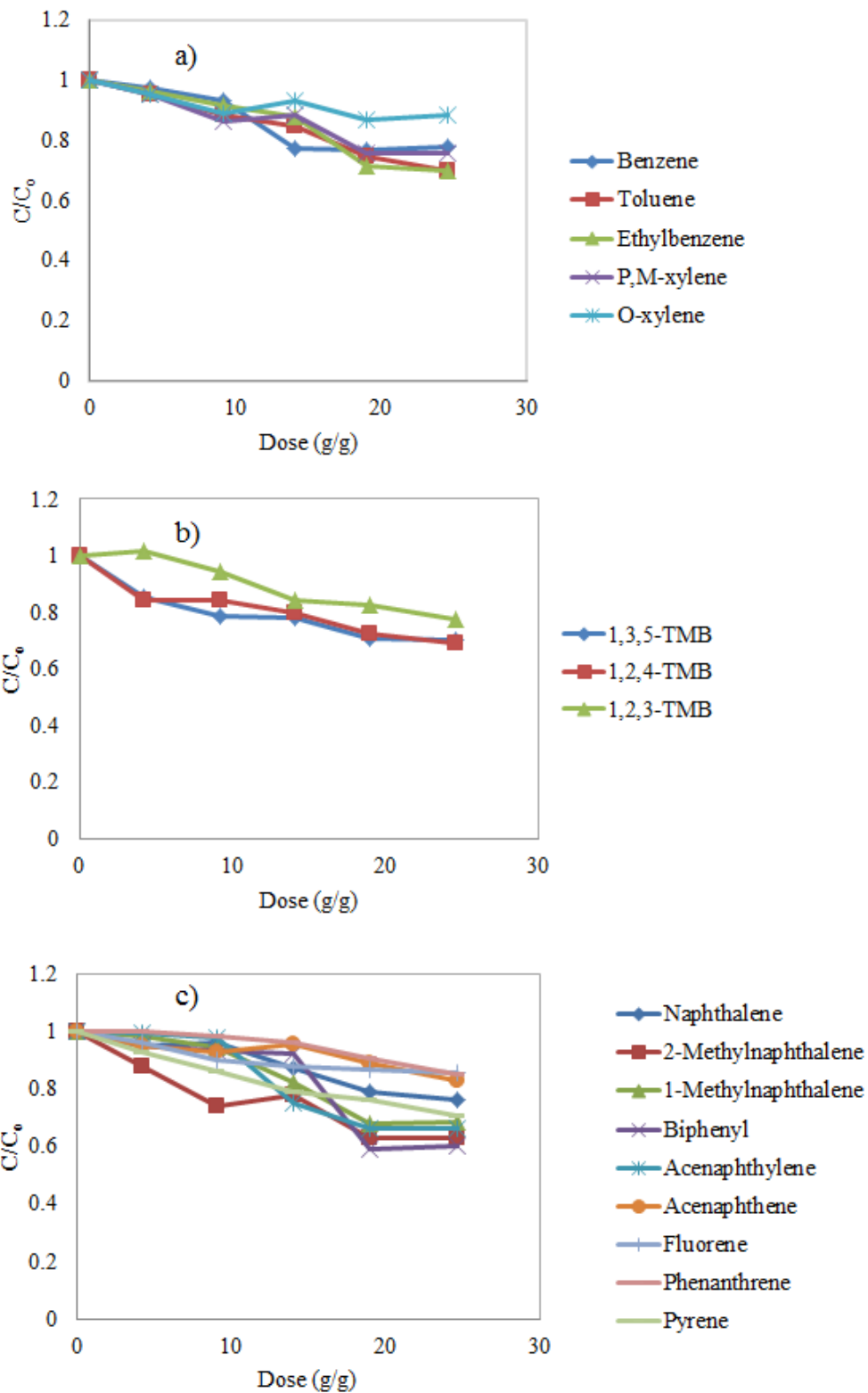


Figure E.4. Control iron(II) activated persulfate dose-response curve for (a) BTEX, (b) trimethylbenzenes, and (c) PAHs.

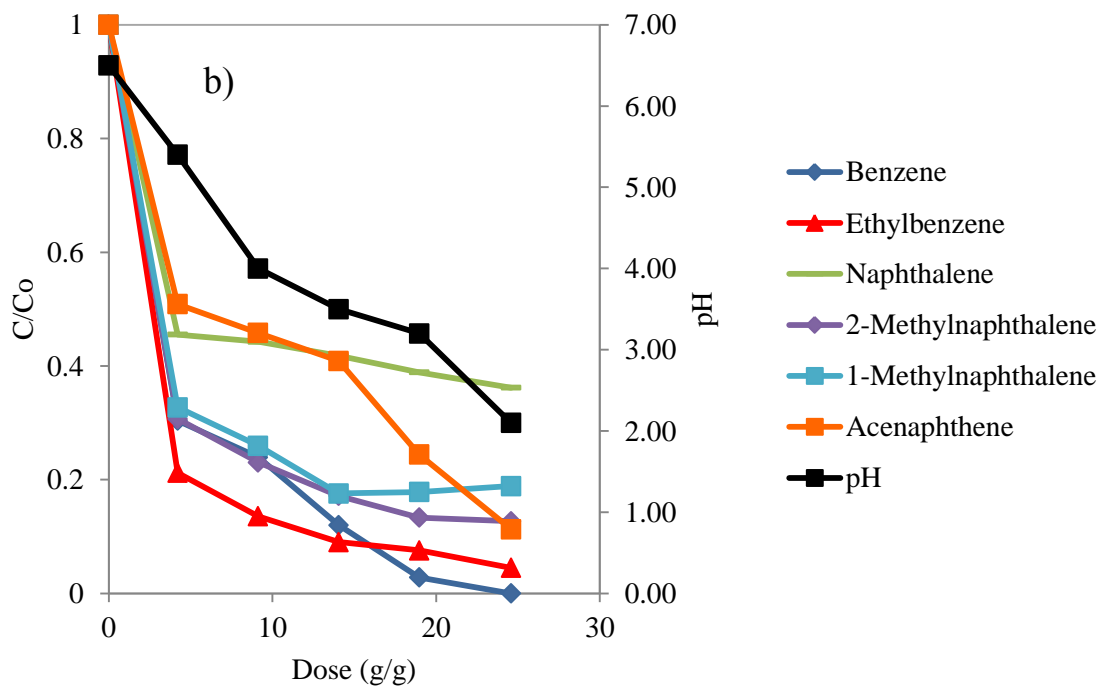
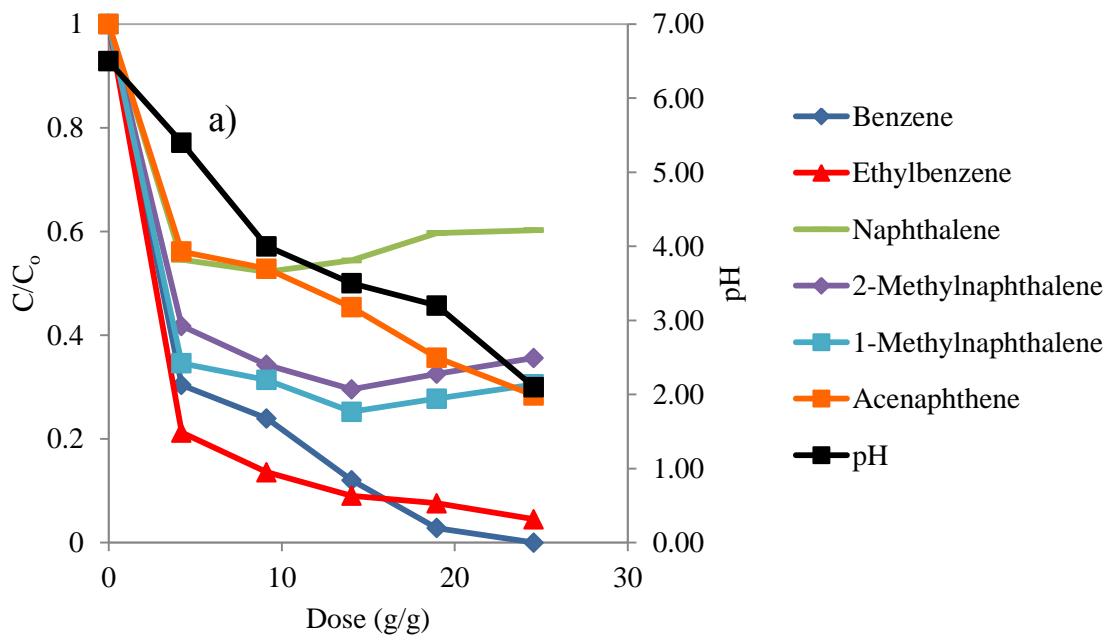


Figure E.5. Average iron(II) activated dose-response curves for (a) control adjusted (b) measured COCs..

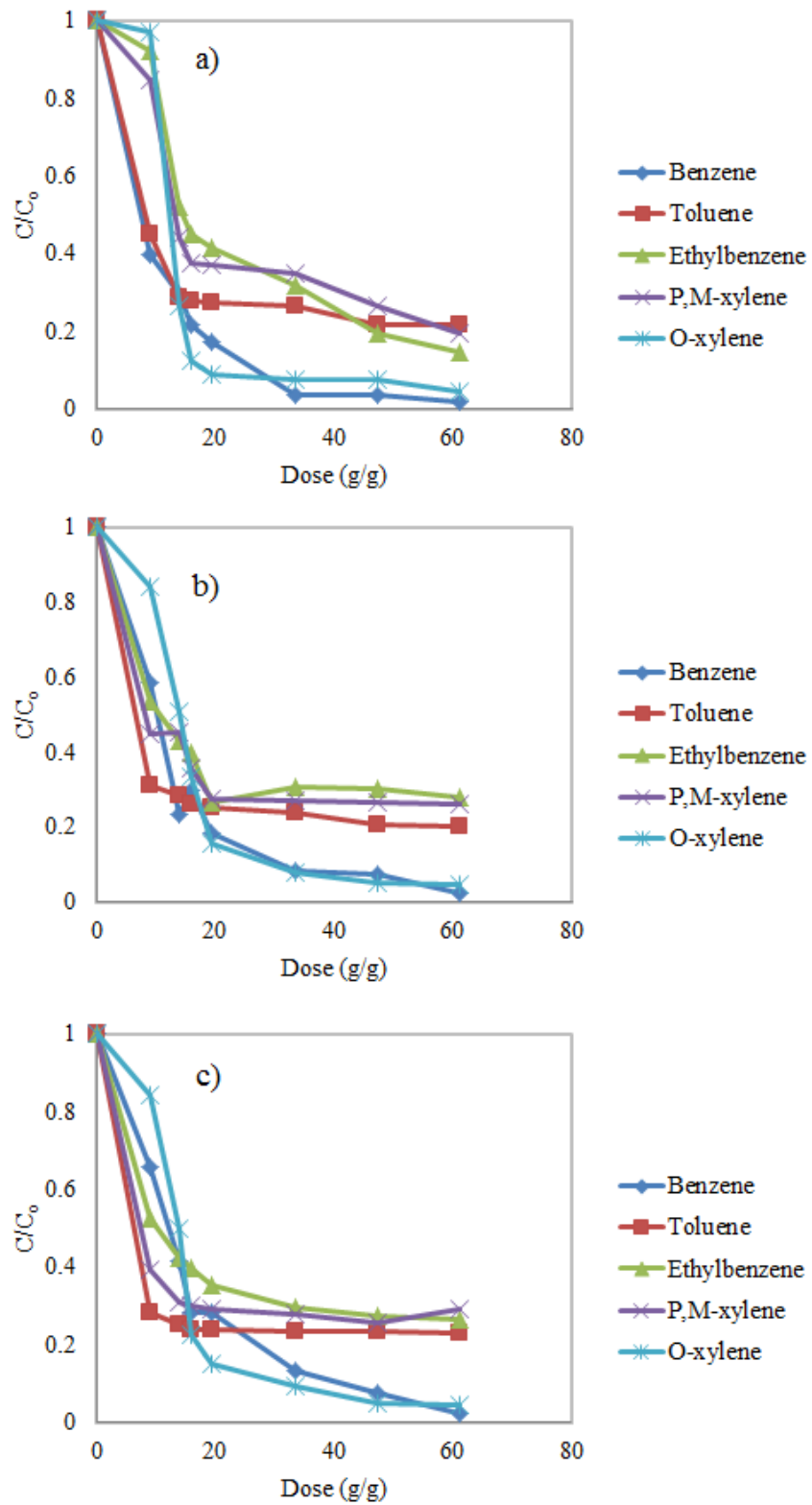


Figure E.6. Unactivated persulfate dose-response curve for BTEX in (a) column 1, (b) column 2 and (c) column 3.

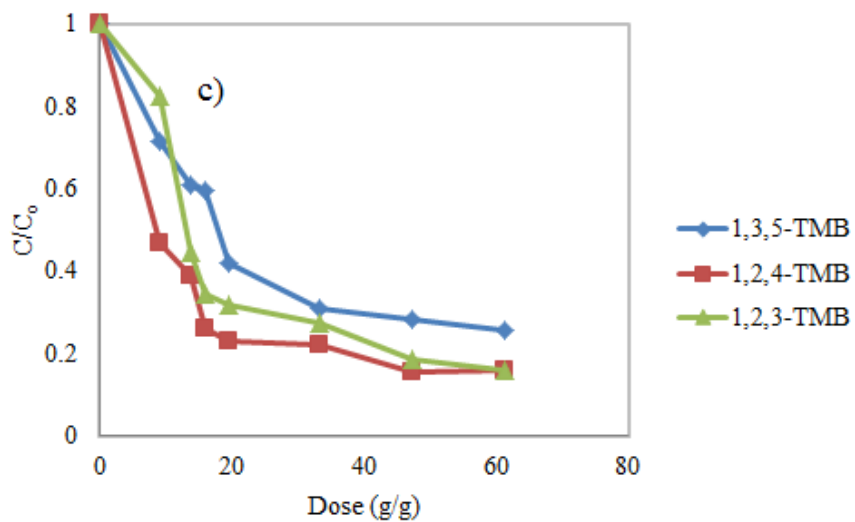
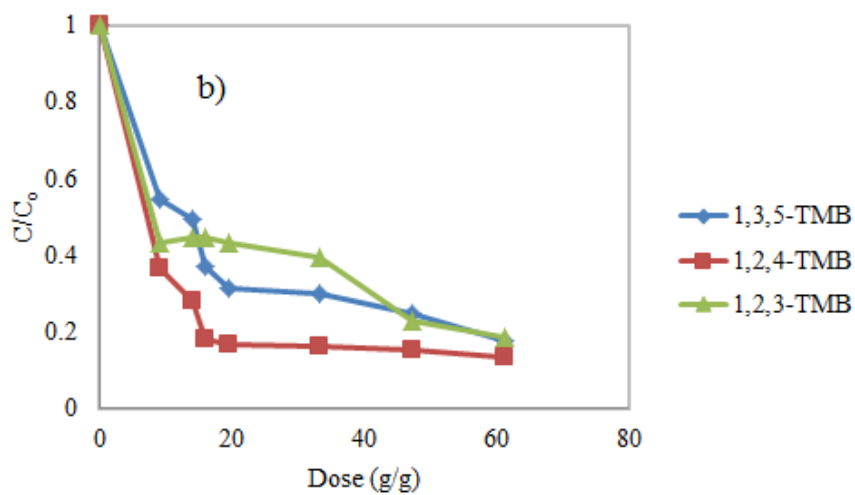
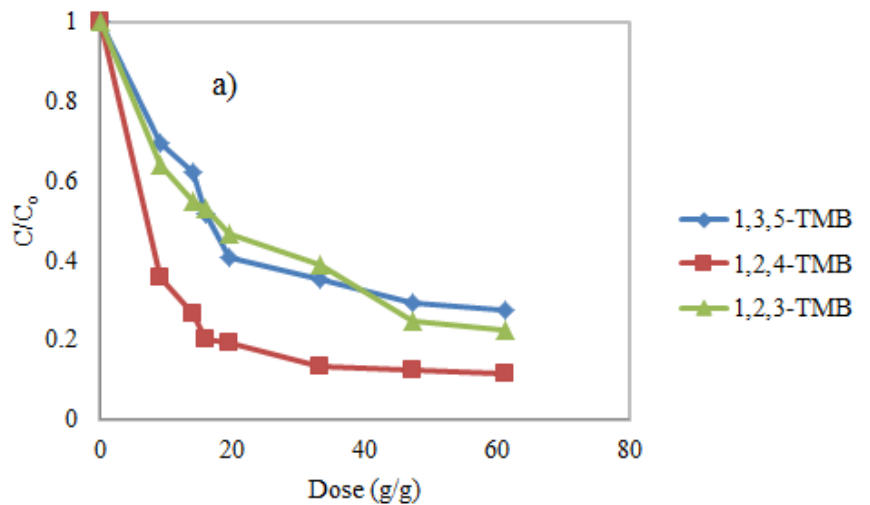


Figure E.7. Unactivated persulfate dose-response curve for TMBs in (a) column 1, (b) column 2 and (c) column 3.

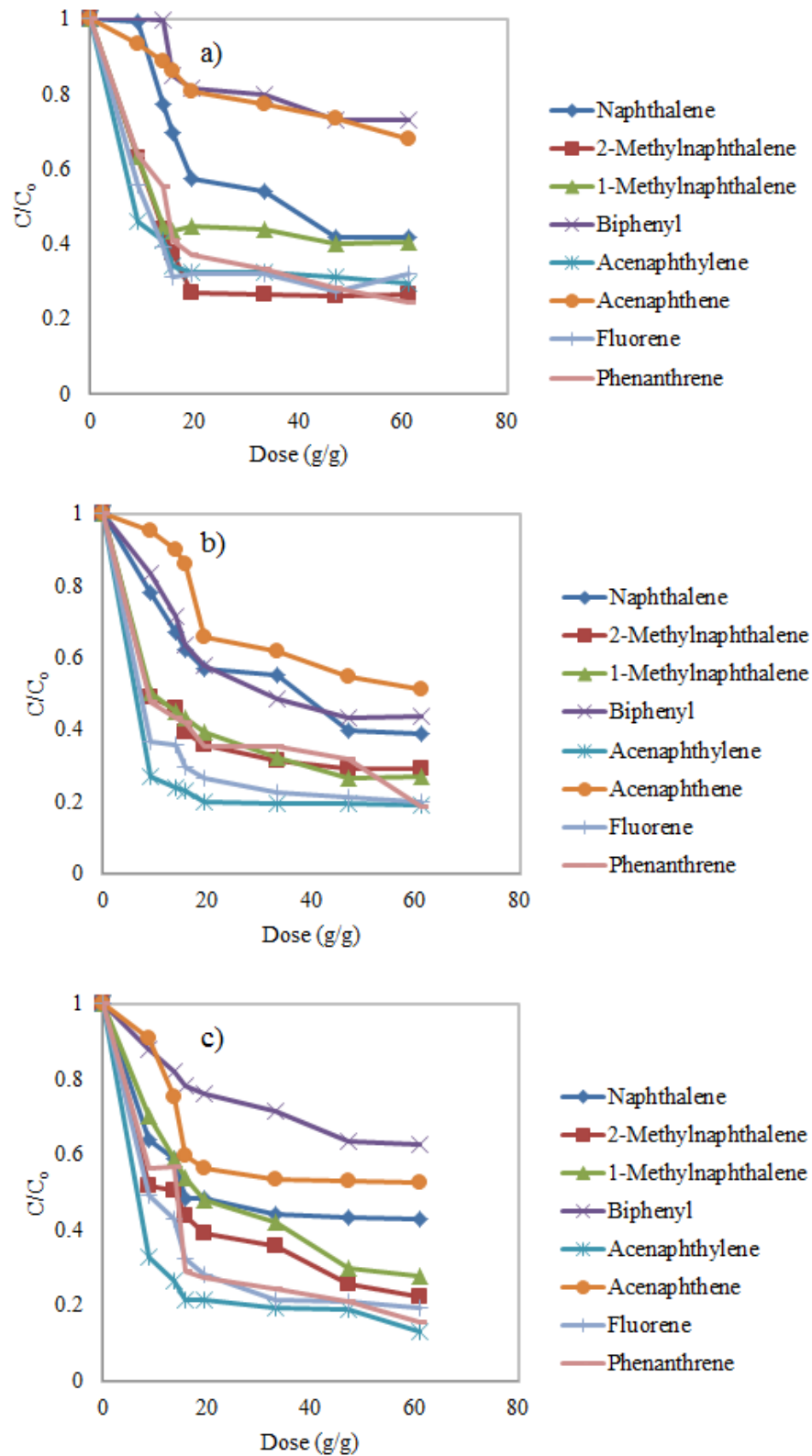


Figure E.8. Unactivated persulfate dose-response curve for PAHs in (a) column 1, (b) column 2 and (c) column 3.

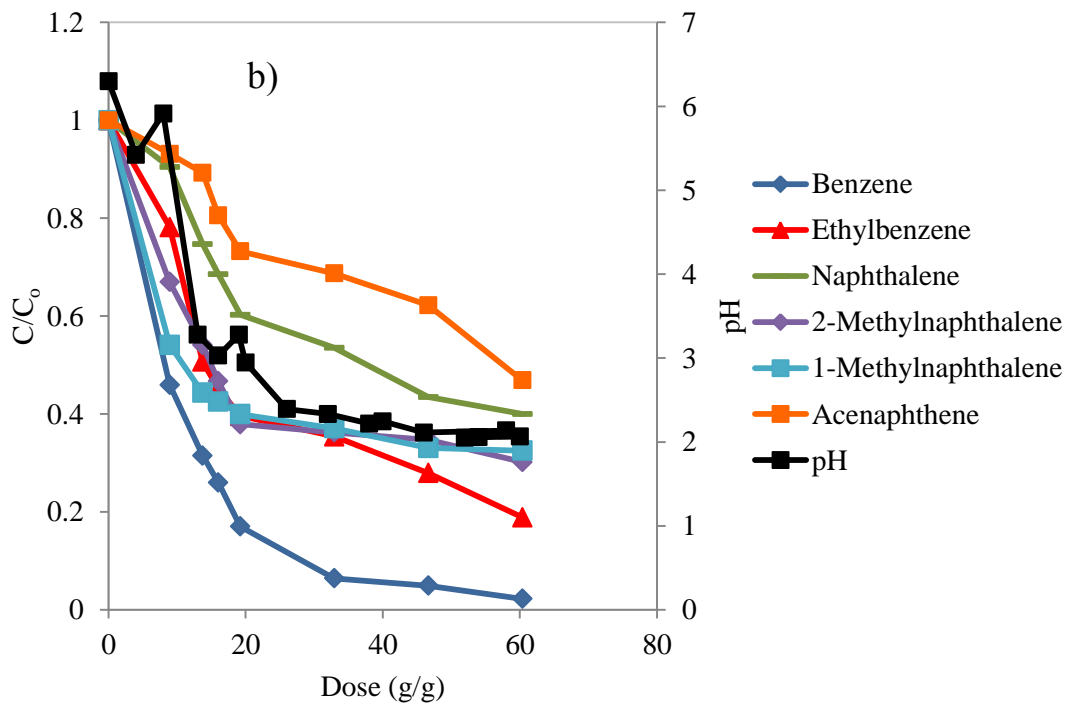
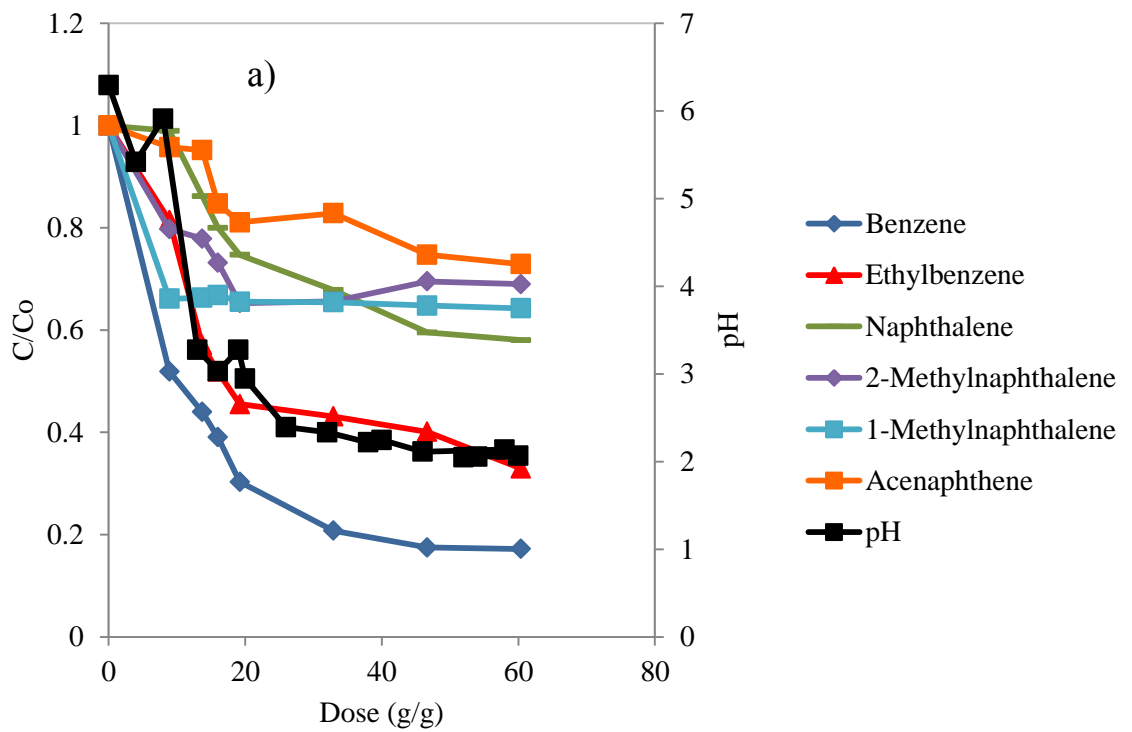


Figure E.9. Average unactivated dose-response curves for (a) control adjusted (b) measured COCs.

Table E.1. Water quality data for unactivated persulfate columns.

Day	Event	Dose (g/L)	Q	V _{ox}	DO (mg/L)				pH				eH (V)				EC (uS/cm)				Temp (°C)			
			(ml/min)	(mL)	CON	C1	C2	C3	CON	C1	C2	C3	CON	C1	C2	C3	CON	C1	C2	C3	CON	C1	C2	C3
0	MilliQ Flush	-	0.025		2.98	3.40	3.52	3.99	6.21	6.40	6.30	6.10	0.84	0.84	0.84	0.85	665	672	680	643	22.1	22.1	22.1	22.1
2	Persulfate Flush	30	0.18	7.78	3.12	2.95	2.85	2.67	6.10	5.00	5.80	5.50	0.85	0.91	0.87	0.90	687	2510	2440	2470	23.1	23.1	23.1	23.1
6	MilliQ Flush	-	0.025		3.05	3.45	3.42	4.19	6.30	5.30	6.30	6.10	0.84	0.90	0.85	0.90	648	612	630	658	25.3	25.3	25.3	25.3
8	Persulfate Flush	35	0.18	9.07	3.10	1.20	1.40	1.40	6.20	3.30	3.20	3.30	0.85	1.02	1.00	1.01	635	2560	2340	2410	22.1	22.1	22.1	22.1
13	MilliQ Flush	-	0.025		3.10	1.30	1.50	1.30	6.10	3.00	3.00	3.10	0.85	1.00	1.00	1.00	624	648	631	709	22.3	22.3	22.3	22.3
15	Persulfate Flush	35	0.18	9.07	3.10	1.10	1.40	1.40	6.20	3.20	3.20	3.30	0.94	1.00	1.00	1.00	635	2560	2340	2410	22.1	22.1	22.1	22.1
20	MilliQ Flush	-	0.025		3.60	2.35	2.00	2.70	6.30	3.10	2.90	2.90	0.84	1.00	1.00	1.00	585	623	614	636	23.2	23.2	23.2	23.2
22	Persulfate Flush	40	0.18	10.37	3.60	1.78	2.00	1.90	6.20	2.40	2.50	2.30	0.85	1.00	1.00	1.00	564	1270	1430	1420	22.5	22.5	22.5	22.5
27	MilliQ Flush	-	0.025		3.10	1.89	2.00	2.00	6.40	3.70	2.40	2.90	0.84	1.00	1.10	1.10	571	642	654	668	22.0	22.0	22.0	22.0
37	Persulfate Flush	100	0.18	25.92	3.10	1.88	2.00	2.00	6.40	2.30	2.10	2.20	0.94	1.10	1.10	1.10	565	1640	1630	1610	22.1	22.1	22.1	22.1
42	MilliQ Flush	-	0.025		3.10	1.79	2.00	1.90	6.00	2.40	2.10	2.20	0.96	1.10	1.10	1.10	526	732	741	804	23.0	23.0	23.0	23.0
44	Persulfate Flush	100	0.18	25.92	3.10	1.80	2.10	1.90	6.10	2.10	2.10	2.10	0.95	1.10	1.10	1.10	599	2090	2120	2020	22.2	22.2	22.2	22.2
49	MilliQ Flush	-	0.025		3.10	1.90	2.00	2.00	6.10	2.20	2.20	2.20	0.86	1.10	1.10	1.10	603	618	606	625	22.0	22.0	22.0	22.0
51	Persulfate Flush	100	0.18	25.92	3.10	1.90	1.90	1.90	6.00	2.10	2.10	2.10	0.84	1.10	1.10	1.10	606	1950	1960	1830	22.7	22.7	22.7	22.7
56	MilliQ Flush	-	0.025		3.10	1.90	1.90	2.00	6.10	2.10	2.10	2.10	0.84	1.10	1.10	1.10	602	607	611	614	22.5	22.5	22.5	22.5
58	Base Activated Flush	30	0.18	7.78	3.00	1.80	1.90	1.80	6.14	2.10	2.10	2.10	0.85	1.10	1.10	1.10	601	2020	2015	2010	22.1	22.1	22.1	22.1
63	MilliQ Flush	-	0.025		3.20	1.90	1.90	1.80	6.10	3.60	3.30	3.30	0.85	1.10	1.10	1.10	610	714	701	698	22.1	22.1	22.1	22.1
70	Base Activated Flush	100	0.18	25.92	3.10	2.00	1.90	2.00	6.11	3.50	3.20	3.20	0.85	1.10	1.10	1.10	600	1850	1840	1770	23.0	23.0	23.0	23.0
75	MilliQ Flush	-	0.025		3.00	1.90	1.90	2.00	6.10	3.50	3.30	3.30	0.86	1.10	1.10	1.10	601	701	723	705	22.5	22.5	22.5	22.5

Table E.2. Water quality data for iron activated persulfate columns.

Day	Event	Dose (g/L)	Q	V _{ox}	DO (mg/L)				pH				eH (V)				EC (uS/cm)				Temp (°C)			
			(ml/min)	(mL)	CON	C1	C2	C3	CON	C1	C2	C3	CON	C1	C2	C3	CON	C1	C2	C3	CON	C1	C2	C3
0	MilliQ Flush	-	0.025		2.98	3.40	3.52	3.99	6.70	6.50	6.70	6.60	0.85	0.84	0.84	0.85	660	677	670	659	22.1	22.1	22.1	22.1
2	Persulfate Flush	30	0.18	7.78	3.12	2.95	2.85	2.67	6.60	3.00	3.10	3.00	0.85	1.30	1.40	1.30	680	2460	2480	2450	22.3	22.3	22.3	22.3
9	MilliQ Flush	-	0.025		3.05	3.45	3.42	4.19	6.60	5.40	5.50	5.50	0.83	0.90	0.85	0.90	672	660	690	685	22.1	22.1	22.1	22.1
11	Persulfate Flush	30	0.18	7.78	3.10	1.20	1.40	1.40	6.70	2.68	2.60	2.75	0.85	1.40	1.30	1.30	630	2200	2280	2250	23.2	23.2	23.2	23.2
16	MilliQ Flush	-	0.025		3.10	1.30	1.50	1.30	6.50	5.10	5.00	5.10	0.87	1.00	1.00	1.00	628	670	630	710	22.5	22.5	22.5	22.5
18	Persulfate Flush	30	0.18	7.78	3.10	1.10	1.40	1.40	6.20	2.54	2.50	2.60	0.89	1.20	1.20	1.20	640	2010	2010	2040	22.0	22.0	22.0	22.0
24	MilliQ Flush	-	0.025		3.60	2.35	2.00	2.70	6.40	4.20	4.10	4.00	0.88	1.00	1.00	1.00	610	623	614	636	22.1	22.1	22.1	22.1
26	Persulfate Flush	35	0.18	9.07	3.60	1.78	2.00	1.90	6.40	2.20	2.20	2.20	0.87	1.30	1.20	1.20	590	1350	1320	1400	22.1	22.1	22.1	22.1
32	MilliQ Flush	-	0.025		3.10	1.89	2.00	2.00	6.30	3.40	3.50	3.30	0.87	1.10	1.00	1.00	587	642	654	668	23.0	23.0	23.0	23.0
34	Persulfate Flush	35	0.18	9.07	3.10	1.88	2.00	2.00	6.30	2.10	2.00	2.10	0.89	1.20	1.00	1.00	579	1700	1610	1650	22.2	22.2	22.2	22.2
40	MilliQ Flush	-	0.025		3.10	1.79	2.00	1.90	6.20	2.10	2.10	2.20	0.9	1.10	1.00	1.10	580	730	750	800	22.0	22.0	22.0	22.0
42	Persulfate Flush	100	0.18	25.92	3.10	1.80	2.10	1.90	6.10	2.10	2.10	2.10	0.9	1.30	1.30	1.20	564	2100	2140	2150	22.7	22.7	22.7	22.7
47	MilliQ Flush	-	0.025		3.10	1.90	2.00	2.00	6.10	2.30	2.30	2.20	0.87	1.10	1.10	1.10	560	618	610	599	22.5	22.5	22.5	22.5
50	Persulfate Flush	100	0.18	25.92	3.10	1.90	1.90	1.90	6.10	2.00	2.00	2.10	0.85	1.30	1.30	1.30	560	2010	2030	2030	22.1	22.1	22.1	22.1

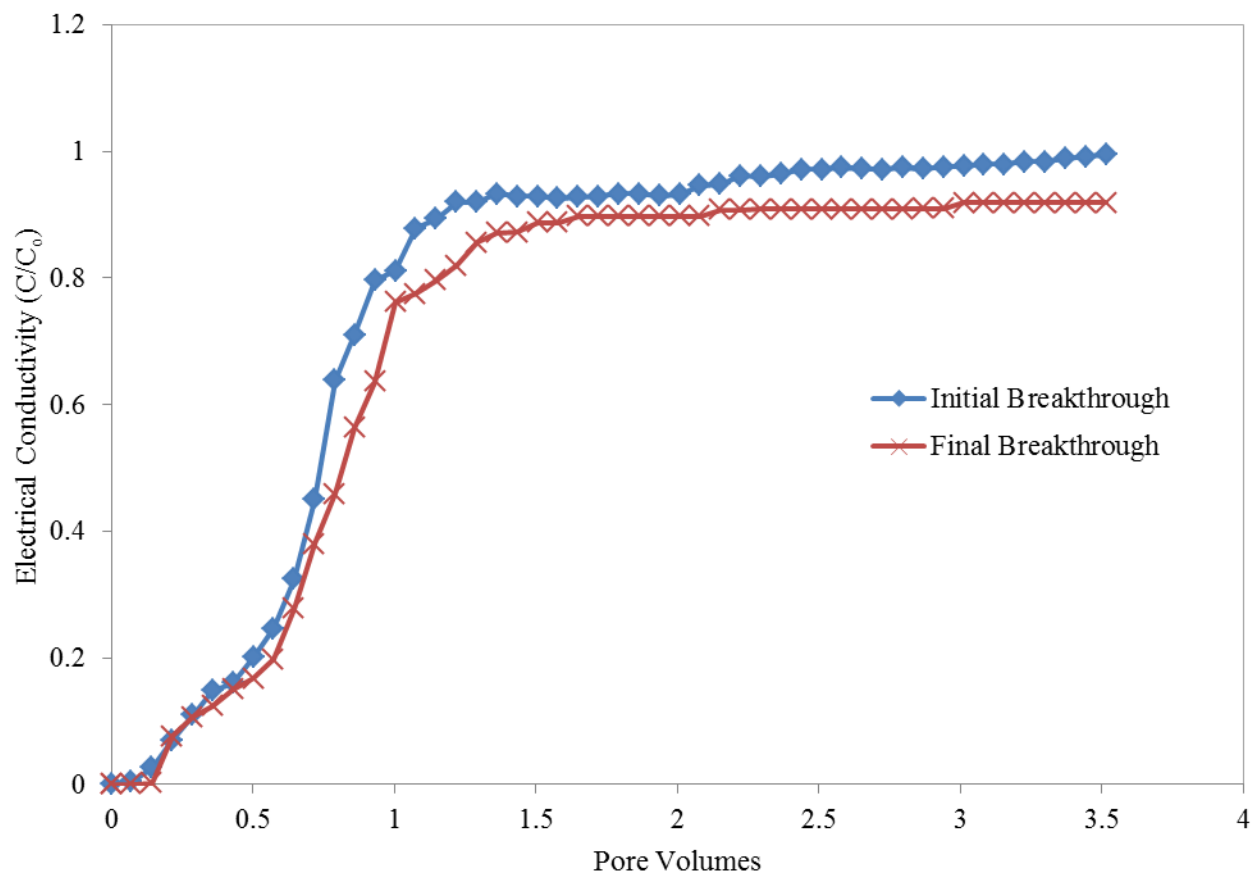


Figure E.10 Initial and final breakthrough curves for unactivated persulfate treatment column

Table E.3. Soil column porosity calculations based on breakthrough curve

$$q_T = \frac{Q}{A} = \frac{0.18 \text{ mL/min}}{13.1 \text{ cm}} * \frac{60 \text{ min}}{\text{hour}} = 0.82 \text{ cm/hr}$$

$$v_T = \frac{L_{\text{column}}}{t_{50\%}} = \frac{10 \text{ cm}}{5.15 \text{ hours}} = 1.94 \text{ cm/hour}$$

$$v = \frac{q_T}{n_T} \rightarrow n_T = \frac{q_T}{v_T} = \frac{0.82 \text{ cm/hr}}{1.94 \text{ cm/hr}} = 0.42$$

$$V_T = \left(\frac{d}{2}\right)^2 \pi \cdot L_{\text{column}} = \left(\frac{4.08 \text{ cm}}{2}\right)^2 \pi \cdot 10 \text{ cm} = 130.7 \text{ mL}$$

$$V_{V_T} = V_T \cdot n_T = 130.7 \text{ mL} \cdot 0.42 = 55.5 \text{ mL}$$

$$V_{T_{\text{endcap}}} = \left(\frac{d}{2}\right)^2 \pi \cdot L_{\text{endcap}} = \left(\frac{4.08 \text{ cm}}{2}\right)^2 \pi \cdot 2 \text{ cm} = 26.1 \text{ mL}$$

$$n_{\text{endcap}} = 0.7$$

$$V_{V_{\text{endcap}}} = V_{T_{\text{endcap}}} \cdot n_{\text{endcap}} = 26.1 \text{ mL} \cdot 0.7 = 18.3 \text{ mL}$$

$$V_{T_{\text{soil}}} = \left(\frac{d}{2}\right)^2 \pi \cdot L_{\text{soil}} = \left(\frac{4.08 \text{ cm}}{2}\right)^2 \pi \cdot 8 \text{ cm} = 104.6 \text{ mL}$$

$$V_{V_{\text{soil}}} = V_{V_T} - V_{V_{\text{endcap}}} = 55.5 \text{ mL} - 18.3 \text{ mL} = 37.2 \text{ mL}$$

$$n_{\text{soil}} = \frac{V_{V_{\text{soil}}}}{V_{T_{\text{soil}}}} = \frac{37.2 \text{ mL}}{104.6 \text{ mL}} = 0.36$$

Where q_T is the total Darcy flux through the column [mL/min]; Q is the volumetric flow rate through the column [mL/min]; A is the cross sectional area perpendicular to flow inside the column [cm]; v_T is the fluid flow velocity in the column [cm/hour]; L_{column} is the total length of the column [cm]; $t_{50\%}$ is the time taken for $\frac{C}{C_0} = 0.50$ [hours]; n_T is the bulk porosity of the total column [-]; V_T is the total column volume [mL]; d is the inner diameter of the column [cm]; V_{V_T} is the volume of the voids for the total column [mL]; $V_{T_{endcap}}$ is the total volume of the column end caps [mL]; L_{endcap} is the length of the end caps [cm]; n_{endcap} is the known porosity of the end caps [-]; $V_{V_{endcap}}$ is the volume of voids in the end caps [mL]; $V_{T_{soil}}$ is the total volume of the soil in the column [mL]; L_{soil} is the length of the soil in the column [cm]; $V_{V_{soil}}$ is the volume of voids in the soil [mL]; and n_{soil} is the porosity of the soil [-].

Table E.4. Parameters and calculations for column experiment design.

Volume of Water Needed		Duplicate?	Total
Analysis	Sample Size		
COCs	40 mL	Yes	80
Persulfate & Iron	5 mL	No	5
SCAP	10 mL	Yes	20
Total	120 mL		

Amount of Soil Available	
277.3 g	per column
104.6 g	per column

Column Dimensions	
Diameter (Inner)	4.08 cm
Volume	104.6 cm ³
Length	8 cm
Area	13.1 cm ²

Hydraulic Calculations	
v	8 cm/day
t (1PV)	1 days
Q	0.025 cm ³ /min
PV	35.6 mL

Sample Times	Baseline Sample
PV	2
Day	2.0

Column Parameters	
Porosity	0.34
Bulk Density	1.8 g/cm ³
V water	35.6 mL
V total	104.6 cm ³
V soil	69.0 cm ³

COCs	Detection Limit (ppb)
Benzene	3.34
1 MethylNaphthalene	3.93
2 MethylNaphthalene	12.82
Napthalene	6.61
Acenaphthene	5.89
EthylBenzene	2.32

Table E.5. Anticipated effluent concentrations based on aqueous solubility values.

Compound	MW (g/mol)	f _S /f _L	C _{max} (mg/L)	C _n (mg/kg)	n (moles)	xi	C _{calc} (mg/L)	C _{calc} (mol/m ³)	C _{calc} (ug/L)	C _{eff} (ug/L)	% Diff
Benzene	78.1	1	1780	73	1.25997E-08	0.000200719	0.357280458	9.18222E-07	27583.93614	2619.433434	953.0497088
Toluene	92.1	1	534.8	635	9.29403E-08	0.001480579	0.791813546	1.2729E-05	1.172342354	2426.387967	-99.95168364
Ethylbenzene	106.2	1	161.2	486	6.16881E-08	0.000982719	0.158414242	1.46588E-06	16822.94581	637.1372283	2540.395988
o-xylene	106.17	1	173	990	1.25702E-07	0.002002494	0.346431494	6.53442E-06	0.693727053	36984.49146	-99.99812428
m,p-xylene	106.17	1	174	467	5.9296E-08	0.000944611	0.164362296	1.46243E-06	17449.5231	1045.759909	1568.597443
C9	120.00	0.03	3.3	265	2.97683E-08	0.000474222	0.05	1.97593E-07	-	-	-
1,2,3-Trimethylbenzene	120.19	1	69	225	2.52348E-08	0.000402002	0.027738125	9.27755E-08	3333.872926	109.9133099	2933.183996
1,2,4-Trimethylbenzene	120.19	1	56	767	8.60227E-08	0.001370379	0.076741251	8.74979E-07	9223.607724	941.8219721	879.3366472
1,3,5-Trimethylbenzene	120.19	1	48.9	248	2.78144E-08	0.000443095	0.021667361	7.98787E-08	2604.221819	140.459121	1754.078112
Naphthalene	128.2	0.3	31.7	72800	7.65479E-06	0.121944099	12.88542641	0.012256644	495573.4997	5355.196543	9154.067442
2-Methylnap	142	0.86	25.4	47200	4.48068E-06	0.071379103	2.108173515	0.001059715	257450.1496	1079.976648	23738.49227
1-Methylnap	142.2	1	28.05	27700	2.62585E-06	0.041830938	1.173357819	0.000345166	166851.4818	952.9023611	17409.81933
Acenaphthylene	154	0.22	9.8	6580	5.75964E-07	0.009175349	0.408720105	2.43516E-05	13847.43715	169.8521065	8052.643751
Acenaphthene	154.2	0.2	3.93	2250	1.96693E-07	0.003133398	0.061571273	1.25115E-06	1898.858058	71.61439404	2551.503351
2,6-Dimethylnaphthalene	156.22	0.97	2	11300	9.75061E-07	0.01553314	0.032	3.1818E-06	4853.174114	-	-
Fluorene	166.2	0.16	1.98	5530	4.48522E-07	0.007145153	0.088421271	3.80134E-06	2351.298436	104.5578104	2148.802291
2,3,5-Trimethylnaphthalene	170.25	0.33	1.37	1100	8.70954E-08	0.001387468	0.0058	4.72676E-08	-	-	-
Phenanthrene	178.2	0.28	1.18	17400	1.31623E-06	0.020968095	0.088365545	1.03976E-05	4409.087209	120.6113949	3555.61414
Anthracene	178	0.01	0.05	2980	2.25676E-07	0.003595123	0.017975613	3.63059E-07	31.9965904	-	-
Dibenzothiophene	184.2	0.20	0.21	1600	1.1709E-07	0.001865296	0.002	2.02529E-08	72.15338506	-	-
C10-C14	185	0.13	0.0043	11465	8.35396E-07	0.013308214	0.00045	3.23713E-08	-	-	-
Methylphenanthrene	192.1	0.679	0.27	2700	1.89464E-07	0.00301824	0.0012	1.88542E-08	-	-	-
Fluoranthene	202.3	0.11	0.26	4860	3.2384E-07	0.005158908	0.012193784	3.10957E-07	271.348266	271.9771528	-0.231227813
Pyrene	202.3	0.04	0.13	7680	5.11747E-07	0.008152349	0.026495135	1.06771E-06	214.3986299	98.984395	116.5984142
BaA	228	0.0097	0.014	2230	1.31844E-07	0.00210033	0.003031404	2.79252E-08	6.704252029	-	-
Chrysene	228	0.039	0.002	2150	1.27114E-07	0.002024981	0.000103845	9.22301E-10	0.923391535	-	-
Naphthobenzothiophene	234.3	0.02	0.0616	534	3.07227E-08	0.000489425	0.002	4.17777E-09	-	-	-
C15-C36	245	0.02	0.000023	37408	2.0582E-06	0.032788069	3.44723E-05	4.61339E-09	-	-	-
BbF	252	0.03	0.00323	2001	1.07038E-07	0.001705155	0.000183588	1.24225E-09	1.387928342	-	-
BaP	252	0.0451	0.0038	2060	1.10194E-07	0.001755432	0.000147908	1.03033E-09	1.681002078	-	-
Indeno	276	0.004	0.062	430	2.10014E-08	0.000334562	0.005185713	6.28603E-09	5.725027517	-	-
DahA	278	0.003	0.0005	430	2.08504E-08	0.000332155	5.53592E-05	6.61433E-11	0.046169577	-	-
BghiP	276	1	0.00026	2990	1.46033E-07	0.002326374	6.04857E-07	5.09828E-12	0.1669406	-	-
Phytane	282.6	1.33	1.68E-05	3310	1.57887E-07	0.002515204	3.18097E-08	2.83114E-13	0.011920061	-	-

Fraction Quantified		0.280844	2.3996E-05	0.382267383
Remaining Mass	250	0.719156	3.87769E-05	0.617732617
TOTAL		1	6.27729E-05	1

Volume of Column (m3)	0.00003556
V pores (cm3)	1.20904E-05
% Saturation	0.04
Area of Source (m2)	0.00131
Density NAPL	1.1
q (m/min)	0.000085
n	0.34
mass of NAPL (kg)	0.00001348
t=	1411.764706

C = (moles of compound - (flux*Area perpendicular to flow * Time * Initial C))/Total Sum of Moles

Solubility data obtained from: <http://www.mfe.govt.nz/publications/hazardous/oil-guide-jun99/appendix-4b-jun99.pdf>

Appendix F:
Raw Data

Table F.4. Raw results from NOI Tests.

Day	0	0.041667	1	2	3	4	7	12	15	20	25	50
Flask 1		0.461	0.440	0.441	0.434	0.413	0.435	0.405	0.398	0.205	0.211	0.191
		0.418	0.434	0.414	0.439	0.411	0.432	0.381	0.388	0.203	0.201	0.198
		0.529	0.404	0.410	0.450	0.410	0.457	0.440	0.388	0.203	0.208	0.191
Flask 2	1	0.9319799	0.8462362	0.8376618	0.8259167	0.8172153	0.8063784	0.7919387	0.7876413	0.7718357	0.7787923	0.7733333
		0.436	0.450	0.438	0.445	0.417	0.407	0.406	0.435	0.211	0.238	0.211
		0.472	0.404	0.430	0.443	0.419	0.457	0.454	0.439	0.209	0.227	0.219
		0.439	0.454	0.477	0.398	0.432	0.431	0.439	0.438	0.218	0.239	0.212
Flask 3	1	0.8917463	0.8760232	0.8704272	0.8685127	0.8646405	0.8612449	0.8590871	0.8486615	0.8475311	0.8402415	0.836
		0.464	0.468	0.450	0.456	0.452	0.450	0.457	0.448	0.233	0.248	0.212
		0.445	0.463	0.457	0.457	0.453	0.452	0.450	0.442	0.231	0.241	0.210
		0.499	0.471	0.451	0.454	0.455	0.456	0.458	0.448	0.243	0.243	0.215
Flask 4	1	0.9319799	0.9180225	0.9109002	0.9064938	0.9003207	0.8950015	0.8903619	0.8858102	0.8878197	0.8806406	0.8593333
		0.436	0.455	0.448	0.419	0.450	0.412	0.438	0.438	0.214	0.220	0.189
		0.45	0.392	0.439	0.427	0.407	0.429	0.431	0.431	0.213	0.215	0.188
		0.471	0.412	0.494	0.413	0.411	0.425	0.438	0.432	0.202	0.215	0.191
Control	1	0.918342	0.9037044	0.8941716	0.8637044	0.8596405	0.8483214	0.8353636	0.8310765	0.8254577	0.7850242	0.7573333
		0.499	0.477	0.478	0.500	0.477	0.501	0.501	0.493	0.243	0.291	0.244
		0.482	0.479	0.489	0.497	0.458	0.511	0.486	0.501	0.254	0.263	0.234
		0.51	0.489	0.482	0.487	0.483	0.485	0.478	0.482	0.282	0.266	0.244
	1	0.9867239	0.98	0.9590221	0.9821069	0.95	0.97	0.96	0.96	0.9783445	0.970	0.963

Table F.4(b). Raw pH results from NOI Tests.

Day	0	1	2	3	4	7	12	15	20	25	53
Flask 1	7.82	7.39	7.12	6.95	6.80	6.33	5.47	4.68	3.91	3.73	3.30
Flask 2	8.82	7.96	7.44	7.36	7.39	7.30	6.80	6.77	6.53	6.24	4.85
Flask 3	8.51	7.8	7.40	7.39	7.38	7.38	6.89	6.81	6.64	6.31	4.20
Flask 4	7.95	7.42	7.18	6.98	6.83	6.40	5.56	4.96	4.23	3.80	3.58
Control	3.65	3.71	3.69	3.68	3.7	3.62	3.55	3.45	3.55	3.53	3.54

Table F.5. Raw results from unactivated persulfate treatability study.

ID	Benz	Tol	Ethyl- benzene	P,M-xylene	O-xylene	1,3,5 TMB	1,2,4 TMB	1,2,3 TMB	Nap	Indole	2-Metnap	1-Metnap	Bi-phenyl	Ace- naphthylene	Ace- naphthene	DbF	Fluorene	Phenan	Anth	Carb	Fluoran	Pyrene	B(a)A	Chrys	B(b)F+		I[1,2,3-c,d]P		
																									B(k)F	B(a)P	+ D[a,h]A	B[g,h,i]P	
MDL	1.11	0.83	0.77	1.46	0.37	0.74	0.82	0.76	2.20	2.12	4.27	1.31	1.09	1.53	1.83	1.10	1.88	3.78	5.53	2.39	1.80	1.60	4.77	5.75	5.62	13.33	18.65	11.49	
LOQ	3.34	2.49	2.32	4.38	1.11	2.21	2.47	2.28	6.61	6.36	12.82	3.93	3.26	4.60	5.49	3.31	5.64	11.34	16.60	7.18	5.40	4.81	14.32	17.24	16.85	39.99	55.95	34.47	
Control-1	6188.4	10725.2	2774.6	2882.1	1740.1	149.7	487.0	203.0	7026.4	10.9	777.4	542.8	48.5	11.4	31.2	20.3	27.1	20.1	5.5	8.0	-	1.3	2.0	-	-	-	-	-	-
1-A	5337.4	8123.5	2142.2	2395.2	1442.8	118.3	465.1	176.0	6670.4	6.3	623.4	461.4	31.8	9.2	8.4	11.4	21.4	21.0	5.5	-	-	-	2.2	-	-	-	-	-	-
1-B	5233.6	8317.5	2192.1	2448.1	1475.0	120.8	475.7	180.0	6650.5	6.4	629.6	468.2	34.1	6.6	7.4	11.7	21.8	21.2	5.5	-	-	-	2.4	-	-	-	-	-	-
1-C	5161.8	8214.9	2164.5	2415.0	1456.6	119.9	470.2	178.5	6602.4	6.4	628.2	464.1	33.3	5.8	7.4	11.8	21.8	20.9	5.2	-	-	-	1.9	-	-	-	-	-	-
Control-2	6125.1	10542.8	2697.8	2800.3	1701.5	145.5	473.4	198.5	6935.6	10.8	770.6	536.0	50.8	9.6	31.2	20.3	28.4	21.5	-	7.9	-	-	1.5	-	-	-	-	-	-
3-A	2930.9	3268.1	915.1	1142.8	649.1	75.5	380.9	89.5	5637.5	2.2	495.6	341.7	31.2	2.3	2.7	9.5	17.4	16.6	4.8	-	-	-	3.0	-	-	-	-	-	-
3-B	2926.2	3306.3	978.9	1222.8	698.4	74.3	398.3	90.0	5516.6	2.3	440.4	362.3	31.6	2.5	2.5	10.0	18.4	17.7	4.6	-	-	-	3.4	-	-	-	-	-	-
3-C	2826.8	3198.7	898.1	1105.4	614.4	75.5	370.2	85.6	5514.3	2.3	451.8	358.7	34.6	2.3	2.5	10.5	17.4	16.8	1.6	-	-	-	2.0	-	-	-	-	-	-
Control-3	6256.7	10784.6	2699.7	2791.7	1712.2	135.5	452.7	191.7	6942.3	10.2	731.6	514.6	37.3	10.7	27.9	21.6	26.1	18.4	-	7.3	-	-	1.7	-	16.4	-	-	-	-
5-A	363.7	94.3	34.0	46.4	23.5	4.6	83.8	3.0	3786.6	-	243.3	216.9	31.7	1.5	1.8	4.4	14.4	11.5	4.9	-	-	-	1.6	-	-	-	-	-	-
5-B	367.2	82.4	35.6	47.7	25.5	4.9	20.1	4.5	3661.7	-	240.3	233.7	21.3	1.2	1.8	4.5	9.9	12.3	-	-	-	-	2.2	-	-	-	-	-	-
5-C	324.7	84.3	31.4	42.9	23.8	4.1	80.7	4.1	3850.9	-	241.9	218.3	33.5	1.2	1.8	4.3	16.9	12.0	4.3	-	-	-	2.0	-	-	-	-	-	-
Control-4	6201.0	10652.7	2639.0	2726.0	1670.3	130.4	437.7	184.9	6614.7	10.1	705.3	501.6	37.4	17.6	27.8	21.7	24.9	18.3	-	6.5	-	-	1.7	-	-	-	-	-	-
7-A	29.1	6.0	3.2	5.1	-	-	8.5	-	2779.9	-	160.1	147.8	21.8	-	-	3.3	4.4	9.3	-	-	-	-	1.9	-	-	-	-	-	-
7-B	39.1	6.8	3.4	5.4	-	-	11.4	-	2959.3	-	161.3	152.9	29.0	-	-	3.6	5.1	9.9	-	-	-	-	1.9	-	-	-	-	-	-
7-C	26.9	4.2	3.3	3.5	-	-	3.8	-	2786.9	-	169.6	121.1	22.1	-	-	3.1	5.6	8.6	2.2	-	-	-	1.4	-	-	-	-	-	-
Control-5	5829.4	9529.4	2397.2	2472.8	1527.6	119.2	403.5	171.8	6139.4	9.7	648.6	466.3	33.4	13.9	25.8	18.3	21.8	15.7	-	5.1	-	-	-	-	-	-	-	-	-
14-A	3.8	1.8	-	2.1	-	-	2.4	-	609.4	-	9.0	8.0	16.6	-	-	2.3	-	3.8	-	-	-	-	1.5	-	-	-	-	-	-
14-B	4.2	0.8	-	1.7	-	-	2.4	-	625.7	-	10.1	8.0	15.1	-	-	1.1	-	3.9	-	-	-	-	1.7	-	-	-	-	-	-
14-C	4.0	1.8	-	1.9	-	-	2.1	-	622.5	-	12.2	7.2	15.8	-	-	1.1	-	3.7	-	-	-	-	1.5	-	-	-	-	-	-

Note: (-) < MDL

Table F.5(b). Raw persulfate results from unactivated persulfate treatability study.

Sample ID	Concentration (mg/L)
1-A	20.9
1-B	20.1
1-C	20.1
3-A	19.9
3-B	18.0
3-C	19.1
5-A	19.2
5-B	19.4
5-C	N/A
7-A	18.5
7-B	18.5
7-C	18.7
14-A	15.7
14-B	17.5
14-C	17.9

Table F.6. Raw BTEX and PAH results from iron activated persulfate treatability study (Fe=150 mg/L).

ID	Benz		Ethyl-benzene		P,M-xylene	O-xylene	1,3,5 TMB	1,2,4 TMB	1,2,3 TMB	Nap	Indole	2-Metnap	1-Metnap	Bi-phenyl	Ace-naphthylene	Ace-naphthene	DbF	Fluorene	Phenan	Anth	Carb	Fluoran	Pyrene	B(a)A	Chrys	B(b)F+		I[1,2,3-c,d]P	
	MDL	1.11	0.83	0.77																						1.46	0.37	0.74	0.82
	LOQ	3.34	2.49	2.32	4.38	1.11	2.21	2.47	2.28	6.61	6.36	12.82	3.93	3.26	4.60	5.49	3.31	5.64	11.34	16.60	7.18	5.40	4.81	14.32	17.24	16.85	39.99	55.95	34.47
Control-1	7420.4	14362.0	3192.0	3683.6	2153.9	184.9	616.0	251.1	7681.7	-	976.4	664.7	84.7	15.5	65.0	28.7	35.8	28.6	-	8.5	-	-	6.0	-	-	-	-	-	-
1-A	2717.0	4065.7	848.3	1847.3	913.8	105.1	459.7	114.0	7365.7	-	821.7	564.8	82.2	8.7	18.1	7.0	29.6	25.4	-	2.2	-	-	5.5	-	-	-	-	-	-
1-B	2836.1	4304.4	899.9	1961.3	956.8	112.8	467.0	118.5	7350.4	-	808.3	577.0	82.8	9.2	19.9	8.0	27.7	22.7	-	2.4	-	-	5.2	-	-	-	-	-	-
Control-2	7191.7	14048.5	3146.9	3642.7	2127.1	188.0	611.3	248.9	7530.3	-	942.0	643.9	84.8	27.7	69.7	28.9	34.9	32.9	-	8.5	-	-	5.2	-	-	-	-	-	-
3-A	1902.0	2611.6	530.8	1425.7	645.0	91.0	397.7	81.9	7604.3	-	814.3	565.8	82.3	5.3	17.2	6.1	24.4	25.0	-	-	-	-	3.9	-	-	-	-	-	-
3-B	2095.5	2868.6	587.0	1502.5	684.2	96.8	417.4	87.0	7676.4	-	819.5	569.6	81.8	13.5	19.5	7.7	26.5	24.0	-	1.8	-	-	3.3	-	-	-	-	-	-
Control-3	7461.1	14441.5	3221.1	3741.0	2188.4	199.2	631.5	256.0	7694.6	-	983.1	671.3	53.7	30.5	68.1	31.0	38.1	32.6	-	11.3	-	-	6.0	-	-	-	-	-	-
6-A	1246.9	1402.3	280.6	907.1	387.8	70.8	315.9	49.7	7237.4	-	706.1	500.8	81.1	4.3	10.4	7.0	20.2	21.8	-	-	-	-	3.0	-	-	-	-	-	-
6-B	1166.4	1285.6	252.9	859.1	355.2	66.7	298.6	45.5	7253.8	-	720.5	500.8	81.5	3.6	11.0	7.0	20.4	22.7	-	-	-	-	3.2	-	-	-	-	-	-
Control-4	7326.4	14245.0	3184.0	3691.8	2157.7	193.6	621.4	252.5	7612.5	-	962.5	657.6	55.7	29.1	68.9	30.0	36.5	32.7	-	9.9	-	-	5.6	-	-	-	-	-	-
12-A	310.0	161.4	29.1	167.9	53.0	17.7	94.8	6.5	5175.9	-	418.6	311.8	73.7	-	8.9	6.0	11.6	14.1	-	-	-	-	-	-	-	-	-	-	-
12-B	543.1	369.6	68.8	327.0	109.4	30.3	152.0	13.7	5441.7	-	466.3	406.2	81.3	2.0	9.3	6.2	13.1	14.0	-	-	-	-	-	-	-	-	-	-	-
Control-5	6729.3	13027.7	2898.5	3386.4	1994.9	191.9	575.0	234.0	6993.0	-	892.9	607.7	53.5	15.5	46.5	24.7	34.1	26.5	-	8.8	-	-	4.0	-	-	-	-	-	-
24-A	2.4	2.6	6.1	25.6	-	-	-	-	41.7	-	17.0	-	29.2	-	3.5	-	2.9	-	-	-	-	-	-	-	-	-	-	-	-
24-B	3.0	5.5	7.6	1.9	-	-	-	-	46.2	-	13.4	-	26.9	-	3.6	-	3.9	-	-	-	-	-	-	-	-	-	-	-	-
Control-6	6286.0	12638.4	2835.1	3422.7	2041.3	225.3	603.0	243.0	6687.7	-	817.3	566.2	54.6	14.7	56.5	25.4	34.3	24.9	-	9.5	-	-	1.3	-	-	-	-	-	-
48-A	-	-	6.1	27.2	-	-	-	-	4.2	3.1	11.2	-	13.5	-	-	-	-	-	-	-	-	-	-	-	-	-	-	-	-
48-B	-	-	6.6	-	-	-	-	-	3.2	4.0	10.5	-	11.1	-	-	-	-	-	-	-	-	-	-	-	-	-	-	-	-
Control-7	4976.5	9605.2	2100.4	2683.3	1592.6	39.8	466.5	190.3	4953.4	-	635.1	445.9	49.6	7.1	47.0	9.6	28.2	20.2	-	7.6	-	-	-	-	-	-	-	-	-
72-A	-	-	6.1	-	2.7	-	1.4	-	3.2	-	4.9	-	3.8	-	-	-	2.8	-	-	-	-	-	4.1	-	-	-	-	-	-
72-B	-	-	6.5	-	2.2	-	-	-	3.2	4.1	4.9	-	9.7	-	-	-	3.0	-	-	-	-	-	-	-	-	-	-	-	-
Control-8	5156.7	9861.6	2188.2	2633.2	1565.7	40.1	462.3	186.6	5025.9	-	635.2	445.1	46.1	22.9	37.4	21.5	28.1	20.3	-	7.4	-	-	-	-	-	-	-	-	-
7-A	-	-	5.0	-	-	-	-	-	-	-	11.4	-	-	-	-	-	-	-	-	-	-	-	4.9	-	-	-	-	-	-
7-B	-	-	4.9	-	-	-	-	-	-	-	6.4	-	6.1	-	-	-	-	-	-	-	-	-	-	-	-	-	-	-	-
14-A	-	-	-	-	-	-	-	-	-	-	7.4	-	3.2	-	-	-	1.9	-	-	-	-	-	-	-	-	-	-	-	-
14-B	-	-	-	-	-	-	-	-	-	-	7.2	-	3.3	-	-	-	2.4	-	-	-	-	-	-	-	-	-	-	-	-

Note: (-) < MDL

Table F.6(b). Raw persulfate results from iron activated persulfate treatability study (Fe=150 mg/L).

Sample ID	Concentration (mg/L)
1-A	18.3
1-B	18.2
3-A	19.1
3-B	21.2
6-A	19.5
6-B	19.5
12-A	20.0
12-B	19.3
24-A	18.3
24-B	18.8
48-A	18.4
48-B	19.3
72-A	17.7
72-B	16.7
7-A	16.5
7-B	17.5
14-A	14.6
14-B	17.5

Table F.10(a). Raw results from iron activated persulfate column experiment for treatment column 1.

ID	Benz	Tol	Ethyl- benzene	P,M- xylene	O- xylene	1,3,5 TMB	1,2,4 TMB	1,2,3 TMB	Nap	Indole	2- Metnap	1- Metnap	Bi- phenyl	Ace- naphthylene	Ace- naphthene	DbF	Fluorene	Phenan	Anth	Carb	Fluoran	Pyrene	B(a)A	Chrys	B(b)F+	B(k)F	B(a)P	I[1,2,3-c,d] P	+ D[a,h]A	B[g,h,i]P
MDL	1.11	0.83	0.77	1.46	0.37	0.74	0.82	0.76	2.20	2.12	4.27	1.31	1.09	1.53	1.83	1.10	1.88	3.78	5.53	2.39	1.80	1.60	4.77	5.75	5.62	13.33	18.65	11.49	18.65	11.49
LOQ	3.34	2.49	2.32	4.38	1.11	2.21	2.47	2.28	6.61	6.36	12.82	3.93	3.26	4.60	5.49	3.31	5.64	11.34	16.60	7.18	5.40	4.81	14.32	17.24	16.85	39.99	55.95	34.47	55.95	34.47
C1-1A	487.7	1807.8	756.4	1206.6	15210.4	138.4	1312.9	295.8	8444.7	-	2014.2	\	167.4	342.4	253.3	70.1	276.7	473.2	54.0	-	74.8	122.6	31.1	-	-	-	-	-	-	-
C1-1B	527.6	1948.8	821.4	1311.2	17568.5	152.4	1366.1	391.3	9148.5	44.2	2190.2	1548.6	183.5	370.6	304.4	73.1	295.0	482.9	55.5	-	66.4	107.2	-	-	-	-	-	-	-	-
C1-2A	181.9	1075.7	188.2	284.2	8882.4	89.0	551.7	173.8	4327.7	-	937.7	698.3	85.5	267.2	105.1	-	225.1	69.85	-	-	-	36.7	-	-	-	-	-	-	-	-
C1-2B	182.1	834.8	188.7	258.4	8897.2	86.5	537.3	161.9	4337.2	-	950.8	708.9	81.4	251.4	113.7	-	218.9	70.60	-	-	-	31.9	-	-	-	-	-	-	-	-
C1-3A	151.5	199.9	123.2	211.2	6983.0	-	175.9	86.6	4190.1	-	586.0	467.0	80.5	145.4	101.69	-	102.07	61.9	66.2	-	-	27.1	-	-	-	-	-	-	-	-
C1-3B	154.3	204.0	121.8	210.1	6191.2	-	171.6	85.7	4160.9	-	564.1	445.9	81.8	150.8	102.55	-	99.63	77.8	73.3	-	-	28.2	-	-	-	-	-	-	-	-
C1-4A	143.8	181.0	107.8	179.1	5519.5	-	129.1	-	4159.1	-	449.7	416.8	78.4	118.4	80.3	-	79.2	71.9	-	-	-	17.2	-	-	-	-	-	-	-	-
C1-4B	136.5	157.0	109.3	182.7	5937.6	-	130.6	-	4147.1	-	514.7	443.5	80.8	110.8	81.4	-	83.4	79.7	-	-	-	17.1	-	-	-	-	-	-	-	-
C1-5A	-	106.9	92.3	172.3	4882.7	-	91.8	-	3676.8	-	490.1	385.8	59.3	87.7	49.6	-	50.5	63.9	-	-	-	-	-	-	-	-	-	-	-	-
C1-5B	-	104.9	98.2	186.2	4958.3	-	96.3	-	3699.9	-	477.0	353.8	56.6	84.6	49.3	-	60.7	61.7	-	-	-	-	-	-	-	-	-	-	-	-
C1-6A	-	50.6	87.4	179.9	4664.8	-	92.3	-	3251.1	-	392.5	391.8	49.6	51.4	20.3	-	51.5	63.0	-	-	-	-	-	-	-	-	-	-	-	-
C1-6B	-	58.5	83.2	171.7	4581.2	-	93.4	-	3439.6	-	379.5	336.1	49.2	52.0	21.4	-	57.3	63.4	-	-	-	-	-	-	-	-	-	-	-	-
C1-7A	-	52.3	77.4	185.6	5610.4	-	96.4	-	3330.2	-	393.9	364.7	53.1	44.1	-	-	41.3	61.0	-	-	-	-	-	-	-	-	-	-	-	-
C1-7B	-	54.0	80.0	189.0	5297.6	-	95.1	-	3310.6	-	381.5	351.4	53.3	49.9	-	-	48.9	61.6	-	-	-	-	-	-	-	-	-	-	-	-

Note: (-) < MDL

Table F.10(b). Raw results from iron activated persulfate column experiment for treatment column 2.

ID	Benz	Tol	Ethyl- benzene	P,M- xylene	O- xylene	1,3,5 TMB	1,2,4 TMB	1,2,3 TMB	Nap	Indole	2- Metnap	1- Metnap	Bi- phenyl	Ace- naphthylene	Ace- naphthene	DbF	Fluorene	Phenan	Anth	Carb	Fluoran	Pyrene	B(a)A	Chrys	B(b)F+	B(k)F	B(a)P	I[1,2,3-c,d] P	+ D[a,h]A	B[g,h,i]P
MDL	1.11	0.83	0.77	1.46	0.37	0.74	0.82	0.76	2.20	2.12	4.27	1.31	1.09	1.53	1.83	1.10	1.88	3.78	5.53	2.39	1.80	1.60	4.77	5.75	5.62	13.33	18.65	11.49	18.65	11.49
LOQ	3.34	2.49	2.32	4.38	1.11	2.21	2.47	2.28	6.61	6.36	12.82	3.93	3.26	4.60	5.49	3.31	5.64	11.34	16.60	7.18	5.40	4.81	14.32	17.24	16.85	39.99	55.95	34.47	55.95	34.47
C2-1A	553.74	1823	766.285	1223.7	11823.5	149.603	1390.2	316.26	9220.2	43.088	2203	1557.96	217.47	366.92	221.68	70.86	338.03	437.84	50.77	-	59.59	101.3	-	-	-	-	-	-	-	-
C2-1B	530.06	1780.9	764.902	1225.2	12414.3	158.526	1452.9	427.2	9647.1	49.52	2486.3	1740.5	211.97	415.74	180.29	86.54	338.77	558.19	65.68	-	83.48	132.36	38.33	-	-	-	-	-	-	-
C2-2A	174.64	260.84	166.919	257.3	7378.52	-	591.83	64.507	4065.7	-	496.6	356.0	89.69	201.03	110.79	35.37	164.31	74.47	-	-	38.18	27.515	-	-	-	-	-	-	-	-
C2-2B	175.99	265.14	171.117	254.9	7185.59	-	599.53	62.154	4023	-	538.9	434.6	87.33	200.39	115.99	42.64	158.87	72.04	-	-	31.22	27.194	-	-	-	-	-	-	-	-
C2-3A	148.14	228.93	135.376	207.7	3322.43	-	197.08	-	3923	-	450.1	401.6	90.85	143.70	108.77	-	141.27	66.80	51.67	-	36.78	20.5	-	-	-	-	-	-	-	-
C2-3B	142.22	220.84	161.924	203.7	3383.75	-	195.71	-	3966.7	-	456.9	393.8	90.17	144.95	102.56	-	141.58	65.55	-	-	26.35	20.3	-	-	-	-	-	-	-	-
C2-4A	32.1	176.16	97.0353	175.7	2700.3	-	107.42	-	3878	-	320.2	392.7	89.97	99.88	99.80	-	68.60	59.43	-	-	25.85	16.9	-	-	-	-	-	-	-	-
C2-4B	32.2	165.66	92.1	178.3	2691.35	-	160.41	-	3848.4	-	338.7	389.3	89.33	104.22	95.99	-	66.80	61.88	-	-	21.22	16.3	-	-	-	-	-	-	-	-
C2-5A	-	144.78	87.8786	171.3	1863.94	-	107.17	-	3838.2	-	396.9	383.5	76.80	73.45	57.64	-	58.11	53.40	-	-	26.78	-	-	-	-	-	-	-	-	-
C2-5B	-	124.8	85.8055	171.5	1918.04	-	101.62	-	3480.3	-	395.4	384.2	74.53	70.72	55.59	-	58.78	53.97	-	-	-	-	-	-	-	-	-	-	-	-
C2-6A	-	82.579	77.5	166.3	1105.72	-	93.1	-	3404.2	-	348.5	397.2	72.17	43.06	18.78	-	50.34	51.99	-	-	-	-	-	-	-	-	-	-	-	-
C2-6B	-	88.735	78.4	161.2	1127.16	-	108.04	-	3539.9	-	305.6	310.6	74.71	44.49	22.47	-	53.36	50.61	-	-	-	-	-	-	-	-	-	-	-	-
C2-7A	-	75.784	79.8	178.7	1172.44	-	97.143	-	3527.8	-	303.5	334.2	77.25	40.10	21.1	-	49.41	66.00	-	-	-	-	-	-	-	-	-	-	-	-
C2-7B	-	75.038	76.8	172.9	1015.04	-	96.306	-	3506.6	-	303.9	355.1	70.06	48.61	20.3	-	48.18	65.99	-	-	-	-	-	-	-	-	-	-	-	-

Table F.10(c). Raw results from iron activated persulfate column experiment for treatment column 3.

ID	Benz	Tol	Ethyl- benzene	P,M- xylene	O- xylene	1,3,5 TMB	1,2,4 TMB	1,2,3 TMB	Nap	Indole	2- Metnap	1- Metnap	Bi- phenyl	Ace- naphthylene	Ace- naphthene	DbF	Fluorene	Phenan	Anth	Carb	Fluoran	Pyrene	B(a)A	Chrys	B(b)F+	B(k)F	B(a)P	I[1,2,3-c,d] P + D[a,h]A	B[g,h,i]P
MDL	1.11	0.83	0.77	1.46	0.37	0.74	0.82	0.76	2.20	2.12	4.27	1.31	1.09	1.53	1.83	1.10	1.88	3.78	5.53	2.39	1.80	1.60	4.77	5.75	5.62	13.33	18.65	11.49	
LOO	3.34	2.49	2.32	4.38	1.11	2.21	2.47	2.28	6.61	6.36	12.82	3.93	3.26	4.60	5.49	3.31	5.64	11.34	16.60	7.18	5.40	4.81	14.32	17.24	16.85	39.99	55.95	34.47	
C3-1A	546.1	2032.6	896.2	1420.9	15437.9	163.3	1340.9	428.6	8863.4	40.5	2129.0	1476.6	176.3	345.0	211.0	70.3	272.0	441.5	53.8	-	79.1	121.1	-	-	-	-	-	-	
C3-1B	472.4	1868.9	830.7	1316.9	18148.8	155.2	1384.1	425.8	8613.9	41.8	2070.5	1443.6	172.3	338.7	215.4	68.9	267.6	437.4	53.4	-	77.0	119.2	38.6	-	-	-	-	-	
C3-2A	111.8	287.8	252.3	448.7	6877.8	-	168.8	76.1	3817.1	-	522.2	413.3	88.9	248.6	121.9	32.10	194.6	77.69	-	-	46.0	31.0	-	-	-	-	-	-	
C3-2B	122.5	285.7	253.6	420.5	7422.3	-	161.2	82.5	3953.5	-	532.2	374.2	80.1	256.3	121.1	35.28	196.2	78.96	-	-	40.1	30.3	-	-	-	-	-	-	
C3-3A	87.6	171.0	151.5	236.3	4924.7	-	113.3	-	3726.5	-	449.2	386.1	63.8	191.1	103.3	-	67.19	76.6	-	-	39.8	25.6	-	-	-	-	-	-	
C3-3B	64.5	175.6	151.7	200.9	5525.6	-	118.8	-	3868.6	-	493.9	342.3	65.8	191.6	102.24	-	71.62	77.5	-	-	36.6	25.1	-	-	-	-	-	-	
C3-4A	44.4	174.7	114.8	199.3	3384.8	-	91.6	-	3210.9	-	304.7	261.2	74.5	139.7	99.74	-	73.0	68.1	-	-	23.7	17.9	-	-	-	-	-	-	
C3-4B	41.5	173.9	112.4	196.3	3385.4	-	93.5	-	3282.0	-	302.9	231.3	71.0	137.4	92.0	-	81.3	68.4	-	-	27.6	16.5	-	-	-	-	-	-	
C3-5A	40.9	175.2	42.3	171.5	3271.0	-	63.3	-	3169.7	-	290.7	236.3	75.6	65.5	58.9	-	55.6	64.7	-	-	-	-	-	-	-	-	-	-	
C3-5B	44.8	163.4	46.6	175.8	3220.9	-	80.9	-	3105.8	-	291.2	230.2	70.7	61.4	57.9	-	59.8	68.1	-	-	-	-	-	-	-	-	-	-	
C3-6A	-	165.1	35.0	151.7	2518.6	-	49.2	-	3156.6	-	242.4	247.8	72.6	56.3	33.3	-	61.8	60.1	-	-	-	-	-	-	-	-	-	-	
C3-6B	-	166.9	35.2	153.9	2416.0	-	68.6	-	3180.4	-	279.7	252.4	72.9	57.1	35.5	-	64.7	60.8	-	-	-	-	-	-	-	-	-	-	
C3-7A	-	136.1	44.4	146.4	7837.7	-	63.6	-	3160.8	-	233.3	255.3	72.2	36.5	-	-	64.2	64.4	-	-	-	-	-	-	-	-	-	-	
C3-7B	-	150.1	45.9	167.5	7880.9	-	55.2	-	3182.2	-	263.1	241.2	74.2	34.8	-	-	65.1	66.4	-	-	-	-	-	-	-	-	-	-	

Note: (-) < MDL

Table F.10(d). Raw results from iron activated persulfate column experiment for control column.

ID	Benz	Tol	Ethyl- benzene	P,M- xylene	O- xylene	1,3,5 TMB	1,2,4 TMB	1,2,3 TMB	Nap	Indole	2- Metnap	1- Metnap	Bi- phenyl	Ace- naphthylene	Ace- naphthene	DbF	Fluorene	Phenan	Anth	Carb	Fluoran	Pyrene	B(a)A	Chrys	B(b)F+	B(k)F	B(a)P	I[1,2,3-c,d] P + D[a,h]A	B[g,h,i]P
MDL	1.11	0.83	0.77	1.46	0.37	0.74	0.82	0.76	2.20	2.12	4.27	1.31	1.09	1.53	1.83	1.10	1.88	3.78	5.53	2.39	1.80	1.60	4.77	5.75	5.62	13.33	18.65	11.49	
LOO	3.34	2.49	2.32	4.38	1.11	2.21	2.47	2.28	6.61	6.36	12.82	3.93	3.26	4.60	5.49	3.31	5.64	11.34	16.60	7.18	5.40	4.81	14.32	17.24	16.85	39.99	55.95	34.47	
CON-1A	487.7	1807.8	756.4	1206.6	15210.4	138.4	1212.9	295.8	8444.7	-	2014.2	1427.8	167.4	342.4	105.1	70.1	276.7	473.2	54.0	-	74.8	122.6	31.1	-	-	-	-	-	
CON-1B	527.6	1948.8	821.4	1311.2	17568.5	132.4	1266.1	391.3	9148.5	44.2	2190.2	1548.6	183.5	370.6	113.7	73.1	295.0	482.9	55.5	-	66.4	107.2	-	-	-	-	-	-	
CON-2A	541.2	1847.6	829.1	1391.9	11258.8	140.8	1034.3	352.4	7499.0	-	1476.4	1018.8	96.9	220.9	101.2	51.3	153.9	190.9	-	-	-	98.3	-	-	-	-	-	-	
CON-2B	448.0	1861.5	830.4	1210.3	11853.3	131.5	1055.6	344.4	6635.0	-	1531.2	1050.5	99.1	226.9	103.5	55.1	160.9	197.1	-	-	-	99.3	-	-	-	-	-	-	
CON-3A	492.2	1717.5	839.6	1131.2	9772.7	134.8	997.3	322.9	6782.3	-	1112.3	980.9	86.9	219.1	90.50	-	141.51	190.83	-	-	-	84.00	-	-	-	-	-	-	
CON-3B	451.4	1721.3	740.4	1235.3	11799.3	116.2	1090.7	323.8	6792.2	-	1109.7	976.2	96.1	217.7	99.80	-	141.20	189.84	-	-	-	86.00	-	-	-	-	-	-	
CON-4A	386.5	1647.7	760.4	1203.5	11294.7	123.6	935.1	289.6	6159.6	-	1170.9	856.3	90.2	168.1	95.5	-	138.3	191.8	-	-	-	77.0	-	-	-	-	-	-	
CON-4B	398.1	1659.6	759.7	1214.9	11305.7	124.8	1041.2	287.2	6186.9	-	1162.8	848.1	90.2	168.8	100.0	-	138.3	181.3	-	-	-	79.0	-	-	-	-	-	-	
CON-5A	393.8	1675.7	657.8	1059.1	10519.5	109.0	951.7	273.8	5251.1	-	937.7	698.3	59.3	145.4	90.3	-	179.2	171.9	-	-	-	76.0	-	-	-	-	-	-	
CON-5B	386.5	1234.8	579.3	1012.7	10537.6	116.5	837.3	291.9	5939.6	-	950.8	708.9	56.6	150.8	91.4	-	93.4	179.7	-	-	-	75.0	-	-	-	-	-	-	
CON-6A	394.4	1338.0	545.9	1006.3	10879.1	104.7	825.9	266.5	5158.4	-	919.3	689.8	55.8	144.6	89.3	-	99.6	165.8	-	-	-	70.0	-	-	-	-	-	-	
CON-6B	396.9	1379.0	665.2	1067.2	10598.8	117.8	889.7	266.0	5572.6	-	978.4	724.8	62.2	152.1	80.4	-	169.3	163.6	-	-	-	70.0	-	-	-	-	-	-	
CON-7A	395.6	1358.5	605.6	1036.8	10738.9	111.2	857.8	266.2	5365.5	-	948.8	707.3	59.0	148.4	84.8	-	134.5	164.7	-	-	-	70.0	-	-	-	-	-	-	
CON-7B	396.3	1368.8	635.4	1052.0	10668.9	114.5	873.7	266.1	5469.1	-	963.6	716.0	60.6	150.3	82.6	-	151.9	164.1	-	-	-	70.0	-	-	-	-	-	-	

Note: (-) < MDL

Table F.11(a). Initial soil concentrations for unactivated column experiment.

Column	Location	Benz	Tol	Ethylbenzene	P,M-xylene	O-xylene	1,3,5 TMB	1,2,4 TMB	1,2,3 TMB	Nap	Indole	2-Metnap	1-Metnap	Bi-phenyl	Ace-naphthylene	Ace-naphthene	DbF	Fluorene	Phena n	Ant h	Car b	Fluor an	Pyre ne	B(a) A	Chry s	B(b)F + B(k)F	B(a) P	I[1,2,3-c,d] P + D[a,h]A	B[g,h,i]P
Control	LOW	8.87	52.0	47.9	75.9	46.3	21.0	91.1	31.3	635	6.3	430	254	52.5	85.7	36.7	34.5	65.3	221	26.9	-	55.7	94.7	16.6	17.1	18.1	14.0	4.7	5.0
	MID	9.34	51.9	47.3	74.4	45.5	20.4	89.7	30.4	620	6.5	429	253	52.6	85.3	36.6	35.1	64.8	219	27.1	-	54.7	92.9	16.5	16.9	17.4	13.4	-	4.7
	HIGH	9.39	53.1	49.1	77.1	48.2	21.1	95.0	32.3	649	6.4	445	261	51.3	85.6	37.4	36.9	69.1	222	24.0	-	55.6	91.8	17.3	17.4	16.7	12.9	-	4.3
1	LOW	7.52	52.0	50.3	79.9	49.2	22.2	96.4	32.7	658	6.6	461	272	57.1	92.5	39.5	37.6	70.2	236	29.0	-	59.6	101	18.0	18.4	19.3	14.9	5.5	4.5
	MID	7.84	54.7	53.9	85.0	53.3	23.8	105.9	36.1	730	6.8	496	290	61.4	96.8	42.2	41.1	78.8	250	26.8	-	64.0	106	21.1	20.7	20.1	16.1	-	4.9
	HIGH	7.68	53.4	52.1	82.4	51.2	23.0	101.2	34.4	694	6.7	478	281	59.3	94.7	40.8	39.4	74.5	243	27.9	-	61.8	103	19.5	19.5	19.7	15.5	2.7	4.7
2	LOW	5.42	46.9	49.1	77.7	48.3	22.4	97.0	32.8	669	6.9	470	277	58.2	94.6	40.5	38.7	123	244	29.7	-	61.6	104	18.8	18.9	19.7	15.4	5.9	5.6
	MID	5.30	46.5	48.7	76.9	47.5	22.1	96.3	32.6	667	7.2	467	275	57.7	93.0	40.0	38.4	121	240	29.7	-	60.3	102	18.8	18.9	19.2	15.1	5.4	4.6
	HIGH	5.60	48.4	51.1	80.8	51.0	23.3	103.2	35.2	703	6.9	491	287	60.3	95.4	42.0	40.5	77.2	246	26.8	-	62.3	103	20.9	20.3	19.2	15.4	-	4.8
3	LOW	7.83	45.5	41.9	65.8	40.5	18.1	78.0	26.6	542	5.8	376	222	46.1	75.3	32.2	30.4	56.9	193	23.7	-	48.1	81.5	14.6	14.9	15.4	12.1	4.4	4.4
	MID	8.11	46.5	42.8	67.3	41.5	18.5	80.0	26.9	553	5.7	384	227	47.2	76.7	32.8	31.5	99.7	197	24.3	-	48.7	82.4	14.7	14.8	15.0	11.3	-	-
	HIGH	8.59	48.8	45.1	70.8	44.3	19.6	86.3	29.2	596	6.1	406	237	46.9	78.8	34.4	33.5	62.3	203	22.3	-	50.9	83.6	16.5	16.1	15.4	12.1	-	-

Note: (-) < MDL

Table F.11(b). Final soil concentrations for unactivated column experiments.

Column	Location	Benz	Tol	Ethylbenzene	P,M-xylene	O-xylene	1,3,5 TMB	1,2,4 TMB	1,2,3 TMB	Nap	Indole	2-Metnap	1-Metnap	Bi-phenyl	Ace-naphthylene	Ace-naphthene	DbF	Fluorene	Phena n	Ant h	Car b	Fluor an	Pyre ne	B(a) A	Chry s	B(b)F + B(k)F	B(a) P	I[1,2,3-c,d] P + D[a,h]A	B[g,h,i]P
Control	LOW	-	15.4	41.3	71.6	49.2	23.1	104	35.0	689	5.8	500	295	32.7	90.4	41.2	38.6	124	243	30.2	-	58.1	93.1	17.7	19.3	16.7	10.3	-	-
	MID	-	13.2	48.9	88.5	55.1	25.9	115	38.3	729	6.0	526	310	33.5	94.2	42.8	40.0	129	253	30.9	-	59.4	94.3	18.4	19.6	16.6	10.5	-	-
	HIGH	-	10.9	12.8	33.1	23.2	15.5	68.3	21.2	431	4.4	357	211	23.4	63.5	28.6	27.0	86.2	167	18.8	-	38.4	60.9	10.5	12.0	10.4	6.45	-	-
1	LOW	-	7.86	34.0	60.4	38.5	19.9	80.6	26.2	586	3.7	433	255	28.7	60.5	33.4	33.1	99.3	213	20.2	-	50.8	78.1	15.4	17.2	15.5	8.67	-	-
	MID	-	8.50	37.4	65.3	39.3	20.9	84.4	27.2	593	3.9	441	259	28.7	61.5	33.5	33.5	99.7	211	20.0	-	49.6	75.2	14.4	16.1	13.9	7.13	-	-
	HIGH	-	4.87	48.4	86.6	56.8	35.9	147	47.5	1075	5.8	753	440	46.8	106	56.3	56.1	168	355	31.8	-	86.9	133.2	29.8	32.5	28.9	17.2	-	-
2	LOW	-	8.76	34.8	63.9	39.5	23.0	91.3	29.8	689	4.4	507	299	33.2	66.9	38.5	39.3	114	250	22.7	-	61.3	94.0	18.6	21.0	19.7	10.7	-	-
	MID	-	8.50	37.4	65.3	39.3	20.9	84.4	27.2	593	3.9	441	259	28.7	61.5	33.5	33.5	99.7	211	20.0	-	49.6	75.2	14.4	16.1	13.9	7.13	-	-
	HIGH	-	5.88	37.4	68.0	44.2	28.3	113	34.8	807	4.8	611	359	38.8	81.4	46.1	46.5	91.8	299	25.9	-	73.0	112	23.4	25.8	23.3	12.7	-	-
3	LOW	-	5.10	33.1	60.9	42.7	22.0	91.8	28.4	680	4.1	500	295	32.4	64.0	37.5	37.6	113	246	20.5	-	59.8	92.0	16.3	19.3	17.8	7.79	-	-
	MID	-	6.5	36.6	65.1	43.6	22.5	94.9	28.7	664	4.0	493	290	32.7	65.8	37.2	37.6	112	244	20.3	-	58.8	89.0	17.3	20.1	17.6	8.10	-	-
	HIGH	-	-	16.9	32.5	28.9	19.1	81.3	23.3	588	3.5	450	265	29.8	59.9	33.5	33.4	101	217	17.8	-	52.5	80.6	15.2	18.2	16.4	8.06	-	-

Note: (-) < MDL

Table F.11(c). Initial soil concentrations for iron-activated column experiments.

Column	Location	Benz	Tol	Ethylbenzene	P,M-xylene	O-xylene	1,3,5 TMB	1,2,4 TMB	1,2,3 TMB	Nap	Indole	2-Metnap	1-Metnap	Bi-phenyl	Acenaphthylene	Acenaphthene	DBF	Fluorene	Phenanthrene	Anthracene	Carb	Fluoranthene	Pyrene	B(a)A	Chrys	B(b)F + B(k)F	B(a)P	I[1,2,3-c,d] P + D[a,h]A	B[g,h,i]P
1	LOW	9.28	52.3	49.2	75.8	46.7	20.8	91.9	31.3	635	6.4	435	256	52.2	85.5	36.9	35.5	66.4	221	26.0	-	55.3	93.1	16.8	17.1	17.4	13.4	1.58	4.69
	MID	9.34	52.1	49.2	75.7	46.1	20.3	90.4	30.9	627	6.8	432	254	52.4	85.4	36.7	35.3	65.6	220	26.5	-	55.0	93.0	16.7	17.3	17.6	13.3	0.850	4.37
	HIGH	9.31	52.1	49.2	75.1	46.1	20.6	90.8	30.9	627	6.5	432	254	52.4	85.4	36.7	35.3	65.6	220	26.5	-	55.0	93.0	16.7	17.0	17.4	13.4	0.789	4.70
2	LOW	8.00	53.0	52.0	83.0	51.0	23.0	97.0	34.0	661	7.0	486	274	59.0	94.0	41.0	38.0	74.0	239	26.4	-	60.0	104	19.0	20.0	20.0	15.0	2.50	5.00
	MID	7.00	54.0	52.0	84.0	52.0	23.0	103	36.0	699	6.5	488	282	59.0	94.0	42.0	41.0	74.0	242	27.0	-	62.0	105	20.0	20.0	20.0	15.0	2.40	4.90
	HIGH	7.76	54.1	53.0	83.7	52.3	23.4	104	35.3	712	6.7	487	286	60.3	95.7	41.5	40.2	76.7	246	27.4	-	62.9	104	20.3	20.1	19.9	15.8	1.37	4.83
Control	LOW	5.51	47.6	50.1	79.2	49.7	22.8	100	34.0	686	6.9	480	282	59.2	95.0	41.3	39.6	100	245	28.2	-	62.0	104	19.9	19.6	19.4	15.4	2.97	5.21
	MID	5.44	47.3	49.6	78.4	48.9	22.6	98.9	33.5	680	7.0	476	280	58.7	94.4	40.9	39.2	107	243	28.7	-	61.4	103	19.5	19.4	19.4	15.3	3.77	5.02
	HIGH	5.48	47.4	49.9	78.8	49.3	22.7	99.5	33.8	683	6.9	478	281	59.0	94.7	41.1	39.4	104	244	28.5	-	61.7	103	19.7	19.5	19.4	15.3	3.37	5.12
3	LOW	8.21	47.2	43.5	68.3	42.4	18.8	82.2	27.9	569	5.9	391	230	46.5	77.1	33.3	31.9	59.6	198	23.0	-	49.5	82.6	15.5	15.5	15.4	12.1	2.18	2.22
	MID	8.40	48.0	44.3	69.5	43.4	19.2	84.2	28.6	583	6.0	398	233	46.7	77.9	33.8	32.7	60.9	200	22.7	-	50.2	83.1	16.0	15.8	15.4	12.1	1.09	1.11
	HIGH	8.49	48.4	44.7	70.2	43.8	19.4	85.3	28.9	589	6.1	402	235	46.8	78.4	34.1	33.1	61.6	201	22.5	-	50.6	83.4	16.2	16.0	15.4	12.1	0.544	0.554

Note: (-) < MDL

Table F.11(d). Final soil concentrations for iron-activated column experiments.

Column	Location	Benz	Tol	Ethylbenzene	P,M-xylene	O-xylene	1,3,5 TMB	1,2,4 TMB	1,2,3 TMB	Nap	Indole	2-Metnap	1-Metnap	Bi-phenyl	Acenaphthylene	Acenaphthene	DBF	Fluorene	Phenanthrene	Anthracene	Carb	Fluoranthene	Pyrene	B(a)A	Chrys	B(b)F + B(k)F	B(a)P	I[1,2,3-c,d] P + D[a,h]A	B[g,h,i]P
1	Top	-	3.35	20.5	39.9	26.4	17.9	73.9	25.6	702	3.4	522	309	42.4	82.2	44.2	43.0	90.8	302	21.3	-	78.2	128	20.7	22.5	22.8	12.8	7.17	5.52
	Mid	-	2.51	21.7	42.4	27.1	19.6	80.5	26.2	741	3.7	561	331	36.6	90.3	48.0	46.1	97.7	319	24.3	-	80.4	131	22.4	23.0	22.2	13.0	6.76	4.98
	Bot	-	-	15.7	31.3	21.7	17.5	72.6	21.0	669	3.5	506	299	32.0	80.9	42.6	42.0	88.4	293	21.3	-	75.1	122	20.7	22.0	21.8	12.6	6.53	4.89
2	Top	-	7.86	34.0	60.4	38.5	19.9	80.6	26.2	586	3.7	433	255	28.7	60.5	33.4	33.1	99.3	213	20.2	-	50.8	78.1	15.4	17.2	15.5	8.67	-	-
	Mid	-	8.50	37.4	65.3	39.3	20.9	84.4	27.2	593	3.9	441	259	28.7	61.5	33.5	33.5	99.7	211	20.0	-	49.6	75.2	14.4	16.1	13.9	7.13	-	-
	Bot	-	4.87	48.4	86.6	56.8	35.9	147	47.5	1075	5.8	753	440	46.8	106.2	56.3	56.1	168	355	31.8	-	86.9	133	29.8	32.5	28.9	17.2	-	-
Control	Top	-	8.76	34.8	63.9	39.5	23.0	91.3	29.8	689	4.4	507	299	33.2	66.9	38.5	39.3	114	250	22.7	-	61.3	94.0	18.6	21.0	19.7	10.7	-	-
	Mid	-	5.26	28.7	52.9	34.1	21.0	83.5	26.9	632	3.7	473	278	31.2	62.1	35.5	36.1	106	232	20.5	-	55.0	83.3	16.3	18.1	16.0	8.47	-	-
	Bot	-	5.88	37.4	68.0	44.2	28.3	113	34.8	807	4.8	611	359	38.8	81.4	46.1	46.5	91.8	299	25.9	-	73.0	112	23.4	25.8	23.3	12.7	-	-
3	Top	-	5.10	33.1	60.9	42.7	22.0	91.8	28.4	680	4.1	500	295	32.4	64.0	37.5	37.6	113	246	20.5	-	59.8	92.0	16.3	19.3	17.8	7.79	-	-
	Mid	-	6.53	36.6	65.1	43.6	22.5	94.9	28.7	664	4.0	493	290	32.7	65.8	37.2	37.6	112	244	20.3	-	58.8	89.0	17.3	20.1	17.6	8.10	-	-
	Bot	-	-	16.9	32.5	28.9	19.1	81.3	23.3	588	3.5	450	265	29.8	59.9	33.5	33.4	101	217	17.8	-	52.5	80.6	15.2	18.2	16.4	8.06	-	-

Note: (-) < MDL

**Appendix G:
Photos**



Figure G.1. Angled drilling under the meter shop.



Figure G.2. Drilling inside operations building.



Figure G.3. NAPL saturated pores in DPT-14 at 20-25 ft bgs.



Figure G.4. NAPL saturated pores in DPT-23 at 13 ft bgs.



Figure G.5. Non-impacted sand in DPT-27 20 to 50 ft bgs.



Figure G.6. NAPL saturated soil from DPT-23 used for column experiments.



Figure G.7. Unactivated column #1.

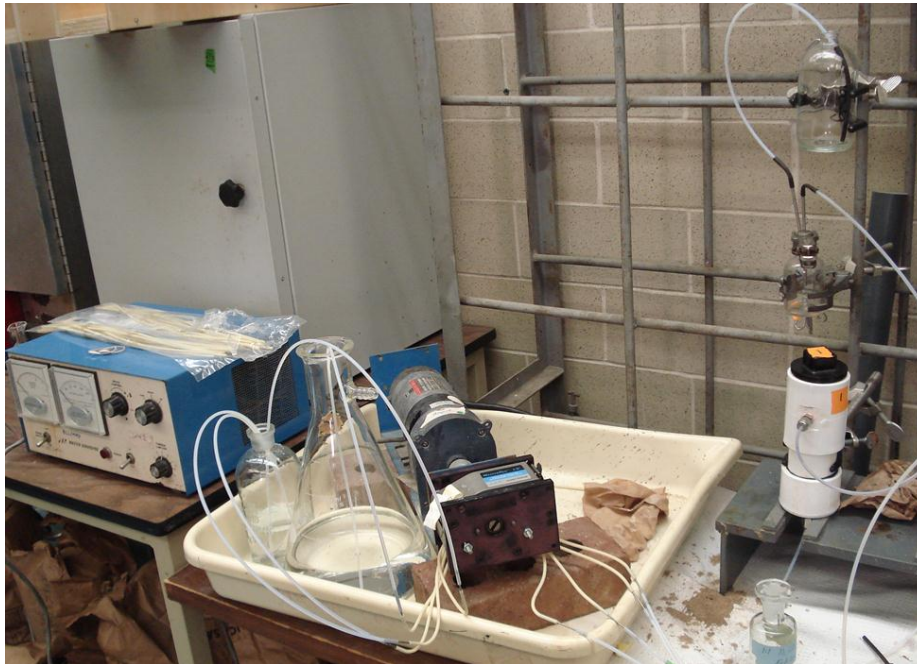


Figure G.8. Column experimental set-up.

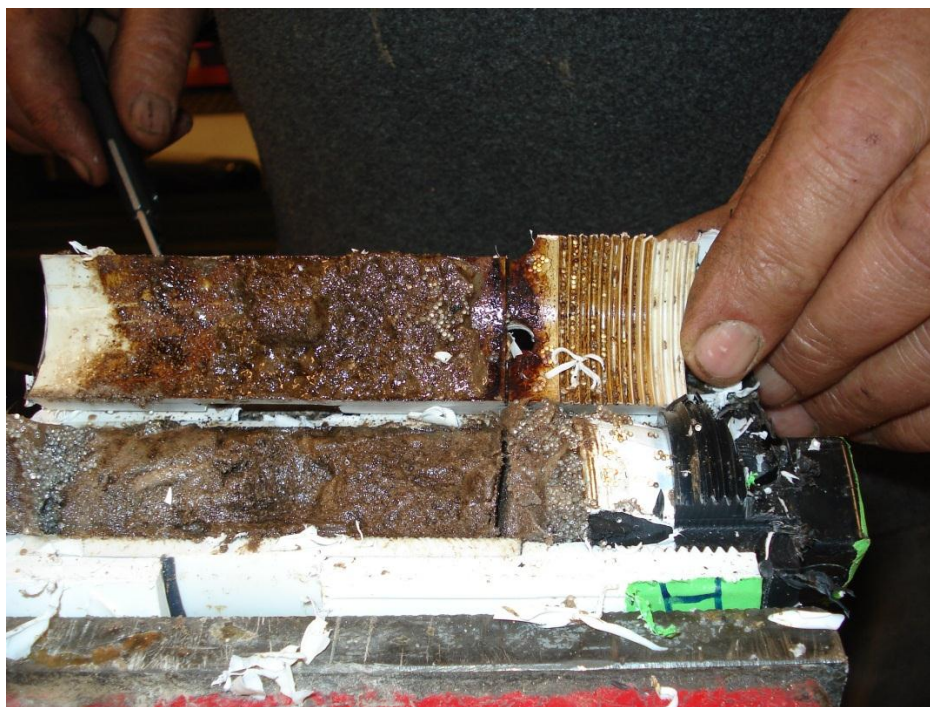


Figure G.9. Iron-activated control column at the conclusion of the experiment.



Figure G.10. Unactivated treatment column #1 at the conclusion of the experiment.



Figure G.11. Iron activated treatment column #1 at the conclusion of the experiment.